

*Genetic, Metabolic and Physiological Studies of Indigenous Halomonas BVR 1
Isolated from Electronic Industry Effluent for Remediation of Heavy Metals*

THESIS

Submitted in partial fulfillment of
the requirements for the degree of

DOCTOR OF PHILOSOPHY

by

MANASI

ID. No: 2010PHXF432H

Under the Supervision of

Prof. VIDYA RAJESH

Department of Biological Sciences

&

Prof. N. RAJESH

Department of Chemistry



BIRLA INSTITUTE OF TECHNOLOGY AND SCIENCE, PILANI

Hyderabad Campus, Hyderabad, INDIA

2017



BIRLA INSTITUTE OF TECHNOLOGY & SCIENCE, PILANI
Hyderabad Campus, Hyderabad, Telangana

CERTIFICATE

This is to certify that the thesis entitled “*Genetic, Metabolic and Physiological Studies of Indigenous Halomonas BVR 1 Isolated from Electronic Industry Effluent for Remediation of Heavy Metals*” submitted by **Manasi, ID.No. 2010PHXF432H** for the award of Ph. D. degree of the Institute embodies the original work done by her under our supervision.

Signature in full of the supervisor : _____

Name in capital block letters : **VIDYA RAJESH**

Designation : **Associate Professor**

Department of Biological Sciences

Date : _____

Signature in full of the supervisor : _____

Name in capital block letters : **N. RAJESH**

Designation : **Professor**

Department of Chemistry

Date : _____

Acknowledgement

- *The following PhD thesis encompasses my individual work although I could never have reached the heights or explored the depths without the help and guidance from lot of people.*
- *I owe my sincere gratitude to **Prof. B. N. Jain**, Ex-Vice Chancellor (BITS), **Prof. V.S.Rao**, Ex-Director (BITS-Pilani, Hyderabad Campus), **Prof. Souvik Bhattacharya** (Vice Chancellor (BITS) and **Prof. G Sundar** (Director BITS Pilani Hyderabad Campus) for funding my research work and permitting me to carry out my doctoral work in this campus.*
- *I express my heartfelt thanks and owe a deep sense of gratitude to my faculty supervisor and co-Supervisor **Prof Vidya Rajesh** and **Prof N. Rajesh** for their sincere guidance, encouragement, suggestion and very constructive criticism that has contributed immensely to the evolution of ideas on the subject. This thesis would not have been possible without their support. Under their supervision, it has been a period of intense learning for me not only in scientific arena, but also on a personal level.*
- *I am grateful to **Prof. Suman Kapur** and **Prof. Ramakrishna Vadrevu** (Ex-HOD, Department of Biological Sciences), **Prof. Naga Mohan Kommu** (HOD, Department of Biological Sciences), **Dr. Sridev Mohapatra** (Convener, DRC, Department of Biological Sciences) and my Doctoral Advisory Committee **Prof. P. Sankar Ganesh** and **Prof. Jayanty Subbalakshmi** for their insightful comments and encouragement, which incited me to widen my research from various perspectives. I would also like to thank **Dr. Vikranth Kumar Surasani** and his students for helping me with the theoretical*

modelling of column studies and giving his valuable comments on drafts that was highly appreciated.

- *I wish to express my thanks and take immense pleasure in acknowledging all the faculty of Department of Biological Sciences, BITS-Pilani, Hyderabad Campus for their support and encouragement to carry out this research work. I also extend my acknowledgement to **Prof. K. Sumithra and Prof. Anupam Bhattacharya** (Ex-HOD Department of Chemistry), **Prof. Manab Chakravarty** (HOD, Department of Chemistry), for granting me permission to carry out heavy metal adsorption based experiments in Department of Chemistry.*
- *I would like to thank the Departmental Research Committee (Department of Biological Sciences) and Academic Research Division for their assistance when ever required.*
- *I would like to acknowledge support from various industries for helping me collect effluents for my thesis work.*
- *I would like to thank **Indian Institute of Chemical Technology (IICT), Nishka Laboratories, Sophisticated Analytical Instrumentation Facility (SAIF), Cochin** for helping me in characterizing the adsorbent for adsorption studies. My heartfelt thanks to **Bioserve Biotechnologies Pvt. Ltd, Hyderabad, India** for providing the DNA sequencing facilities.*
- *I would specially like to thank my uncle, **Dr. K. Nagaiah** (Sr. Principal Scientist CSIR-Indian Institute of Chemical Technology) for his constant encouragement and support.*
- *I would like to acknowledge my deep regards to my fellow research students **Dr. S. Kalidhasan, Dr. Santhanam Krishna Kumar, Madhu Poornima Mamidala, C N Rahul, T. Sathvika, Shivani Sharma and M. Bharathi** for their encouragement and*

*maintaining a healthy, positive and cordial environment all through the years of my research work in this campus. My heartfelt thanks to **Megha Sravani Bondada** for helping me out with the coloum experiments and **Aditya** for his assistance in carrying out the biochemical characterisation of five strains. I would also like to thank the **research scholars** from various departments, **lab technicians**, **Central analytical laboratory** for their support in every possible manner and help me complete my work smoothly.*

- *Last but not the least I place my deep sense of gratitude and loving thanks to my family members, my mother and father **Mrs. Kalpana Mudaliyar & Mr. Shriram Mudaliyar** for their blessings and kind advice. My heartfelt thanks to my in-laws and husband **Mr. Anil Kumar**, my lovely twins, **Aarav and Aarana** for their love, constant encouragement support and motivation to complete this work successfully.*
- *Lastly, I offer my regards to all of those who supported me in any other respect during the completion of my thesis.*
- *I dedicate this thesis to my family and most of all to our great creator, our almighty God, the author of knowledge and wisdom who made this possible.*

I humbly dedicate this thesis to my FAMILY

DATE:

MANASI

Abstract

The industrialization of world has witnessed several changes in the environment. The outcome of this effect is a huge generation of unwanted, toxic and hazardous substances/chemicals that tend to leach into landfills and contaminate surface waters thus polluting air, water and soil. All this, in total, contributes to environmental pollution.

E-waste is one of the fastest growing waste streams that is a major contributor of environmental metal pollution. Various industries in the electronic sector releases heavy metals in the environment through their effluents. Pollution of the natural environment by these heavy metals is a worldwide problem as they cannot be destroyed and most of them have toxic effects on living organisms, when present beyond their permissible levels. Several physical and chemical methods proposed for removal of these heavy metals have become obsolete due to some major reasons such as high capital input and reduced efficiency at dilute concentrations of the metal solutions, generation of hazardous by-products or inefficiency when the concentration of the pollutant is below 100 mg l^{-1} . This necessitates cost effective and environmental friendly techniques for their removal.

Biological methods solve these drawbacks since they are easy to operate, do not produce secondary pollutants, sludge and show higher efficiency at low metal concentrations. Microbes found in heavy metal rich habitats have resistance mechanisms to tolerate high concentrations of heavy metals by efflux, complexation, cell wall adsorption, transformation to a less toxic state, expression of polyamines, metallothioneins, phytochelatin, synthesis of metal binding peptides

and so on. These potent abilities of the microbes could thus be exploited to remediate heavy metals. However, there are several disadvantages and demerits associated with the direct use of bacterial biomass. Microbial masses are basically small particles with low density, little rigidity and poor mechanical strength. Immobilization of these microbes on suitable polymers is one of the key elements for practical application of the biosorbent in upscale metal removal studies. This eventually enhances the adsorption capacity of the biosorbent.

This thesis focuses on the isolation and characterization (chemical and microbiological) of the electronic industry effluent to explore for some novel heavy metal resistant microbial strains to remediate heavy metals. Various culture independent and dependent methods of identification involving biochemical tests and molecular biology based methods like 16 S r - DNA sequencing and lipid analyses (FAME analysis) were carried out to identify and confirm the strains isolated from an electronic industry effluent. Several adsorbents were prepared by using the biomass as such and subsequent immobilization of the microbe on various biopolymer matrices for enhanced remediation of lead, cadmium and zinc. Various parameters such as effect of pH, temperature, concentration, contact time, interference from diverse ions etc, were optimized to achieve maximum adsorption of the metal cations. Additionally, physicochemical characterizations (SEM-EDAX, XRD, FTIR) of the adsorbent before and after metal adsorption were also carried out to analyze the metal adsorption on the adsorbent.

Our study showed the presence of a diverse group of resistant microbes and revealed a total of ten bacterial and two fungal isolates. All these isolates were found to survive in presence of heavy metals like cadmium, lead and zinc and were resistant to antibiotics like ampicillin, tetracycline, streptomycin, penicillin and chloramphenicol as indicated by their Minimum Inhibitory Concentrations (MIC). Such resistant isolates harbor possibilities of metal

adaptive/selective pathways which render them as economically beneficial bio-sorbent and a better alternative in bioremediation of heavy metals.

One of the isolated microbe *Halomonas sp. strain BVR 1*, was selected as our model organism for this study based on its heavy metal resistance for the removal of heavy metals. The surface characterizations of the adsorbent before and after adsorption of metal ions showed significant differences indicative of effective metal binding. Langmuir isotherm gave good fit to the experimental data with a maximum adsorption capacity of 12.023 mg g⁻¹, 11.11 mg g⁻¹ and 9.152 mg g⁻¹ for cadmium, zinc and lead respectively.

To achieve a high metal binding capacity and metal selectivity, *Halomonas BVR 1* was immobilized in sodium alginate, chitosan and graphene oxide. These combinations of the adsorbents proved to be beneficial as the adsorption capacities of the metal ions increased significantly by two folds.

Halomonas BVR 1 has been proved to be a good host for metal cations, understanding the physiology of this organism under heavy metal stress and delineating the genetic basis of its heavy metal resistance is of paramount importance. In this context, we demonstrate a correlation between cellular content of three major polyamines (putrescine, spermidine and spermine) upon exposure to lead in this bacteria. The physiological response to lead occurs within 6 h post metal treatment. During the same time interval there was a surge in the growth of bacteria along with the enhancement in putrescine levels. The FTIR data of the extracted polyamines post metal treatment also showed significant shift in the spectral peaks in comparison to the ones without any metal treatment. Thus, it could be hypothesized that, the endogenous polyamines contribute towards scavenging lead in these bacteria.

The present study also proved the genetic contribution of heavy metal resistance in this strain to be plasmid mediated. Plasmid curing experiments affirmed plasmid mediated heavy metal resistance. Additionally, genetic transformation of a non metal resistant lab strain *E.coli* and the cured strain of *Halomonas BVR 1* with the isolated plasmid increased their metal tolerance level by 50 % confirming the genetic determinant to be present on the plasmid.

Keywords: E-waste, *Halomonas BVR 1*, Heavy metal, Bioremediation, Adsorption isotherms, Kinetics, Thermodynamics, Heavy metal stress, Polyamines, Plasmid

Table of contents

<i>Certificate</i>	i
<i>Acknowledgement</i>	iii
<i>Abstract</i>	vi
<i>Abbreviations & Symbols</i>	xi
<i>List of figures</i>	xiii
<i>List of Tables</i>	xvii
1. Introduction	3
2. Characterization and remediation of electronic industry effluents.	26
3. Enhancing metal remediation by immobilization of <i>Halomonas BVR 1</i> in chitosan and Graphene Oxide.	83
4. <i>Halomonas BVR 1</i> immobilized in Sodium alginate for effective removal of cations and their modelling studies to assess the upscale removal of heavy metal lead.	128
5. Understanding the effect of heavy metal stress on <i>Halomonas BVR 1</i> and delineating the genetic basis of its heavy metal resistance.	166
6. Summary, Conclusions and Future Perspective	196
<i>References</i>	202
<i>Appendix I</i>	225
<i>List of publications</i>	235
<i>Brief biography of the Supervisor</i>	236
<i>Brief biography of the Co-supervisor</i>	237
<i>Brief biography of the Candidate</i>	237

Abbreviations & Symbols

e-waste	Electronic waste
μL	Micro litre
$^{\circ}\text{C}$	Degree Celsius
AAS	Atomic Absorption Spectrophotometer
B	Langmuir constant
CETP	Common Effluent Treatment Plant
C_0	Initial Concentration
DNA	Deoxy ribonucleic Acid
dNTPs	Deoxy Ribonucleotide Triphosphate
EDAX	Energy Dispersive X-Ray Spectroscopy
EDTA	Ethylene Diamine Tetra Acetic Acid
EPA	US Environmental Protection Agency
FAME	Fatty Acid methyl Ester
FTIR	Fourier Transform Infrared Spectroscopy
G	Gram
GMOs	Genetically Modified Organisms
GO	Graphene Oxide
H	Hours
IAA	Isoamyl alcohol
KDa	Kilo Dalton
k_{int}	Intra-particle diffusion constant
M	Molar
MIC	Minimum Inhibitory Concentration
Min	Minute
mL	milli litre

MSA	Multiple Sequence Alignment
MTs	Metallothioneins
n & K _f	Freundlich constants
Ng	Nano Gram
Nm	Nanometer
OD	Optical Density
PAs	Polyamines
PCR	Polymerase Chain Reaction
mg L ⁻¹	Parts per million
q ₀	Maximum adsorption capacity
q _e	Equilibrium concentration
rDNA	ribosomal DNA
R _L	Dimensionless constant in Langmuir isotherm model
RNA	Ribonucleic acid
ROS	Reactive Oxygen Species
Rpm	Revolutions Per Minute
SDS	Sodium Dodecyl Sulphate
SEM	Scanning Electron Microscopy
T	Time
WHO	World Health Organization
ΔG ⁰	standard Gibb's free energy
ΔH ⁰	standard enthalpy
ΔS ⁰	standard entropy

List of Figures

Figure No	Caption/Legend	Page No
1.1	Schematic representation of the environmental pollutants as per EPA guidelines.	4
1.2	Schematic representation Percentage contribution of various electronic sectors.	7
1.3	Schematic representation of protective mechanisms of bacteria under metal stress.	13
1.4	Depiction of metal microbe interaction.	18
1.5	Overview of the remediation of heavy metals.	23
2.1	Gram staining depiction of strains isolated.	35
2.2	Resistance patterns of the microbes towards antibiotics.	41
2.3	MIC of strains against various heavy metals.	44
2.4	1.5 Kb amplicon of 16 S r-DNA of one of the isolate.	47
2.5	Multiple Sequence Alignment of the variable regions of all the strains.	49
2.6	Phylogenetic analysis of the isolated strains.	50
2.7	FAME profiles of the four different strains <i>Halomonas, Bacillus, Pseudomonas, Kocuria</i> .	53
2.8	Phylogenetic relationship of the isolated <i>Pseudomonas</i> with the other strains.	54
2.9	Fungal DNA isolated.	55
2.10 A-D	SEM Images of the biomass before and after adsorption.	60
2.11 A-D	EDAX spectrum of the biomass before and after adsorption.	61
2.12 A-D	FTIR spectrum of the biomass before and after the metal adsorption.	64
2.13	Effect of pH on the metal adsorption.	65
2.14 A-D	Adsorption isotherms for the removal of cadmium, lead and zinc using <i>Halomonas BVRI</i> .	68
2.15 A-D	Kinetic Plots for the adsorption of cadmium, lead and zinc using <i>Halomonas BVRI</i> .	73
2.16 A-D	Van't Hoff plot showing the variation of $\ln K$ against $1/T$.	77
3.1	Illustration of the microbe immobilized in chitosan crosslinked with glutaraldehyde.	85

3.2	SEM and optical images of the adsorbent (<i>Halomonas BVR 1</i> immobilized in chitosan) before and after the metal adsorption.	89
3.3 A-D	EDAX analysis of the adsorbent (<i>Halomonas BVR 1</i> immobilized in chitosan) before and after metal adsorption.	90
3.4A-B	FTIR of the adsorbent (<i>Halomonas BVR 1</i> immobilized in chitosan) before and after metal adsorption.	92
3.5	Percentage of metal removal at different pH.	93
3.6 A-D	Adsorption isotherms for the removal of cadmium, lead and zinc using <i>Halomonas BVR1</i> immobilized in chitosan.	94
3.7 A-D	Kinetic Plots for the adsorption of cadmium, lead and zinc using <i>Halomonas BVR1</i> immobilized in chitosan.	97
3.8 A-D	Intra-particle diffusion plot for intraparticle diffusion.	98
3.9	Van't Hoff plot showing the variation of $\ln K$ against $1/T$.	100
3.10	Effect of eluent on desorption.	104
3.11 A-D	SEM and EDAX analysis of the adsorbent (<i>Halomonas BVR1</i> immobilized in graphene oxide) before and after adsorption.	107
3.12	XRD pattern of the adsorbent (<i>Halomonas BVR1</i> immobilized in graphene oxide) before and after metal adsorption	109
3.13	FTIR analysis of the adsorbent (<i>Halomonas BVR1</i> immobilized in graphene oxide) before and after metal adsorption.	111
3.14	A. Effect of pH on the adsorption of metal ions. B. Mechanistic interaction of the biosorbent with the metal ions.	112
3.15 A-D	Cadmium adsorption isotherms using <i>Halomonas BVR1</i> immobilized in graphene oxide for the removal of cadmium, lead and zinc.	114
3.16 A-D	Lead adsorption isotherms (A: Langmuir isotherm, B: Freundlich isotherm, C: D-R isotherm, D: Elovich isotherm)	115
3.17 A-D	Zinc adsorption parameters (A: Langmuir isotherm, B: Freundlich isotherm, C: D-R isotherm, D: Elovich isotherm)	116
3.18 A-C	A) Pseudo Second order, B) Pseudo first order and C) Weber Morris diffusion plots.	118
3.19	Van't Hoff plot depicting $\ln K$ Vs. $1/T$.	120
3.20	A) Concentration of HCl against % desorption B) Regeneration efficiency of adsorbent	123
3.21	Effect of sample volume on metal adsorption	124

4.1	Structure of sodium alginate.	128
4.2 A-D	FTIR analysis of the adsorbent (<i>Halomonas BVR 1</i> immobilized in sodium alginate) before and after metal adsorption.	133
4.3 A-D	SEM image of the immobilized adsorbent (<i>Halomonas BVR 1</i> immobilized in sodium alginate) before and after metal adsorption.	134
4.4 A-C	EDAX of the adsorbent (<i>Halomonas BVR 1</i> immobilized in sodium alginate) before and after metal adsorption.	135
4.5	Effect of pH on metal removal.	136
4.6	Adsorption isotherms A) Langmuir isotherm, B) Freundlich isotherm, C) Elovich isotherm and D) DR isotherm for heavy metals lead, cadmium and zinc.	138
4.7	Kinetic plots A) Pseudo first order B) Pseudo second order C) Intraparticle diffusion and D) Van't Hoff's plots depicting $\ln K$ Vs. $1/T$ for heavy metals Lead, Cadmium and Zinc.	142
4.8	Depiction of the adsorbent used for column packing.	147
4.9	Schematic representation of the experiments carried out for modeling studies.	148
4.10	Breakthrough curves for 20, 30, 40 and 50 mg L ⁻¹ of lead at 2.3 mL min ⁻¹ .	150
4.11	Breakthrough curves for 20, 30, 40 and 50 mg L ⁻¹ of lead at 15 mL min ⁻¹ .	151
4.12	Breakthrough curves for 20 mg L ⁻¹ concentration of Pb(NO ₃) ₂ in 100 mL MilliQ water at the maximum flow rate 15 mL min ⁻¹ . Eight runs performed with a total of 800mL treated for 1hr 45mins.	151
4.13	Breakthrough curves for 20 mg L ⁻¹ concentration of Pb(NO ₃) ₂ in 250 mL MilliQ water at the maximum flow rate 15 mL min ⁻¹ . Four runs performed with a total of 800 mL treated for 1 hr 45 mins.	152
4.14	Dithizone test for the <i>Halomonas BVR 1</i> immobilized sodium alginate beads before and after adsorption.	153
4.15	Comparison of experimental data and generated breakthrough curves using Linear Model for 20, 30, 40 and 50 mg L ⁻¹ of Pb(NO ₃) ₂ in 100 mL in MilliQ water at the least flow rate of 2.3 mL min ⁻¹ .	161
4.16	Comparison of experimental data and generated breakthrough curves using Langmuir Model for 20, 30, 40 and 50 mg L ⁻¹ of Pb(NO ₃) ₂ in 100 mL in Milli Q water at the least flow rate of 2.3 mL min ⁻¹ .	162
4.17	Comparison of experimental data and generated breakthrough curves using Freundlich Model for 20, 30, 40 and 50 mg L ⁻¹ of Pb(NO ₃) ₂ in 100 mL in MilliQ water at the least flow rate of 2.3 mL min ⁻¹ .	163
5.1	Growth curve of <i>Halomonas BVR 1</i> in the presence and absence of metal.	174
5.2	Extracellular concentration of metal in growth medium.	175

5.3	Membrane damage assay of the cells in the presence of metal.	176
5.4	Respiratory activity of the cells in the presence of the metal.	180
5.5	Polyamine content in the control and metal treated cells as determined through fluorescence.	182
5.6A-C	Mass data of the polyamines over a period of time.	183
5.7	FTIR analysis of the polyamines from control and metal treated bacterial cells.	184
5.8	SDS gel analysis of the varying proteome expression profiles of the control bacteria and under stress.	185
5.9	Plasmids isolated from various strains	190
5.10	Restriction digestion of the isolated plasmid from <i>Halomonas BVR 1</i>	191
5.11	Transformed bacterial growth in the presence of heavy metal.	192
5.12	Metal evaluation of test, transformed and wild strain	193

List of Tables

Table No.	Caption	Page No.
1.1	Various microorganisms used for metal removal.	15
1.2	Functional groups on bacterial cell wall for binding metal.	17
2.1	Chemical characterization of the effluents.	30
2.2	Heavy metal analysis of the effluents.	31
2.3	Details of the biochemical tests.	37
2.4	Biochemical and morphological characteristics of the isolated strains.	40
2.5	Carbohydrate utilization pattern by the isolated strains.	40
2.6	Primers for amplification of 16 S r -DNA.	46
2.7	List of the strains isolated.	49
2.8	Isotherm parameters obtained from chosen models.	71
2.9	Kinetic and intraparticle rate constant data for the adsorption of metal ions.	76
2.10	Thermodynamic data for the adsorption of metal ions.	78
2.11	Effect of diverse ions on the adsorption of metal ions.	79
2.12	Adsorption capacity comparison against various bacterial and fungal strains.	80
3.1	Isotherm parameters obtained from various models for microbe immobilized chitosan as biosorbent.	95
3.2	Kinetic and Intraparticle rate constant data for the adsorption of metal ions.	99
3.3	Thermodynamic data for the adsorption of metal ions.	101
3.4	Effect of diverse ions on the adsorption of metal ions.	102
3.5	Comparison of the maximum adsorption capacities of the other	103

	adsorbents.	
3.6	Adsorption parameters calculated from their respective models for microbe immobilized graphene oxide adsorbent.	117
3.7	Kinetic parameters for the adsorption of metal ions.	119
3.8	Thermodynamic data for the adsorption of metal ions.	120
3.9	Effect of various ions on the removal of lead, cadmium and zinc.	122
3.10	Comparison of the maximum adsorption capacities of the other adsorbents.	125
4.1	Isotherm parameters obtained through various models using microbe immobilized sodium alginate adsorbent.	139
4.2	Kinetics and Intraparticle rate constant data for the adsorption of metal ions.	140
4.3	Thermodynamic data for the adsorption of the metal ions.	143
4.4	Effect of interfering ions metal adsorption.	144
4.5	Recovery of lead with various eluents.	145
4.6	Comparison of the adsorption capacities with other similar adsorbents.	146
4.7	List of parameters considered to obtain the numerical model.	159

CHAPTER I

INTRODUCTION

INTRODUCTION

Rapid industrialization, changing consumerist life style and industrial pollution in recent years increased significantly with an increase in the consumer demand and anthropogenic activities [Klaus et al, 2005]. This outcome results in a huge generation of unwanted, toxic and hazardous substances/chemicals. These substances tend to get leached into landfills, contaminate surface waters, thus contributing to environmental pollution.

Environmental pollutants

The major pollutants in air include sulfur oxides, carbon monoxide, nitrogen oxides, volatile particulate matter and organic compounds [Sharma et al, 2013]. They result in various environmental effects such as acid rains, smog, eutrophication, ozone depletion and global climate change. The associated health effects mainly include respiratory illness, pulmonary and neurological disorders.

All these contaminants fall under the category of either hazardous waste or non-hazardous wastes (**Fig.1.1**). The details listed by EPA for these wastes are as follows:

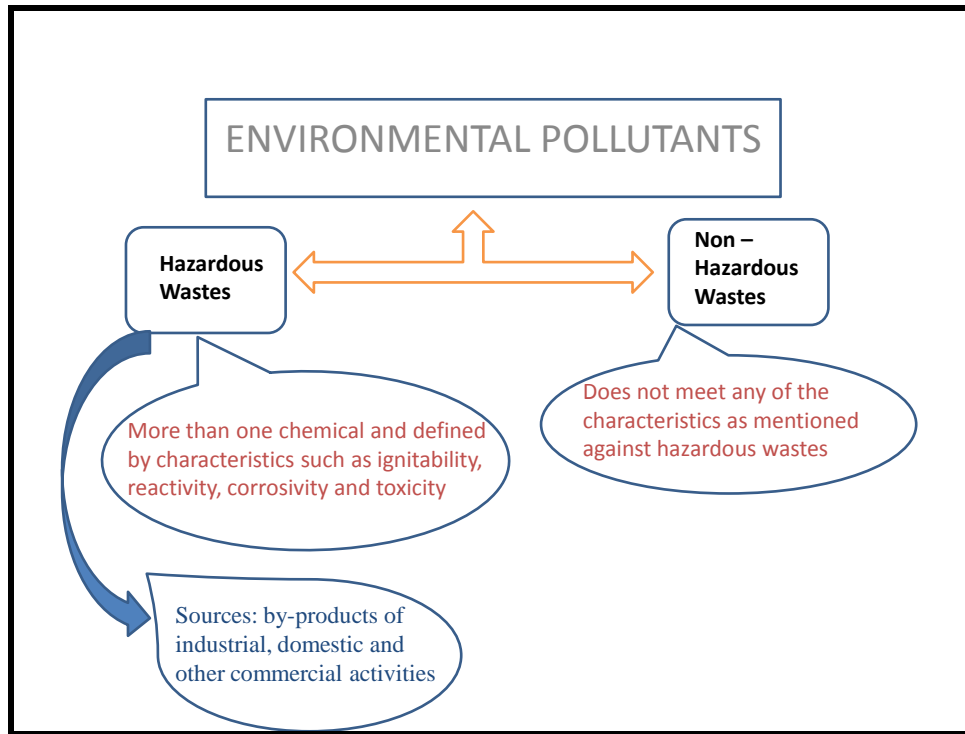


Fig 1.1: Schematic representation of the environmental pollutants as per EPA guidelines. (EPA September 2005).

Among the various types of pollutions caused due to these pollutants, environmental metal pollution from natural as well as anthropogenic sources and minerals is rapidly increasing [Oancea et al, 2003]. Heavy metals are grouped under the category of hazardous waste and thus their disposal needs to be addressed.

Heavy metal and their hazardous health effects

Pollution of the environment due to heavy metals is a worldwide problem as these metals cannot be destroyed and some of them have toxic effects on living organisms, when present beyond desired levels. [Mmolawa et al, 2011]. The term 'heavy metal' refers to any metallic element that has a density between 3.5 g/cm^3 to above 7g/cm^3 . It is toxic or poisonous even at low concentrations [Duruibe et al, 2007]. Heavy metals include cadmium (Cd), lead (Pb), zinc (Zn), silver (Ag), mercury

(Hg), arsenic (As), copper (Cu), iron (Fe), chromium (Cr) and platinum (Pt) group elements. Heavy metals can be emitted into the environment by both anthropogenic and natural factors, which include forest fires, volcanic activity, dust particles, coal powder stations, automobile exhausts etc. Among these heavy metals, WHO has classified lead, cadmium, mercury and Arsenic to be extremely hazardous and are extensively studied for their effects on human health. [Morrow et al, 2010].

Cadmium

Cadmium occurs naturally in ores together with copper, lead and zinc [Dinis et al, 2011]. Sources that release cadmium, include industrial emissions and application of fertilizer, sewage sludge to farm land, that leads to contamination of soils. This eventually increases cadmium uptake by crops grown for human consumption [Muhammad et al, 2012]. The uptake process of soil cadmium by plants is enhanced at low pH 4 [Veeraiah et al, 2013]. Metallic cadmium has mostly been used as an anticorrosion agent, a principle called as cadmiation [Gairola et al, 1991]. Cigarette smoking is a major source of cadmium exposure. Inhalation of cadmium fumes or particles can be life threatening, and leads to acute pulmonary effects. Although deaths are uncommon, periodic cases still occur [Nriagu, 1979]. Animal experiments have also suggested that cadmium may be a risk factor for cardiovascular diseases. The IARC has classified cadmium as a human carcinogen (group I) on the basis of sufficient evidence in both humans and experimental animals [Huff et al, 2007].

Mercury

A major use of mercury is as an electrode in the chlor alkali industry in the electrochemical process of manufacturing chlorine. [Handbook of chlor alkali technology Volume I]. Metallic mercury is also used in thermometers, barometers and instruments for measuring blood pressure. Methyl mercury poisoning has a prolonged latency and the main symptoms relate to nervous system damage

[Bernard, 1984]. A high dietary intake of mercury from consumption of fish has been hypothesized to increase the risk of coronary heart disease [Yoshizawa et al, 2002].

Lead

The general population is exposed to lead from air and food in roughly equal proportion. During the last century, lead emissions have further polluted our ambient air environment, with over 50% of lead emissions originating from petrol [Tong et al, 2000]. Occupational exposure to inorganic lead occurs in mines and smelters as well as welding of lead painted metal, and in battery plants. Up to 50% of inhaled inorganic lead may be absorbed in the lungs [Mohajer et al, 2013].

Adults take up 10–15% of lead in food and about 50% gets adsorbed via the gastrointestinal tract in children. In adults, inorganic lead does not penetrate the blood–brain barrier, whereas in children, this barrier is less developed and leads to its easy penetration. The symptoms of acute lead poisoning include abdominal pain, headache, irritability and various symptoms related to the nervous system. Recent research has shown that long-term low-level lead exposure in children may also lead to decreased intellectual capacity [Ruiz et al, 2008].

Electronic waste / e waste: a major source of heavy metals

One of the major source of all these heavy metals is the electronic industry. Rapid economic growth, coupled with urbanization and a growing demand for consumer goods, has increased both the production and consumption of the electronic waste [Pinto, 2008]. The Indian Information Technology (IT) industry has contributed significantly to the digital revolution being experienced by the world and has been one of the major drivers responsible for the change in economy in the last decade. Electronic gadgets and appliances have infiltrated every aspect of our daily lives, providing our society with easy

information acquisition and exchange. Various industries in the electronic sector (Fig. 1.2) investigated by Greenpeace International that contribute of heavy metal pollution through their effluents were the manufacturing units of printed wiring boards (PWBs), semiconductor chip manufacturing, and component assembly

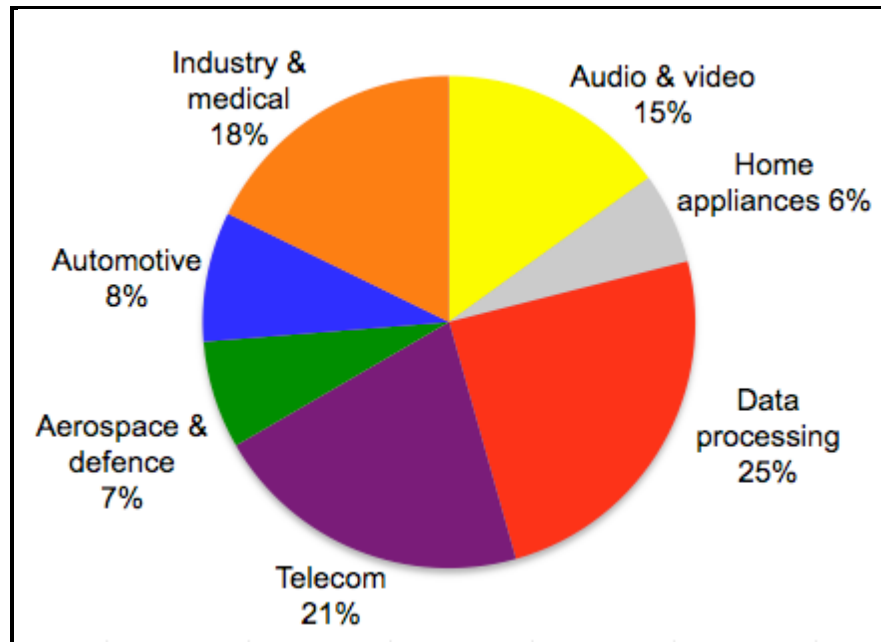


Figure 1.2: Percentage contribution of various electronic sectors.

Composition of electronic goods is very diverse and broadly consists of ferrous and non-ferrous metals. Iron and steel constitutes about 50% of e-goods while non-ferrous metals constitute about 13%. Non-ferrous metals include aluminum, copper and other precious metals [Pinto, 2008].

The same frienzied technology of electronic production that is considered as a key source for future modern societal development, it does not have so-modern downside to it i.e the electronic waste

(e-waste). This knowledge electronic society is simultaneously creating its own toxic footprints [Oteng-Ababio, 2012]. The fate and effects of the hazardous chemicals and substances generated during the manufacture of these products have been very poorly documented.

E-waste broadly covers waste from all electronic and electrical appliances that comprises of items such as mobile phones, refrigerators, computers, televisions (TVs), digital music recorders/players, washing machines and many other household consumer items (Guidelines for environmentally sound management of e-waste) .

The increasing ‘market penetration’ in the developing countries, ‘replacement market’ in the developed countries and ‘high obsolescence rate’ make e-waste one of the fastest growing waste streams [Kurniawan et al, 2006]. This new kind of waste is posing a serious challenge in disposal and recycling to both developed and developing countries. Though India has some of the world's most advanced high-tech software and hardware developing facilities, its recycling sector is in the nascent stage. The hazardous waste management has now been complicated with the dumping of e-waste ('green passport' according to Gutierrez), particularly computer waste, into India from developed countries [Pinto, 2008]. This has made e-waste management an issue of environment and health concern.

Even though India is trying to devise various environmental friendly ways to dispose e-waste, the spectre of this waste destroying the nation’s ecological health is alarming. According to a report named “E-waste in India” by Rajya Sabha Secretariat, E-waste from old computers would jump by 400 per cent in China and by 500 per cent in India by 2020. Such predictions highlight the urgent need to address all the problems related to e-waste (recycling or treatment of the e-waste effluents) in developing countries like India which is a dumping ground for e-waste. Furthermore, the collection

and management of E-waste and the recycling process is yet to be properly regulated. Considering the growth rate, the volume of e-waste is estimated to reach nearly 2 million Metric Tonnes by 2025. This figure shows that e-waste is a serious matter of concern for countries like India (Economic Times news bulletin, Jun 03, 2016).

In our study, one such e- waste stream i.e; electronic industry effluent has been considered as a source for the isolation of heavy metal resistant organisms.

Over view of the metal remediation processes

Heavy metals released from these electronic industrial effluents and e-waste recycling units can be treated by various methods. Chemical methods include chemical oxidation or reduction or formation of an insoluble gas, chemical precipitation [Barakat et al, 2011]. Also, it includes, other processes like ion exchange, solvent extraction and electrolytic recovery. Physico-chemical precipitation include ferrite treatment, carbonate precipitation and sulfide precipitation. These processes results in the formation of insoluble metal oxide salt sludge. The various disadvantages associated with these methods involves high chemical requirement, and sludge generation [EPA guidelines, Office of air and radiation, 2010]. Solvent extraction utilizes membrane systems for the removal of heavy metals. The end product is in the form of concentrated metals ions present in solvent stream [Quintelas et al, 2008]. Ion exchange involves an adsorption based phenomenon in which the metal ions bind on the immobilized solid support of the column. Electrolytic recovery gives us a solid metal at the end of the process. However, Intensive energy is needed to bring about this process. All these proposed methods of metal removal are inefficient owing to some of the reasons such as high capital input [Gakwisiri et al, 2012], reduced efficiency at dilute concentrations of the metal solutions, generation of hazardous by-products or inefficiency when the concentration of the pollutant is below

100mg l⁻¹ [Gavilescu, 2004; Wang and Chen 2009]. This necessitates cost effective and environmental benign techniques for their removal.

Alternate green methodology

Biological methods solve these drawbacks since they do not produce secondary pollutants and sludge, are easy to operate and show higher efficiency at low metal concentrations [Chen et al. 2005]. One of the viable environmental friendly option proposed to remediate heavy metals are microorganisms. Microbes found in heavy metal rich habitats have developed resistance mechanisms to tolerate high concentrations of heavy metals by efflux, complexation and transformation to a less toxic state or as terminal electron acceptor as in case of anaerobic respiration [Gadd, 1990].

Mechanism of metal tolerance in microbes

Bacteria have a high surface to volume ratio and provide a large contact area for interactions with the surrounding environment [Brandl et al, 2001]. The net negative charge of the cell envelope make these organisms prone to accumulate metal cations from the environment [Silvahy et al, 2010]. This accumulation is linked to the concentration and the speciation of the metal which also determines whether the metal is useful or harmful to the bacterial cell. Homoeostasis is therefore essential and bacteria have developed a fine-tuned regulatory system of incorporation and excretion of the metal. Some of the mechanisms that protect the bacterial cells against heavy metal stress have been briefed here (**Fig 1.3**):

Redoxolysis: Metals are microbially oxidized or reduced during oxidation-reduction processes. As result, metal mobility is decreased depending on the type of metal and its oxidation state [Weber et al, 2010].

Acidolysis: The mechanism is also called proton-induced metal solubilization. Protons released from microorganisms results in changes of the metal mobility. These protons are bound to the surface and aids in replacement of metal ions from the aqueous solutions.

Complexolysis: The mechanism is also termed ligand-induced metal solubilization. Microbial formation of complexing or chelating agents leads to an increase of metal mobility. Metal complexes are formed on microbial surfaces by ligand exchange and polarization of critical bonds thus facilitating the detachment of metals species from the surface.

Mobilization: Mobilization occurs through alkylation of Alkyl groups on the bacterial surface that is enzymatically transferred to the metal ions. The process is often described as “metal volatilization”, because alkylated metals show an enhanced volatility as compared to their elemental or ionic forms. One of the best known alkylation process is methylation.

Immobilization and precipitation: Soluble metal species are immobilized (precipitated) by microbially formed complexing agents, e.g., sulfide. Metal sulfides show very low solubility such that metals are efficiently precipitated even at low sulfide concentrations. Additionally, the bacterial activities can result in a reduction of the acidity in an environment leading to the precipitation of metals as hydroxides [Gadd et al, 2001].

Few molecular mechanisms of cell that involves the intracellular synthesis of biological molecules/ proteins for increased metal tolerance includes:

Polyamines: Polyamines are considered to be simple primordial stress molecules that are produced in response to stress. Physiological polyamines putrescine, spermidine and spermine are ubiquitous polycationic molecules that are endogenously synthesized in all organisms. Polyamines are also known to regulate biochemical activities of DNA, RNA and proteins apart from their role in helping bacteria to combat heavy metal stress by sequestering the toxic metal ions. Polyamines are known to

scavenge the Reactive Oxygen Species (ROS) generated in response to heavy metal stress and protect the cell from damage [Rhee et al, 2007].

Metallothioneins: These are one among the major proteins that play a central role in heavy metal metabolism. Metallothioneins (MTs) are low molecular (6-7 KDa) cysteine-rich protein residues that are divided into different classes based on the amount of cysteine content and structure. MTs lack histidine and any other aromatic amino acid. The mammalian Mts have two distinct domains that can accommodate about seven divalent metal ions and twelve monovalent metal ions [Cong et al, 2012]. The only difference between the mammalian metallothionein and the MTs present in cyanobacteria, yeast and a few higher plants is the distribution pattern of the cysteine residues. Heavy metals including mercury (Hg), zinc (Zn), gold (Au), copper (Cu), silver (Ag), cobalt (Co), Cadmium (Cd), nickel (Ni) and bismuth (Bi) regulate the Mts synthesis at the transcriptional level [Singh et al, 2011].

Phytochelatins: The members of the third class of Mts are considered to be phytochelatins (PCs). It has been reviewed that PCs are used for metal complexation in plants. The biosynthesis of PCs is also induced by certain metals [Maitani et al, 1996].

Expression of metal binding peptides: Metal binding peptides offers great advantage in metal remediation due to the fact that they enhance the metal specificity and selectivity. These metal peptides are either designed *de-novo* or selected by screening peptide libraries. Apart from the cysteine rich metallothionein protein molecules, histidine which are known to have more affinity towards the transition metal ions, peptides comprising of a combination of cysteine and histidine are being exploited for metal remediation. Cadmium (Cd^{2+}) and Mercury (Hg^{2+}) binding was enhanced by the expression of a fusion protein involving a maltose-binding protein in *E. coli* and a repetitive cysteine rich metal-binding motif (CGCCG). Expression of this fused protein lead to a tenfold increase in the metal

binding [Mejare et al, 2001]. A schematic representation of the tolerance mechanisms discussed has been given below:

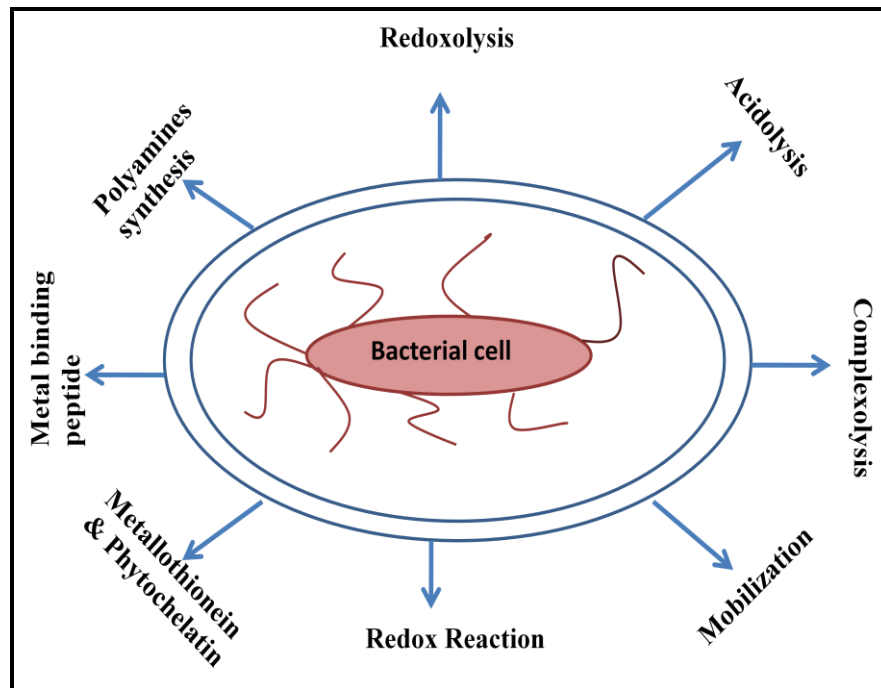


Figure 1.3: Schematic representation of protective mechanisms of bacteria under metal stress.

Some of these mechanisms are of biotechnological importance owing to their metal removal and recovery capacity from industrial effluents. Thus heavy-metal-resistant microorganisms suggest their plausible role in heavy metal remediation

Bioremediation, is therefore a viable, eco-friendly and cost effective option that utilizes the microbial cells or their metabolites for pollution abatement. This is a feasible method to accelerate the process of decay and remove metals by encouraging the microbial and associated biota within the contaminated site to degrade, accumulate and/or remove the pollutants from the identified site. It is a cost effective technology and is aptly called as insitu bioremediation [Atlas and Unterman,1999]. Bioremediation has been labeled by many researchers as a technology, employed in the removal of hydrocarbons, oil-based pollutants and many heavy metals [Atlas and Untermann, 1999, Sabate et al,

2004, Jain et al 2011]. These days researches have focused upon the intrinsic bioremediation which relies on degradative capacity of indigenous microorganisms, micro flora, isolated from contaminated sites, to remove metals, without having to employ any additional treatment [Jain et al, 2005].

Heavy metal resistant microorganism for use as a biosorbent

Selection of a novel organism for its use as an effective bioadsorbent would require a detailed characterization of the microbial communities from various heavy metal rich habitats. There has been numerous reports on the microbial characterization of various industrial effluents. However, reports on microbes inhabiting a electronic industrial effluent is not available till date. Screening of microbial communities involves isolation and characterization of indigenous microorganisms that are a resident of these effluents. Detailed identification and characterization of microorganisms can broadly be classified into morphological, biochemical and molecular procedures [Spiegelman et al, 2005].

Morphological methods are relatively easy to be performed and is rapidly done. They rely on growth and microscopic examination that give a general characteristic to the morphology of an organism.

Molecular biology based methods involve diverse range of techniques that involve microbial DNA. This analysis involves a culture independent method which does not require the growth of microorganisms nor the analysis of any secondary metabolite. This eliminates the time required for the growth of the microorganism and any bias associated with the growth. **Biochemical methods**

involves more varied set of recent technologies. These involve gas chromatography and mass spectroscopy experiments that separate a mixture of compounds and identify a range of biomolecules.

Fatty Acid methyl Ester (FAME) analysis is a kind of lipid analyses that identify the lipid profile pattern specific to the organism. Similar to the molecular biology methods, biochemical methods is a culture independent technique.

Literature reports have suggested that there has been extensive research for the heavy metal removal using microbes. Several organisms are still being tested to remove heavy metals from industrial wastes with higher adsorption capacity. **Table 1.1** summarizes few of the important results of metal biosorption using bacterial strains [Ahluwalia and Goyal, 2007; Vijayaraghavan and Yun, 2008].

Table 1.1: Microorganisms used for metal removal.

Heavy metal	Organism	Adsorption capacity (mg g⁻¹)
Ni	<i>Ascophyllum nodosum</i>	2.316
Pb	<i>Ascophyllum nodosum</i>	2.307
Cd	<i>Chaetomorpha linum</i>	0.48
Ni	<i>Chlorella miniata</i>	0.237
Cu	<i>Aspergillus niger</i> pretreated with NaOH	25.5
Pb	<i>Aspergillus niger</i> pretreated with NaOH	32.6
Pb	<i>Corynebacterium glutamicum</i>	567.7
Pd	<i>Desulfovibrio desulfuricans</i>	128.2
Cd	<i>Staphylococcus xylosus</i>	250.0
Pd	<i>Pseudomonas aeruginosa</i> PU21	0.7
Pd	<i>Streptomyces noursei</i>	1.6
Pd	<i>Penicillium</i> sp.	5.0
Pd	<i>Aspergillus niger</i> (live)	2.25
Pd	<i>Mucor rouxii</i> (Na ₂ CO ₃ pretreated)	3.26
Cd	<i>Pseudomonas putida</i>	8.0
Cd	Free cell suspended in solution Lab culture	14.3–20.0
Cd	Immobilized cells on sepiolite	10.9
Cd	<i>Penicillium digitatum</i>	3.5
Cd	<i>Penicillium notatum</i>	5.0
Cd	<i>Aspergillus niger</i>	1.31

The complex structure of the microorganisms implicit that there are many ways by which the microorganism can adsorb/absorb metal ions from the surrounding environment that aids in the biosorption of heavy metals.

Heavy metal resistant microorganisms and their mechanism for heavy metal removal.

The heavy resistant organisms chosen as a biosorbent, remove heavy metals by one of the following mechanisms:

Intracellular accumulation

Microbes potentially accumulate metals either by a metabolism dependent, active process or a metabolism-independent, passive process. Thus, overall accumulation is determined by sorptivity of the cell envelope and capacity for intracellular movement of metals into the cytosol. Passive adsorption is likely to be the dominant mechanism in metal accumulation since it does not require continuous supply of nutrients for growth of organisms. Active uptake into the cytosol is usually slower than passive adsorption and is dependent on element-specific transport systems [Haferburg et al, 2007]. This occurs rarely as it requires energy and is usually associated with the viable cells. Additionally, microbes lack highly specific uptake systems for most metals.

Metal sorption

The surface characteristics of bacteria determine their metal-adsorption properties. The differences in cell wall construction of Gram-positive and Gram-negative bacteria influence the sorption behaviour of different metals [Johnson et al, 2004]. Metal sorption can be more or less selective, depending on the organisms used and environmental conditions (e.g., pH, salinity) [Haferburg et al, 2007]. The presence of many functional groups acts as binding site for the formation of heavy metal crystals. These groups include hydroxyl, sulfhydryl, carboxyl, carbonyl, thioether,

amine, sulfonate, imine, amide, imidazole, phosphonate, and phosphodiester groups (**Table 1.2**). The bulk functional group chemistry of both classes of bacterial surfaces is similar, but particular single constituents of the cell envelope can have great importance for metal binding. For example, phosphoryl groups of lipopolysaccharides, carboxylic groups of teichoic and teichuronic acids, or capsule forming extracellular polymers influence the metal sorption of the cell envelope [Chen et al, 2015].

Table 1.2 : Functional groups on bacterial cell wall for metal binding.

Formula of Functional Group	Name	Formula of Functional Group	Name
$R^* - O - H$	Hydroxyl	$R - S - H$	Sulhydryl
$R - C \begin{matrix} \nearrow O \\ \searrow OH \end{matrix}$	Carboxyl	$R - C \begin{matrix} \nearrow O \\ \searrow H \end{matrix}$	Carbonyl
$R - C \begin{matrix} H \\ NH_2 \\ H \end{matrix}$	Amino	$R - C \begin{matrix} O \\ C - \\ \end{matrix}$	Carbonyl
$R - C \begin{matrix} \nearrow O \\ \searrow O - R \end{matrix}$	Ester	$R - O - P \begin{matrix} O \\ OH \\ OH \end{matrix}$	Phosphate

Metal Immobilization

The exopolymers or biopolymers produced by the bacteria as cell defence mechanism helps in immobilization of the toxic heavy metals and prevents them from entering the cell (Meenakshi et al, 2004). Thus, this is also a surface phenomenon of metal removal.

Precipitation

Precipitation process may or may not be dependent on the cells metabolism. It is independent of the cells metabolism, in case of a chemical interaction between ligands and functional group on the bacterial cell wall [Silvahy et al, 2010].

All these processes are exploited commercially for effective bioremediation of heavy metals effectively and is schematically represented below (**Fig. 1.4**).

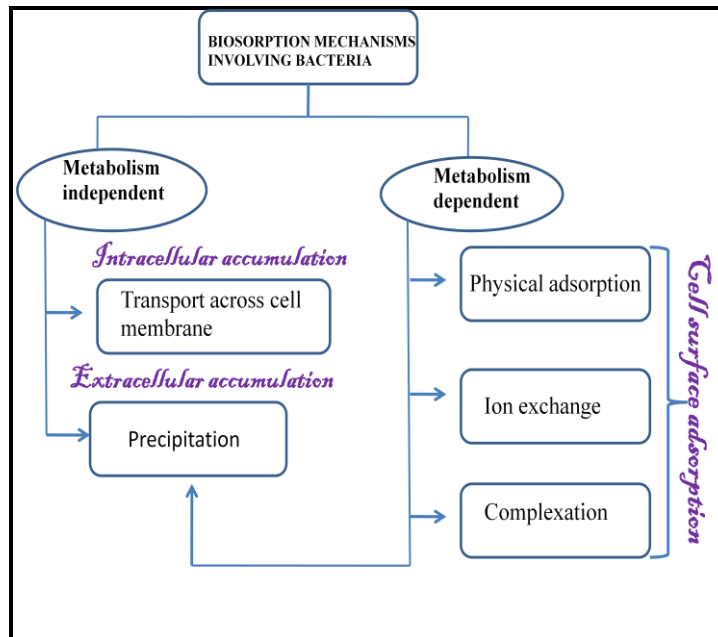


Figure 1.4: Metal microbe interaction.

Microbial masses cannot be used independently for a continuous scale up operation owing to their low density, small particle size, less rigidity, and poor mechanical strength. It may result in the inability to regenerate/reuse, biomass swelling, solid–liquid separation problems and development of high pressure drop in the column mode in real application [Mahamadi et al, 2014]. Increased hydrostatic pressures generated to develop suitable flow rates in a fixed or expanded bed reactor might cause disintegration of free biomass. All these problems can be avoided by the use of immobilized cell systems. Hence, immobilization of these microbial masses on suitable solid support matrices ought to be carried out to overcome these limitations. Microbial immobilization involves confinement of microbial cells in a three dimensional mode in the lattice. This allows free diffusion of the metal ions in and out of the lattice and ensures effective removal of metal ions from the aqueous solutions [Haynes et al, 2010]. Thus, the enhancement of metal removal by immobilization has been sought for owing to its long term operation capability and also the simplified treatment of effluents to larger volumes by column studies [Gupta et al, 2016].

Enhanced metal removal

Immobilization in biopolymers

Use of biopolymers for immobilization and subsequent remediation of heavy metals is a promising technology [Jan Koshtal et al, 2005]. Support matrices suitable for biomass immobilization include alginate, polyacrylamide, polyvinyl alcohol, polysulfone, silica gel, cellulose, chitosan, glutaraldehyde graphene oxide etc [Zang et al, 2002, Vijayaraghavan and Yun, 2008]. The immobilization of the microbial biomass in solid structures would create a biosorbent material with the right size, mechanical strength, rigidity and porosity necessary for use in practical processes. The immobilized materials can be used in a manner similar to ion exchange resins, enabling ease of metal

removal, efficient adsorption–desorption cycles (recovery of the adsorbed metal, reactivated and re-use of the biomass) [Veglio and Beolchini, 1997].

Various combinations of microbes immobilized polymeric matrices are still being explored that can be used in practical biosorption [Veglio and Beolchini, 1997] to enhance metal remediation. Our contribution adds few more novel adsorbents to this existing pool of immobilized biosorbents.

Apart from immobilization, enhancement of metal adsorption can also be achieved by the process of genetic engineering.

Genetic engineering

Non genetically engineered biomass usually lack specificity in metal binding, which may cause difficulties in the recovery and recycling of the desired metal(s). Several genetic approaches have been developed to improve or redesign microorganisms, where biological metal-sequestering systems will have greater resistance to environmental conditions, higher intrinsic capability as well as specificity to metal ions [Bae et al, 2000; Majare & Bulow, 2001]. Many bacterial strains contain genetic determinants of resistance to heavy metals on plasmids, transposons or can be chromosomal mediated. The resistant determinant can hence be transferred to any non tolerant bacteria, thus increasing the threshold of metal tolerance. The potential to alter the metabolic functions is also advantageous, as they tend to adsorb, accumulate and sequester more number of metal ions.

Naturally occurring bacteria cannot specifically take up a single heavy metal. Genetic engineering alters such an bacteria with the desired traits, thus increasing its specificity [Sauge-Merle et al, 2003].

The use of recombinant bacteria to remove specific metals from contaminated water is a promising area of research. A genetically engineered *E.coli*, which expresses the Hg²⁺ transport system and metallothionein (a metal binding protein), was able to selectively accumulate 8 μmole

Hg²⁺/g cell dry weight [Perpetuo et al, 2011]. The presence of the chelating agents Na⁺, Mg²⁺ and Ca²⁺ did not affect its bioaccumulation. Krishnamurthy and Wilson constructed an *E. coli* strain by introducing a gene nix A (coding for nickel transport system) that expressed a glutathione S-transferase metallothionein fusion protein. This recombinant strain was able to accumulate four times more nickel than the control strains. Metal resistant *R. Eutropha* isolate engineered to produce a metallothionein accumulated more cadmium than its wild type counterpart [Valls et al, 2000]. This thesis focuses on one such genetic approach of increasing the threshold of metal tolerance in non resistant strains by transferring the plasmid, harbouring the genetic determinant for heavy metal resistance.

Another important aspect that was considered in the present work is, understanding the physiology of the bacterial cell under metal stress. Environmental stress has a significant negative impact on the growth of bacteria. Irrespective of their habitat, bacteria are constantly exposed to a variety of environmental stresses such as salinity, heat, metal stress etc. and they have evolved numerous mechanisms to combat stress [Sharma et al, 2006]. Sensing and responding correctly to these stresses is crucial for the survival of all bacteria [Moat et al, 2000]. Stress in bacteria leads to increased metabolite production due to changes in physiological processes contributing to their protective mechanisms [Ramakrishna et al, 2011]. These stress related adaptive and protective responses include, alteration of gene expression patterns such as changes in the control of transcription, translation, stability of transcripts and proteins etc [Ron et al, 2013]. Accumulation of diverse range of metabolites involving amino acids and amines is commonly seen in response to exposure to heavy metals. This indicates that fluctuations in nitrogen metabolism is central to the heavy metal response [Sharma et al, 2006; Chen et al, 2011]. Among these metabolites, the major players are polyamines (PA), which are ubiquitous polycationic aliphatic amines present in all living

organisms. The three major PA's include putrescine, spermidine and spermine [Pang et al, 2007]. This thesis focusses on this three centered interaction between the polyamines, heavy metal and bacteria.

Gaps in the existing research

1. There is no report on the microbial characterisation of the effluents from electronic industries.
2. Non- availability of the identified microbes which can remove heavy metals from electronic industrial effluents.
3. Improvise on the existing methods of e-waste bioremediation.
4. Specific role of polyamines in a metal stressed bacteria.

Scope and objective of the work

The research work presented in this thesis represents the microbial diversity of the electronic industry effluent and its use for bioremediation of metal cations. The overall objective has been represented below (**Fig. 1.5**).

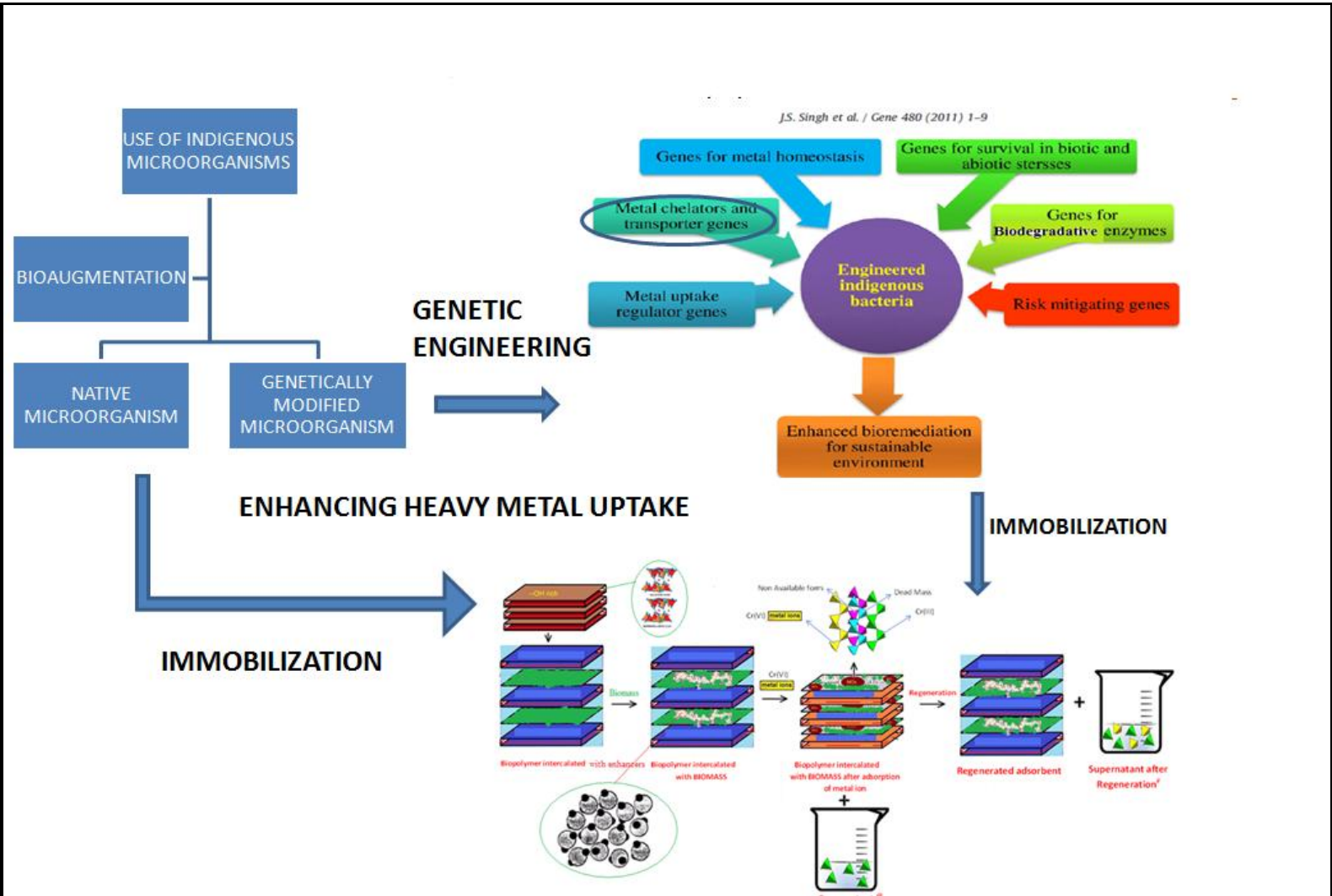


Figure 1.5: Overview of the remediation of heavy metals.

The above brief review on the current status of the electronic waste and their hazards, shows us that there is an urge to overcome the deficiency of the existing methods of metal removal. Since, each methodology differs with respect to selectivity, their actual use in practice depends on the particular analytical problem. A careful introspection reveals that there is a compelling need to look for more effective strategies. Keeping these aspects in mind, and other factors such as biosorbent availability, cost effectiveness, greener solvents, etc efforts were directed towards the development of novel

microbial biosorbents that could remediate heavy metals such as lead, zinc, cadmium etc. thus solving the existing problems of bioremediation strategies.

Detailed microbial characterization of the electronic industry effluents to explore novel heavy metal resistant microbes for their use as biosorbent was carried out. Various physicochemical and spectroscopic techniques were applied for the characterization and analysis of the prepared adsorbent before and after the adsorption. The effect of various analytical parameters such as pH, concentration of metal ions, contact time, temperature *etc.* were studied in detail. Thermodynamics and kinetics of the adsorption processes were investigated in detail. The developed adsorbents were tested for the remediation of heavy metals from real industrial samples such as battery industry effluent. The greener aspects in the adsorption processes are illustrated through the regeneration of the metal ions from adsorbents in a facile manner.

The following are the **specific objectives** proposed for the study:

- To isolate and characterize the heavy metal resistant microorganisms in the effluents from electronic industry.
- Immobilization of the microbes on various biosorbents and testing for the best possible combination to remediate major cations in electronic industry effluents.
- Genetic transformation of microbes to enhance the property of metal remediation.
- To understand the role of polyamines in bacteria under heavy metal stress.
- To develop a new microbial package and detoxify heavy metals.

CHAPTER II

CHARACTERIZATION AND REMEDIATION OF HEAVY METALS IN ELECTRONIC INDUSTRY EFFLUENTS

Characterization and remediation of heavy metals in electronic industry effluents

Introduction

Microorganisms are ubiquitous and pioneer colonizers of the environment that symbolizes the richest repertoire of microbial and molecular diversity in nature. The available literature on the microbial communities represents only a tiny fraction of the natural diversity representing both natural and manmade ecosystems [Elshahed et al, 2012]. Out of the 300,000 to one million species of prokaryotes existing on earth, only 3,100 bacteria have been described in the Bergey's Manual of Systematic Bacteriology [Varadarajan et al, 2014]. Industrial effluents are one such ecological niche where diverse range of microbiota can be found. A detailed chemical and microbiological characterization of these effluents, would thus reveal the severity of metal pollution and the microbial community inhabiting the heavy metal rich effluents.

Ours is the first attempt, to characterize an electronic industry effluent with a view to map its microbial population. This would reveal the presence of any metal resistant microbe that can tolerate metals to a high concentration. Using this innate capability of the organism, microbial biosorbents can be developed that is universally applicable to remove heavy metals.

The increasing concern about environmental metal pollution, has stimulated active research in the field of remediation of heavy metals and significant advancement in the search for novel eco friendly adsorbents that can effectively remediate heavy metals is in progress [Alkorta et al, 2014; Bansode et al, 2003 Babel et al, 2003]. In this context, this part of the thesis focuses on microbial metal adsorption.

Some of the key factors that control and mediate the metal adsorption are

1. The type of functional groups acting as ligands for effective metal binding [Phoenix et al, 2002].
2. The type of the biosorbent (i.e. living /non-living) [Wang et al, 2009]
3. Characteristics of the metal solution (e.g. pH and the interfering ions) [Wang et al, 2009]

Microbes possess the ability to bind to metal ions present in the external environment, at their cell surface through the carboxyl, hydroxyl and amine functional groups [Crist et al, 1981]. The metal adsorption could involve a surface phenomenon through physisorption or an ion adsorption on the surface of dead or live bacteria. Alternatively, microorganisms could also accumulate these metals quite slowly according to their metabolic activity (metabolism dependent) [Gadd et al, 1990; Gadd et al, 1992; Umrana et al, 2006]. They develop resistance mechanisms to these toxic heavy metals and hence heavy metal resistant microorganisms have paved way to alleviate the problems of heavy metal contaminants in various effluents [Nourbakhsh et al, 2002]. Studies involving the use of various fungi and yeasts for the removal of toxic metals like lead and cadmium have been reported [Yoshida et al, 2006]. Kirkelund et al. [Kirkelund et al, 2012] recently reported the electro-dialytic removal of cadmium from biomass combustion fly ash. Reports also suggest the use of *Bacillus subtilis*, *Rhizopus arrhizus*, *Saccharomyces cerevisiae*, algae and various halophilic bacteria for the adsorption of heavy metals from industrial wastes [Wang et al, 2009]. All these studies illustrate that metals is known to bind to the microbial cell surface through various biosorption mechanisms [Amoozegar et al., 2012; Kimmek et al, 2001].

Biosorption involving microbial biomass, can be carried out using live or dead microbe. Practically, the use of dead biomass, is beneficial as it removes the constraint of hindrance to bacterial

growth upon exposure to high concentration of heavy metals. Moreover, use of a live microbe requires continuous supply of nutrients to promote its growth. This would result in a high cost input.

The pH of the aqueous solution is another important parameter that changes the affinity of the cationic and anionic functional groups on the biosorbent surface towards the metals ions [Barakat, M.A., 2011].

To sum up all, these microbial sorbents have been drawing constant attention due to their extraordinary ability to metabolize waste materials and thereby help in removal of the hazardous materials from the effluents. Furthermore, the concept of zero discharge, at a low cost is the major prerequisite for all the industries releasing effluents. Taking all the above facts into consideration, the study of microbial flora including bacteria, fungi and actinomycetes was deliberated upon in order to explore heavy metal resistant microbe that can be used as a wonder microbial biosorbent for the remediation of heavy metals.

Till date, there has been no report on the microbial characterization and the presence of microorganisms in the electronic industry effluents. This chapter, therefore, presents one of the few studies aimed at characterizing the effluents to determine the hazardous compounds and evaluate the microbial diversity prevalent in the effluent of a battery industry unit. It also elucidates the use of the microbial biomass for the removal of metals like zinc, cadmium and lead.

Chemical and microbiological characterization of the electronic industry effluent

This section deals with the chemical and microbiological characterization of the electronic industry effluent collected from an industry located close to Hyderabad. There are many industries that are located in and around Hyderabad namely ECIL (Electronic corporation of India Limited), HBL Power systems, IONICS Power systems, MNR industries etc where electronic industry effluents are available. The electronic industries generate large quantities of effluents rich in metals, phosphates, sulphates, acids etc [Barakat et al, 2011].

The approach adopted to do this part of the work helps in understanding chemical and microbiological characteristics of effluents and in identifying a resistant microbe for subsequent metal adsorption studies. The 'Materials & Methods' and Results obtained for each method have been presented together in the following sections for ease of understanding. The results have been independently discussed

Materials and Methods

Collection points and transport of effluents

Industrial effluents were collected from entry points of CETP (Common Effluent Treatment Plant) and Reverse Osmosis (RO) units in sterile sample collecting bottles and transported to our laboratory for further microbiological and chemical characterization of the effluents. Various parameters such as the pH, colour and odour were measured at the site of collection.

Chemical characterization of effluents.

Detailed characterisation of the effluents involving Biological Oxygen Demand (BOD), Chemical Oxygen Demand (COD), Dissolved Oxygen (DO), Chlorides, Sulphates and alkalinity were carried out in our laboratory at BITS Pilani Hyderabad Campus. The details are given in **Table 2.1**.

Table 2.1 Chemical characterisation of the effluents.

Name of the test	Materials and Methods	Reference	Result Obtained
Chemical Oxygen Demand (COD)	Determination of COD was done by adding 2.2 mL of COD solution A (Mercury (II) sulphate & sulphuric acid) and 1.8mL of COD solution B (Potassium dichromate & sulphuric acid) to 3 mL of effluent sample. The reaction was agitated and placed on a thermoreactor set at 140°C for 120 min After two hours of digestion of the sample, the reaction contents were used for spectrophotometric analysis	Guide manual waste water analysis by Central Pollution Control board	437.21 mg L⁻¹
Biological Oxygen Demand (BOD)	BOD test is to compute a difference between initial and final DO of the samples incubation. A standard protocol was followed for this measurement	Guide manual waste water analysis by Central Pollution Control board	27.39 mg L⁻¹
Alkalinity	Alkalinity of the effluent sample was calculated by titrating the sample with 0.02N H ₂ SO ₄ till the pink colour of the sample due to the addition of phenolphthalein indicator disappears. Subsequent to this 2-3 drops of methyl red indicator was also added and titrated with 0.02N H ₂ SO ₄ till the yellow colour changed to orange. The total alkalinity was calculated by the following formula: T-alkalinity, as mg CaCO ₃ /L = B x 1000/mL sample	Guide manual waste water analysis by Central Pollution Control board	1096 mg L⁻¹
Chloride	Chloride measurement was carried out by diluting the effluent sample in the ratio of 1:2.The pH was maintained at	Guide manual waste water	0.16 %

measurement	7-10. To this 1mL of K ₂ CrO ₄ indicator was added and the reaction mixture was titrated with 0.0141 N AgNO ₃ till yellowish solution turns red. The volume of AgNO ₃ consumed in the titration was noted for further calculations	analysis by Central Pollution Control board	
Total Dissolved Solids (TDS)	Procedure was carried out in the analytical lab of the industry from where the samples was collected.		49626 mg L⁻¹
Sulphate measurements	Procedure was carried out in the analytical lab of the industry from where the samples was collected.		3.28 g L⁻¹

Heavy metals in the effluents were measured using Atomic Absorption Spectrophotometer (AAS).

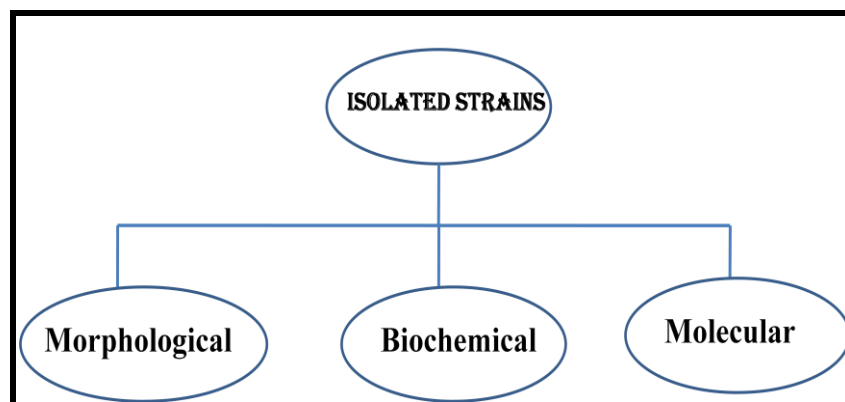
They were detected as given in **Table 2.2**.

Table 2.2: Heavy metal analysis of the effluents.

Characteristic	Value
pH	12.0
Temperature	35 ⁰ C
Zinc	4.0 mg L ⁻¹
Cadmium	1.0 mg L ⁻¹
Nickel	22.5 mg L ⁻¹
Aluminium	Nil
Chromium	Nil
Magnesium	5.5 mg L ⁻¹
Lead	2.5 mg L ⁻¹

Discussion: The effluents collected from the electronic industry, were found to be rich in heavy metals like zinc, cadmium, nickel and lead in the concentrations of 4.0 mg L^{-1} , 1 mg L^{-1} , 22.5 mg L^{-1} and 2.5 mg L^{-1} respectively (**Table 2.2**). However, the metals that are hazardous, majorly represent the electronic industry effluent and cause acute toxicity are lead, cadmium, zinc and mercury [Tchounwou et al, 2012]. Therefore, lead, cadmium and zinc were specifically chosen for the present study. Surprisingly, the concentrations of sulphates (207.9 gm/lit) and chlorides (3.54 gm/lit) was found to be reasonably high in comparison to the heavy metal concentrations. However, these values were within the limits of secondary Maximum Contaminant Levels (MCLs) as per the United States Environmental Protection Agency (EPA) (EPA, 2016). The TDS for the effluent was found to be 49626 mg L^{-1} . The acceptable MCL for the TDS according to these guidelines is 500 mgL^{-1} . The high TDS indicated a higher amount of dissolved ion content in the effluent sample. This might be due to the probability that the effluent was an RO feed water and had not undergone the effluent treatment procedures. The total BOD_5 and COD for the effluent samples was found to be 27.39 and 437.21 respectively.

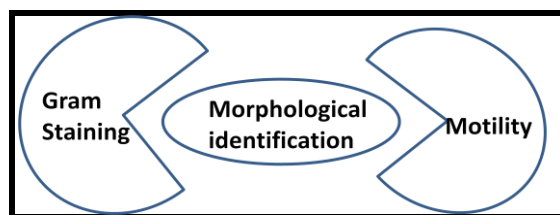
A comprehensive effluent characterization involves the microbial characterizations in addition to the chemical characterization. Microbial characterization involve the identification of the microbial flora inhabiting the effluent. Reviews suggest the methods for identification and characterization of microbial communities can be grouped under three broad categories viz., morphological, biochemical and molecular biology based methodology. Accordingly, a detailed microbial characterization has been performed to arrive at a taxonomic identification of the individual strains of the microbial community present in the collected effluent [Bergey et al, 1974; Spiegelman, 2005]. The basic approach followed to identify the isolated strains is schematically represented as



Identification of the bacterial communities in effluents

Bacterial population in the effluent sample was determined by the standard spread plate count method with serial dilutions of the effluent and subsequent inoculation in Nutrient Agar medium (NA) [Smrithi et al, 2012]. Isolation experiments were performed in triplicates.

Morphological identification of the microbes.



A total of ten isolates were selected based on their distinct cultural characteristics. These were further subjected to various biochemical tests for their genus identification.

The isolates were morphologically evaluated by **gram staining** and **motility tests**. **Gram staining**, also called Gram's method, is a method of differentiating two diverse groups of bacteria Gram-positive and Gram-negative species. This test is based on the ability of a cell to retain the crystal violet dye during staining procedure. The cell walls for gram-negative microorganisms have a lower peptidoglycan and higher lipid content than gram-positive cells. Principally, this difference in the microbial cell wall is amplified that helps in the identification. Originally, crystal violet is penetrated

in both kinds of cells. Iodine is subsequently added as a mordant to form the crystal violet iodine complex so that the dye cannot be removed too easily. This step is commonly referred to as fixing the dye. However, the subsequent treatment with the decolorizer (ethanol), removes the complex from the gram-negative cells. In contrast, the complex is retained in a gram positive cells and hence they remain stained. Finally, a counter stain, safranin is applied to the smear. The decolorized Gram negative bacteria take up this counter stain readily (Bartholomew et al., 1952). The Gram staining images of the bacteria isolated has been depicted in **Fig. 2.1**.

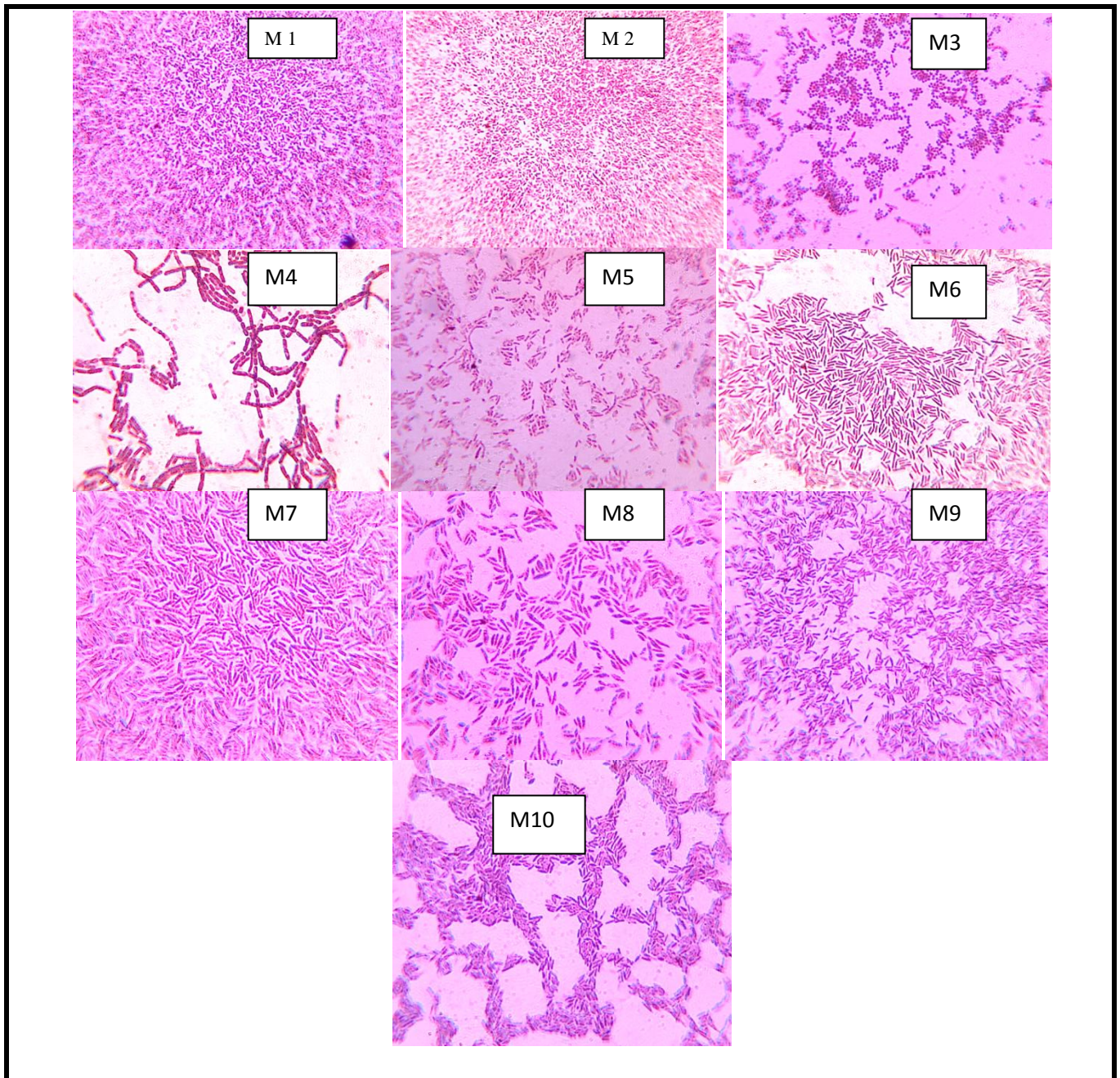


Figure 2. 1: Gram staining depiction of isolated strains.

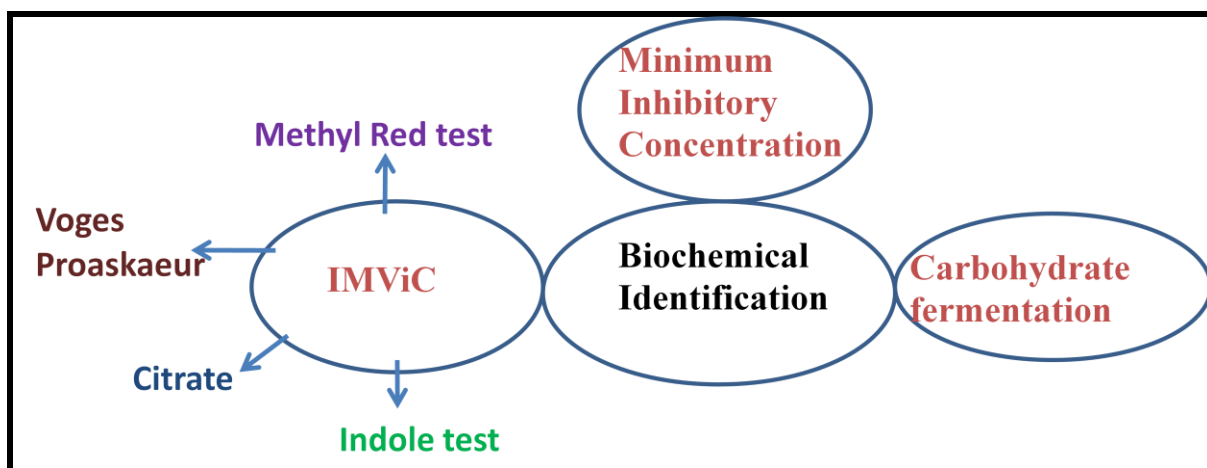
Gram staining revealed that M1, M3, M8, M9 and M10 were Gram positive while M2, M4, M5, M6 and M7 belonged to the group of Gram negative bacteria. (**Fig 2. 1**).

Some bacteria have the property to propel themselves through the liquids by means of their flagella. The type of motility is specific to genera of the bacteria that also aids in taxonomic

classification [Seymour et al, 2006]. **Hanging drop preparation** is a special kind of preparation of wet mount that is used to observe the motility of bacteria. A drop of culture was taken on a cover slip and was inverted on a concave slide such that the culture drop hangs in the well with support from the overlying cover slip [Aygan et al, 2007]. This prepared mount was observed for the motility under different magnification using optical microscope. The results have been tabulated in **Table 2.4**


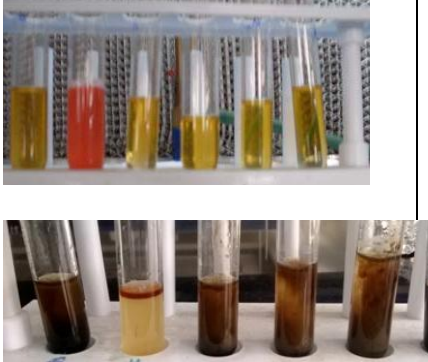
Biochemical characterization

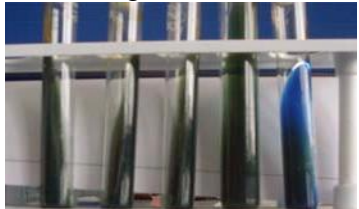

The following tests presented below are grouped under the head biochemical identification of bacteria

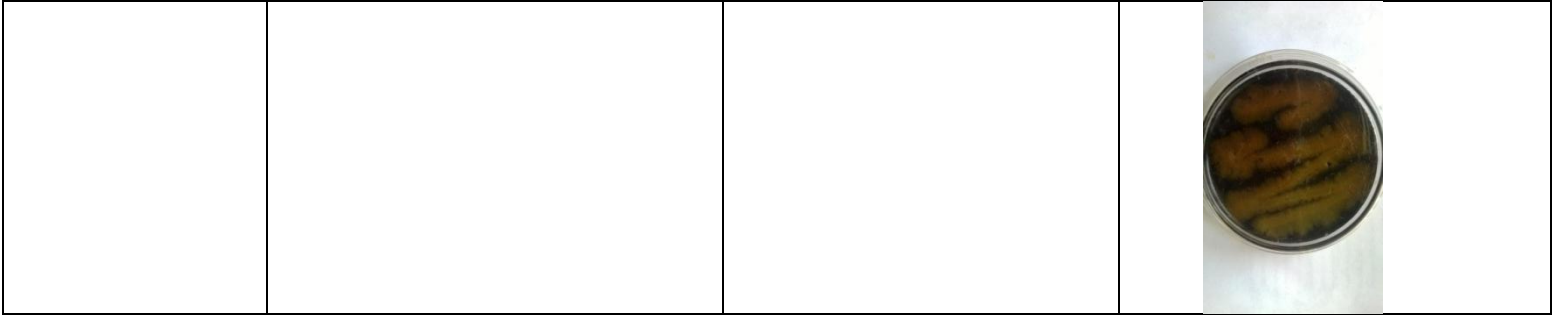


The detailed test procedure principle involved and result obtained has been represented in **Table 2.3**.

Table 2.3 : Details of the biochemical tests.

Name of the test	Principle	Materials & Methods	Result obtained
Indole test	Identifies the organism that is metabolically able to degrade tryptophan in the presence of tryptophanase to indole, pyruvate and carbon dioxide.	The organism was grown in a peptone broth supplemented with tryptophan	<p>A positive test was indicated by the conversion of the yellow colour broth to cherry red on reaction with a indicator, Kovacs reagent (Hydrochloric acid and p-dimethylaminobenzaldehyde in amyl alcohol).</p> 
MR-VP	The test determines whether the microbe performs mixed acids fermentation when supplied with glucose. Methyl red test indicates the production of acids during metabolism, while the VP test indicates the butanediol fermentation as a part of the bacterial cell metabolism.	The organisms were grown in a MR-VP broth at 37°C till sufficient growth was observed.	<p>A positive MR test was indicated by the appearance of red colour on addition of methyl red indicator that suggests the production of acid due to mixed acid fermentation. [Ljutov et al., 1963]. Organisms that respond positive to the VP test, produce acetoin that react with alpha-naphthol (VP reagent #1) and potassium hydroxide (VP reagent #2) to form a red color.</p> 

<p>Citrate test</p>	<p>Upon utilization of citrate as a sole carbon and energy source, carbonates and bicarbonates is produced along with liberation of carbon dioxide. This reacts with the water and other cations in the medium to change the pH to alkaline.</p>	<p>This test exploits the use of Simmons citrate agar medium to determine the ability of the test organism to use citrate as a sole carbon source. Citrate, ammonium ions and bromothymol blue indicator are the sole constituents of this agar medium</p>	<p>An organism that is able to utilize citrate as a carbon source was indicated by the change in the colour of agar from green to blue</p> 
<p>Carbohydrate fermentation test</p>	<p>The test classifies the organisms depending on the ability of the organism to take up the given carbohydrate as a carbon source</p>	<p>phenol red broth comprising of trypticase, sodium chloride, phenol red and a carbohydrate that acts as an energy source is used. The trypticase component of the broth is a source of nitrogen and helps in maintaining osmotic balance and electrolytes for the transport of metabolites through the cell. Durhams tubes were also placed in an inverted position inside the broth tubes. Once the bacterium was inoculated into the broth, it ferments carbohydrate with a simultaneous generation of acid</p>	<p>In tubes where the test organism is able to ferment glucose the medium colour changes to yellow owing to the generation of acid and reduction in the pH. Few of the tubes also shows the liberation of gas (CO₂) which accumulates at the tip of the Durhams tube</p>
<p>Starch Hydrolysis</p>	<p>The purpose of the test is to classify an organism that has the ability to use starch, a complex carbohydrate made from glucose, as a source of carbon and energy for growth. Use of starch is accomplished by an enzyme called alpha-amylase.</p>	<p>The organism was grown on a starch agar medium. Subsequent to the growth of the organism the starch agar plate was flooded with iodine solution</p>	<p>Organism capable of utilizing the starch will have clear zones around their growth</p> 



The **results** obtained for all the tests mentioned above is tabulated in the following tables (**Table 2.4** and **Table 2.5**).

Table 2.4: Biochemical and morphological characteristics of the isolated strains.

Strain	Shape	Motility	Grams reaction	Methyl red	Vogespro skauer	Catalase	Starch	Citrate	Indole
M1	Rods	Motile	Gram Positive	-	-	+	-	-	-
M2	Rods	Motile	Gram negative	-	-	+	+	+	+
M3	Cocci	Sluggish motile	Gram Positive	-	+	+	+	-	-
M4	Rods	Motile	Gram negative	-	-	+	-	-	-
M5	Rods	Motile	Gram negative	+	+	+	-	-	-
M6	Rods	Motile	Gram negative	-	-	+	-	-	-

M7	Rods	motile	Gram negative	-	-	+	-	-	-
M8	Rods	Motile	Gram Positive	+	-	+	+	-	-
M9	Rods	Motile	Gram Positive	+	-	+	+	-	-
M10	Rods	Motile	Gram Positive	-	-	+	-	-	-

'+' indicates the strains give a positive reaction to the test; '-' indicates the strains give a negative reaction to the test

Table 2.5: Carbohydrate utilization pattern by the isolated strains.

Strain	Sucrose (1%)		Dextrose (1%)		Galactose (1%)		Lactose (1%)		Fructose (1%)	
	Acid	Gas	Acid	Gas	Acid	Gas	Acid	Gas	Acid	Gas
M1	+	-	+	-	+	-	+	-	+	-
M2	+	-	-	-	+	-	+	-	+	-
M3	-	-	-	-	-	-	+	-	-	-
M4	-	-	-	-	+	-	+	-	+	-
M5	+	-	+	-	+	-	+	-	+	-
M6	+	-	+	-	+	-	-	-	+	-
M7	+	-	-	-	+	-	+	-	+	-

M8	+	-	+	-	-	-	+	-	+	-
M9	+	-	+	-	-	-	+	-	+	-
M10	+	-	-	-	-	-	+	-	+	-

'+' (Acid) indicates the strains produces acid ;' -' (Acid) indicates the strains does not produces acid ; '+' (Gas) indicates the strains liberates gas;' -' (Gas) indicates the strains does not liberate gas.

Additionally, **Minimum Inhibitory Concentration (MIC)** against various antibiotics and heavy metals was also carried out to analyse the resistance pattern of the isolated microbes.

The lowest concentration of the antimicrobial agent that inhibits the growth of bacteria is considered as the MIC. To assess the susceptibility to antibiotics, disc diffusion assay methods were performed. Approximately 2×10^{12} cells of each culture were plated on an LB agar plate [Aleem et al., 2003]. Different commercially procured antibiotic discs with known concentrations were added on the plate and allowed to incubate overnight. The zones of inhibition developed was measured in millimeter and was compared with the zone criteria distances **Fig. 2.2** published by the Clinical and Laboratory Standards Institute.

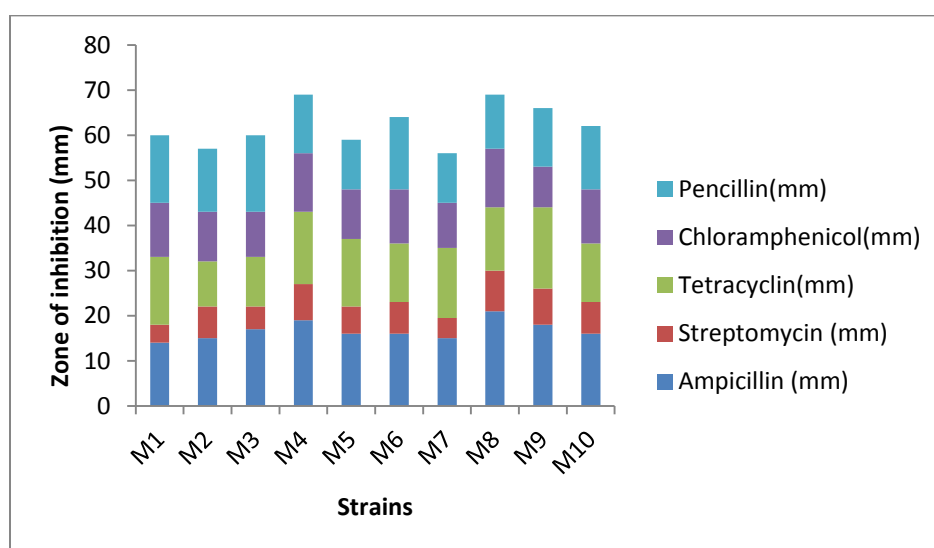


Figure 2.2 Resistance patterns of the microbes towards antibiotics.

Strain	Ampicillin	Streptomycin	Tetracyclin	Chloramphenicol	Pencillin
M1	Resistant	Resistant	Sensitive	Resistant	Resistant
M2	Resistant	Sensitive	Intermediate Resistant	Resistant	Resistant
M3	Resistant	Resistant	Resistant	Resistant	Sensitive
M4	Sensitive	Resistant	Sensitive	Resistant	Resistant
M5	Resistant	Resistant	Sensitive	Resistant	Resistant
M6	Resistant	Sensitive	Intermediate Resistant	Resistant	Sensitive
M7	Intermediate Resistant	Resistant	Sensitive	Resistant	Resistant
M8	Sensitive	Sensitive	Resistant	Intermediate Resistant	Sensitive
M9	Resistant	Sensitive	Sensitive	Resistant	Sensitive
M10	Resistant	Sensitive	Intermediate Resistant	Resistant	Intermediate Resistant

When the antibiotic sensitivity of these strains were tested, most of the strains were resistant to chloramphenicol and ampicillin except strain 8 which had intermediate resistance to chloramphenicol and was sensitive towards ampicillin. Apart from this strain, M4, belonging to *Pseudomonas* genus was also sensitive towards ampicillin. Among the different antibiotics used, majority of the strains were sensitive to streptomycin and penicillin.

The concentration of metal that hindered the growth of the microorganism was considered as the MIC against that specific heavy metal. A range of concentrations of the metal solutions (Lead, zinc, cadmium and chromium (50-500 mg L⁻¹)) were individually added to the LB broth cultures. After incubation of the organism overnight, spectrophotometric readings were taken at 600nm [Malik et al, 2000; Aleem et al, 2003]. All the ten isolated microbes were tested for their MIC towards the heavy metals. Among these strains M3 and M8 were the least tolerant to metals. Strain 5 was one

among the most resistant organism. It could resist lead, cadmium and zinc upto 200 mg L⁻¹. Beyond this metal concentration there was a total cessation of the growth at 250 mg L⁻¹ and above. However, the strain was sensitive to chromium at about 150 mg L⁻¹. (**Fig 2.3**). M1 and M4 were the most resistant strains that could tolerate majority metals to a relatively higher concentration.

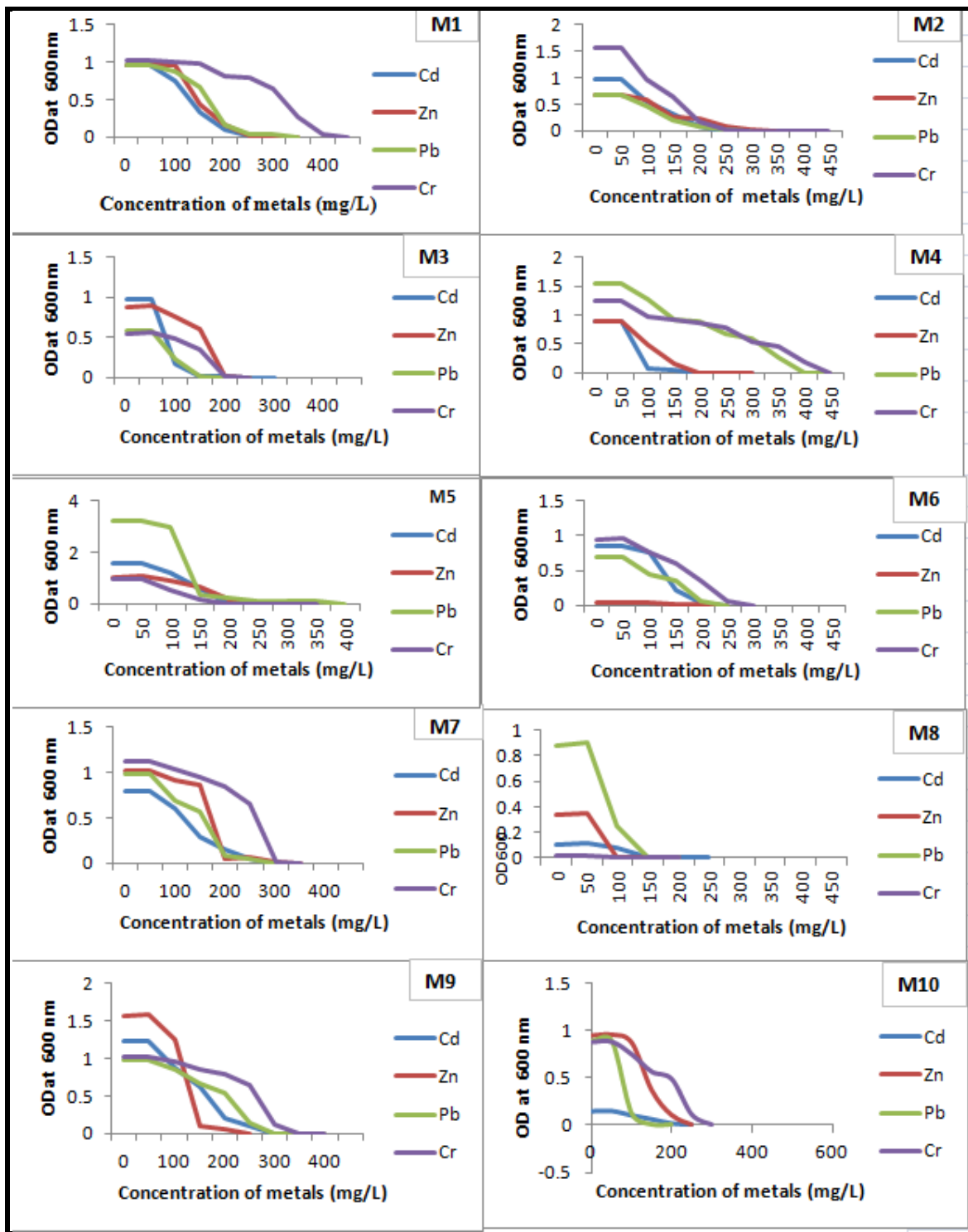


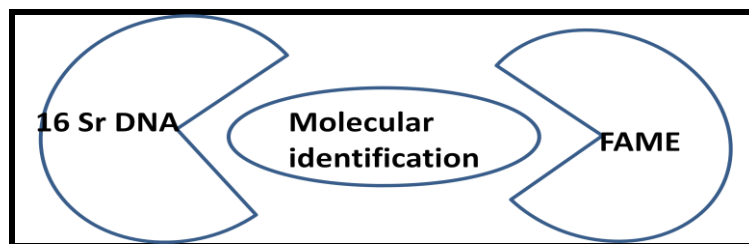
Figure 2.3: MIC of strains against various heavy metals.

Overall the difference in the tolerance to metals might be attributed to the fact that these bacteria have specific genetic mechanisms that aid in tolerating high levels of toxic metals. The bacterial

association of metal and antibiotic resistance is relatively common as both the resistant genes are located on the same mobile genetic element [Silva et al, 2012]. Therefore, the selective pressure exerted by the metals result in an indirect selection of the antibiotic resistance pattern.

The results obtained from these tests were compared with the Bergey's manual of systemic classification of bacteria and the available literature to arrive at a genus level confirmation of the isolated strains. These strains were further tested to confirm their identity using molecular characterization.

Molecular characterization



Materials and Methods

16S r DNA sequencing

Bacterial 16 S r-DNA region contains about nine hypervariable region (V1-V9) which has considerable sequence diversity, and is characteristic to one organism. Each of these variable regions are flanked by the conserved regions, to which the universal primers are designed [Chakravorty et al, 2007]. The 16 S r- DNA region is of 1.5 kb length. The pair of primers used to amplify this region were 27F and 1492R (**Table 2.6**). These primers are of 19 nucleotide length that bind at the 27th and 1492nd position of the 1.5 kb region of 16 S r- DNA. [Robertson et al, 2016] .

Primers	Nucleotide sequence
27 F	5'-AGAGTTTGATCMTGGCTCG-3'
1492R	5'- GGTTACCTTGTTACGACTT-3'

Table 2.6 Primers for amplification of 16 S r- DNA.

In order to sequence the 16 S r- DNA region of the genomic DNA, standard sambrook protocol was followed for the isolation of genomic DNA. (Appendix I)

PCR amplification of the 16 S r- DNA region of the genomic DNA

Bacterial genomic DNA was used as a template for amplification. The amplicons of the 16 S r- DNA region was obtained through regular PCR or colony PCR. The standard protocol was followed to prepare the PCR mixture (Appendix I). The thermocycling profile was set up as follows: Initial denaturation was carried out at 94 °C for 3min followed by 34 cycles of denaturation at 94 °C for 1 min. This was followed by an annealing step at 58 °C for 50 sec. Extension was carried out at 72 °C for 2 min, and a final extension was programmed at 72 °C [Widmer et al, 1998].

One major difference in the thermocycling profiles of colony PCR, is in the initial denaturation step. In colony PCR the time was extended to 5 min at 95 °C. This high temperature for a longer period of time takes care of the cell wall damage of bacteria and release of the cellular contents outside. One of the obtained amplicon is represented below **Fig. 2.4:**

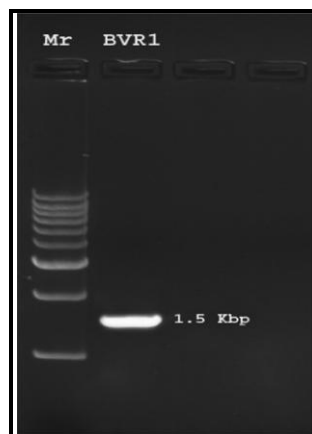


Figure 2.4: Lane 1 Mr-StepUp 1 Kb DNA ladder [Banglore Genei Cat # 612652070501730: 1000 bp, 2000 bp, 3000 bp, 4000 bp, 5000 bp, 6000 bp, 7000 bp, 8000 bp, 10000 bp.], lane 2 *Halomonas BVR 1*-16S r-DNA PCR amplified product.

The PCR amplicons from the above reaction were commercially sequenced at Bioserve Pvt. Ltd, Hyderabad, using ABI 3730x1s Genetic analyser (Applied Biosystems). According to the available literature, among the nine variable regions, V1-V3 is considered to be relatively significant in identification of a species. Reports also suggest that the other variable regions are less suitable for the identification, pertaining to their higher degree of conservation in comparison to the first three variable regions [Chakravorty et al, 2007; Dong et al, 2014]. These variable regions were therefore sequenced to confirm the identity.

DNA Sequencing

The gel-purified Amplicons were sequenced by commercial sequencing at :

- 1) Bioserve Pvt. Ltd. Hyderabad, India.
- 2) ABI Life Technologies-Invitrogen, Gurgaon, India.

About 50–100 ng of the purified DNA was used for sequencing PCR using BigDye® Terminator v3.1 Cycle Sequencing Kits [Applied Biosystems]. The cycling conditions for sequencing PCR were as follows: Initial denaturation at 97 °C for 10 sec, annealing at 55 °C for 10 sec and extension at

60 °C for 4 min. After 35 cycles, the templates were purified using Ethanol/EDTA precipitation method and sequenced on ABI 3730x1s Genetic Analyzer.

Sequences were read multiple times (were read using Finch TV version 1.4.0) per sample using both the forward and reverse primers. Only chromatograms lacking overlapping peaks were judged to be pure and were chosen for further analysis. Few samples showed overlapping peaks and were non conclusive, and were hence, eliminated. Good quality reads were selected and analysed using the Gene Bank database (Nucleotide Blast). Based on the maximum similarity hit to the organism reported in the database, generic and species name were assigned to the isolates.

Results and discussion

Blast hit analysis of V1-V3 variable regions of these isolates categorized them into four different genera of *Pseudomonas*, *Bacillus*, *Halomonas* and *Kocuria*. Genus and species level identification criteria were defined as a 16 S- r DNA sequence similarity greater than 97% and 99% respectively when compared against the test strain sequence [Riccardi et al, 2005]. The data from the molecular sequencing, corroborated well with the result from biochemical analysis. Four strains out of the ten strains belonged to genera *Halomonas*, 3 belonged to the genera *Bacillus*, 2 grouped under *Pseudomonas* and one was categorized under the genus *Kocuria* (**Table 2.7**). These partial sequences (V1-V3) of the strains have been subsequently deposited with the gen bank under the accession numbers: KT699196, KT699197, KT699198, KT699200, KT699202, KT699203, KT699204, KT699205, KT699206 and KC178681.

Table 2.7: List of the strains isolated.

Strain No:	Source of isolation	Strain Name	Similarity index	Reported strain
M1	Entry point of RO	<i>Halomonas</i>	96 %	<i>Halomonas clone HA 74</i>
M2	Entry point of RO	<i>Pseudomonas</i>	93 %	<i>Psuedomonas stutzeri Z102</i>
M3	Entry point of CETP	<i>Kocuria</i>	94 %	<i>Kocuria TS 13</i>
M4	Entry point of CETP	<i>Pseudomonas</i>	93 %	<i>Pseudomonas balearica S1-4-1</i>
M5	Entry point of RO	<i>Halomonas</i>	94 %	<i>Halomonas clone TV-G01-52</i>
M6	Entry point of CETP	<i>Halomonas</i>	97 %	<i>Halomonas clone ACH 14S-95</i>
M7	Entry point of CETP	<i>Halomonas</i>	95 %	<i>Halomonas clone NTN89</i>
M8	Entry point of CETP	<i>Bacillus</i>	94 %	<i>Bacillus sps. SBRh2</i>
M9	Entry point of RO	<i>Bacillus</i>	99 %	<i>Bacillus sps.4J</i>
M10	Entry point of CETP	<i>Bacillus</i>	99 %	<i>Bacillus JAPSK2</i>

A Multiple Sequence Alingment (MSA) was also carried out using CLUSTALW to analyse the percentage of variability among the strains (**Fig. 2.5**).



Figure 2.5: Multiple Sequence Alignment of the variable regions of all the strains.

Additionally, to analyse the evolutionary relationship among the isolated organisms, phylogenetic tree was constructed using Neighbour-joining (NJ) method in MEGA version 5.0. This showed clear bunching of the ten isolates among four different genera (**Fig. 2.6**).

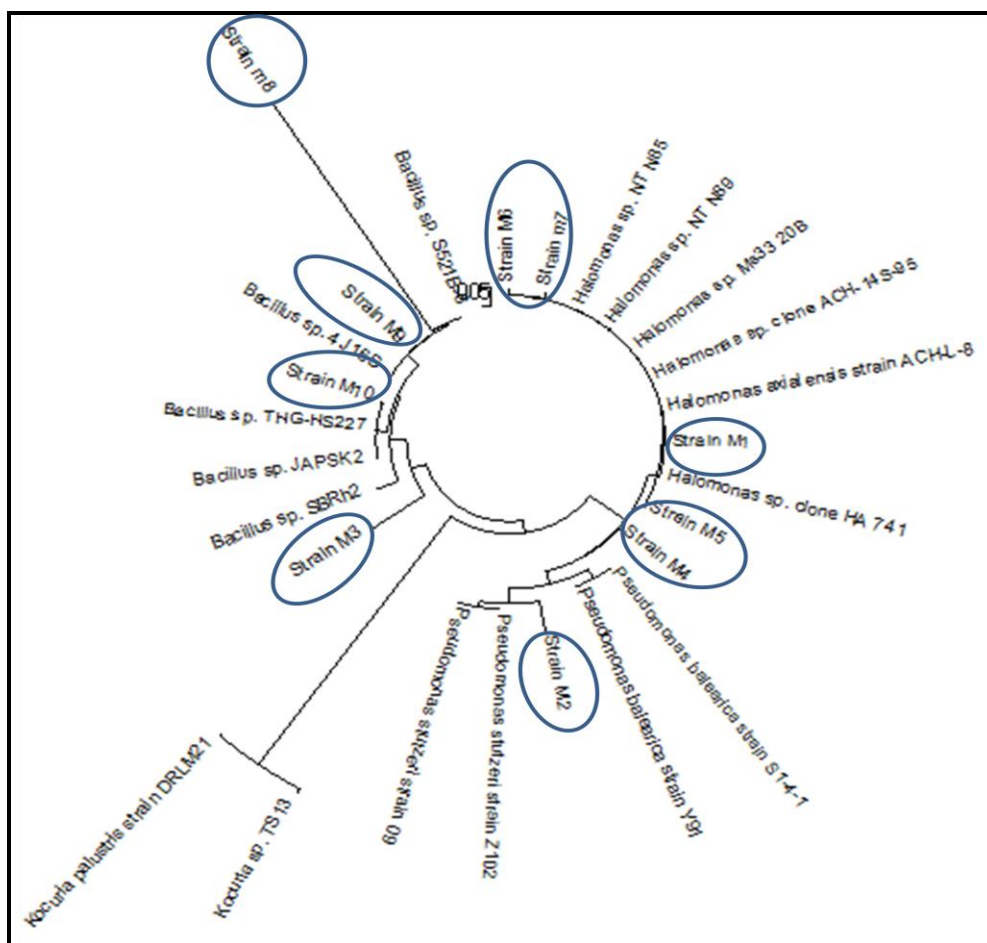


Figure 2.6: Phylogenetic analysis of the isolated strains.

Fatty Acid Methyl Esters (FAME) analysis of the isolates was carried out as a part of molecular identification. For this, one strain from each of the genera were selected and outsourced to Royal Life Sciences Pvt. Limited, India for FAME analysis.

FAME analysis methodology

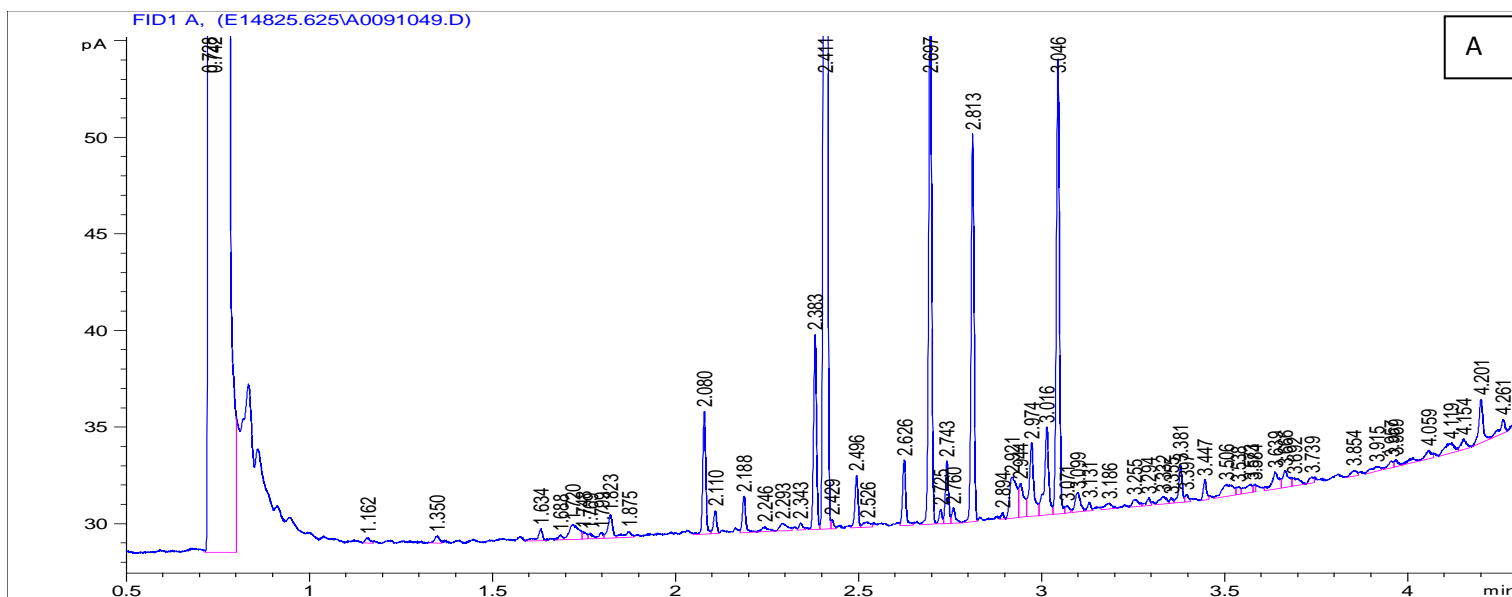
The Gas Chromatographic (GC) analysis of the short chain fatty acids of the microbial cells was carried out as a part of the biochemical analysis to confirm the results from the molecular 16 S-

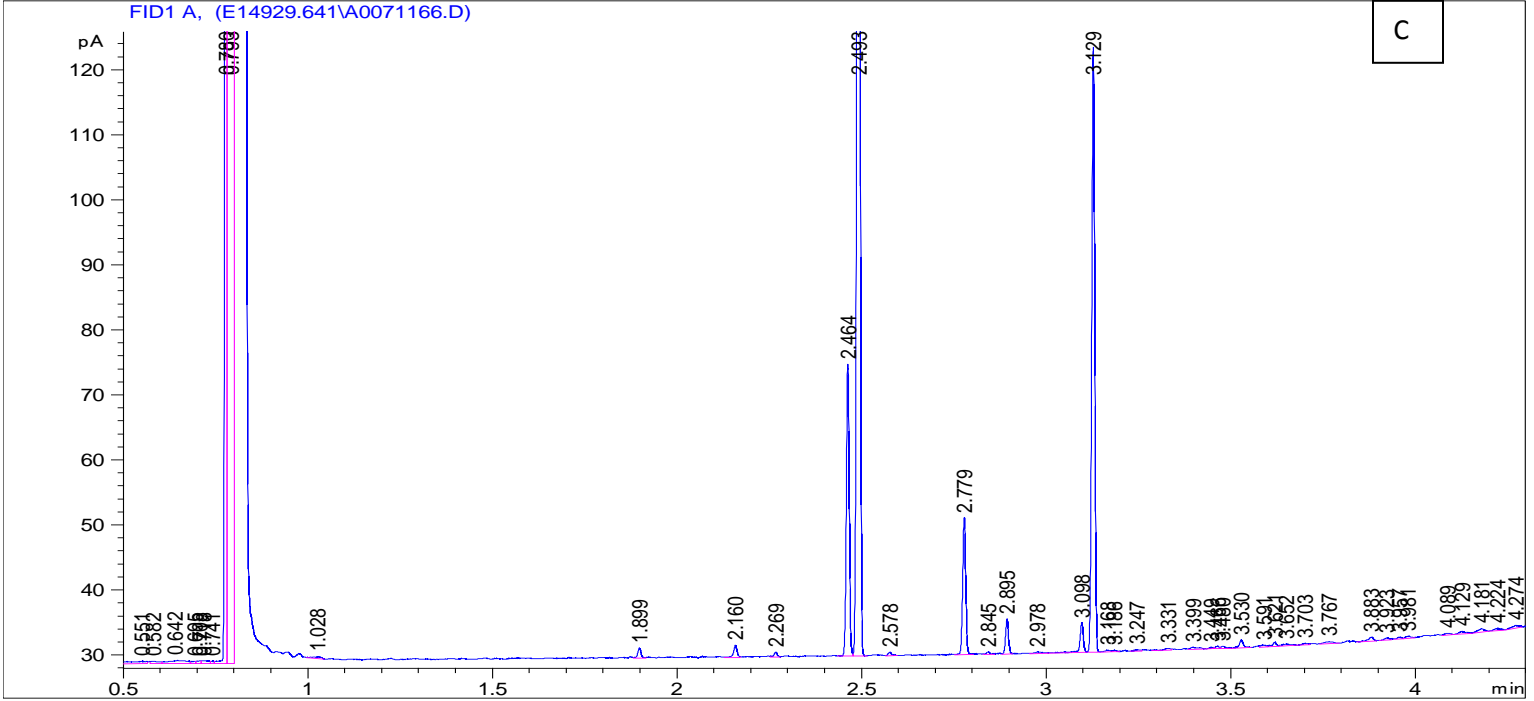
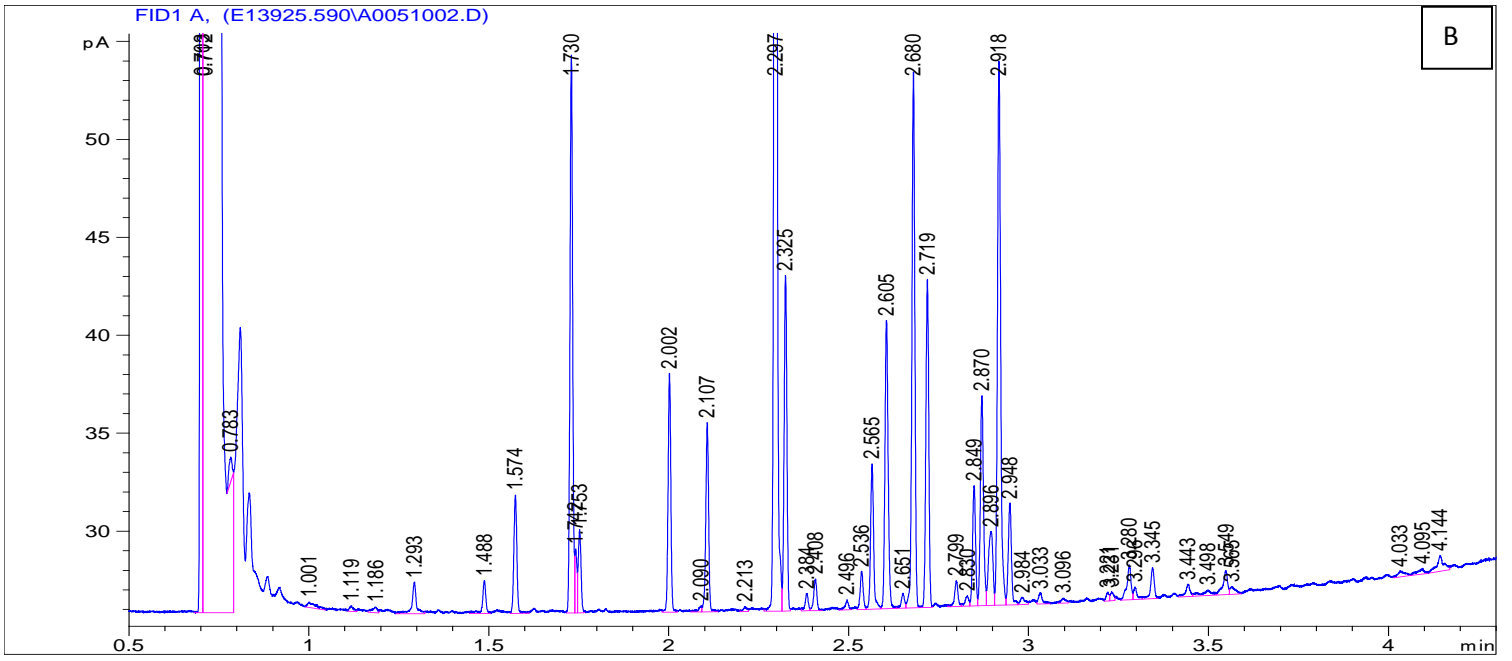
rDNA sequencing. For many years now, analysis of the short chain fatty acids specific to an organism is an important tool for bacterial identification. This wealth of information was also used in our study to confirm the identity on the unknown genera [Clarridge et al, 2004].

Phenyl methyl silicon columns (25mX0.2mm) was used to analyze the bacterial fatty acid methyl esters. An Agilent 6850 GC was equipped with the flame ionization detector. An initial column temperature of 170 °C was used at injection which continued till a final temperature of 270 °C. The injection port and detector temperature was set at 250 °C. By using hydrogen gas, the sample was injected at a flow rate of 30mL /min. Volume of sample injected was 2 microlitre.

The FAME profile of the organisms were compared with the Sherlock Microbial Identification System to report the identity of unknown strain [Chen et al, 2015] (**Fig 2.7**).

FAME profile of the isolated *Bacillus* sps. had a similar profile to that of *Bacillus cereus* with a similarity index of 0.717. Isolated strain *Kocuria* also had a profile similar to *Kocuria varians* with 0.358 similarity index. However, there was a little ambiguity with respect to *Halomonas* and *Pseudomonas* species.





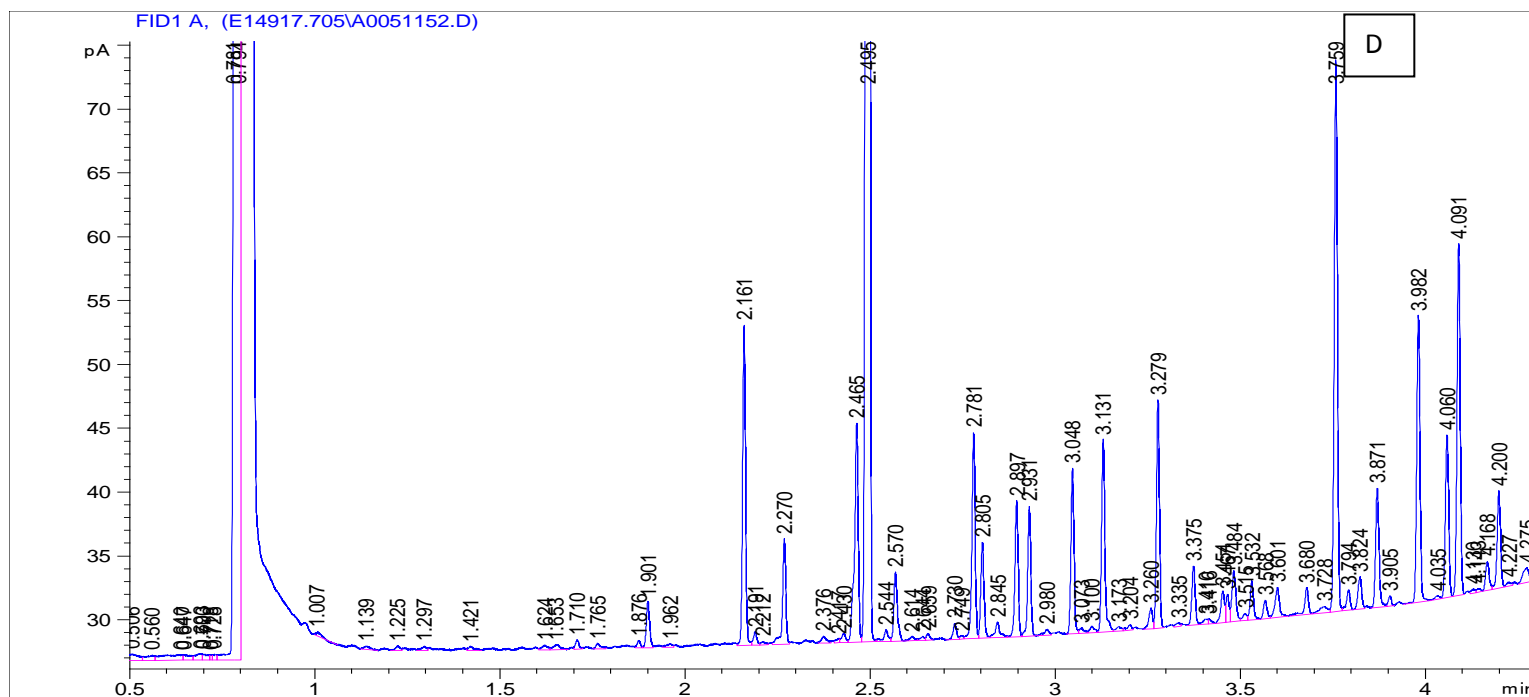


Figure 2.7: FAME profiles of the four different strains A-D: *Halomonas*, *Bacillus*, *Pseudomonas*, *Kocuria*.

Results and discussion

FAME profiles conclusively authenticated the isolated organisms as *Kocuria*, *Pseudomonas* and *Bacillus*. FAME analysis of *Halomonas* showed it to be similar to *Bacillus* with a similarity index of 0.582. Reports have suggested that FAME profile of *Halomonas* and *Bacillus* are similar because of which the identification through FAME analysis becomes difficult and inconclusive. This is because *Halomonas* is a moderate halophile and exhibit a *Bacillus* like morphology. Moreover, a number of *Bacillus* species that are moderately halophilic have been isolated from hyper saline habitat which make their FAME profiles to be similar. The members of *Halomonas* in general has been difficult to identify based on the chemotaxonomic and phenotypic characterizations [Johnson et al, 2007]. A similar feature was observed in our study too. However, the characteristic fatty acid marker such as 15:0 anteiso, 16:0 iso and 17:0 anteiso corresponding to *Halomonas* genera in the database, was observed to be present in higher percentages in our strain [Ventosa et al, 1998]. FAME profile of the

isolated *Pseudomonas* showed a profile similar to *Brevibacterium* strain. However when a phylogenetic dendrogram was constructed considering the FAME profiles of these strains (**Fig 2.8**), our isolate bunched along with *Psuedomonas balearica* strain indicating its similarity to the strain. This data was well substantiated with the 16 S r-DNA sequencing data, where, upon multiple sequence alignment our strain hit *Psuedomonas balearica* in the database with 95 % similarity index.

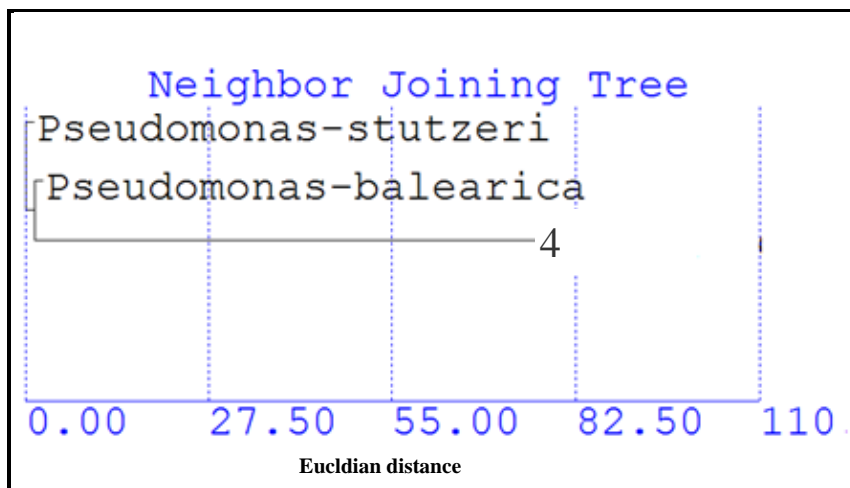


Figure 2.8: Phylogenetic relationship of the isolated *Pseudomonas* with the other strains.

Fungal isolation and identification method

The effluents were plated on Sabourauds Dextrose Agar medium (SDA) and incubated at 28 °C. Morphology of the individual fungal strains was observed after staining their hyphae and spores with Lactophenol Cotton Blue. Fungal isolates were then confirmed using the 18 S r-DNA sequencing analysis. The fungal DNA was extracted using the protocol given by Mollers et al [Moller et al. 1992]. About 100 mg of the fungal mycelium was extracted from the SDA plates. These were ground manually using a pestle and motor with simultaneous addition of SET (2% SDS, 10 mM EDTA pH 8.0 and 100mM Tris pH 8.0) buffer at 60 °C. Proteinase K at a concentration of 100 µg was added to this mixture and was incubated at 60 °C for 60 min. Furthermore, the mixture was

incubated for 10 min subsequent to which 5M NaCl and 10 % (w/v) CTAB was added. Later the fungal DNA was extracted using isoamylalcohol:chloroform (24:1). Followed by this DNA was precipitated using three volumes of cold isopropanol and single volume of sodium acetate (3M). This mixture was centrifuged and washed using 70 % alcohol. The fungal DNA was subsequently resuspended in 100 µl of TE buffer (10 mM Tris pH 8.0 and 1 mM EDTA pH 8.0).

This isolated DNA was used for the amplification of the 18 S r -DNA using universal fungal primers nu-SSU-0817-5' (TTAGCATGGAATAATRRAATAGGA), and nu-SSU-1536-3' (TCTGGACCTGGTGAGTTTCC) [Borneman et al. 2000]. This set of primer has been reported to represent major taxonomic groups of fungi that amplify a 762-bp region and contain the V4 (partial), V5, V7, and V8 (partial) variable regions. The amplified product was gel purified and further processed for sequencing by Bioserve Technologies Pvt. Ltd, Hyderabad, using ABI 3730x1 Genetic analyser (Applied Biosystems).

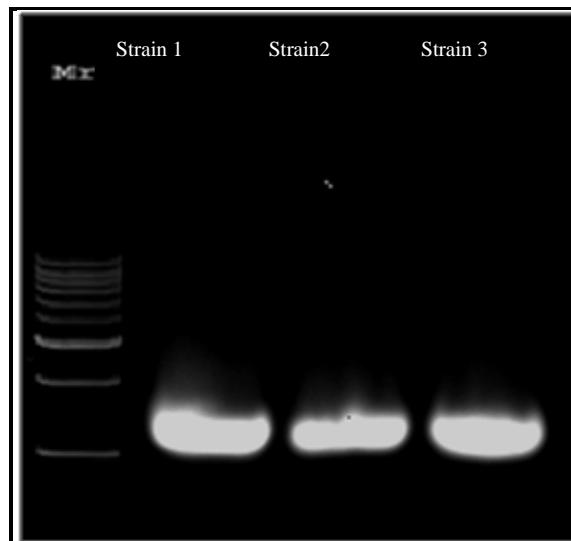


Figure 2.9: Fungal DNA isolated (Mr-500bp, 1000bp, 1.5kb, 3kb, 4kb, 5kb, 6kb, 8kb, 10kb).

Result & Discussion: 18 S r-DNA of our isolated fungal strains revealed two different types of fungal strains. One strain was similar in morphology to the *Cladophialophora* genus with respect to the culture characteristics, with the fungal colony appearing black and velvety in texture. The 18 S r - DNA of this isolate also showed 97% similarity to *Cladophialophora* genus. Two other isolated strains were 98 % similar to an unclutured *hypocrea* clone. These fungal isolate sequences have been deposited with the Gen Bank under the accession numbers: KT699199 and KT699201.

Isolation of Actinomycetes

Effluents were plated on Actinomycetes Isolation Medium (AIM). However, there was no actinomycetes population growth observed in the effluent collected.

Biosorption of cadmium, lead and zinc using *Halomonas BVR 1* isolated from an electronic industry effluent

SYSTEM 1: Halomonas BVR 1

This section deals with the selection of a microbe based bio adsorbent and its preparation, optimization of the various analytical parameters for the efficient removal of lead, cadmium and zinc.

Materials and Methods

Selection of a microbe based bio sorbent for metal removal

From the set of isolated microbial flora discussed earlier in this chapter, organisms belonging to the genera *Bacillus* and *Pseudomonas* were not selected for further studies as there has been enormous work on the remediation of metals using these organisms. Genera *Kocuria* was also eliminated as it is a pathogenic strain to work with and requires a Class II Bio Safety Cabinet for its culturing. Among the four isolates that belonged to the genera *Halomonas*, M5 strain i.e *Halomonas BVR 1* was chosen as our standard organism for all the further experimentation. This bacterial strain was chosen based on its high level resistance to various heavy metals and antibiotics. Moreover, this strain has not been reported till date for the remediation of metal cations.

Preparation of the biosorbent

Halomonas BVR 1 was inoculated into 100 mL LB containing 0.5 mol L⁻¹ NaCl and incubated at 37 °C for 48 hrs. The cells were grown to late exponential phase, harvested at 4 °C by centrifugation and the pellet was washed three times with deionized water. This was dried in a hot air oven at 40 °C. The dried pellet was used as a biosorbent.

Preparation of the metal solutions and their analysis

Heavy metals analysed in our study were cadmium, lead and zinc. The standard stock solutions of the metals were prepared using CdCl₂, Pb(NO₃)₂ and ZnSO₄ respectively. The concentration of the metal solutions in the aqueous medium was measured using Atomic Adsorption Spectrophotometer (AAS-Shimadzo 7000) and Ion selective electrode (Hanna).

Optimization of various parameters studied for efficient adsorption of the metal ion

Optimization of the various parameters involving adsorption isotherms, kinetics, and thermodynamics has been carried out. The physicochemical characterization of the biosorbent before and after adsorption was performed to evaluate the effectiveness of heavy metal adsorption. The theory and basis of the isotherms, kinetics and thermodynamics has been given in detail in the Appendix I.

Adsorption Studies

A 20 mL volume of a known concentration of each of the metal solution was equilibrated with a known weight of the prepared biosorbent in an orbital incubator shaker (Biotechnics, India) at room temperature for varying time periods. The amount of metal adsorbed (mg g⁻¹) at equilibrium q_e can be obtained by the expression

$$q_e = \frac{(C_o - C_e) V}{W} \quad (1)$$

where C_o and C_e are the initial and final concentrations of metal in solution, V is the volume of aqueous phase (L) and W is the weight (g) of the biosorbent used in the batch adsorption study. All of these above mentioned procedures were also carried out for the systems 2-4 discussed later in this thesis

Physicochemical Characterisations of the biosorbent

The scanning electron microscopy images (SEM) and energy dispersive spectral analysis (EDAX) of the adsorbent, before and after the adsorption of metal ions were recorded with a Hitachi-S520 model, Japan. Microbial pellet before and after adsorption was processed for SEM analysis as per the standard protocol [Fischer et al, 2012]. Pellet was fixed in 4% glutaraldehyde in 0.02 mol L⁻¹ phosphate buffer (pH 6.9) for 1 h. This was followed by washing the pellet twice in distilled water. Pellet was later washed with 10%, 20%, 30%, 50%, 70%, 90%, 100% alcohol, for 20 min at each step. Pellet was air dried and used for SEM-EDAX analysis. The pH measurements were done using an Elico LI-127 pH meter (Elico, India). ISE HI98185 ion meter equipped with ion selective electrode (Hanna Instruments, USA) was used to measure the concentration of metal ions at various stages of the adsorption process. The amount of metal adsorbed was also confirmed through AAS measurements (Analyst 300 – Perkin Elmer) using an air-acetylene flame.

Results and discussion

The biosorbent after metal adsorption appeared as a dense homogenous surface in contrast to the biosorbent before metal adsorption that showed a rough surface. This difference indicates effective interaction of metal ions. The morphological change in the biomass (**Fig. 2.10A-D**) subsequent to metal adsorption was also evident from the shiny and bright areas in the SEM micrographs which highlight the electrostatic affinity [Guo et al, 2012] between the biosorbent and divalent metal ions.

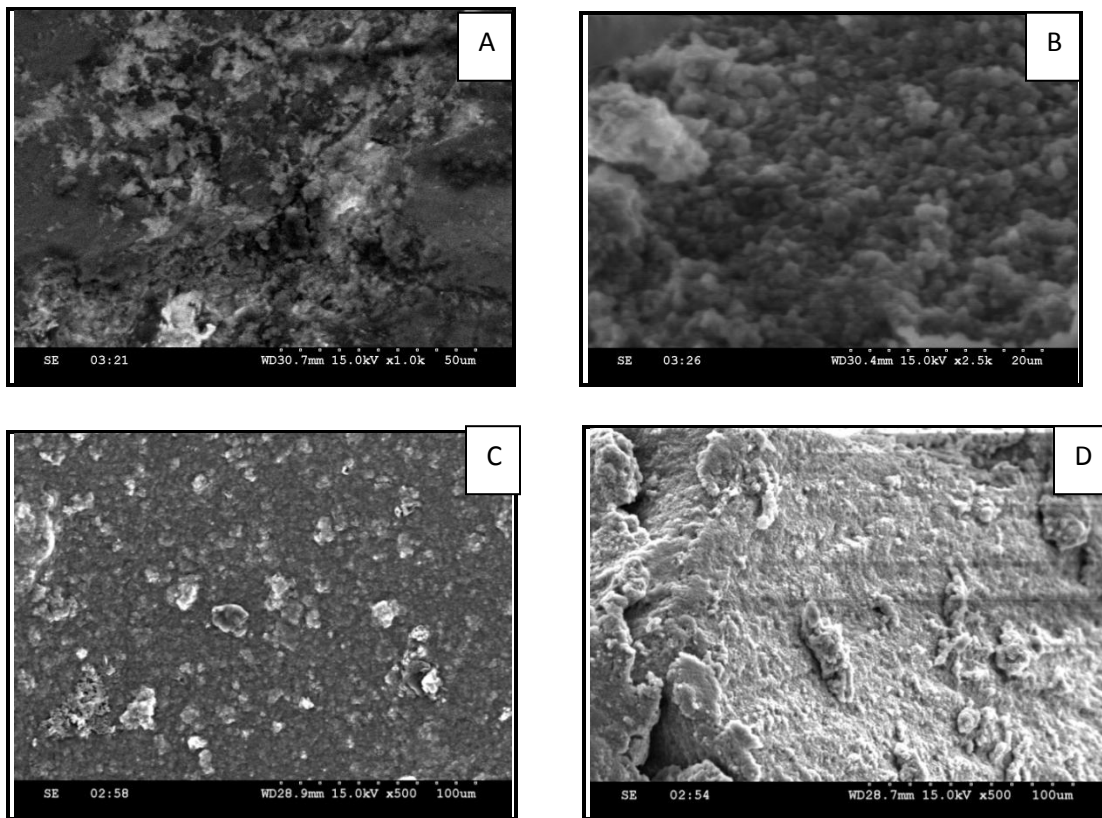


Figure 2.10 A) SEM image of the adsorbent before adsorption B) SEM image of the adsorbent after cadmium adsorption C) SEM image of the adsorbent after lead adsorption. D) SEM image of the biosorbent after Zinc adsorption.

EDAX analysis

The EDAX spectral analysis (**Fig. 2.11A-D**) of the *Halomonas* pellet gave some interesting insights to the process of adsorption. The EDAX pattern after metal adsorption indicates the electrostatic and coordinate bonding between metal ions and other negatively charged groups present in the cell wall of the bacterium. The peaks of C, N, O, P, and Ca corresponding to cell surface functional groups were retained after treatment with M^{+2} solution. Additionally, the M^{+2} (Pb^{+2} , Cd^{+2} , Zn^{+2}) peak was distinctive on the cell surface, indicating that M^{+2} was adsorbed by the cells. In general, the biosorption processes involve an ion exchange mechanism [Krishnani et al, 2008a] wherein, some of the Ca ions in the biosorbent surface were exchanged for the respective metal ions (Cd^{+2} , Pb^{+2} , Zn^{+2})

respectively. In this system too, the Ca peak intensity decreased [Guo et al, 2012] that further indicates that Ca was released in the process of M^{+2} adsorption. These observations confirm the presence of ionic exchange mechanism in the M^{+2} adsorption.

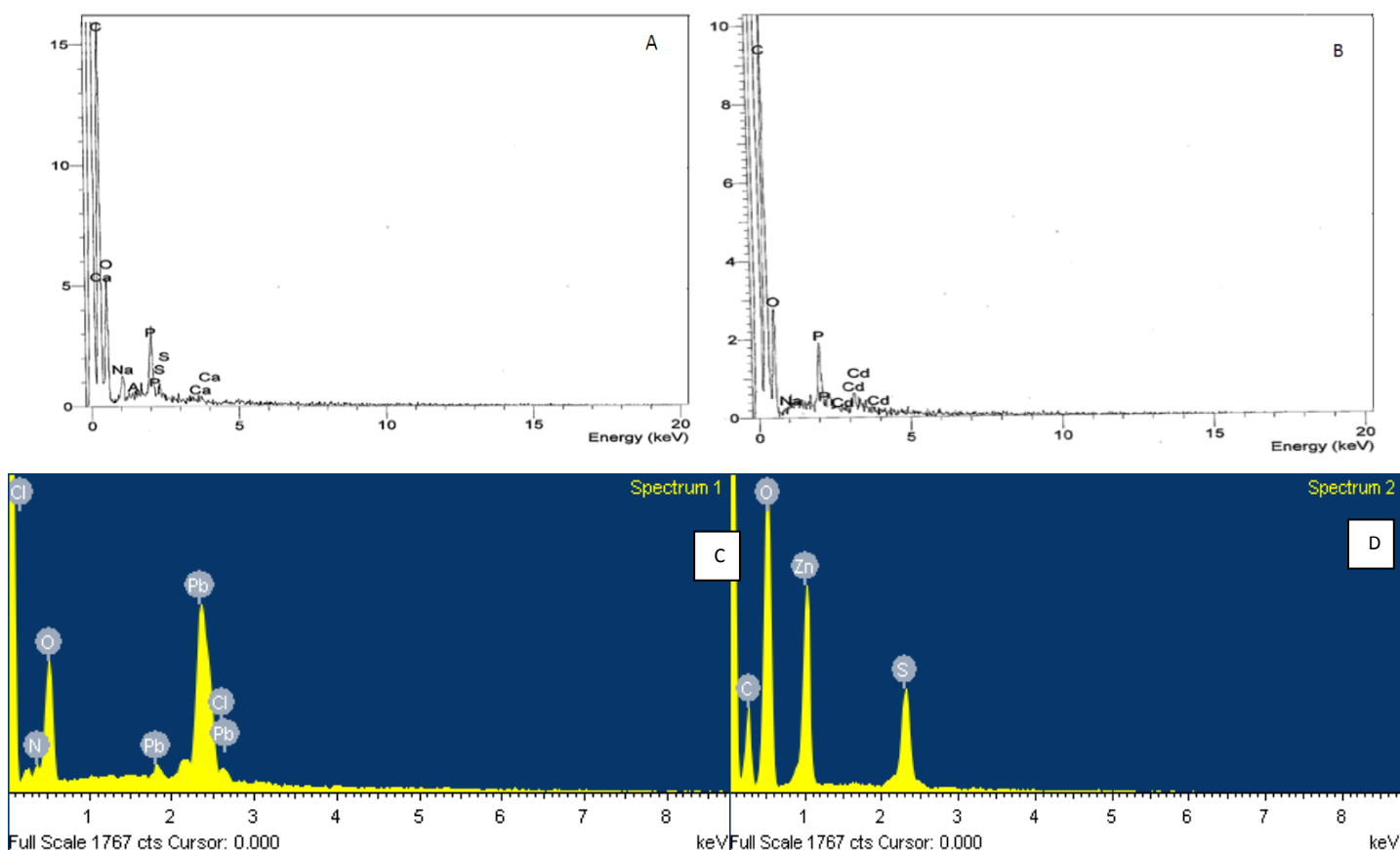


Figure 2.11 A) EDAX spectrum of the adsorbent before adsorption B) EDAX spectrum of the adsorbent after cadmium adsorption C) EDAX spectrum of the adsorbent after lead adsorption D) EDAX spectrum of the adsorbent after zinc adsorption.

FTIR spectral characterization:*Methodolgy*

The FTIR spectral analysis of the *Halomonas sps.* was performed using a Jasco 4200 FTIR spectrometer in the range $400\text{--}4000\text{ cm}^{-1}$. The biosorbent (free and metal treated) was dried overnight and this was followed by encapsulation into dry potassium bromide (KBr) powder.

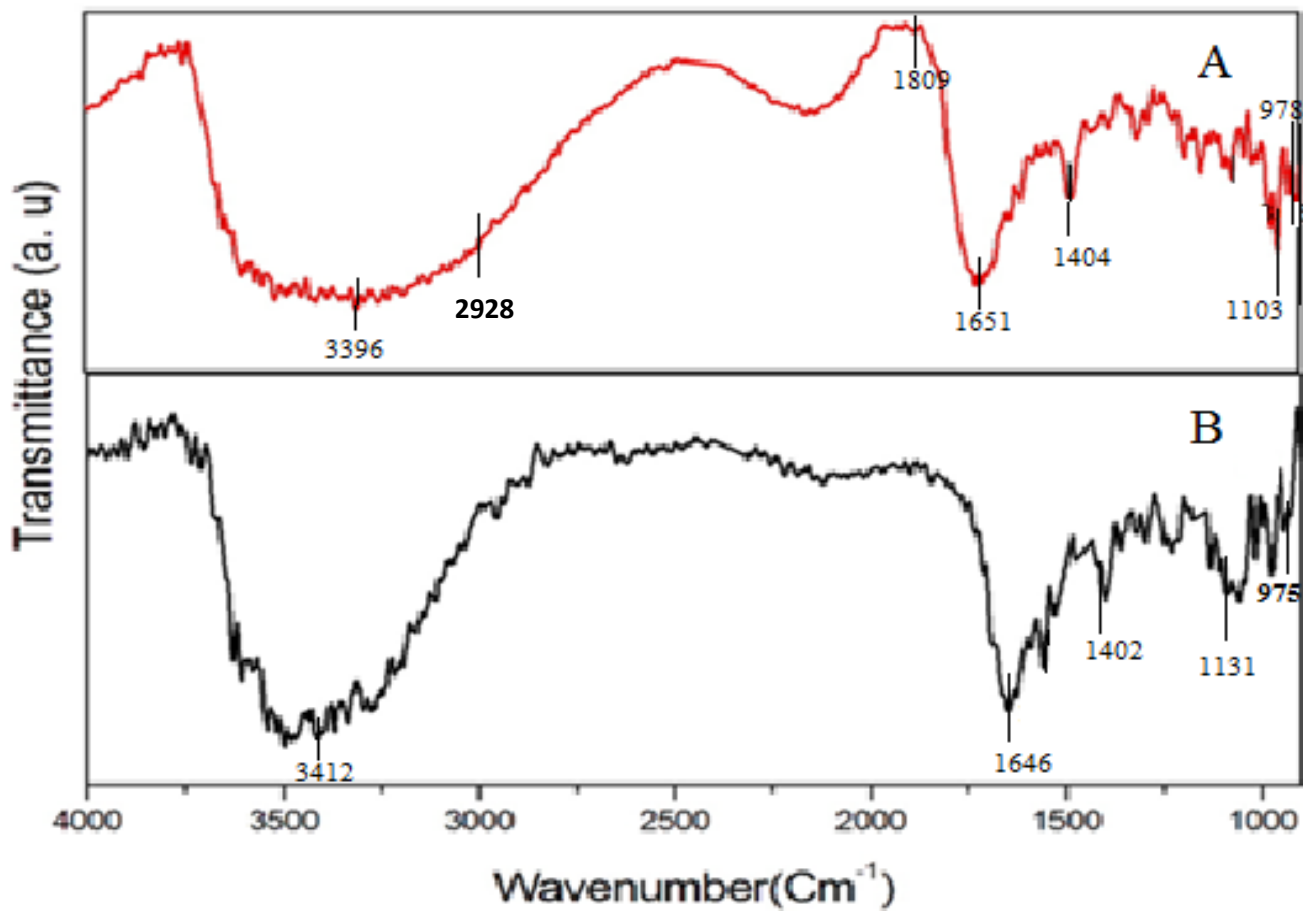
The prepared pellet was then scanned and the spectra of control and metal treated biomass were recorded.

Results and discussion: In the FTIR spectral analysis of the biomass (**Fig. 2.12**), we observed characteristic bands corresponding to O-H and N-H stretching vibrations at 3396 cm^{-1} and 1651 cm^{-1} respectively. The C-H and the C-O stretching were observed at 2916 cm^{-1} and 1103 cm^{-1} respectively [Sarkar et al, 2011]. The phosphoryl bending vibrations were observed at 978 cm^{-1} . A characteristic peak at 1809 cm^{-1} corresponding to C=O was also observed in the adsorbent [Souza et al., 2008]. The spectrum showed characteristic difference in the peaks of the biomass after adsorption of cadmium. The N-H bending vibration at 1651 cm^{-1} was shifted to 1646 cm^{-1} after the adsorption with cadmium [Elzinga et al, 2007]. The hydroxyl peak broadened with a corresponding shift from 3396 cm^{-1} to 3412 cm^{-1} . Similarly, the C-O stretching vibration observed at 1103 cm^{-1} resulted in a shift to 1131 cm^{-1} . Cadmium is mainly known to bind to carboxyl and phosphate groups. Accordingly, an increase in the peak intensity with a corresponding shift in the phosphoryl vibrations confirms the same [Elzinga et al, 2007]. These changes could be attributed to the effective interaction of cadmium with the organic functional groups on the cell wall.

FTIR pattern of the adsorbent after lead adsorption also suggested the involvement of various functional groups in metal binding. The spectral shift of peak from 2916 cm^{-1} to 2928 cm^{-1} suggest the involvement of C-H in lead binding. The peaks corresponding to the O-H and N-H also shifted to 3354 cm^{-1} and 1615 cm^{-1} respectively depicting their involvement in metal binding [Sarkar et al, 2011].

The change in the FTIR pattern of the adsorbent subsequent to zinc adsorption also is indicative of the metal adsorption. The functional group, C=C at 1404 cm^{-1} shifted to 1421 cm^{-1}

is indicative of this group in zinc adsorption. Similar to the other two metals, the shift in the N-H stretching to 1640 cm^{-1} indicates effective zinc adsorption [Elzinga et al, 2007].



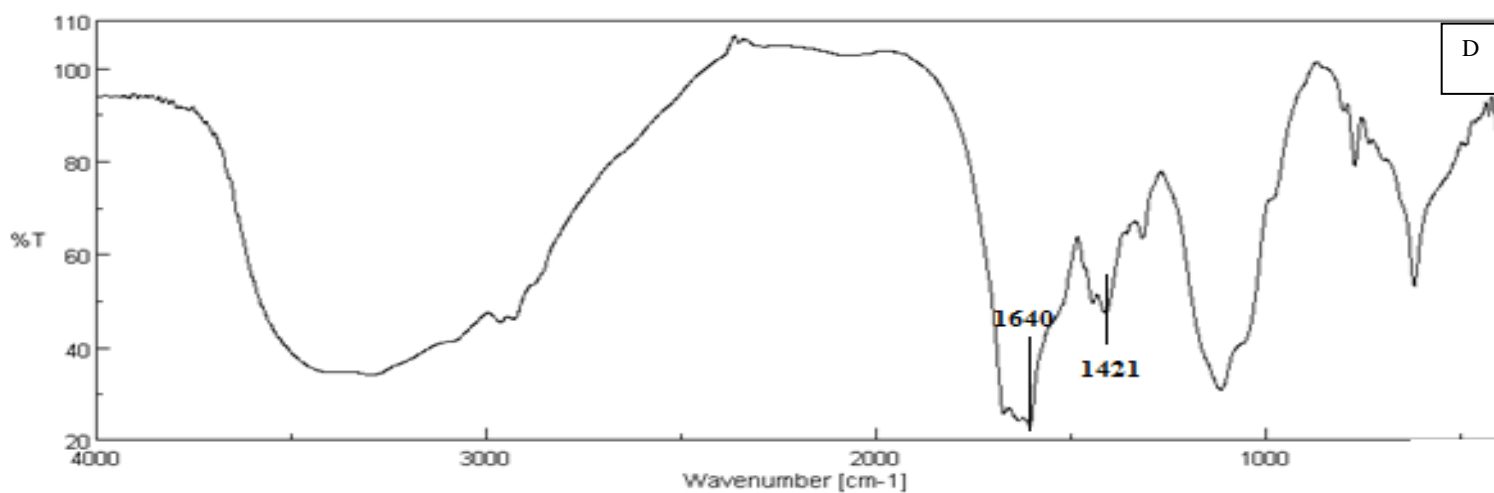
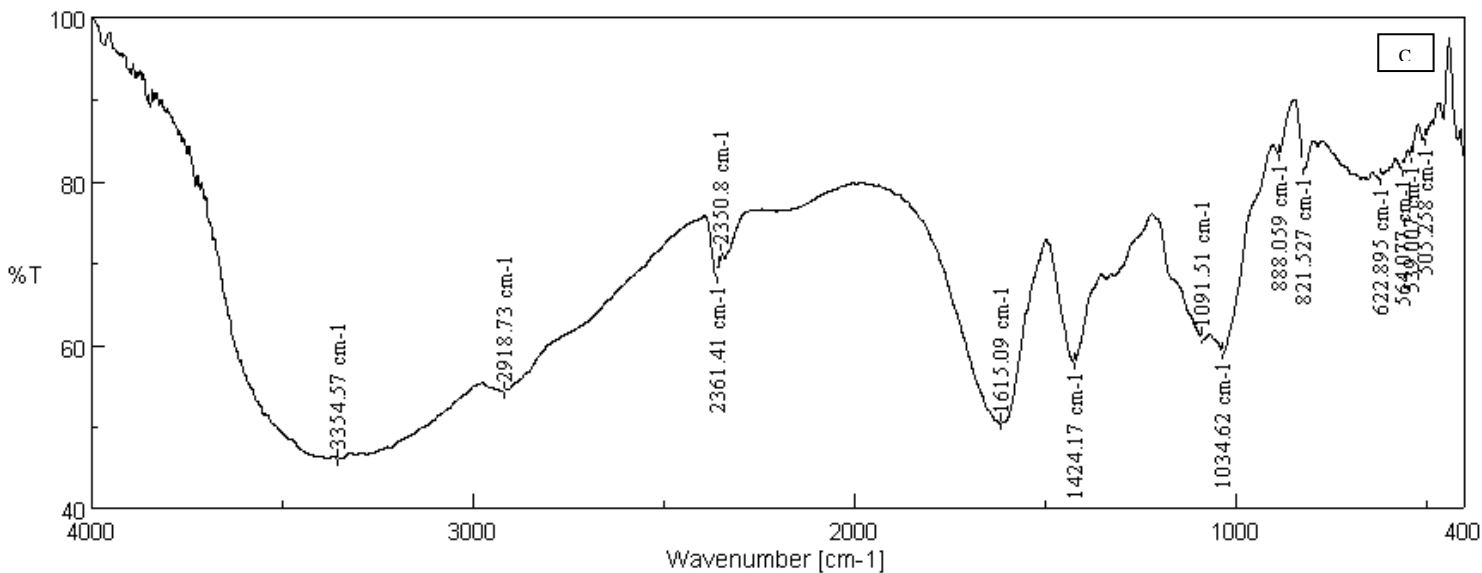


Figure 2.12 A) FT-IR spectrum of pellet before adsorption B) FT-IR spectrum of pellet after cadmium adsorption C) FT-IR spectrum of pellet after lead adsorption. D) FT-IR spectrum of pellet after zinc adsorption.

Effect of pH on adsorption.

The effect of pH has an important role in most adsorption processes. The adsorption of metals was found to be maximum above pH 8 (**Fig. 2.13**), and it is expected that the surface precipitation

and complexation mechanisms would favour metal ions uptake. In acidic pH, the functional groups in the cell surface attain a positive charge leading to repulsion between such groups and metal ions [Chakravarthy et al, 2012]. Lead adsorbed effectively at pH above 8.5, while adsorption of zinc was maximum at 8 pH. This can be attributed to the fact that at this pH the strong negatively charged groups such as carboxyl anions are available for metal binding.

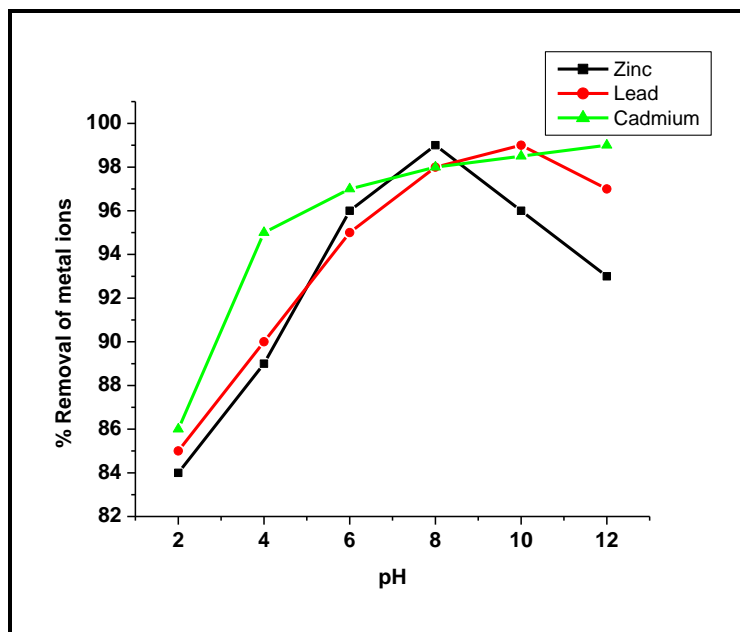


Figure 2.13 Effect of pH on adsorption

Equilibrium adsorption isotherms reflect the distribution of the metal ion between the biomass and aqueous phase at equilibrium as a function of concentration.

Isotherm studies

The detailed theory and methodology of adsorption isotherms, kinetics and thermodynamics is given in Appendix I

Langmuir isotherm

The Langmuir adsorption capacity, q_0 and the constant b (adsorption energy) obtained from the slope and intercept of the plot of C_e/q_e against equilibrium concentration, C_e (**Fig. 2.14A**) for cadmium

were found to be 12.023 mg g^{-1} and 0.108 L mg^{-1} (**Table 2.8**) respectively with a regression coefficient of 0.89. The maximum adsorption capacity obtained for the removal of zinc and lead was 11.11 mg g^{-1} and 9.152 mg g^{-1} respectively. Therefore, it can be inferred that this adsorbent could effectively remove cadmium as compared to lead and zinc. The following sections, hence deals in detail with the mechanistic interaction of cadmium and the biosorbent. The value of R_L for the adsorption of cadmium ($C_o = 80 \text{ mg L}^{-1}$) and lead on the biomass was found to be 1.103 and 0.0037 respectively which signifies effective adsorption [Mohan et al, 2012]. The R_L value incase of zinc adsorption (1.801) was higher than the other two metals. This indicates that adsorption of zinc did not favour Langmuir isotherm.

Freundlich isotherm

An efficient adsorption process yields the Freundlich constant 'n' in the range 1 and 10. A higher value of n implies stronger interaction between the adsorbent cell surface and divalent metal ions. The logarithmic plot of q_e against C_e (**Fig. 2.14A**) gives the constants K_F and n for the adsorption of cadmium as $4.920 \text{ mg}^{1-1/n} \text{ g}^{-1} \text{ L}^{1/n}$ and 7.215 respectively (**Table 2.8**). Adsorption of zinc obeyed the Freundlich model of multilayer adsorption with a higher regression coefficient than Langmuir isotherm. Also, the n value in case of zinc adsorption was highest (8.354) indicating that the sorption was favorable. Moreover, the value of $1/n = 0.15$ which indicates the normal adsorption phenomenon [Venkatesh et al, 2010].

Dubinin–Radushkevich [D-R] and Elovich isotherm

The adsorption mechanism and the interaction between divalent metal ion and the bacterial cell surface can also be modeled through D–R isotherm to understand the mechanism of interaction between the metal ions and biosorbent [Igwe et al, 2007]. This isotherm relates important parameters adsorption energy β and Polanyi potential ϵ to q_e and q_m .

$$\ln q_e = \ln q_m - \beta \varepsilon^2$$

The slope and intercept of the plot of $\ln q_e$ versus ε^2 (**Fig. 2.14 A**) gives β and q_m (**Table 2.8**) and the adsorption energy is related to the mean free energy of adsorption (E_{DR}).

$$E_{DR} = 1/(2\beta)^{-0.5}$$

A mean free energy of adsorption of $5.6274 \text{ kJ mol}^{-1}$ obtained for the adsorption of cadmium on the bacterial cell surface is ascribed to physical adsorption. In case of lead and zinc adsorptions also, a physisorption mechanism was observed owing to its free energy value less than 8 kJ mol^{-1} .

The Elovich model can be expressed as, [Hamdaoui et al., 2007]

$$\ln \left(\frac{q_e}{C_e} \right) = \ln (K_E q_m) - \frac{q_e}{q_m}$$

Where K_E is the Elovich constant (L mg^{-1}). The relevant isotherm parameters (**Table 2.8**) are obtained from the plot of $\ln [q_e/C_e]$ against q_e (**Fig. 2.14A**).

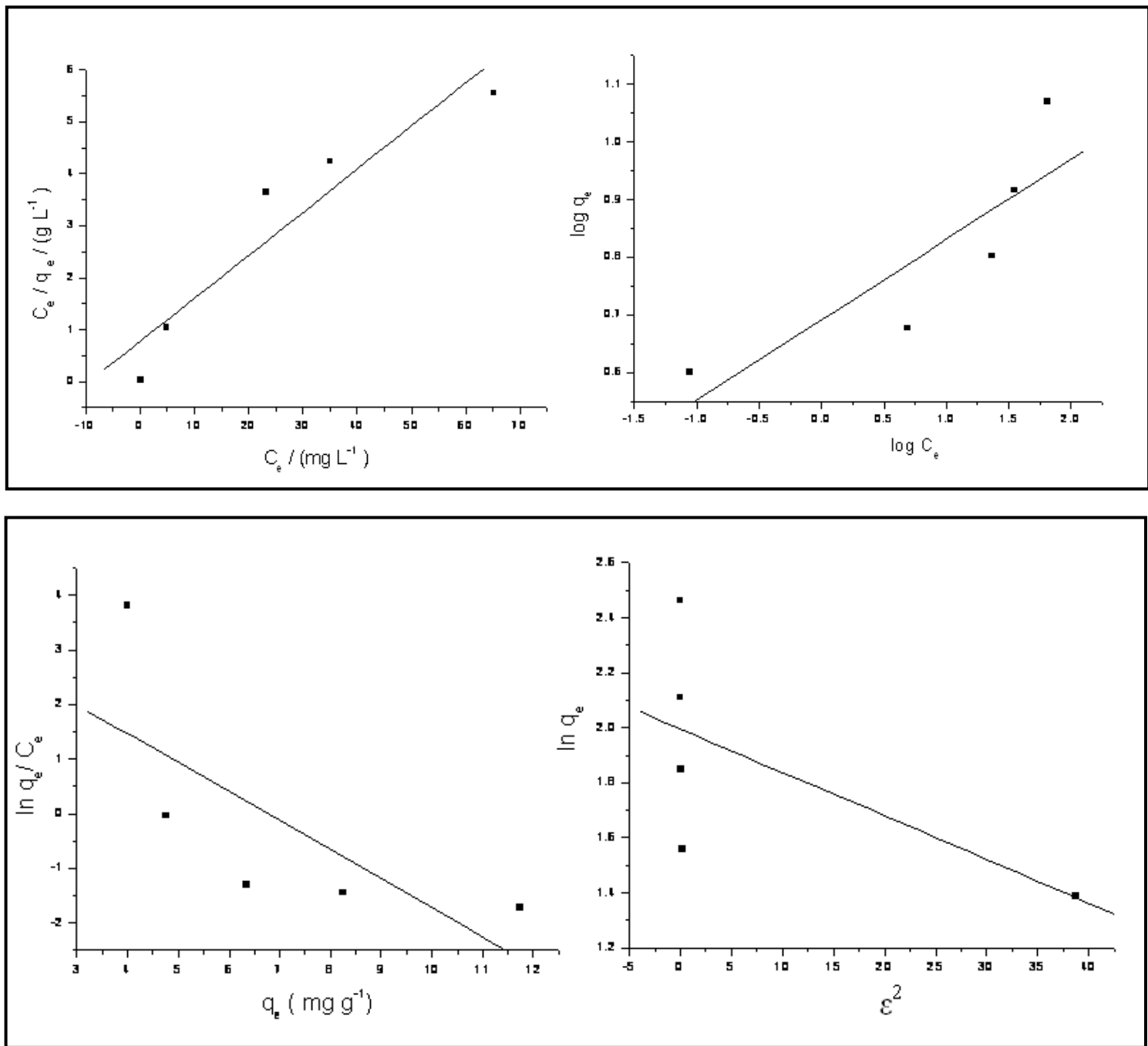


Figure 2.14A Cadmium adsorption (A) Langmuir isotherm (B) Freundlich isotherm (C) Elovich isotherm (D) D-R isotherm

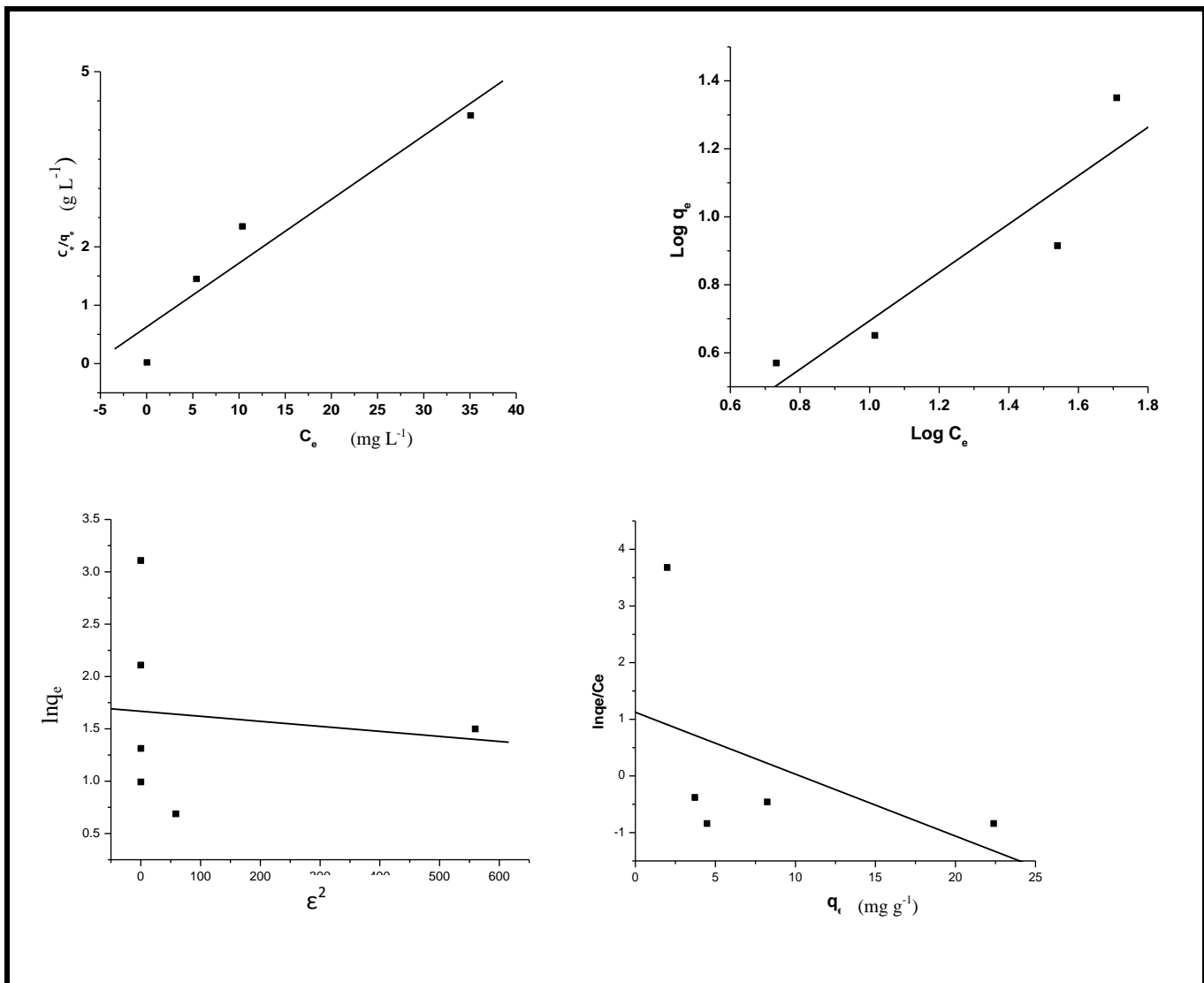


Figure 2.14B Lead adsorption (A) Langmuir isotherm (B) Freundlich isotherm (C) D-R isotherm (D) Elovich isotherm.

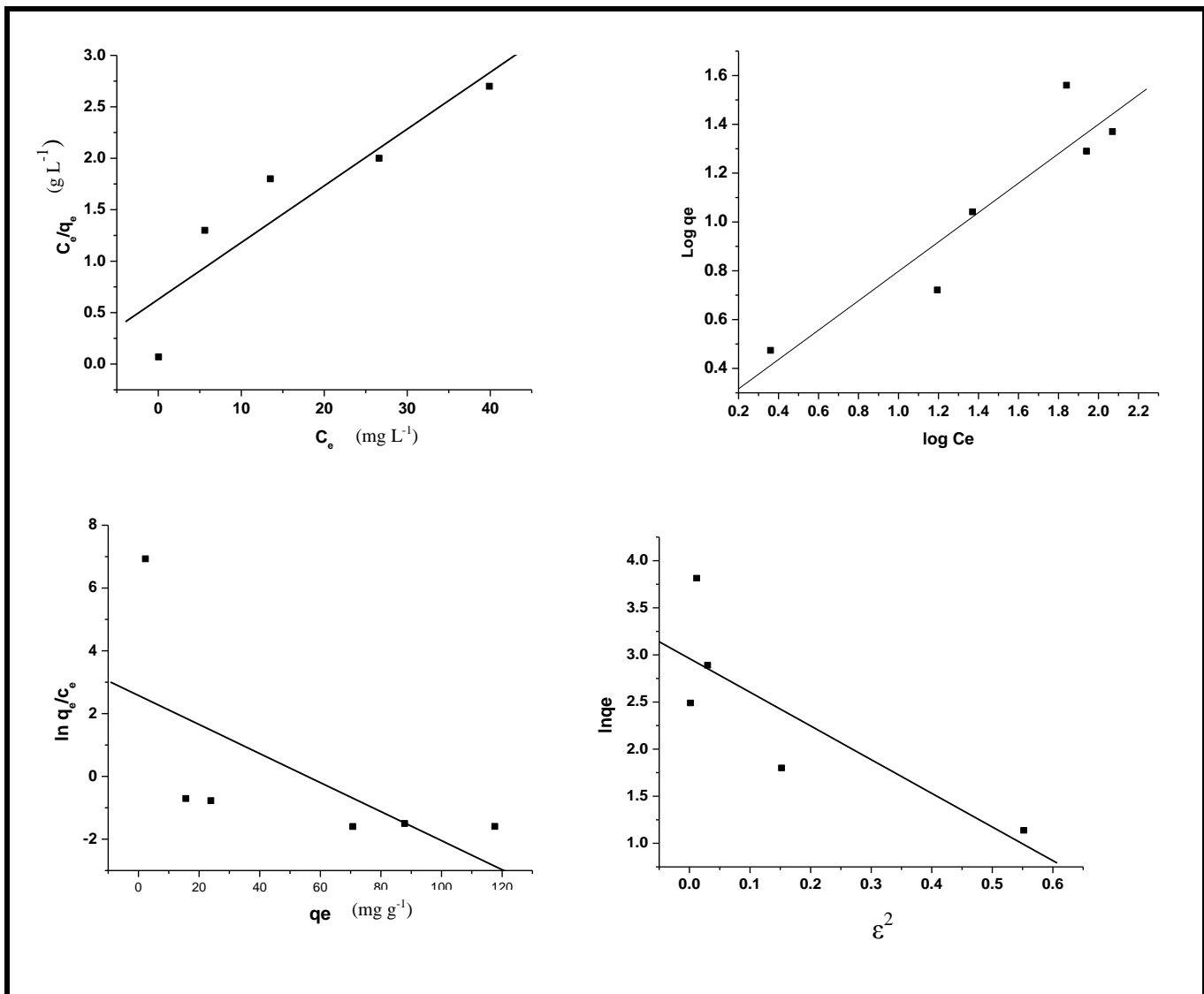


Figure 2.14C Zinc adsorption (A) Langmuir isotherm (B) Freundlich isotherm (C) Elovich isotherm (D) D-R isotherm.

Table 2.8 Isotherm parameters obtained from chosen models.

Sl. No.	Isotherm models	Parameters	Cadmium	Lead	Zinc
1.	Langmuir	$q_0(\text{mg g}^{-1})$ $b (\text{L mg}^{-1})$ R_L r^2	12.023 0.108 1.103 0.8947	9.152 5.747 0.0037 0.912	11.11 0.050 1.801 0.887
2.	Freundlich	$K_F(\text{mg}^{1-n} \text{g}^{-1} \text{L}^{1/n})$ n r^2	4.920 7.215 0.731	0.960 1.405 0.847	5.128 8.354 0.928
3.	Dubinin-Radushkevich	$q_m(\text{mg g}^{-1})$ β $E (\text{kJ mol}^{-1})$ r^2	7.358 0.0158 5.6274 0.404	5.299 4.7966 0.322 0.0151	6.253 1.256 4.325 0.69
4.	Elovich	q_m K_E r^2	1.885 19.144 0.512	9.157 0.371 0.2116	5.365 5.365 0.356

Kinetics of adsorption

The uptake of metals by the *Halomonas* sp./biosorbent depends on the contact time and hence the study of the kinetics of adsorption is an essential factor. The pseudo first order and pseudo second order kinetic models [Lagergren et al, 1898; Ho et al, 2006] relate the amount of metal adsorbed on the cell surface at equilibrium and at various time intervals to the respective kinetic rate constants (k_1 and k_2).

The kinetic plots (**Fig. 2.15**) and the parameters (**Table 2.9**) yield a higher regression coefficient for the second order kinetic model in case of all the metal ions. This indicates that the experimental data can be well described through this model. In addition, the experimental and calculated equilibrium adsorption capacity values for cadmium were found to be 3.7 mg g^{-1} and 4.9

mg g⁻¹ as per the second order kinetic model. Diffusion processes such as film, pore and surface diffusion [Sengil, 2009] could also influence the transport of the metal ions from the bulk to the bacterium cell surface. Intraparticle diffusion of the metal from the bulk into the pores of the biomass could also influence the kinetics of sorption. The Weber and Morris [Weber et al, 1963] intraparticle diffusion model gives the intraparticle diffusion rate constant k_{int} (**Table 2.9**).

$$q_t = k_{int} \sqrt{t} + C$$

The Weber–Morris plot (**Fig. 2.15**) yielded a finite intercept for all the metals under study and this is attributed to the fact that boundary layer effect also could influence the uptake of the metal ion from the bulk to the bacterium cell surface.

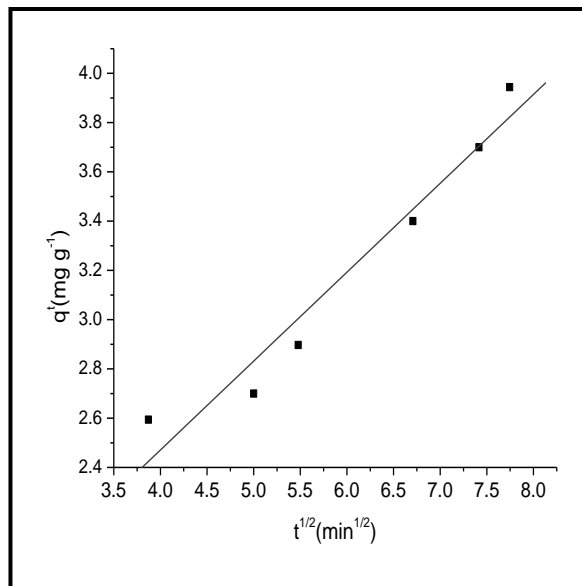
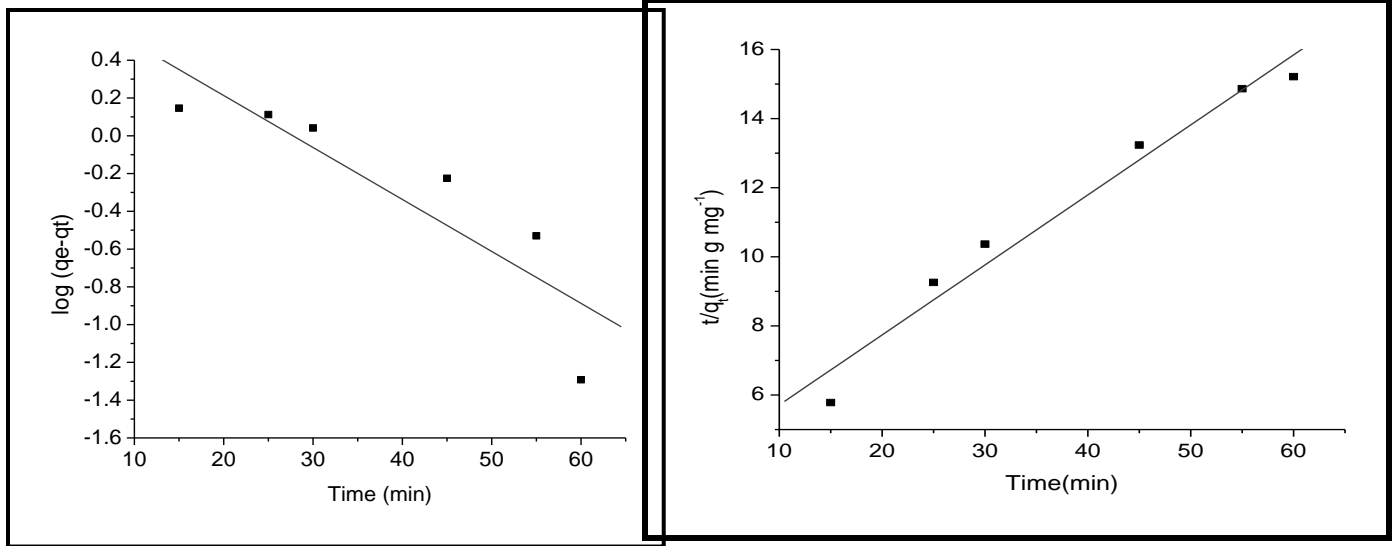


Figure 2.15 Cadmium adsorption A) Pseudo first order kinetic plot B) Pseudo second order kinetic plot C) Plot of q_t against square root of time

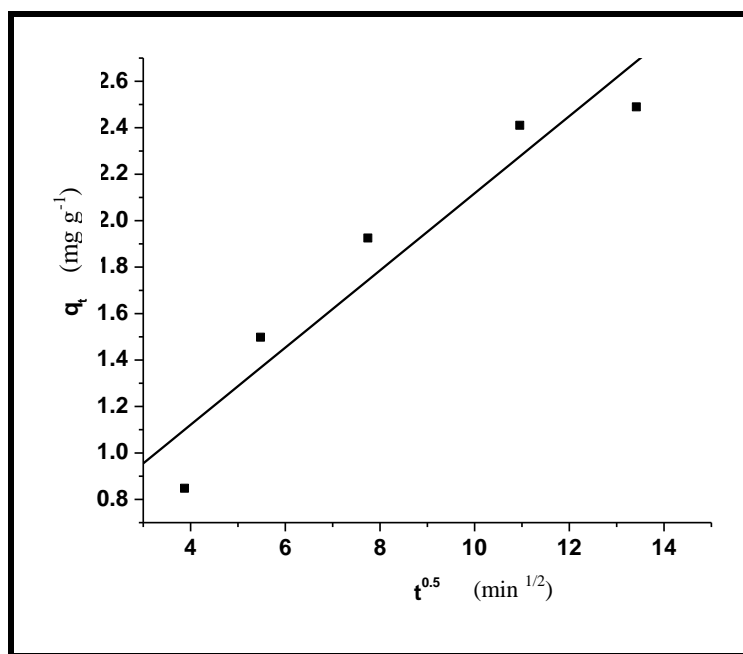
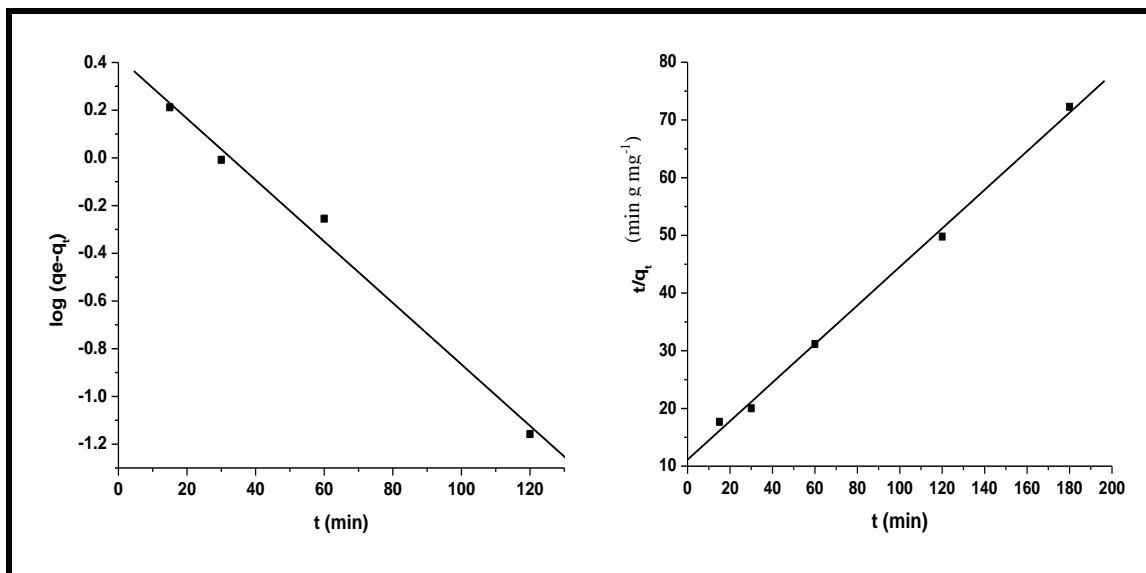


Figure 2.15 Lead adsorption Pseudo first order kinetic plot B) Pseudo second order kinetic plot C) Plot of q_t against square root of time

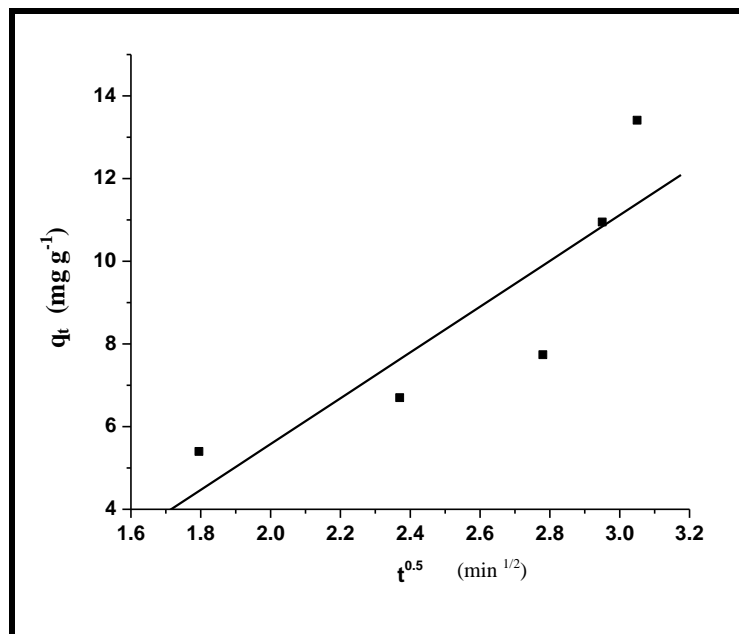
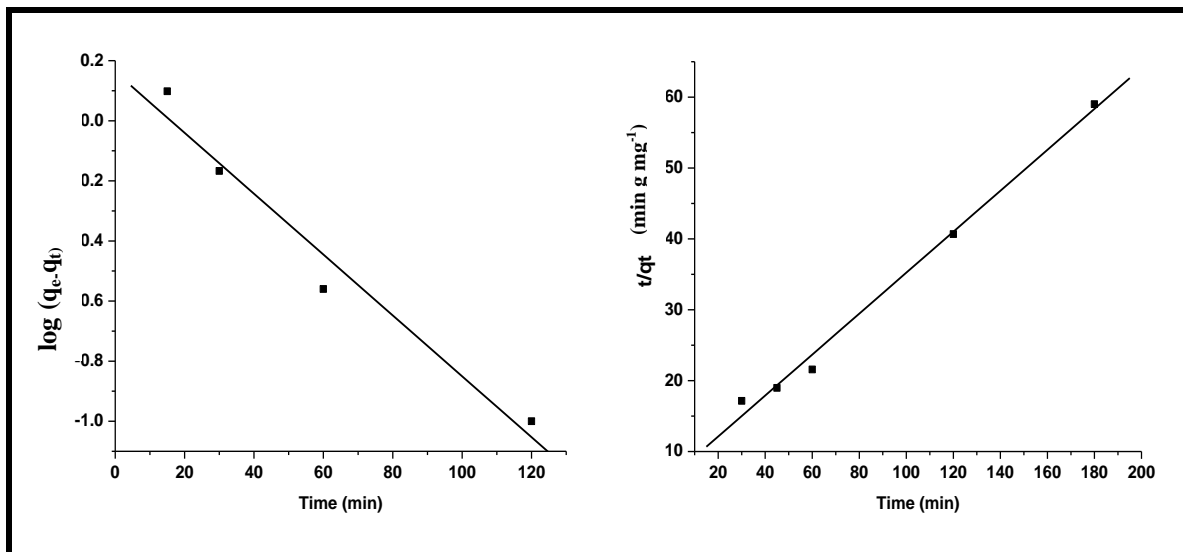


Figure 2.15 Zinc adsorption Pseudo first order kinetic plot B) Pseudo second order kinetic plot C) Plot of q_t against square root of time

Table 2.9 Kinetic and intraparticle rate constant data for the adsorption of metal ions

Metals	Second order rate constant k_2 [$\text{g mg}^{-1} \text{min}^{-1}$]	Regression Coefficient	First order rate constant k_1 [min^{-1}]	Regression coefficient	Intraparticle rate constant k_{int} [$\text{mg g}^{-1} \text{min}^{-1/2}$]
Cadmium	0.0110	0.9682	0.062	0.886	0.3684
Lead	0.0100	0.996	0.027	0.994	0.166
Zinc	0.0123	0.99	0.023	0.98	5.53

Thermodynamics of adsorption

The effect of temperature on the adsorption of divalent metal ions over the bacterium cell surface was studied. The equilibrium constant K is evaluated from the ratio of concentration of ions adsorbed on the microorganism to that in the solution phase. The $\ln K$ against $1/T$ plot gives ΔH^0 (Enthalpy) and ΔS^0 (Entropy) respectively (**Fig. 2.16**). The negative free energy change and the exothermic adsorption nature of the adsorption process (**Table 2.10**) indicates that metal adsorption on the bacterium cell surface is spontaneous [Yousif et al, 2016]. The *Halomonas* sp. thereby functions as an excellent host towards the adsorption of cadmium and the host-guest interaction is manifested through the surface active hydroxyl, carboxyl and amino groups present in the bacterium strain.

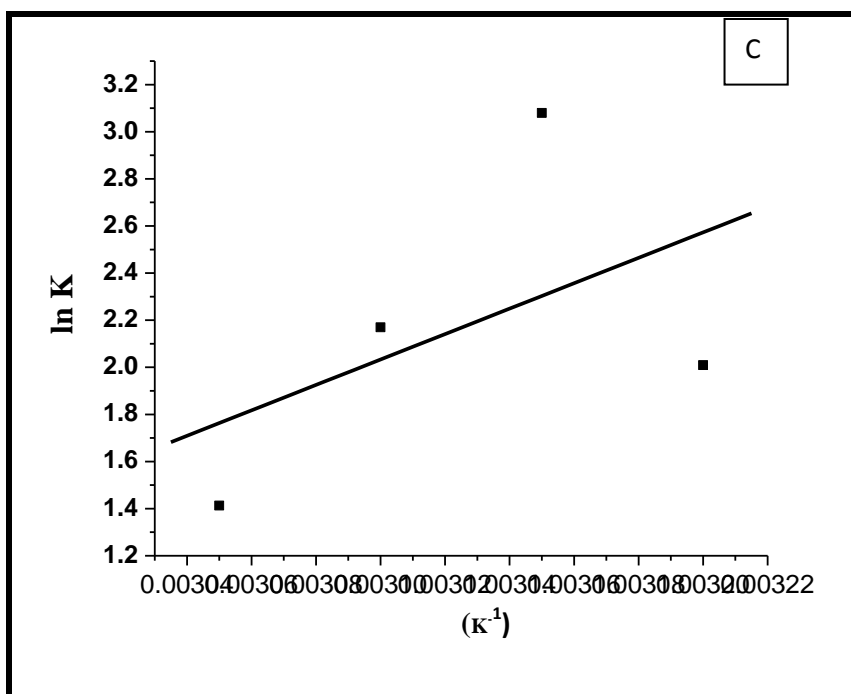
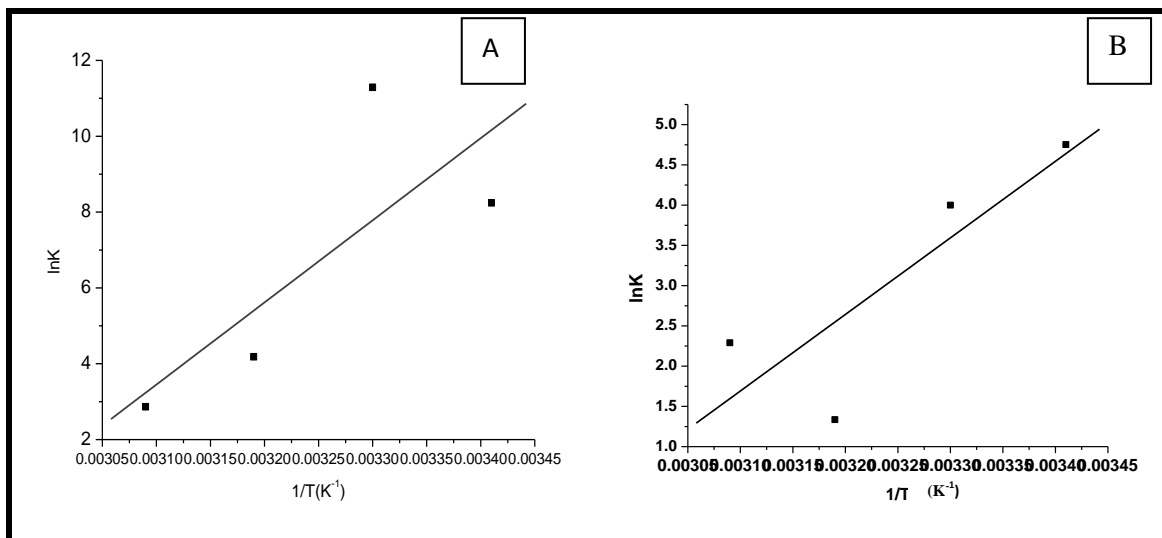


Figure 2.16 Van't Hoff plot showing the variation of lnK against 1/T in A) cadmium B) lead and C) zinc adsorption.

Table 2.10 Thermodynamic data for the adsorption of metal ions

Temperature [K]	ΔG° Cadmium	ΔG° Lead	ΔG° Zinc	Metal ions	ΔS° [J mol ⁻¹ K ⁻¹]	ΔH° [kJ mol ⁻¹]
293	-20.082	-11.575	-3.325	Cadmium	-545.91	-180.034
303	-28.438	-10.076	-5.299			
313	-10.885	-3.747	-7.526	Lead	-330.07	- 108.73
323	-7.696	-0.993	-4.595			
				Zinc	- 48.81	- 11.64

Effect of interfering ions on adsorption of metal ions

The influence of certain cations and anions that could be commonly associated with the electronic industry effluents were investigated at different concentrations. Ions such as nickel and cobalt did not interfere up to 70 mg L⁻¹ in the adsorption of lead and cadmium. Beyond 60 mg L⁻¹ concentration cadmium and iron caused a reduction in lead adsorption. Cobalt and manganese showed their interference at 60 mg L⁻¹ in case of zinc adsorption. Anions such as chloride and sulphate did not affect the adsorption of metals when their concentration levels were in the range 60 mg L⁻¹. Nitrate and phosphate caused a decrease in the percentage adsorption of lead and cadmium beyond 80 mg L⁻¹. Sulphates were the major anions that interfered with the metal adsorption beyond 70 mg L⁻¹ and caused a reduction upto more than 20 percentage (**Table 2.11**). The adsorption of the metal ions significantly reduced beyond 75 mg L⁻¹ of other cations. Presence of anions beyond 80 mg L⁻¹ also affected the adsorption of metal ions.

Table 2.11 Effect of diverse ions on the adsorption of metal ions.

Concentration of Anions mg l ⁻¹	% adsorption of cadmium	% adsorption of lead	% adsorption of zinc	Concentration of Cations mg l ⁻¹	% adsorption of cadmium	% adsorption of lead	% adsorption of zinc
SO ₄ ²⁻ (60)	89±0.6	90±0.8	92±0.7	Zn ²⁺ (100)	NI*	NI*	NI*
PO ₄ ³⁻ (80)	95±1.5	93±0.6	NI*	Ni ²⁺ (70)	99±1.3	98±0.5	NI*
Cl ⁻ (60)	NI*	NI*	NI*	Co ²⁺ (70)	98±0.6	99±0.2	91±0.3
NO ₃ ⁻ (70)	92±0.8	96±0.1	NI*	Mn ²⁺ (60)	NI*	NI*	89±0.8
				Fe ²⁺ (60)	NI*	94±1.2	NI*
				Mg ²⁺ (50)	NI*	NI*	NI*
				Cd ²⁺ (60)	NI*	95±0.7	NI*

*NI: No Interference

Comparison with other strains

The developed method was compared in terms of the adsorption capacity against other bacterial and fungal strains. The comparison **Table 2.12** shows that *Halomonas* sp. has good adsorption capacity towards the metal ions when compared with other reported strains. *Halomonas* sp proved to be very effective in binding cadmium, lead and zinc on its surface.

Table 2.12 Adsorption capacity comparison against various bacterial and fungal strains

S.No.	Strain	cadmium Adsorption capacity (mg g ⁻¹)	Strain	Lead Adsorption capacity (mg g ⁻¹)	Strain	Zinc Adsorption capacity (mg g ⁻¹)
	Pardo et al 2003 Kapoor et al 2007		(Abbas et al., 2014)		(Abbas et al., 2014)	
1	<i>Pseudomonas putida</i>	8.0	<i>Stenotrophomonas maltophilia</i>	0.41	<i>Pseudomonas Aeruginosa</i>	1.33
2	Free cell suspended in solution Lab culture	14.3–20.0	Brown algae(<i>Fucus vesiculosus</i>)	1.04	Sulphate-reducing bacteria(SRB)	5.6
3	Immobilized cells on sepiolite	10.9	<i>Pleurotus ostreatus</i>	4.84	<i>Geobacillus themocatenulatus</i>	12.3
4	<i>Penicillium digitatum</i>	3.5	<i>Candida spp</i>	1.03	<i>Green algae</i>	7.62
5	<i>Penicillium notatum</i>	5.0	<i>Saccharomyces cerevisiae</i>	0.60	<i>Saccharomyces cerevisiae</i>	11.8
6	<i>Apergillus niger</i>	1.31	-	-	-	-
7 →	<i>Halomonas BVR 1</i>(Present study)	12.023	<i>Halomonas BVR 1</i> (Present study)	9.15	<i>Halomonas BVR 1</i>(Present study)	11.11

Conclusions

This part of the thesis adds knowledge on the unique microbial diversity prevalent in electronic industry effluent, a man-made ecosystem. We report the isolation of a total of ten bacterial strains and two fungal strains from the effluent collected. These bacterial strains belonged to four different genera of *Bacillus*, *Halomonas*, *Pseudomonas* and *Kocuria*, while the fungal strains belonged

to the genus *Cladophialophora* and *Hypocrea*. No actinomycetes were observed in this effluent. These microbial strains, with an ability to thrive in complex metal rich environment add to the repertoire of natural microbial diversity. One of these microbes (*Halomonas BVR 1*) was chosen to remediate heavy metals based on its high level of metal tolerance. This microbe functions as an effective adsorbent for the remediation of heavy metals due to the presence of functional groups such as carboxyl, amine, hydroxyl and phosphate that facilitate metal binding and removal from aqueous solutions. The surface characterization of the adsorbent also showed binding of the heavy metals ion on to the surface of the adsorbent. Langmuir isotherm gave good fit to the experimental data with a maximum adsorption capacity of 12.023 mg g⁻¹, 11.11 mg g⁻¹ and 9.152 mg g⁻¹ for cadmium, zinc and lead respectively. This microbial adsorbent has more specificity to cadmium owing to its higher adsorption capacity in comparison to the other heavy metals. The adsorption was found to be significantly dependent on the pH, contact time and temperature. The adsorption favoured langmuir adsorption in case of cadmium and lead while it obeyed Freundlich isotherm for zinc adsorption. The pseudo second order kinetic model was best suited for the adsorption of all the metals and thermodynamics depicted the process to be spontaneous and exothermic. The highlight of the method is that although the effluent contains large concentrations of salts (chlorides, nitrates and phosphates), their effect on the adsorption of metal ions was negligible. Overall *Halomonas BVR 1* was able to remove cadmium upto a concentration of 100 mg l⁻¹. This biomass was able to remove lead and zinc upto a concentration of 80 mg l⁻¹ and 50 mg l⁻¹ respectively thus making the process economical and benign in environmental remediation.

CHAPTER III
ENHANCED METAL REMEDIATION BY IMMOBILIZATION OF
***Halomonas BVR 1* IN CHITOSAN AND GRAPHENE OXIDE**

Introduction

The most challenging feature in a successful biosorption experiment involves the selection of a promising biosorbent from the vast materials available in nature [Michalak et al, 2013]. Considerable research studies have been conducted to explore efficient biosorbents for the removal of heavy metals from effluents. For a full scale biosorption experiment, the biological materials with high metal binding capacity and high metal selectivity is essentially an important prerequisite. Various biomass from the fermentation wastes or activated sludge act as candidate biosorbents for heavy metal remediation [Das et al, 2008]. Recently, there has been a tremendous increase in the use of microorganisms belonging to diverse genera and groups as prominent biosorbents. Many bacterial species (e.g. *Bacillus*, *Pseudomonas*, *Streptomyces*, *Escherichia*, *Micrococcus* etc), have already been tested for metal uptake [Xu et al, 2012; Mameri et al, 1999; Joo et al, 2010]. However, there are several disadvantages associated with the direct use of bacterial biomass. Microbial biosorbents are basically small particles with low density, little rigidity and poor mechanical strength. Moreover, solid liquid separation problems, biomass swelling and difficulty in regeneration are other important demerits of using the biomass alone for metal removal [Das et al, 2008]. Nevertheless, a lot of variation occurs in the metal adsorption capacity with various adsorbents [Abas et al, 2013].

Immobilization technique is one of the key elements for the practical application of biosorption, especially by dead biomass, that enhances the adsorption capacity of the adsorbent. Nonetheless, the type of polymeric matrix determines the mechanical strength and chemical resistance of the final biosorbent to be utilized for successive sorption–desorption cycles.

There are several reports on the immobilized biosorbents which can be used in practical biosorption. Serbus et al. (1973) invented a new sorbent for treating heavy metal ions containing biological (telomic plants or algae) and water-insoluble polymeric parts. Pieschel et al. (2003) developed phosphorylated cellulose containing material by using phosphoric acid or ammonium phosphate in the presence of urea. As this modified biosorbent exhibited improved mechanical strength, this was used to treat heavy metals from aqueous solutions. Using ceramic material as substrate, Boddu et al. (2004) prepared an innovative composite biosorbent, chitosan-coated substrate. This proposed composite biosorbent was used to remove a number of metal ions including As(V), As(III), Cu(II), Cr(VI), Ni(II), Pb(II), and Hg(II) from aqueous solutions. A biosorption system composed of a bacterial biofilm of *Arthrobacter viscosus* supported in synthetic faujasite zeolite was also developed by Simões et al. (2008).

There have been several reports on the immobilized biosorbents, nevertheless we aimed at developing novel adsorbents by immobilizing our isolated bacteria on various polymeric matrices so as to remediate cadmium, lead and zinc with a higher adsorption capacity and low cost. This thesis focuses on preparation of biosorbent by immobilizing *Halomonas BVR 1* on various polymeric matrices such as chitosan, sodium alginate and graphene oxide and remediation of lead, cadmium and zinc. Among these, use of chitosan and Graphene Oxide (GO) as polymers for immobilization of *Halomonas BVR 1* and removal of cadmium, lead and zinc has been dealt with in detail in this chapter.

Chitosan is a green and biodegradable polymer endowed with amino and hydroxyl groups ideally suited for metal chelation. Furthermore, crosslinking with glutaraldehyde enhances the physical and biological stability by imparting mechanical strength to the polymer matrix especially during scale up operations in column studies. The deacetylated form of chitin i.e., chitosan has proved its worth towards metal complexation [Varma et al, 2004; Sowmya et al, 2011; Miretzky et al, 2009]. Chitosan is a renewable biopolymer composed of -2-amino-2-deoxy-d-glucopyranose and residual 2-acetamido-2-deoxy-d-

glucopyranose units. The free amine and hydroxyl groups present in the chitosan polymer chain interacts with various metal ions through ion exchange and/or chelation mechanism [Chakrabarty et al, 2014]. Additionally, this polymer is of paramount importance to researchers as their applications include properties such as biocompatible, biodegradable, non-toxic, hemostatic, bacteriostatic, fungistatic, anticancerogenic, anticholesteremic, antibacterial, mucoadhesive, selective and capable for the adsorbing metals, high in mechanical strength, cheap and susceptible to chemical modifications [Kocack et al, 2012]. In the present chapter, data representing the immobilization of the indigenously isolated *Halomonas BVR 1* in chitosan cross linked with glutaraldehyde for the remediation of metal cations has been elucidated (Fig. 3.1).

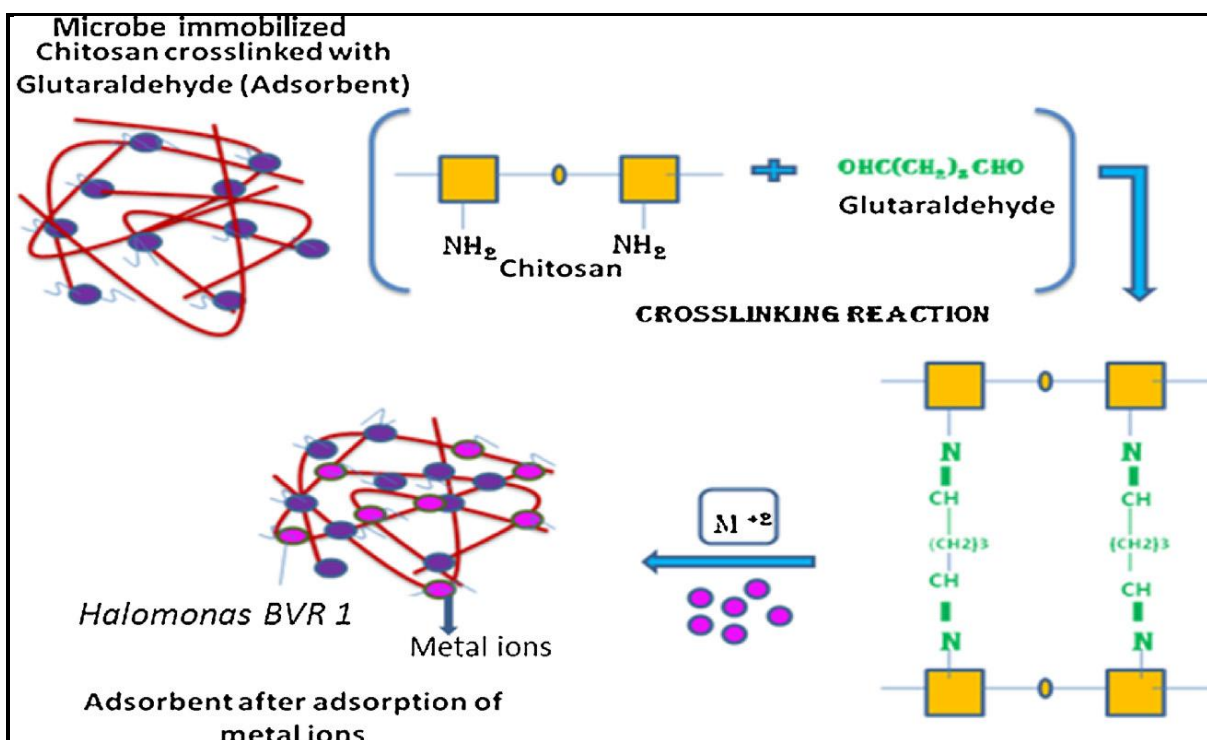


Fig 3.1: Illustration of the microbe immobilized in chitosan crosslinked with glutaraldehyde.

Graphene Oxide (GO) is another adsorbent with great potential for removing cationic heavy-metal contaminants from water [Chen et al, 2013]. The adsorption capacities of GO for lead (Pb^{2+}), cobalt (Co^{2+}), copper (Cu^{2+}), and cadmium (Cd^{2+}) are higher than the adsorption capacities of conventional adsorbents

such as activated carbon and iron-oxide nanoparticles [Mohapatra et al, 2012]. GO is a two-dimensional nanoparticle that can be readily produced by exfoliating naturally occurring graphite under oxidation [Amiri et al, 2016]. GO has emerged as a key member of the carbon family with regard to its excellent properties such as high surface area, good electrochemical [Sanchez et al, 2012], physicochemical and electronic properties and presence of various functional groups (epoxy groups, hydroxyl and carboxylic).

There has been considerable research in this field and various combinations of GO with other materials have been used as an adsorbent for adsorption of heavy metals. There have been several reports on graphene oxide based nanocomposites to remove heavy metals from wastewaters. Magnetic graphene oxide has been examined for the adsorption of metals [Hur et al, 2015]. Silica mesoporous graphene oxide has also been exploited for the removal of lead, cadmium and humic acid [Wang et al, 2013]. However, a careful literature survey shows that there has been no adsorbent prepared in combination with any microorganism for the remediation of the three metals mentioned above. Microbial reduction of GO is a facile process that involves low cost and biodegradable products that makes the method environmentally benign. Reduction of GO makes the material more hydrophilic enabling it to exfoliate in water [Ammar et al, 2016]. Considering such inherent properties of GO, we have embarked on its combination with a microorganism that in turn has numerous functional groups on its cell surface for its use as a bioadsorbent. This combination as a whole would have a synergistic effect in enhancing the adsorption of heavy metals individually and collectively as well.

An indigenous *Halomonas BVR1* strain immobilized in cross linked chitosan for adsorption of cadmium, lead and zinc.

SYSTEM 2: Halomonas BVR 1 immobilized in chitosan

This part of the chapter deals with the remediation of cadmium, lead and zinc using *Halomonas BVR 1* immobilized chitosan as a novel adsorbent.

Materials and Methods

Preparation of the biosorbent

Halomonas BVR 1, being a halophile was grown in a Luria Bertani (LB medium) containing NaCl at an overall concentration of 1.0 mol L⁻¹. Bacterial cells were harvested at the exponential phase by centrifugation at 7800 rpm for 10 min. The harvested cells were dried at 60°C and subsequently used for immobilization in chitosan. About 1.0 g of chitosan was dissolved in acetic acid (2%, v/v) and made into slurry. A 0.5 g of the powdered microbial cells was added and the mixture was stirred for 30 min. In order to foster the crosslinking, 5% glutaraldehyde in aqueous medium was added to chitosan in the ratio 40:1 (v/v) and stirred vigorously for 5 min. The resultant mixture was refrigerated at 4°C for 24 h to promote crosslinking and further washed to obtain neutral pH. The biomass immobilized chitosan obtained through the above procedure was dried in an oven at 60°C [Viswanathan et al, 2010] and used for biosorption experiments.

Adsorption Studies

Batch adsorption experiments were conducted at 25°C using 0.5 g of the immobilized biosorbent and equilibrated individually with 25 mL of varying concentrations of metal ion solutions (Cd, Pb and Zn)

ranging from 40 mg L⁻¹ to 500 mg L⁻¹ for isotherm studies. Similarly, 0.5 g of pure chitosan (without bacteria) was also equilibrated with varying concentrations of the metal ion solutions. The equilibrations were performed using an orbital incubator shaker (Biotechnics, India) at 120 min and 180 min respectively. The concentrations of metal ions in the solution phase were monitored by atomic absorption spectrometry (Shimadzu AA 7000). The equilibrium adsorption capacities (q_e) for the metal ions were obtained from the difference between the initial (C_o) and equilibrium concentrations (C_e) in the solution phase. Based on the optimum concentration at which effective adsorption was observed, 80 mg L⁻¹ cadmium and 40 mg L⁻¹ lead at pH 7.0, 60 mg L⁻¹ zinc at pH 6.8 were chosen as the initial metal ion concentrations for the thermodynamics and kinetic studies respectively.

Physicochemical Characterisations of the biosorbent

The methodology for the processing of sample for SEM-EDAX and FTIR analysis is the same as mentioned for system 1 in chapter 2.

Results and discussion

SEM-EDAX analysis

The SEM images of the microbe immobilized in cross-linked chitosan taken at 300x magnification showed characteristic co-precipitation of the metal ions in the form of salt like deposition over the biosorbent surface post heavy metal adsorption (**Fig. 3.2 B-D**). The biosorbent morphology appeared smooth before the adsorption process (**Fig. 3.2 A**). The optical images (**Fig. 3.2E & 3. 2F**) clearly show that the biosorbent has the potential to accommodate the metal ions. The images were also acquired after adding dithizone as a spot colouring agent [Michalak et al, 2013] to the biosorbent before and after metal adsorption. Accordingly cadmium, lead and zinc which are known to form stable metal chelates with dithizone gave a characteristic pink colour to the biosorbent surface. This suggests that the metal ions

were adsorbed effectively on the microbe immobilized chitosan surface through interaction with the various functional groups.

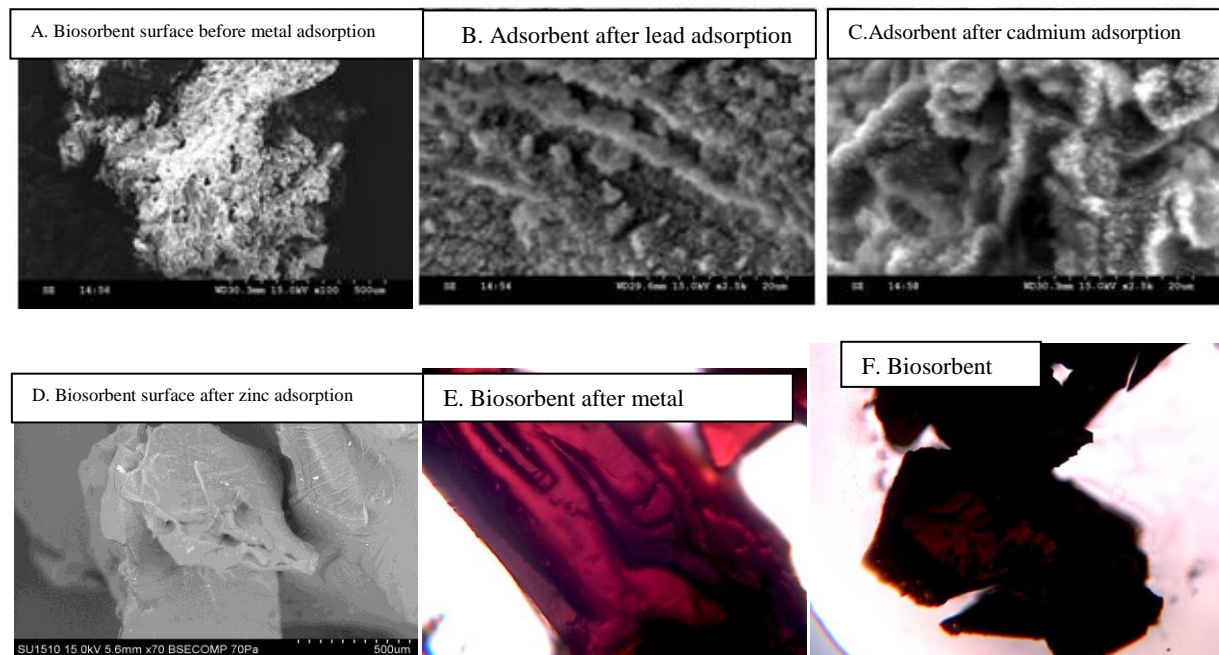


Figure 3. 2: SEM and optical images of the adsorbent before and after the metal adsorption

EDAX analysis

The EDAX spectral analysis (**Fig. 3.3 A- 3.3 D**) of *Halomonas BVR 1* microbe in chitosan shows the presence of C, N, O and Ca as distinct peaks. The decrease in the calcium ion concentration is evident from the disappearance of Ca peak after the adsorption of the respective metal ions. The decrease in intensity of the Ca peaks, as observed in the system 1 and emergence of more prominent peaks due to metal adsorption were also evident from the EDAX spectrum.

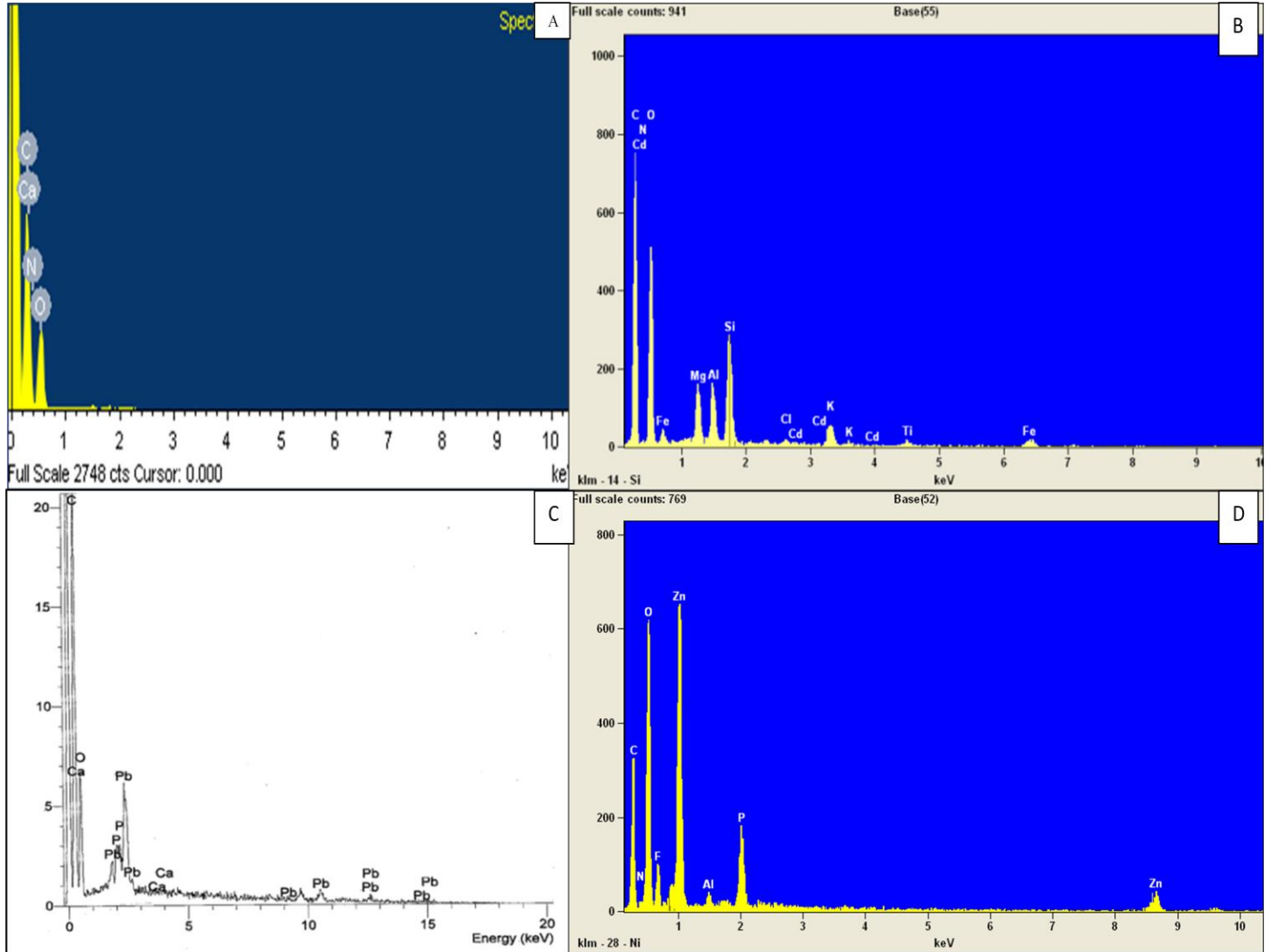


Figure 3.3 A) EDAX analysis of the adsorbent B) EDAX analysis of the adsorbent after Cadmium adsorption C) EDAX analysis of the adsorbent after lead adsorption D) EDAX analysis of the adsorbent after Zinc adsorption

FTIR spectral characterization

The FTIR spectra of chitosan and microbe immobilized chitosan before and after adsorption are shown in **Fig 3.4A**. The broad band around 3440 cm^{-1} corresponds to the $-\text{NH}$ and $-\text{OH}$ stretching vibrations [Sun et al, 2008]. The C-H stretching vibration was observed at 2950 cm^{-1} . The C-H bending vibrations could be identified by a prominent peak at 1424 cm^{-1} . The peak at 1152 cm^{-1} could be attributed to C-O vibration of

the polysaccharide. The peak at 1595 cm^{-1} corresponds to NH amide band II vibrations. Certain characteristic changes were observed after immobilization with the biomass. The emergence of a peak at 1659 cm^{-1} indicates the C=O in amide group [Chen et al, 2011] in the immobilized biosorbent. The biosorbent also showed a shift in the amino peak from 1595 cm^{-1} to 1591 cm^{-1} [Kocak et al, 2012]. The appearance of peak at 1627 cm^{-1} is indicative of C=N imine group of the glutaraldehyde cross linked chitosan. After the adsorption of metal ions, the shift in wave number from 1659 cm^{-1} to 1648 cm^{-1} shows the effectiveness of interaction of lead and cadmium with the C=O of the amide (CONH) group. The amide functionality and the involvement of nitrogen lone pair from the NH_2 group towards the binding of cadmium and lead were evident from the shifts in the peak from 1627 cm^{-1} to 1634 cm^{-1} respectively [Chen et al, 2009; George et al, 2013]. FTIR spectrum of zinc also depicts the involvement of groups such as NH_2 group which is clearly seen by the spectral shift from 1627 cm^{-1} to 1634 cm^{-1} [Chen et al, 2009]. The appearance of peak at 1152 cm^{-1} is also indicative of the C-O group involved in zinc binding **Fig 3.4B**. All these changes shows the effective binding of the metal ions on the *Halomonas* immobilized chitosan biosorbent surface.

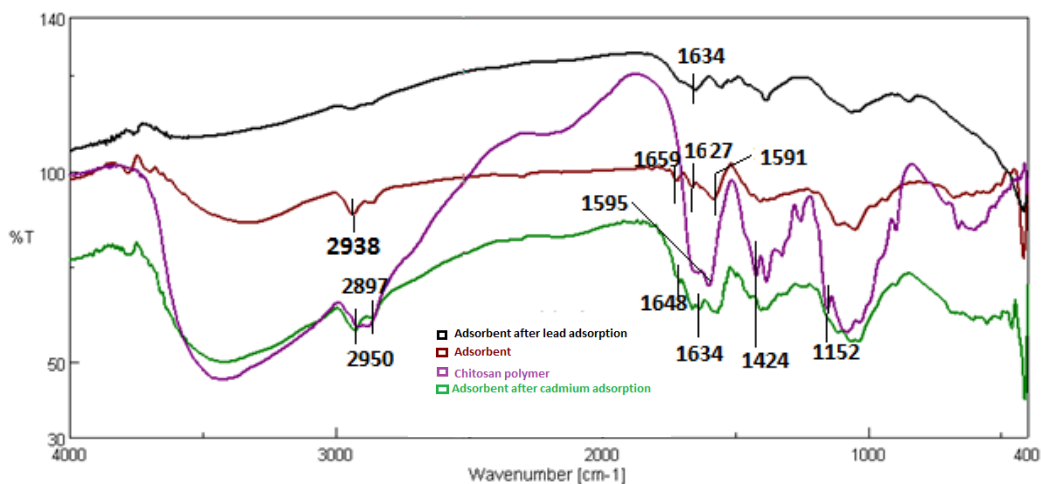


Figure 3. 4A) FTIR spectrum of the immobilized adsorbent before and after the adsorption of lead and cadmium.

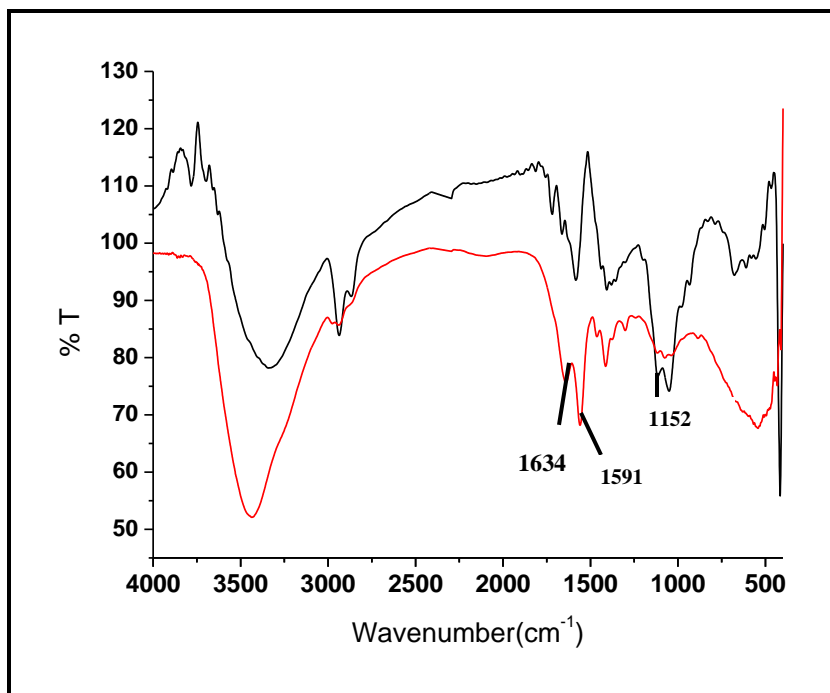
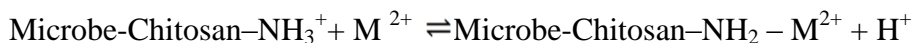


Figure 3. 4B) FTIR spectrum of the adsorbent before (black) and after (red) the adsorption of zinc.

Effect of pH on adsorption.

The influence of pH is a key parameter that needs to be optimized in adsorption processes. The adsorption of metal cations increases with pH and the maximum adsorption was observed near neutral pH. The protonation of amino group in the biosorbent and its subsequent interaction with the metal ions could be expressed as



With increase in pH of the aqueous solution, the deprotonation of the amino groups are more probable with a corresponding decrease in the number of H^+ ions. This leads to an overall decline in the competition of active binding sites on the biosorbent. However, at an acidic pH, the biosorbent acts as a weak base and hence the amino groups readily get protonated using the protons available in the aqueous solution. At low pH, the protons would compete with the cationic metal ions for active adsorption sites leading to a reduction

in the adsorption (Bohli et al, 2013). The metal adsorptions were found to be quite effective (**Fig 3.5**) in the pH range 5-7 where the competition from the H^+ is relatively low. The availability of lone pair of electrons on the nitrogen atom of the amine functionality also contributes to the interaction with metal cations near neutral pH.

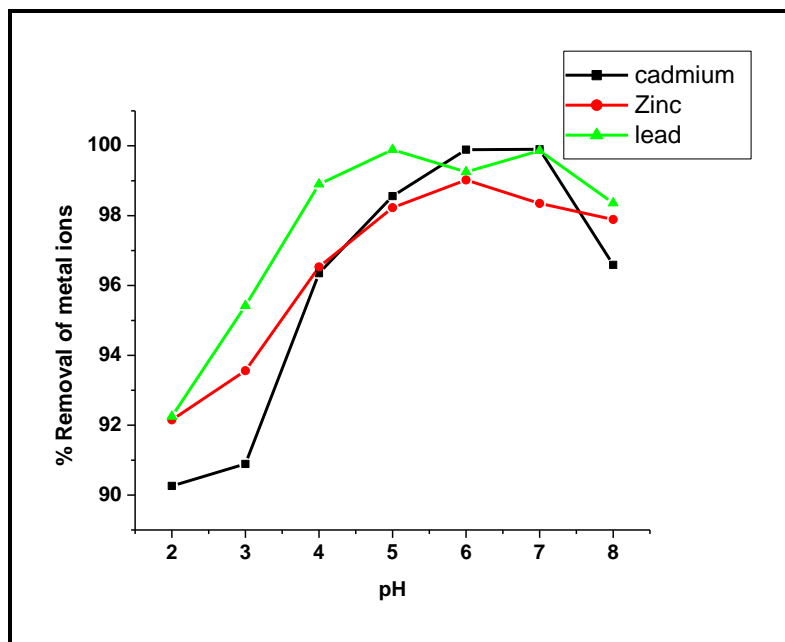


Figure 3.5: Percentage of metal removal at different pH

Isotherm studies

The detailed theory and methodology of adsorption isotherms, kinetics and thermodynamics is given in Appendix I.

Langmiur isotherm

The maximum adsorption capacity (q_0) for cadmium, lead and zinc obtained from the plot of C_e against C_e/q_e (**Fig. 3.6A-D**) were found to be 24.15 mg g^{-1} and 23.88 mg g^{-1} and 42.53 mg g^{-1} respectively .

The R_L (in the range 0-1) values were found to be 0.0820, 0.128 and 0.322 for cadmium, lead and zinc signifying a favorable and reversible adsorption process [Sun et al, 2013].

Freundlich isotherm

The value of the constants K_f and n from the Freundlich plot of $\log C_e$ against $\log q_e$ (**Fig. 3.6A-D**) were found to be $2.02 \text{ mg}^{1-1/n} \text{ g}^{-1} \text{ L}^{1/n}$ and 2.38 for cadmium, $2.365 \text{ mg}^{1-1/n} \text{ g}^{-1} \text{ L}^{1/n}$ and 1.69 for lead and $2.74 \text{ mg}^{1-1/n} \text{ g}^{-1} \text{ L}^{1/n}$ and 1.04 for zinc respectively.

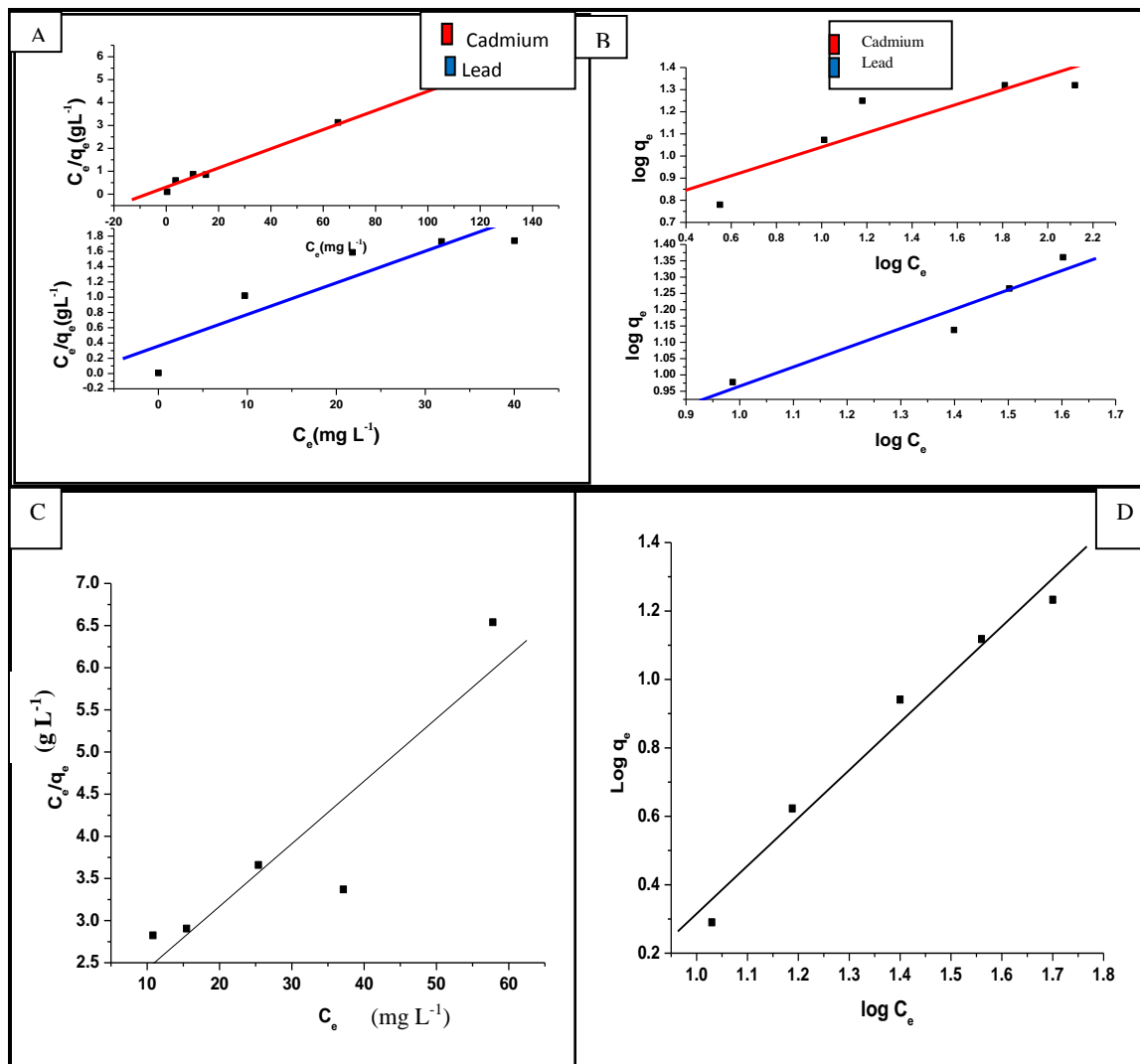


Figure 3.6 Isotherm models A) Langmuir plot for cadmium and lead B) Freundlich plot for cadmium and lead metal ions. C) Langmuir plot for zinc adsorption D) Freundlich plot for zinc adsorption

The equilibrium adsorption data for cadmium suggests the formation of a monolayer following the Langmuir isotherm and this is also evident from the low chi square (χ^2) value (0.222). This feature can be explained by considering the ionic radii of cadmium, lead and zinc. Since, the ionic radius of cadmium and zinc is less than lead (Cd^{2+} (0.97 Å) Pb^{2+} (1.20 Å) and Zn^{2+} (0.74 Å)), a minor difference exists between the neighbouring sites in the biosorbent thus favouring Langmuir isotherm [Molyneux et al, 1964]. However, the equilibrium data for lead and zinc fits well with the Freundlich isotherm model. The mean free energies for cadmium, lead and zinc adsorption obtained from the Dubinin-Radushkevich (D-R) isotherm model ($E_{\text{DR}} = 1/ (2\beta)^{-0.5}$) were found to be 1.98 kJ mol⁻¹, 10.20 kJ mol⁻¹ and 0.374 kJ mol⁻¹ respectively. The isotherm parameters obtained from the above three models are summarized in **Table 3.1**. The D-R model suggests that physisorption phenomenon accounts for the uptake of cadmium and zinc, while an ion exchange mechanism is more probable in case of lead adsorption. Since in physisorption, the energy of interaction between the cadmium ions and the biosorbent is marginally higher than the energy of condensation of the adsorbate, less activation energy is needed for adsorption [Guibel et al, 2004]. Furthermore, in case of lead, the formation of a metal-ligand complex through an electrostatic or coordination interaction is also in accordance with the physico-chemical adsorption phenomenon.

Table 3. 1 Isotherm parameters obtained from various models for microbe immobilized chitosan as biosorbent

S.No	Isotherm models	Parameters	Values		
			Cadmium	Lead	Zinc
1.	Langmuir	q_0 (mg g ⁻¹)	23.88	24.154	12.535
		b (L mg ⁻¹)	0.136	0.1149	0.03
		R_L	0.128	0.0820	0.322
		r^2	0.98	0.820	0.645
2.	Freundlich	K_F (mg ¹⁻ⁿ g ⁻¹ L ^{1/n})	2.02	2.365	2.747
		n	2.38	1.691	1.043
		r^2	0.81	0.925	0.996
		q_m (mg g ⁻¹)	14.497	12.590	8.046

3.	Dubinin-Radushkevich	β	0.127	0.004	3.573
		$E_{DR} \text{ (kJ mol}^{-1}\text{)}$	1.988	10.204	0.374
		r^2	0.646	0.518	0.812

Kinetics of adsorption

The approach to adsorption kinetics could be explained through the following modes:-

- Film diffusion of metal ions to the external surface of the microbe immobilized chitosan matrix.
- Particle diffusion through the pores of microorganism immobilized biosorbent.
- Internal diffusion of Cd^{2+} , Pb^{2+} and Zn^{2+} into the biosorbent.

The particle diffusion followed by an internal diffusion of the metal ions on the biosorbent matrix plays a key role in understanding the kinetics of adsorption. The adsorption was quite effective since the equilibrium was reached within 2-3 hour duration in case of lead and cadmium adsorptions. However, there were slight differences in the exact equilibrium time attained among the three metals [Vold et al, 2003]. Zinc adsorption attained equilibrium within 3-5 hrs with an adsorption capacity lower than the other two metals. This could be associated with the difference in the ion exchange affinities of metal ions. The probability of lead ions having affinity towards the biosorbent is higher than cadmium. With increase in affinity, the rate of adsorption increases and this leads to a marginal decrease in the pH of the solution. The decrease in pH after the adsorption of lead was more as compared to cadmium. Additionally, lead also has a higher ionic radii and this is evident from the differences between the polarizability of the metal ions. This difference accounts for the higher affinity of lead towards the microbe immobilized biopolymer biosorbent. In accordance with the higher affinities, lead reaches equilibrium faster (2 hours) than cadmium (3 hours). The metal adsorption favours pseudo second order kinetics in case of all the three metals.

The experimental and calculated equilibrium adsorption capacity (q_e) values from the pseudo second order model (**Fig. 3. 7 A-C**) were found to be 4.9 mg g^{-1} and 5.68 mg g^{-1} for cadmium, 4.9 mg g^{-1} and 5.02 mg g^{-1} for lead and 3.1 mg g^{-1} and 3.7 mg g^{-1} for zinc respectively. The kinetic parameters (**Table 3.2**) show the applicability of second order model with a high regression coefficient.

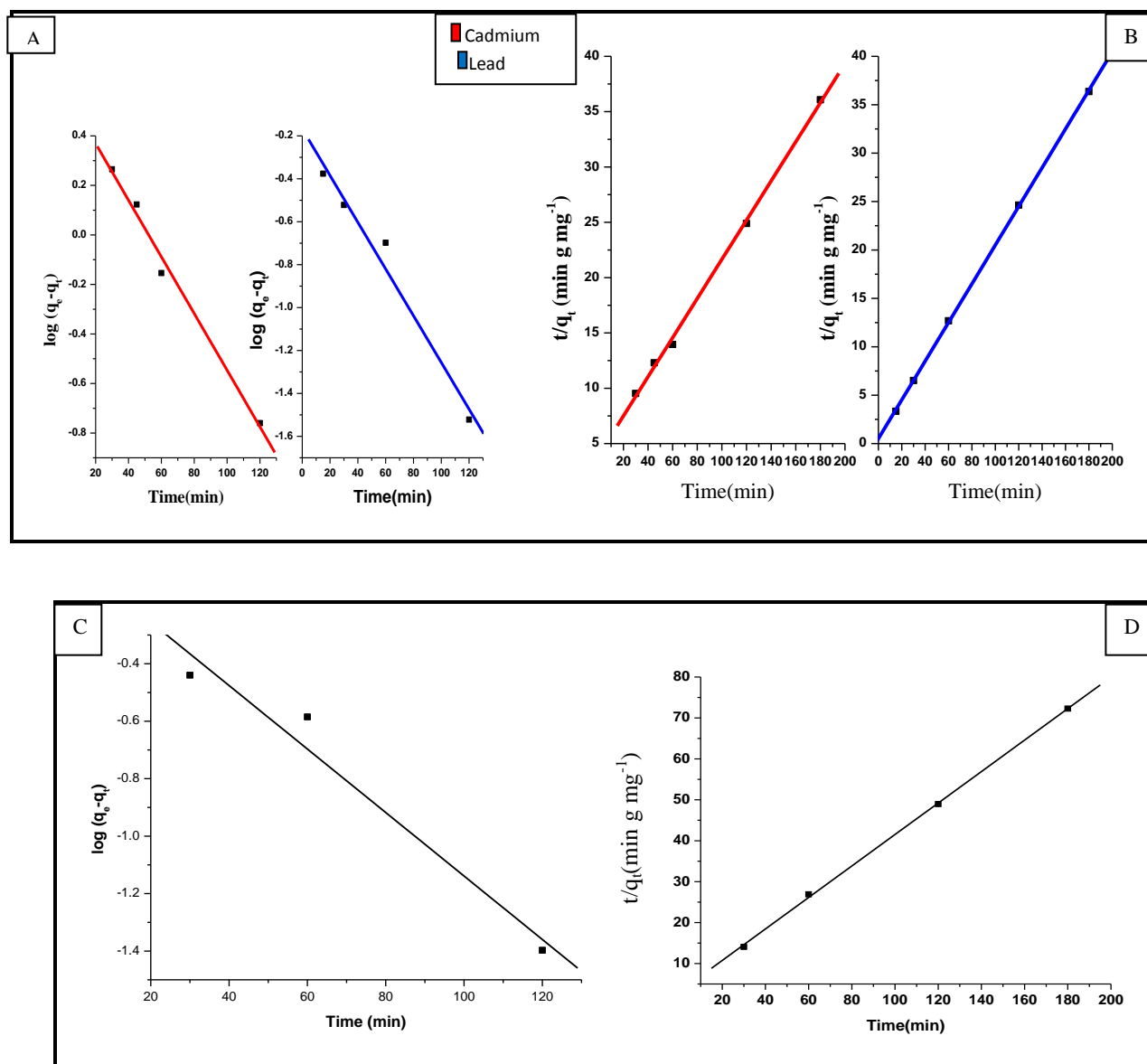


Figure 3.7: A) Pseudo first order kinetics for lead and cadmium adsorption B) Pseudo second order kinetics for lead and cadmium adsorption. C) Pseudo first order kinetics for Zinc adsorption D) Pseudo second order kinetics for Zinc adsorption.

The Weber and Morris intraparticle diffusion model for Cd^{+2} , Pb^{+2} and Zn^{+2} were also studied using the expression [Weber et al, 1963]

$$q_t = k_{\text{int}} \sqrt{t} + C$$

where k_{int} is the intra-particle diffusion constant and q_t is the amount of heavy metals adsorbed at time t . The **Fig. 3.8 A-C** shows the plot of q_t versus $t^{0.5}$ for a particular concentration of lead (40 mg L^{-1}), cadmium (80 mg L^{-1}) and zinc (50 mg L^{-1}). The multilinear fit obtained for cadmium shows that the first portion of curve relates to the instantaneous surface adsorption followed by intraparticle diffusion in the second portion. In case of lead and zinc, the plot shows a good linear fit with a definite intercept (**Table 3.2**). These plots reflect boundary layer as well as diffusion controlled adsorption processes.

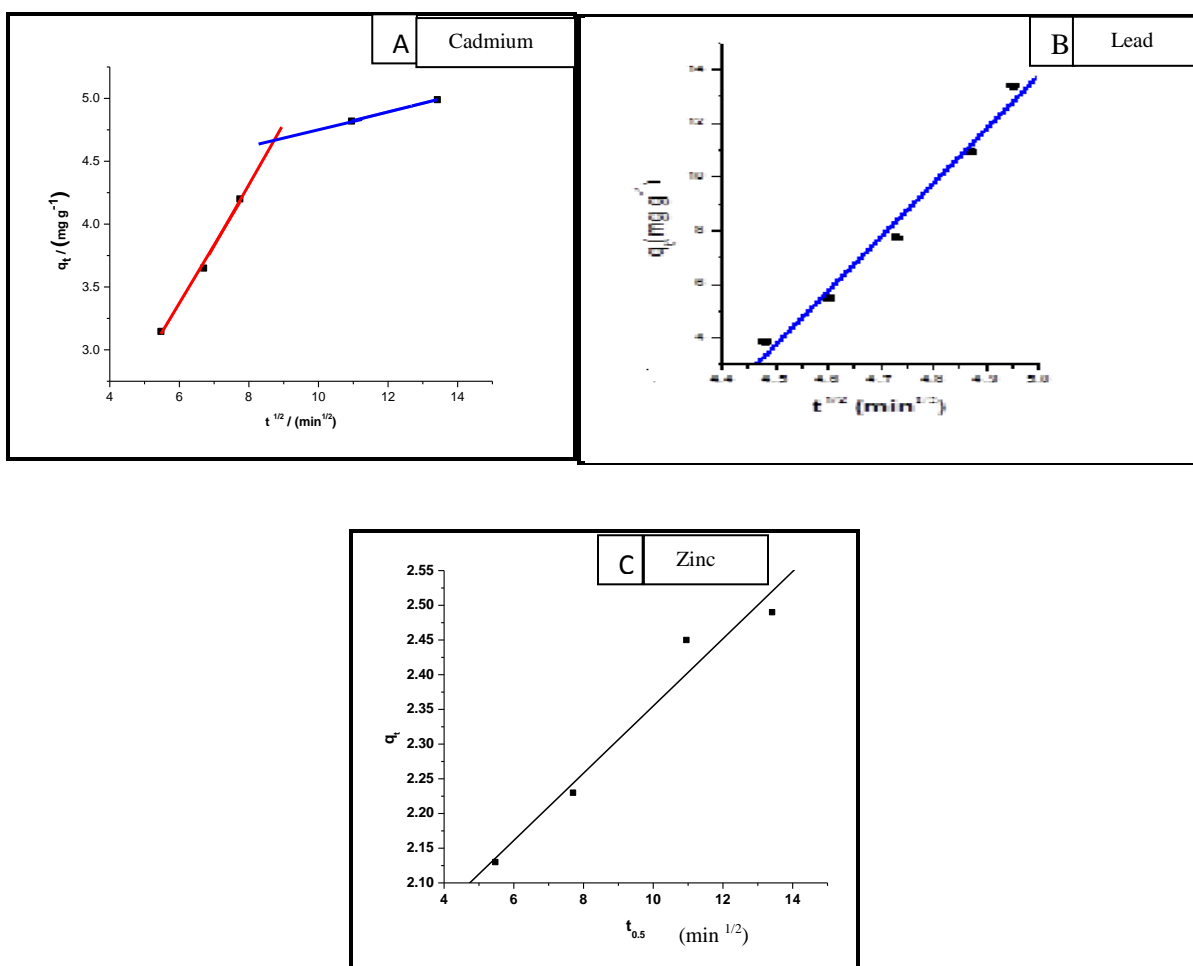


Figure 3.8) Intra-particle diffusion plot of A) cadmium B) lead and C) zinc.

Table 3.2 Kinetic and Intraparticle rate constant data for the adsorption of metal ions.

Metal ion	Second order rate Constant k_2 [g mg⁻¹ min⁻¹]	Regression Coefficient (r²)	First order Rate constant k_1 [min⁻¹]	Regression Coefficient (r²)	Intra particle rate constant k_{int} [mg g⁻¹ min^{-1/2}]
Cadmium	0.007	0.99	0.026	0.98	0.069
Lead	0.07	0.98	0.023	0.974	20.166
Zinc	0.035	0.999	0.026	0.854	0.046

Thermodynamics of adsorption

The energetics of biosorption could be described through the study of various thermodynamic parameters involving free energy (ΔG^0), entropy (ΔS^0) and enthalpy (ΔH^0) changes.

The free energy changes were accordingly found to be -11.77, -11.76, -10.90 and -7.75 kJ mol⁻¹ for the biosorption of lead at 293, 303, 313 and 323 K respectively. Likewise, the ΔG values for cadmium and zinc were also negative at these temperatures (**Table 3.3**). The diffusion of metal ions [Reddad et al, 2002] from the aqueous solution on the polymeric interface is more probable near room temperature. The adsorption was thermodynamically feasible and spontaneous as indicated by the negative free energy values. The enthalpy (ΔH°) and entropy (ΔS°) of biosorption were estimated from the slope and intercept of the plot of $\ln K$ against $1/T$ (**Fig. 3.9**). The enthalpy of biosorption (ΔH°) for the cadmium, lead and zinc systems were found to be -43.6 kJmol⁻¹, -50.04 kJ mol⁻¹ and 11.6 kJ mol⁻¹ respectively. Since, the Gibb's free energy becomes less negative with temperature, the degree of spontaneity decreases with increase in temperature for both the metal ions. The biosorption process was thermodynamically favourable and exothermic resulting in negative ΔG° and ΔH° values. The ΔS° values for adsorption process were also negative (-

118.80 J mol⁻¹ K⁻¹ , -128.63 J mol⁻¹ K⁻¹ and -78.5 J mol⁻¹ K⁻¹) (Table 3.3) for cadmium, lead and zinc respectively suggesting reduced randomness at the solid - solution interface.

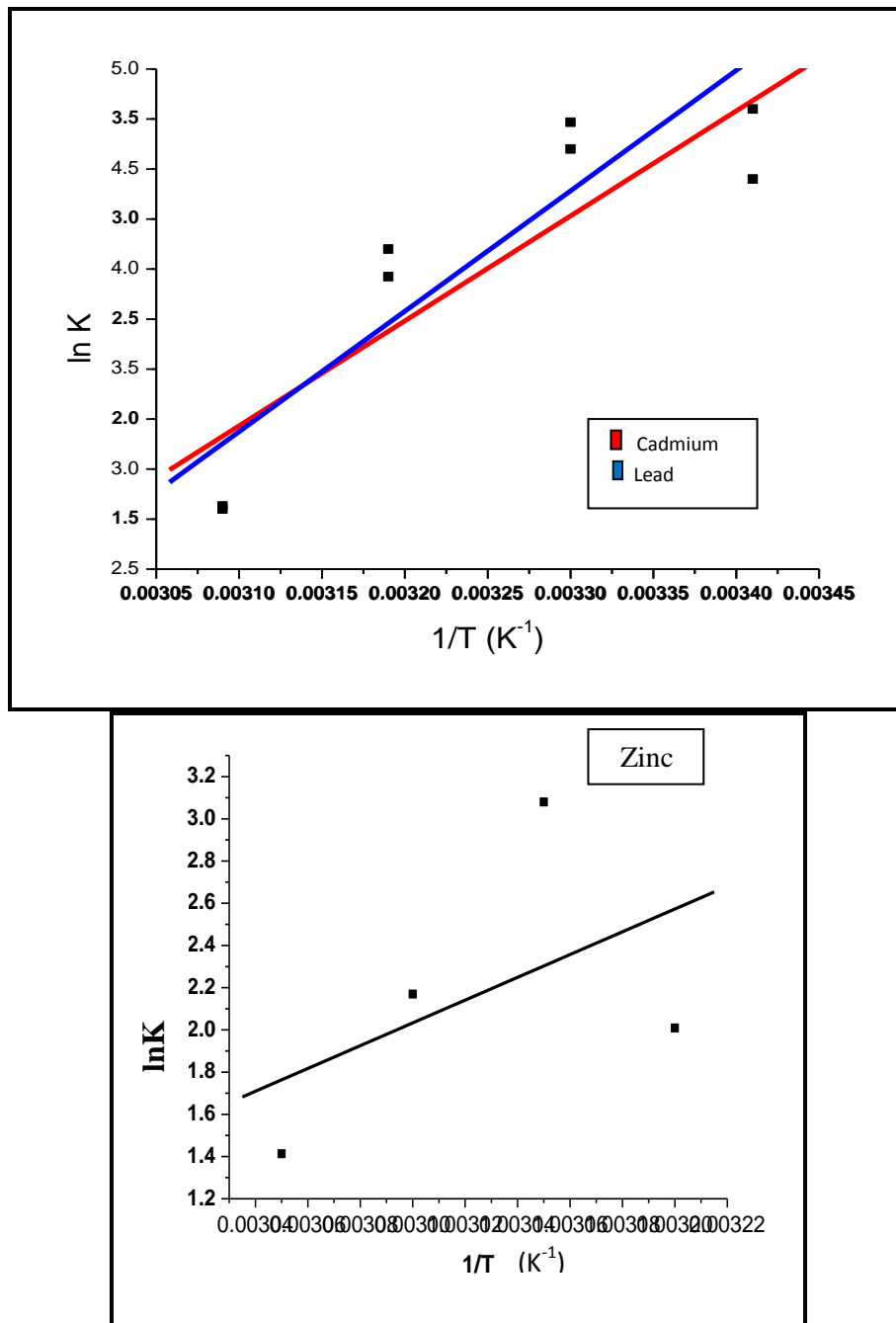


Figure. 3.9. Van't Hoff plot obtained for the adsorption of metal ions on the microbe immobilized chitosan surface.

Table 3.3 Thermodynamic data for the adsorption of metal ions.

Metal ion	Temperature /Kelvin	ΔG° [kJ mol⁻¹]	ΔS° [J mol⁻¹ K⁻¹]	ΔH° [kJ mol⁻¹]
Cadmium	293	-7.99	-118.80	-43.617
	303	-8.76		
	313	-7.057		
	323	-4.202		
Lead	293	-11.77	-128.63	-50.043
	303	-11.76		
	313	-10.90		
	323	-7.75		
Zinc	283	-4.681	-78.45	-11.66
	293	-5.803		
	303	-8.580		
	313	-12.20		
	323	-8.004		

Effect of interfering ions on adsorption of metal ions

The influence of certain cations and anions that could be commonly associated with the electronic industry effluents were investigated at different concentrations. Ions such as zinc and cobalt did not interfere up to 50 mg L⁻¹ level, while nickel and iron caused a reduction in the adsorption of lead and cadmium beyond 60 mg L⁻¹ concentration (**Table 3.4**). Anions such as chloride and sulphate did not affect the adsorption of lead and cadmium when their concentration levels were in the range 10-60 mg L⁻¹. Nitrate and phosphate caused a decrease in the percentage adsorption of lead and cadmium beyond 70 mg L⁻¹. In case of, zinc adsorption, presence of lead caused an inhibition in the metal adsorption at a concentration of 50 mg L⁻¹. Similar to the earlier system, sulphates were the major anions that interfered with the metal adsorption beyond 60 mg L⁻¹ and caused a reduction upto more than 10 percentage. Overall the anions did

not have much effect on the adsorption except for sulphates presence of cations beyond 70 mg L⁻¹ decreased the adsorption of cations.

Table 3.4: Effect of diverse ions on the adsorption of metal ions

Concentration of Anions mg l ⁻¹	% adsorption of cadmium	% adsorption of lead	% adsorption of zinc	Concentration of Cations mg l ⁻¹	% adsorption of cadmium	% adsorption of lead	% adsorption of zinc
SO ₄ ²⁻ (60)	89±0.6	90±0.2	92±0.7	Zn ²⁺ (100)	NI*	NI*	NI*
PO ₄ ³⁻ (70)	96±0.9	93±0.8	NI*	Ni ²⁺ (60)	94±0.3	95±1.2	NI*
Cl ⁻ (60)	NI*	NI*	NI*	Pb ²⁺ (50)	NI*	NI*	93±0.6
NO ₃ ⁻ (70)	92±0.7	95±1.5	NI*	Mn ²⁺ (60)	NI*	NI*	NI*
				Fe ²⁺ (60)	93±0.3	94±1.2	NI*
				Mg ²⁺ (50)	NI*	NI*	NI*
				Cd ²⁺ (60)	NI*	95±0.7	NI*

NI*: No Interference

Column studies

Experiments to treat metal cations from a larger volume were studied by column studies. For this purpose, 2.5 g of the bioadsorbent was packed in the column of 2 cm x 4 cm with the overall concentration of the metal cations maintained at 150 mg L⁻¹. The maximum removal efficiency (96%) was attained with a flow rate of 2mL min⁻¹. The percentage adsorption of the metal ions decreased beyond 350 mL volume of the sample loaded.

Comparison with other strains

The proposed method for removal of cations was compared in terms of the maximum adsorption capacity with other polymeric matrices involving chitosan. The results showed that *Halomonas BVR 1* immobilized chitosan exhibits good adsorption capacity as evident from the comparison shown in **Table 3.5**.

Table 3. 5: Comparison of various adsorbents with their adsorption capacities.

Adsorbent	Heavy metal	Adsorption capacity (mg)	Reference
Chitosan/cotton fibres	Cadmium	15.74	Zhang et al, 2008
Alginate chitosan	Cadmium	6.63	Gotoh et al, 2004
<i>Halomonas BVR 1 immobilized in chitosan</i> →	Cadmium	23.88	<i>Present study</i>
Chitosan/cellulose	Lead	26.31	Sun et al,2009
Chitosan/sand	Lead	12.32	Wan et al, 2010
Chitosan immobilized on bentonite	Lead	15.0	Futalan et al, 2012
<i>Halomonas BVR 1 immobilized in chitosan</i> →	Lead	24.15	<i>Present study</i>
Zeolite, clinoptilolite	Zinc	0.5	Barakat et al, 2011
Pecan shells activated carbon	Zinc	13.9	Barakat et al, 2011
magnetic chitosan modified with diethylenetriamine	Zinc	0.35	Barakat et al, 2011
<i>Halomonas BVR 1 immobilized in chitosan</i> →	Zinc	12.53	<i>Present study</i>

Regeneration of biosorbent

A preliminary study for regeneration of the biosorbent showed that 0.5 m mol L^{-1} EDTA has the potential to complex the metal ions and desorb them effectively (**Fig. 3.10**). A total of 30 mL was used to desorb the cations upto two cycles beyond which the regeneration efficiency gradually reduced. Use of EDTA helps in metal chelation, thereby allowing the bound metal to leave the column and provide free available binding sites for the incoming metal ions.

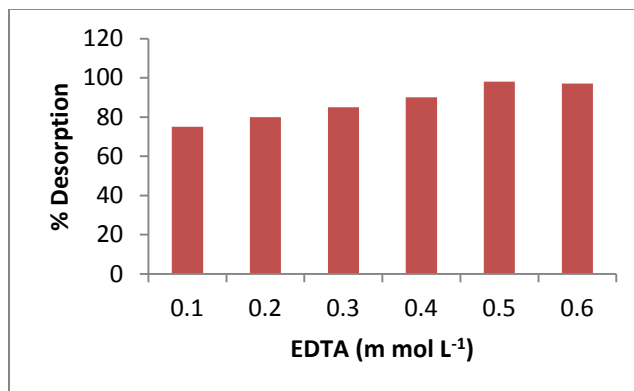


Figure 3.10. Effect of eluent on desorption

Synergistic effect of Reduced Graphene-Oxide and a bacterial species *Halomonas BVR 1* for the sequestration of lead, cadmium and zinc.

SYSTEM 3: Halomonas BVR 1 immobilized in Graphene Oxide

Our objective in this part of the work was to develop a novel bioadsorbent by functionalization of graphene oxide with *Halomonas BVR 1*. The utility of this adsorbent for the remediation of lead, cadmium and zinc has been dealt with in detail. The mechanistic interaction between the metal ions and the adsorbent has also been looked into in this part of the chapter.

Materials and Methods

Preparation of the biosorbent

For the synthesis of GO an improvization of the Hummer's method was –used [Marcano et al, 2010]. According to this about 1.5 g of graphite powder was taken and gradually added to a mixture of concentrated H₂SO₄/H₃PO₄ (9:1). This reaction was constantly stirred for 12h with simultaneous warming to 35-40 °C. This was followed by heating to 60 °C. The above reaction mixture was cooled to room temperature and slowly poured in ice cold peroxide solution. Subsequently, the mixture was centrifuged at 4000 rpm for 4h and the supernatant was discarded. The pelletized material obtained after centrifugation was thoroughly washed with a series of solutions; 200 mL of water followed by 200 mL of 30% HCl and 200 mL of ethanol. After every wash, the filtrate was centrifuged at 4000 rpm for 2h and the supernatant was decanted. The material obtained after centrifugation was kept for drying at 30 °C in vacuum oven (Biotechnics, India) for 48h.

0.5g GO powder obtained from the above step was dispersed in 0.5g *Halomonas BVR 1* bacterial culture [Wang et al, 2011]. This reaction mixture was stirred at 120 rpm for 1h. After the thorough dispersion of GO in microbial culture, the mixture was centrifuged at 7800 rpm for 10 min. The pellet obtained was washed with Milli Q water and dried. This was ground as a smooth powder and used as a biosorbent. The obtained biosorbent is a combination of rGO (due to the action of live *Halomonas BVR 1* on the Graphene Oxide) and the microbial cells.

Physicochemical Characterizations of the adsorbent

The methodology followed for the processing of adsorbent for the SEM- EDAX and FTIR analysis is the same as mentioned for the system 1 in chapter 2.

Results and discussion

SEM-EDAX Analysis.

The SEM images after the adsorption of metal cations showed characteristic changes in the surface morphology. Salt like deposition was observed on the adsorbent after the adsorption of all three metals (**Fig. 3.11A-D**). The adsorbent surface indicated bright spots after metal adsorption.

The EDAX analysis also showed characteristic peaks proving the immobilization of the microbe on the GO surface. Certain peaks like sulphur and nitrogen at 2.3 keV and 0.5 keV respectively (**Fig. 3.11**) could be a contribution from the bacterial cell wall [Petrone et al, 2011]. Other peaks observed in the adsorbent were carbon and oxygen specific to rGO along with the respective metal ions (**Fig. 3.11**). This clearly indicates that the metal ions have been successfully loaded on the microbe immobilized rGO.

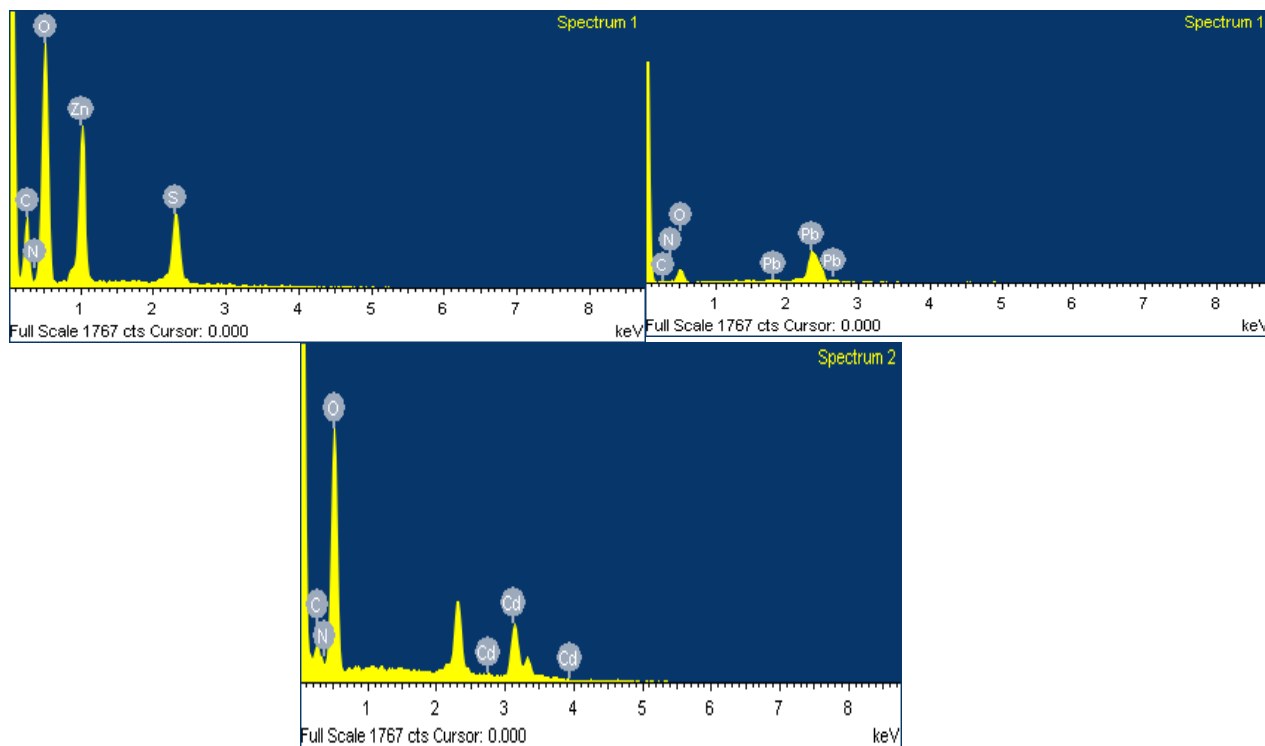
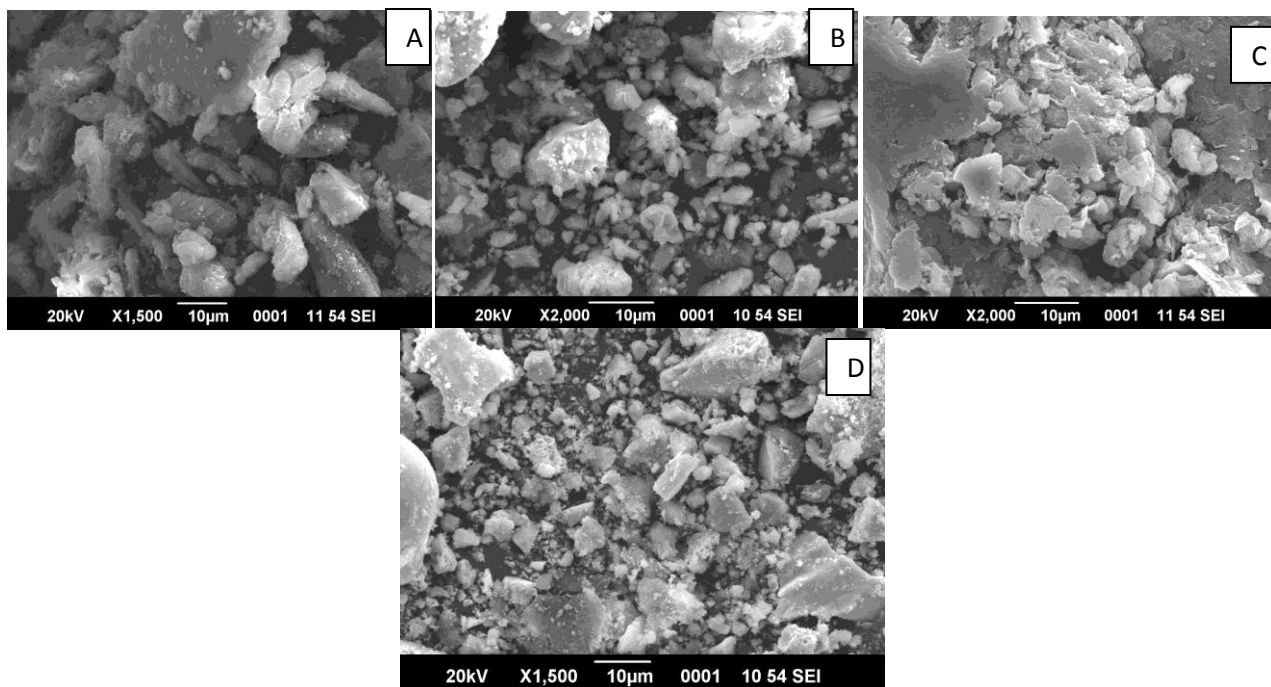


Figure 3.11. SEM A) Adsorbent after cadmium adsorption; B) Adsorbent after lead adsorption ; C) Adsorbent after zinc adsorption; D) Adsorbent before adsorption) and EDAX analysis of the adsorbent after adsorption.

XRD analysis

The X-ray diffraction (XRD) pattern of GO, GO-Microbe adsorbent before and after the adsorption of metal ions were obtained using a Bruker AXS D8 Advance XRD diffractometer with Cu K α radiation source ($\lambda = 1.5406 \text{ \AA}$) source energized at 40 KV and 35 mA with step size and time of 0.020° and 65.6 s respectively. The samples were scanned at the rate $2.0^\circ \text{ min}^{-1}$ in the 2θ range 5° to 100° .

The rGO with the microbial culture showed an intense diffraction peak at around $2\theta = 26.38^\circ$ that is characteristic of reduced graphene oxide (**Fig. 3.12**) [Mishra et al, 2014]. A plausible mechanism that can be explained to describe the appearance of this peak is the microbial reduction of GO to partially reduced GO. The intense characteristic crystalline peak at 10.54° corresponding to GO disappeared with a simultaneous generation of a broad peak starting from 24° to 30° indicative of microbial reduction of GO. This broad peak is also indicative of loss of long range order in graphenes [Kaniyoor, 2010]. The live cultures of *Halomonas BVR 1* would reduce the GO in anaerobic atmosphere with a simultaneous consumption of oxygen by the growing cells. The calculated d-spacing in case of the adsorbent before metal adsorption was higher (3.39 \AA) than the d-spacing for the adsorbent after metal adsorption (2.52 \AA , 2.54 \AA and 2.89 \AA for lead, zinc and cadmium respectively). This indicates that the metal ions have efficiently interacted with the functional groups (OH, COOH, NH₂) present on the microbe-rGO surface [Zhao et al, 2011]. The interaction of the metal ions results in decreased d-spacing values. Furthermore, it also suggests the removal of any oxygen moiety from the interlayer GO sheets. From the spectra it was deduced that the adsorbent was crystalline in nature due to the sharp high intensity Bragg peaks. The average crystallite size of the adsorbent before the metal adsorption was calculated to be 39.4nm. The size significantly reduced to

24.9nm, 26.4nm and 34.1nm after lead, cadmium and zinc adsorption, indicative of effective interaction of the metal ions with the rGO-microbe adsorbent [Susan et al, 1984].

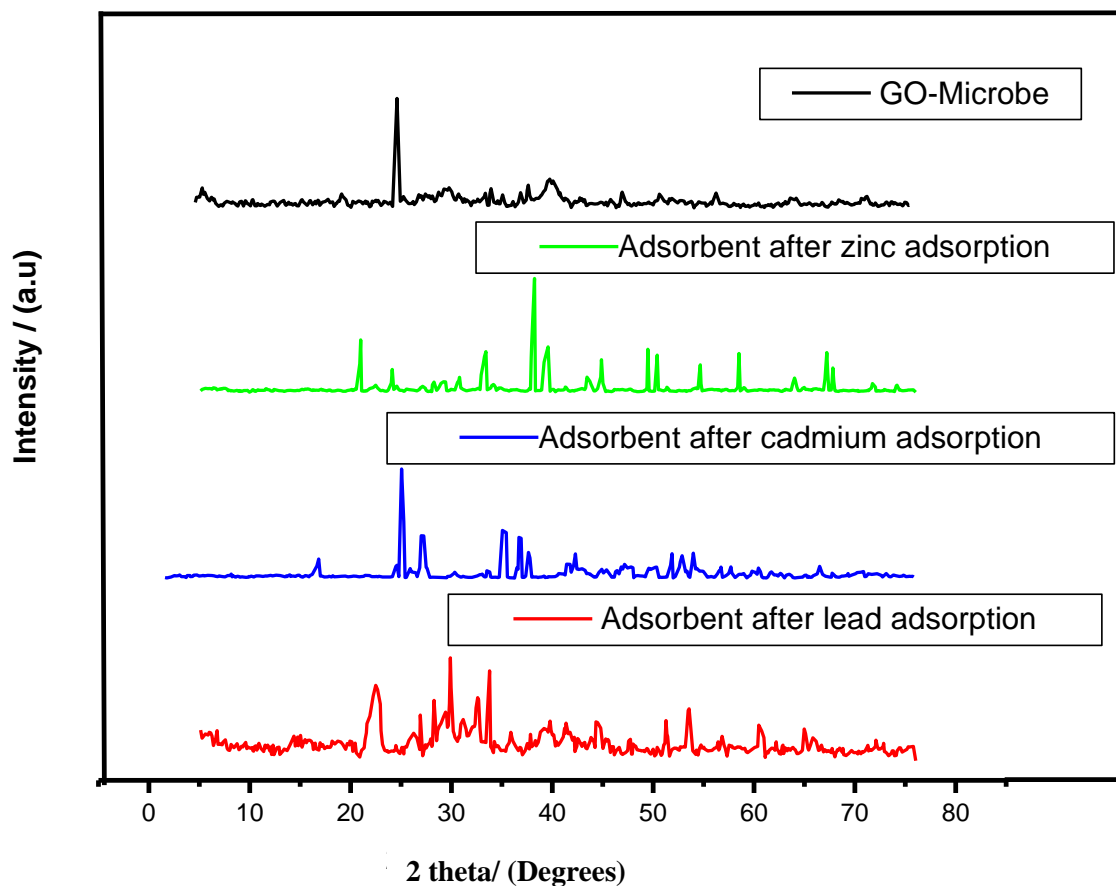


Figure 3.12.: XRD pattern of the adsorbent before and after metal adsorption

FTIR spectral characterization

FTIR spectrum of rGO- Microbe yields two characteristic peaks around 1740cm^{-1} and 1646cm^{-1} corresponding to C=O and C=O stretching of the amide I functional groups [Sun et al, 2014; Stankovich et al, 2006] (**Fig. 3.13**). The carbonyl group, perhaps is contributed by the graphene oxide component of the adsorbent while the amide stretching might be an attribute of the microbial component of the bioadsorbent. The peak at 1396cm^{-1} and 1226cm^{-1} is attributed to the hydroxyl

groups located on the plane of GO and C-O-H stretching respectively [Muthoosamy et al, 2015]. These groups can be correlated to the functional groups on the bacterial cell wall. Prominent changes were observed in the biosorbent after the metal adsorption. Shifting of the peak from 1646 cm^{-1} to 1627 cm^{-1} was noticed subsequent to the adsorption of zinc and cadmium in the bioadsorbent. This group correlates to the C=C stretching and the spectral shift can be attributed cationic- π electron interaction indicative of metal adsorption [Kumar et al, 2012]. However, in case of lead, the same peak was shifted to 1630 cm^{-1} indicating metal binding over the bioadsorbent surface. Involvement of the carbonyl group in metal binding was indicated by the change in the peak position from 1740 cm^{-1} to 1736 cm^{-1} and 1767 cm^{-1} in case of lead and cadmium respectively [Zhang et al, 2013]. Epoxy groups of the reduced GO also played an important role in metal binding as was indicated by the spectral shift from 875 cm^{-1} to 835 cm^{-1} and 887 cm^{-1} in case of zinc and lead adsorption respectively [Liu et al, 2015]. Furthermore, the peak at 835 cm^{-1} broadened indicating the interaction of zinc with the epoxy groups. A common peak observed at 3440 cm^{-1} suggests the involvement of O-H functional group of the partially reduced graphene oxide in metal binding. All these changes in the FTIR spectrums clearly stipulate the involvement of various functional groups in metal binding.

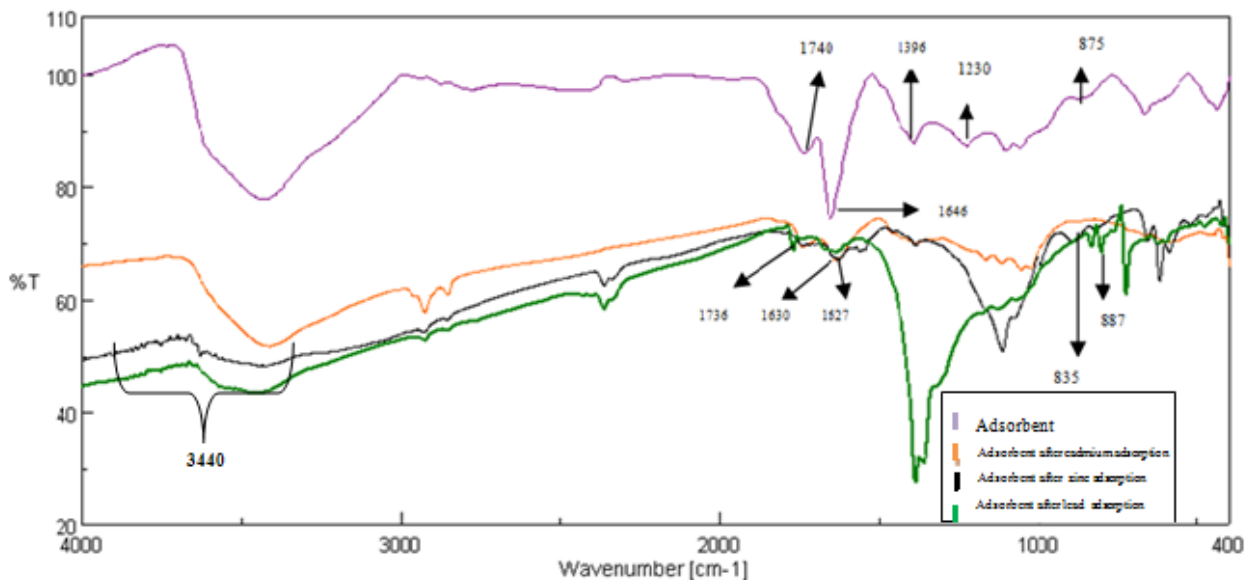


Figure 3.13: FTIR analysis of the adsorbent before and after metal adsorption.

Effect of pH on adsorption.

The effect of pH on the percentage removal of metal ions is an important parameter to be standardized. The pH of the medium was varied in the range 2-9. With the increase in pH, percentage adsorption of heavy metals also increased [Akpomie et al, 2015]. Maximum adsorption was observed within the pH range of 7.5 to 8.5 (**Fig 3.14**) At a lower pH the adsorbent surface attains a net positive charge due to the protonation of acidic functional groups in carbonaceous rGO- microbe adsorbent. This results in the repulsion of the positively charged adsorbent surface and the predominant positive cations [Akpomie et al, 2015] (**Fig. 3.14 A**). Moreover, competition between the H^+ ions and the divalent cations lead to the reduction in the adsorption capacity due to non availability of the metal binding sites on the adsorbent. However, with an increase in pH, expansion of the deprotonated sites on the adsorbent occurs leading to a stronger attraction between the adsorbent surface and metal ions. At a pH higher than 10, turbidity was observed in the aqueous solution due to formation of metal

hydroxides. Despite the similar trends in the pH range at which there is maximum adsorption, there were few differences observed, depending upon the metal ions. In the pH range 7.5-8.5, better removal was observed in case of lead ions as compared to the other two metals. The order of removal in terms of better efficiency was $Pb^{+2} > Cd^{+2} > Zn^{+2}$. This selectivity could be ascribed to the decreasing order of their ionic radii [Hazarika et al, 2015]. A schematic representation of the metal adsorption is depicted in the **Fig. 3.14B**.

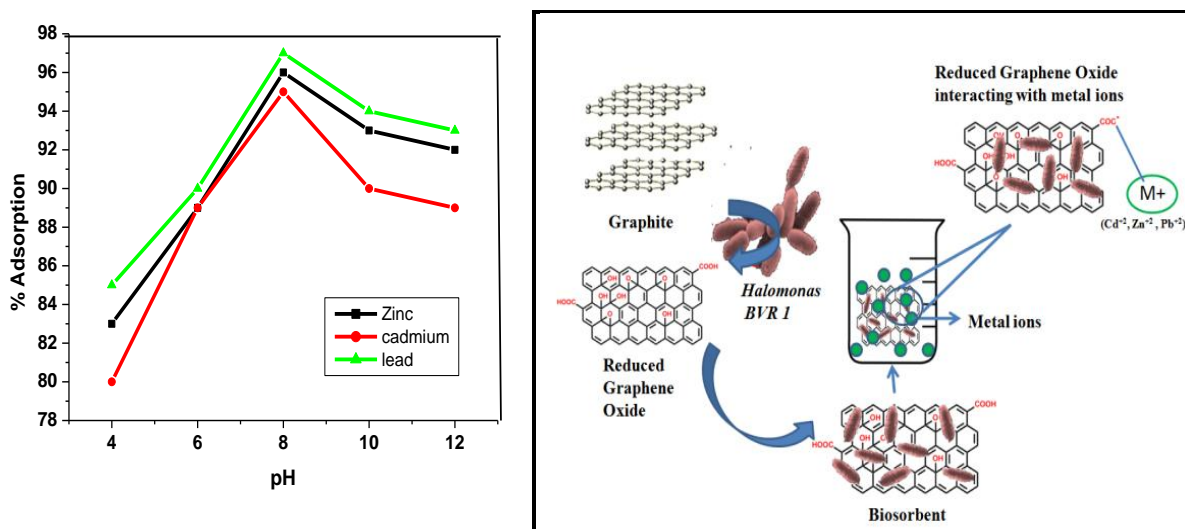


Figure 3.14: A) Effect of pH on adsorption of metal ions B) Schematic representation of metal adsorption on the adsorbent

Isotherm studies

The theory and basis of the isotherms, kinetics and thermodynamics has been given in detail in the Appendix I.

Langmuir isotherm

The Langmuir isotherm parameters was obtained from the plot of C_e/q_e against C_e (**Fig. 3.15-3.17**) The maximum adsorption capacity (q_0) was calculated from the slope of this plot. It was found to be 73.58 mg g^{-1} , 20.30 mg g^{-1} and 42.535 mg g^{-1} for lead, cadmium and zinc respectively. Such a high

adsorption capacity indicates the potency of this bioadsorbent towards metal adsorption. The dimensionless separation factor ($R_L = 1 / 1 + b C_o$) was found to be 0.008, 0.07 and 0.32 for lead, cadmium and zinc respectively. These values being close to unity shows the applicability of Langmuir model to the adsorption process. However, comparing the regression coefficients of the respective metals sorption, lead and zinc had lower coefficients which suggests that it may not be purely monolayer adsorption. This deviation might be ascribed to the existence of surface sites having multiplicity of adsorption free energies [Wu et. al, 2005]. Regression coefficient was as high as 0.95 in case of cadmium adsorption. This can be corroborated with the fact that cadmium has a smaller radii in comparison to lead. This leads to a small difference among the neighbouring metal binding sites in the bioadsorbent, thus favouring a monolayer Langmuir adsorption [Langmuir et al, 1918].

Freundlich isotherm

The Freundlich isotherm model was analysed by plotting $\log q_e$ against $\log C_e$. (**Fig. 3.15-3.17**). The intensity of adsorption (n) and the adsorption capacity (K_F) were obtained from the slope and intercept of this plot. These values for all the metals are clearly tabulated in table 3.6. The n values for all the metals were in between 1 and 10 indicating the favourable adsorption of the metal ions on the bioadsorbent [Freundlich et al, 1906]. The high values of n and K_F as shown in **Table 3.6** signify the effective uptake of these metal ions over the reduced GO-microbe biosorbent surface [Freundlich et al, 1906]. Higher regression coefficients were obtained in case of lead and zinc adsorption indicating their good fit to this isotherm and suggesting a multilayer adsorption phenomenon.

Dubinini–Radushkevich isotherm

The mean free energies for the metals were calculated from the Dubinin–Radushkevich isotherm (D-R)[Hu et al, 2016] (**Fig. 3.15-3.17**) that has similarity to Langmuir isotherm model. The mechanism of interaction between the metal ions and the bioadsorbent surface is also justified from

these calculated adsorption energies. The adsorption energy, E can also be expressed as $-(2\beta)^{-0.5}$ and the positive value of E (+0.77 kJ/mol, 0.75kJ/mol and 1.1947kJ/mol for lead, cadmium and zinc respectively) in all three metals indicated that the interaction between the metals and rGO-microbe biosorbent is endothermic and hence higher temperatures are favourable for adsorption. Additionally, the E value lies in the range of 1-10 signifying a physisorption kind of interaction [Hu et al, 2016] .

All the calculated parameters from various isotherms have been tabulated (**Table 3.6**)

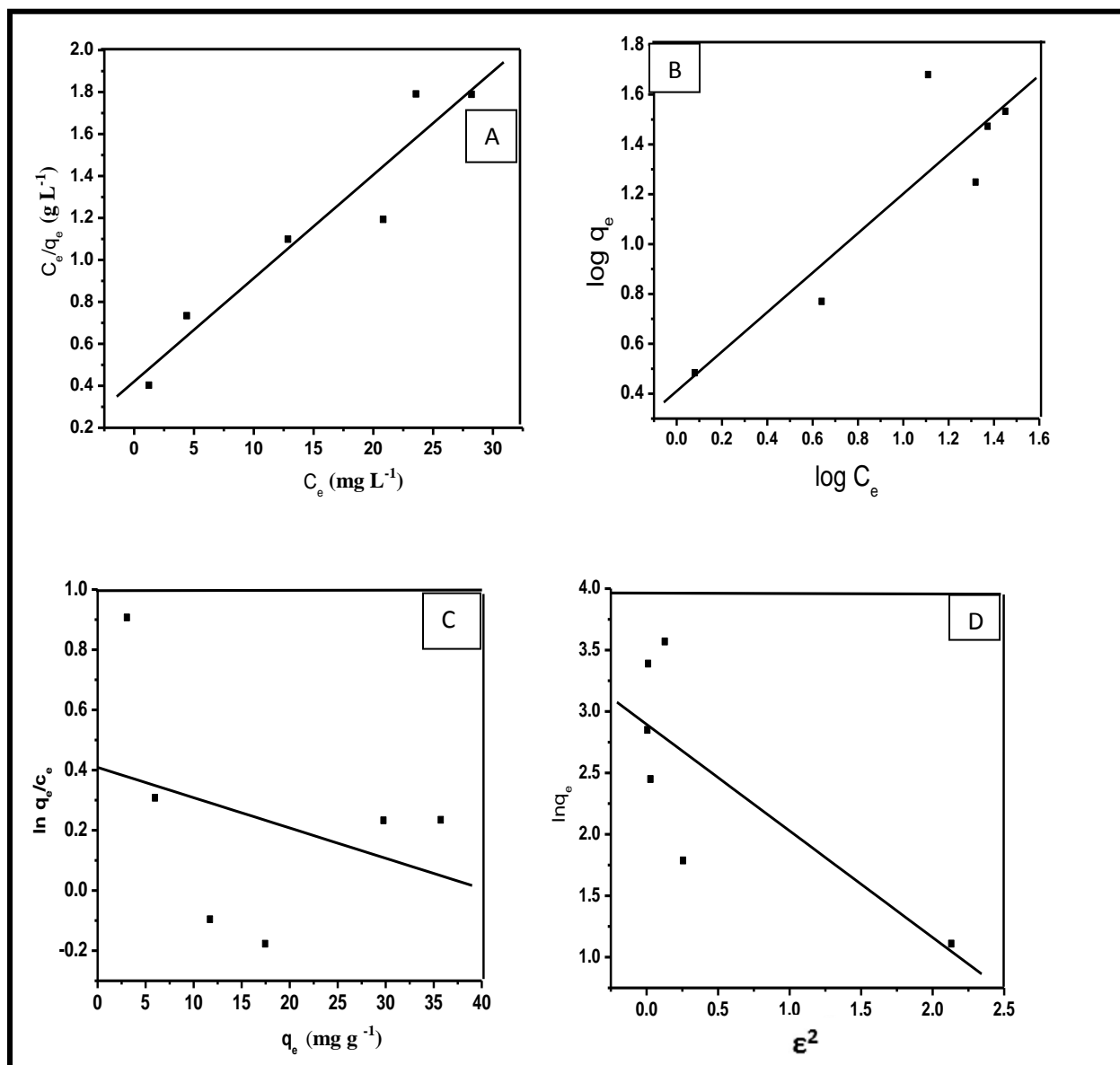


Figure 3.15: Cadmium adsorption isotherms A) Langmuir isotherm B) Freundlich isotherm C) Elovich isotherm D) D-R isotherm.

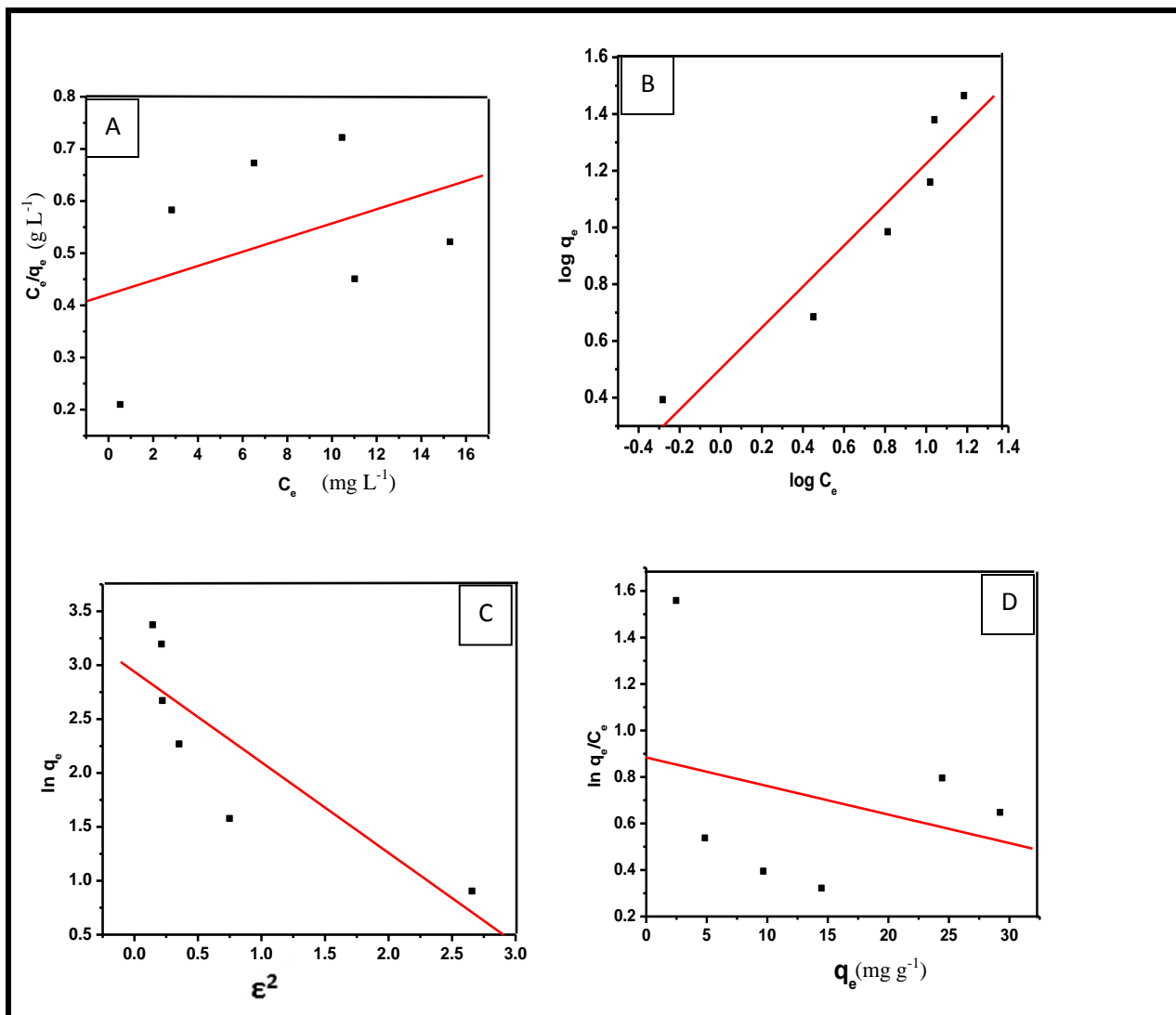


Figure 3.16: Lead adsorption isotherms A) Langmuir isotherm B) Freundlich isotherm C) D-R isotherm, D) Elovich isotherm.

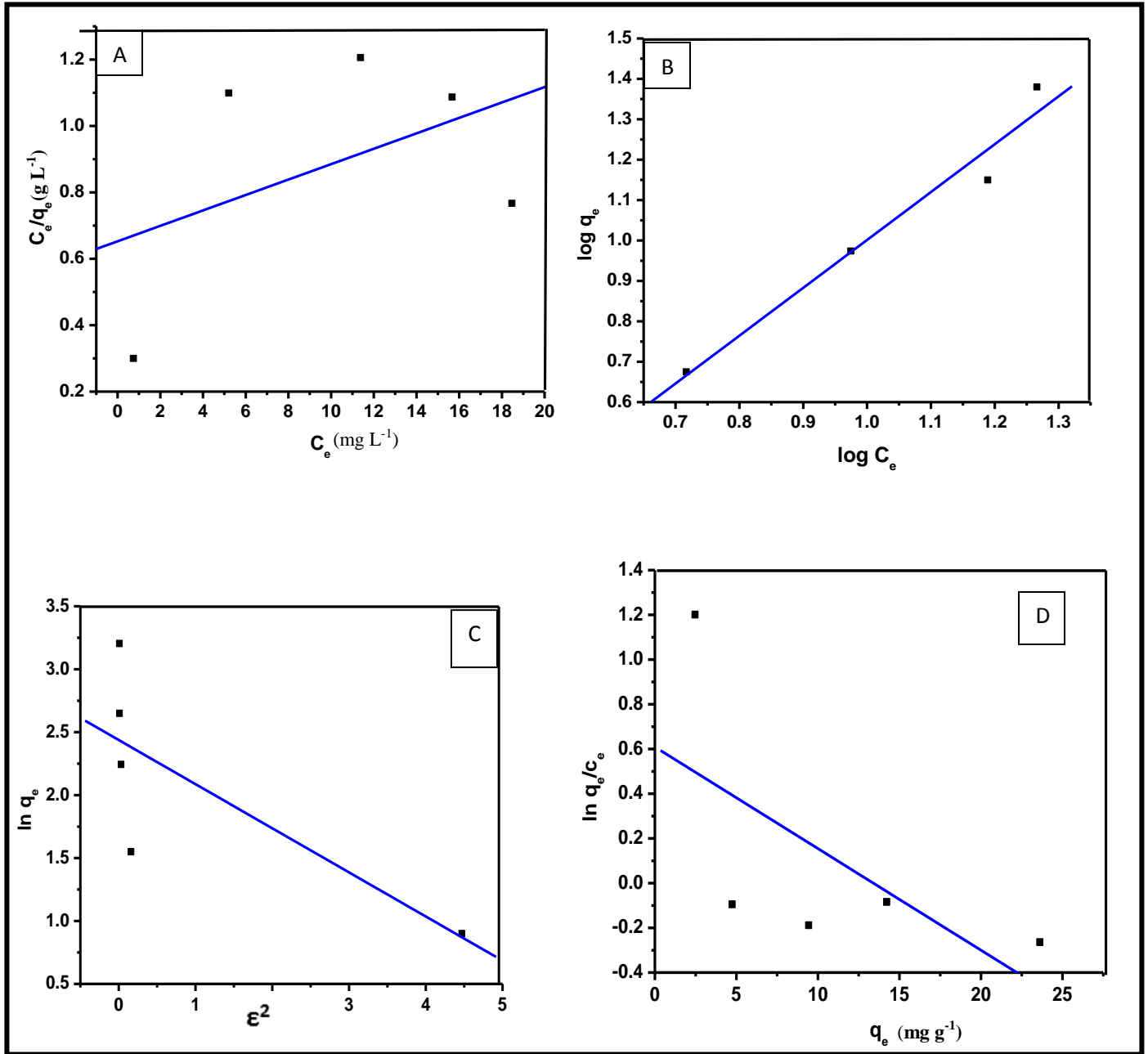


Figure 3.17.: Zinc adsorption parameters A) Langmuir isotherm B) Freundlich isotherm C) D-R isotherm D) Elovich isotherm.

Table 3.6. Adsorption parameters calculated from their respective models for microbe immobilized Graphene Oxide adsorbent

Sl. no.	Isotherm models	Parameters	Cadmium	Lead	Zinc
1.	Langmuir	q_o (mg g^{-1}) b (L mg^{-1}) R_L r^2	20.308 0.117 0.078 0.95	73.58 0.032 0.008 0.598	42.535 0.033 0.322 0.599
2.	Freundlich	K_F ($\text{mg l}^{-1/n} \text{g}^{-1} \text{L}^{1/n}$) n r^2	2.570 1.390 0.896	3.189 1.38 0.955	1.09 1.05 0.98
3.	Dubinin-Radushkevich	q_m (mg g^{-1}) β E (kJ mol^{-1}) r^2	18.08 0.867 0.75 0.76	18.89 0.840 0.77 0.855	11.43 0.3504 1.19 0.76
4.	Elovich	q_m K_E r^2	100 0.015 0.11	83.33 0.029 0.29	35.714 3.043 0.31

Kinetics of adsorption

The kinetics of adsorption were analyzed through the pseudo first order [Lagergren 1898], second order [Ho, 2006], and intraparticle diffusion rate equations [Weber & Morris, 1963] (**Table 3.7**) for the adsorption of metal ions on the rGO-microbe biosorbent. The regression coefficient of the plots that are close to one were considered as the best fit kinetic models for the metal adsorption. The various kinetic plots applied and their corresponding kinetic parameters are shown in **fig. 3.18 A-C**. All the metal adsorption favoured pseudo second order kinetic model. Also, the calculated q_e value through this model matched well with experimental (q_e) value in case of all the metals. Hence, the pseudo second-order kinetic model was considered more suitable to describe the kinetic behavior of metal adsorption on rGO-microbe biosorbent surface.

In Weber–Morris intraparticle diffusion model, a plot of q_t versus $t^{0.5}$ would be linear and if the plot passes through the origin, it would be inferred that intraparticle diffusion is the only rate-determining step. The plot was linear in this adsorption process giving the intraparticle rate constant (k_{int}) and a non-zero intercept (Fig. 3.18. C) pointing out to the fact that boundary layer phenomenon could also direct the adsorption of M^+ ion on the rGO-microbe biosorbent surface

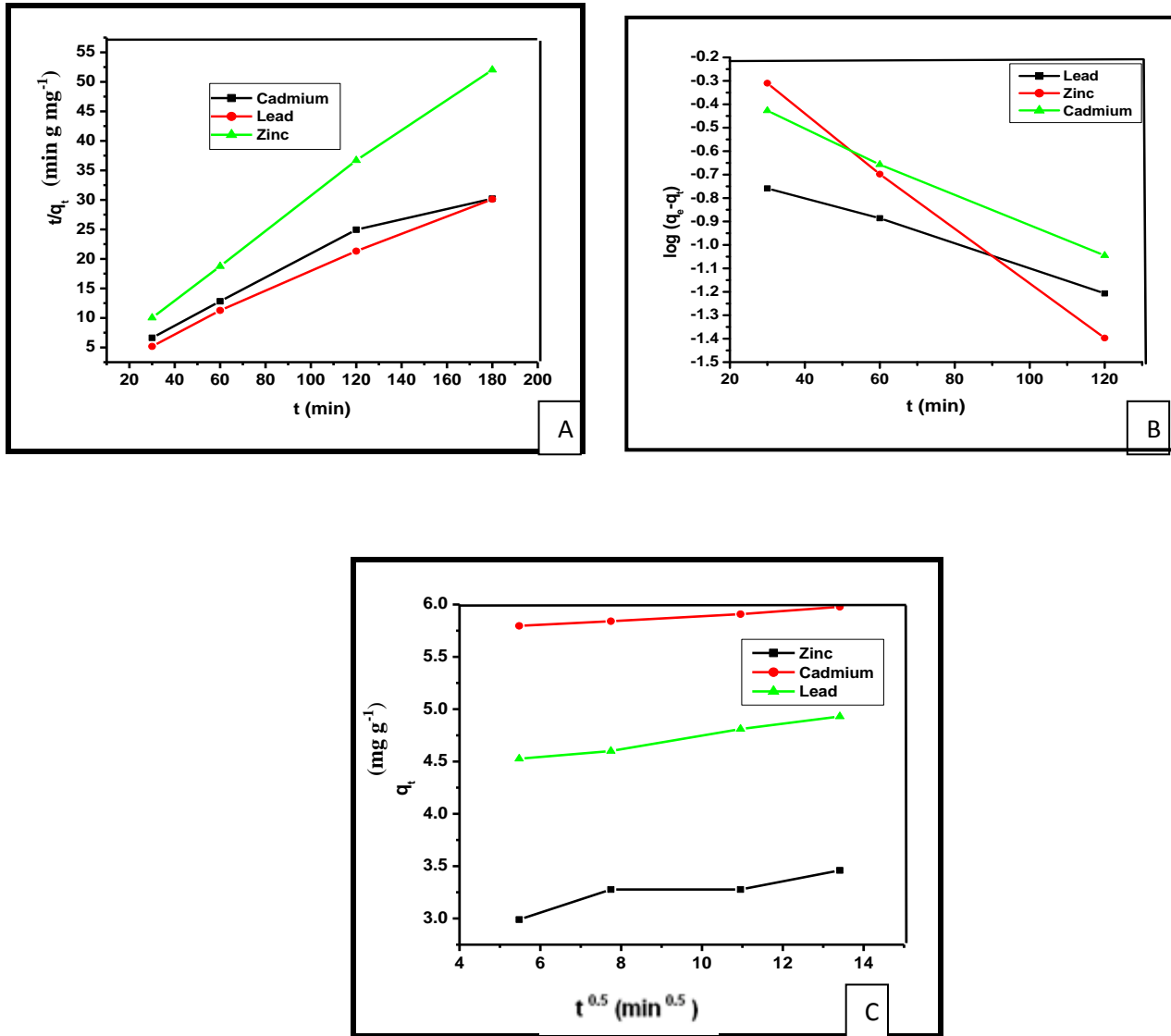


Figure 3.18: A)Pseudo Second order B)Pseudo first order and C)Weber Morris diffusion plots.

Table 3.7 Kinetic and Intraparticle rate constant data for the adsorption of metal ions.

Metal	Second order rate constant k_2 [g mg ⁻¹ min ⁻¹]	Regression Coefficient	First order rate constant k_1 [min ⁻¹]	Regression coefficient	Intraparticle rate constant k_{int} [mg g ⁻¹ min ^{-1/2}]
Cadmium	0.055	0.99	0.015	0.89	0.053
Lead	0.106	0.99	0.009	0.56	0.022
Zinc	0.03	0.98	0.026	0.67	0.047

Thermodynamics of adsorption

Thermodynamic parameters involving enthalpy (ΔH^0), entropy (ΔS^0) and Gibbs free energy (ΔG^0) were calculated to ascertain the spontaneity of the adsorption process. All these parameters were calculated from the classic Van't Hoff plot of $\ln K$ against $1/T$ [Donia et al, 2006] (**Table 3.8**) (**Fig. 3.19**). To obtain this plot the metal ions adsorption was tested at different temperatures using a known concentration of the metal solution. All the metal adsorptions had a positive enthalpy ($\Delta H^0 = 30.127$ kJ/mol, 37.369 kJ/mol and 29.96 kJ/mol for cadmium, lead and zinc respectively) signifying the feasibility adsorption of the metal ions on the rGO-Microbe bioadsorbent. Positive enthalpy values also indicate an endothermic reaction that suggests that adsorption is favorable at high temperatures and the reactions takes energy from the surrounding environment for effective adsorption [Ang et al, 2013]. Moreover an enthalpy value lower than 80 kJ/mol is indicative of an physical adsorption involving a ligand exchange mechanism [Bharathi et al, 2014]. This data is well corroborated with the E value calculated from the DR isotherm. Entropy is an extensive property and the positive value ($\Delta S^0 = 99.23$ J mol⁻¹ K⁻¹, 127.71 J mol⁻¹ K⁻¹ and 122.85 J mol⁻¹ K⁻¹) signifies the feasibility and favorability of the adsorption process. Additionally, the negative Gibbs free energy values also

manifests that the adsorption process is spontaneous. The activation energy (E_a) required for favourable M^+ ion adsorption was also obtained using the expression $E_a = \Delta H^{\circ}_{ads} + RT$ (Table 3.8). The E_a was found to be around 25.45 KJ mol⁻¹ on an average indicating endothermic adsorption reaction.

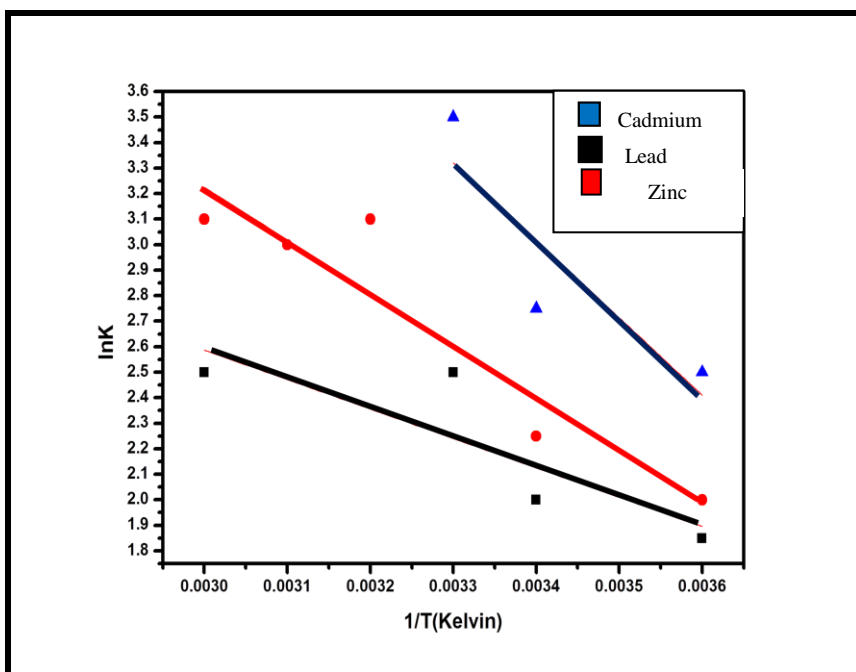


Figure 3.19: Van't Hoff plot depicting ln K Vs. 1/T.

Table 3.8 Thermodynamic data for the adsorption of metal ions.

Metal	Temperature / [Kelvin]	ΔG° [kJ mol ⁻¹]	ΔS° [J mol ⁻¹ K ⁻¹]	ΔH° [kJ mol ⁻¹]	E_a [kJ mol ⁻¹]
Cadmium	283	-3.190	+ 99.23	+30.127	+27.40
	293	-4.604			
	303	-10.66			
	313	-7.234			
	323	-6.391			
Lead	283	-4.517	+127.71	+37.369	+28.49
	293	-5.018			
	303	-6.146			
	313	-11.29			
	323	-8.297			
	283	-4.681			
	293	-5.803			

Zinc	303	-8.580	+ 122.85	+29.969	+27.466
	313	-12.203			
	323	-8.004			

Effect of interfering ions on adsorption of metal ions

The effect of influence of certain cations and anions commonly associated with the electronic industry effluents were investigated at different concentrations. Ions such as nickel and cobalt did not interfere up to 50 mg L⁻¹ level, but beyond this level the percentage adsorption of zinc ions decreased by 5 %. Anions such as phosphates and nitrates did not affect the adsorption of zinc when their concentration levels were in the range 10-60 mg L⁻¹. Chlorides and sulfates caused a slight decrease in the percentage adsorption of lead and cadmium beyond 60 mg L⁻¹. In case of cadmium adsorption, cobalt and iron (II) had maximum interference with the adsorption. Their presence at 70 mg L⁻¹ decreased the metal adsorption by 15%. Anions such as chlorides and phosphates has inhibitory effect on lead adsorption at 60 mg L⁻¹ concentration. Presence of cadmium at 50 mg L⁻¹ reduced the adsorption of lead by 10%. Other cations did not have much effect below 60 mg L⁻¹. Among the anions, presence of sulfate only reduced the adsorption by 10 % (Table 3.9)

Table 3.9: Effect of various ions on the removal of lead, cadmium and zinc

Concentration of Anions mg l ⁻¹	% adsorption of cadmium	% adsorption of lead	% adsorption of zinc	Concentration of Cations mg l ⁻¹	% adsorption of cadmium	% adsorption of lead	% adsorption of zinc
SO ₄ ²⁻ (70)	93±0.4	95±0.1	NI*	Zn ²⁺ (100)	NI*	97±0.1	NI*
PO ₄ ³⁻ (80)	NI*	94±0.5	97±0.1	Ni ²⁺ (100)	NI*	NI*	95±0.1
Cl ⁻ (70)	95±0.2	95±0.1	NI*	Co ²⁺ (100)	85±0.3	98±0.4	95±0.6

NO₃⁻ (80)	NI*	NI*	97±0.1	Mn²⁺ (50)	NI*	NI*	NI*
				Fe²⁺ (100)	85±0.5	99±0.1	NI*
				Mg²⁺ (50)	NI*	NI*	NI*
				Cd²⁺ (50)	NI*	90±0.3	95±0.1

NI*: No Interference

Regeneration of the biosorbent

Regeneration of the adsorbent is an important prerequisite to assess the adsorption efficiency. In case of all the three metals the eluent that gave maximum percentage of desorption was 1.0 mol L⁻¹ HCl. Varying concentrations of the eluent were used to desorb the metal ions. A total volume of 15mL was used to desorb the cations upto two cycles beyond which the regeneration efficiency gradually reduced (**Fig. 3.20**). The desorption was high at this optimum concentration as strong competition between H⁺ ions and metal cations exists for adsorption sites that causes displacement of cations into the acid solution [Zhang et al, 2015].

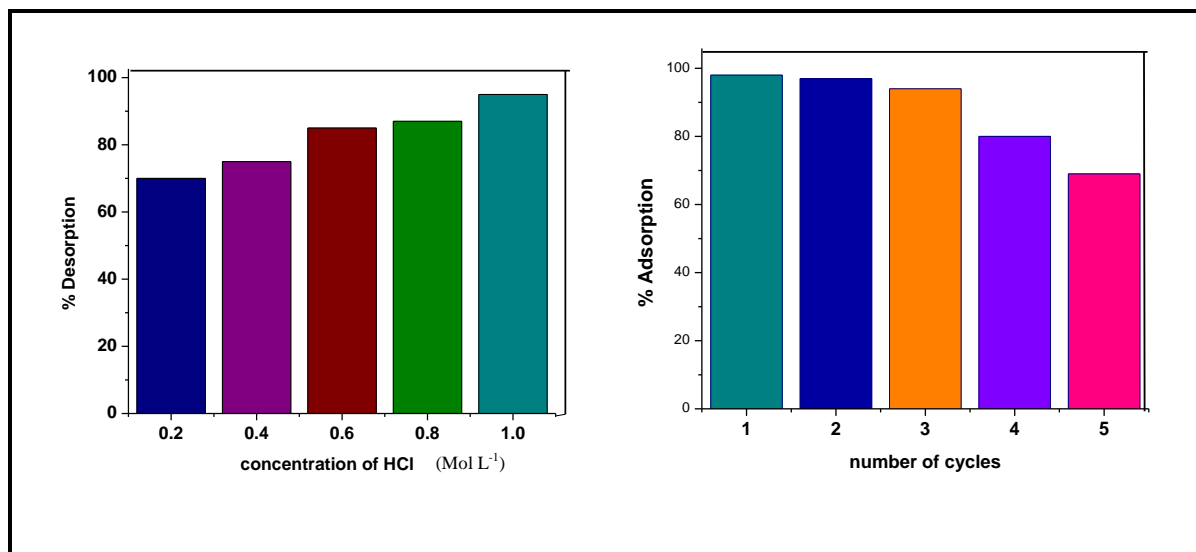


Figure 3.20: A) Concentration of HCl against % desorption B) Regeneration efficiency of adsorbent

Column studies

After optimization of parameters for the efficient adsorption of the metal cations in batch studies, experiments to treat metal cations from a larger volume were also evaluated by column studies. For this purpose, 1.0 g of the bioadsorbent was packed in the column of 2 cm x 4 cm with the overall concentration of the metal cations maintained at 100 mg L⁻¹. The maximum removal efficiency (98%) was achieved with a flow rate of 2mL min⁻¹. The percentage adsorption of the metal ions decreased beyond 500mL volume of the sample loaded (**Fig. 3.21**). The decrease in the percentage of adsorption might be ascribed to the fact that the number of available sites on the adsorbent for the binding of the metal ions decreased significantly. Moreover, the interaction between the adsorbate and the adsorbent also weakens with increased sample volume due to the swelling of the adsorbent. Owing to this the void spaces in the adsorbent increases resulting in the free flow of the aqueous metal solutions and decreased adsorbent- adsorbate interaction.

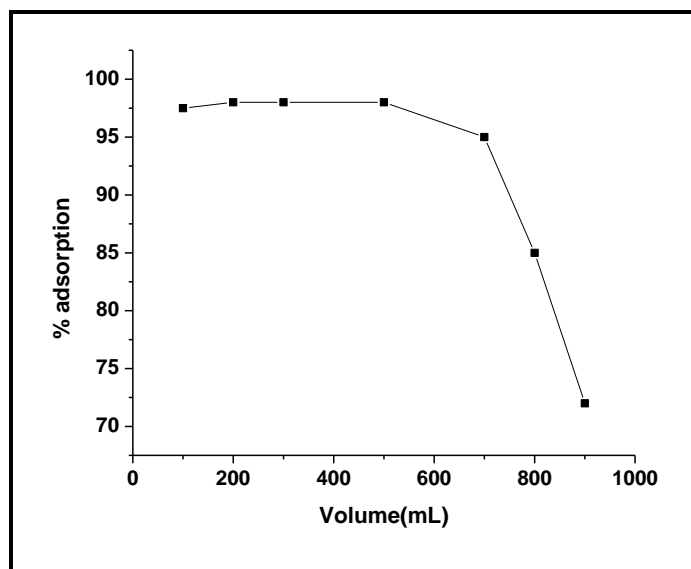


Figure 3.21: Effect of sample volume on metal adsorption

Comparison against other biosorbents

The proposed method for the removal of divalent cations, cadmium, lead and zinc were compared in terms of the maximum adsorption capacities with other adsorbents involving Graphene Oxide. The results showed that Graphene Oxide-microbe biosorbent exhibits good adsorption capacity as evident from the comparison shown in **Table 3.10**.

Table 3.10. Comparison of adsorption capacities of various adsorbents.

Sl.No.	Adsorbent	Metal	Adsorption capacity (mg g ⁻¹)	Reference
1	Graphite doped chitosan composite	Lead	6.711	Gedam et al,2014
2	Multiwalled carbon nanotubes	Lead	27.8	Tehrani et al,2014
3	Magnetic chitosan graphene oxide composites	Lead	76.94	Fan et al, 2013
4	Bare graphene	Lead	30.30	Santosh et al, 2015
5	Bare graphene	Cadmium	15.57	Santosh et al, 2015
6	Magnetic graphite oxide	Lead	38.5	Hur et al,2015
7	Magnetic graphite oxide	Cadmium	5.3	Hur et al,2015
8	Graphene Oxide	Zinc	88.12	Najafi et al, 2015
9	Carbon nanotubes	Zinc	32.68	Lu et al, 2006
10	Activated carbon	Zinc	20.52	Kouakou et al,2013
11 →	<i>Halomonas BVR1</i> immobilized in graphene oxide	Lead	73.58	Present study
12 →	<i>Halomonas BVR1</i> immobilized in graphene oxide	Cadmium	20.308	Present study
13 →	<i>Halomonas BVR1</i> immobilized in graphene oxide	Zinc	42.535	Present study

Conclusions

The metal biosorption process involving the use of *Halomonas BVR 1* immobilized in chitosan as a biosorbent is spontaneous, exothermic and favours pseudo second order kinetics. The Langmuir adsorption capacities were found to be 24.15 mg g⁻¹, 23.88 mg g⁻¹ and 12.53 mg g⁻¹ for lead, cadmium and zinc respectively. Characterisation techniques such as FT-IR, SEM, EDAX and optical imaging techniques ascertained the adsorption of metal ions on the bacteria immobilized chitosan biosorbent. Electrostatic and ion exchange mechanisms govern the interaction between the metal ions and the biosorbent. As a complexing agent, EDTA showed good potential to desorb metal cations. Hence, the combination of

Halomonas BVR 1 and chitosan is capable of adsorbing lead, cadmium and zinc effectively from aqueous solution in comparison to the biomass used as such.

The effective integration of the rGO and microbial cells for the removal of cadmium, lead and zinc has also been demonstrated in this study. Adsorption studies show that cadmium adsorption obeyed a monolayer kind of adsorption phenomenon behaving closely to the Langmuir adsorption isotherm. Lead and zinc adsorption followed the freudlich type of adsorption phenomenon. Adsorption at low pH was not effective due to the protonation of functional groups and repulsion between the protonated functional group and the metal cations. Pseudo second order model was best suited to explain the kinetics of all the three metal adsorption studies. The intraparticle diffusion plot pointed out to the fact that boundary layer phenomenon could also direct the adsorption of M^{2+} ion on the rGO-microbe biosorbent surface. The thermodynamics of the sorption indicates a spontaneous and feasible adsorption for all the three metal cations. The adsorption was effective at higher temperatures indicative of a endothermic reaction and a positive enthalpy. The ability of the biosorbent to treat the synthetic metal solutions and reusabilty of the biosorbent using 0.1 mol L^{-1} HCl opens up new arenas in the field of bioremediation as a sustainable solution to heavy metal pollution.

CHAPTER IV
ENHANCED METAL REMEDIATION USING *Halomonas BVR 1* IN SODIUM
ALGINATE

Enhanced Metal Remediation using *Halomonas BVR 1* in Sodium Alginate: Kinetics and Column Studies

SYSTEM 4: Halomonas BVR 1 immobilized in sodium alginate

Introduction

Sodium alginate was chosen as another polymeric material for use as a carrier matrix that hosts the bacterial cells. Alginates are polysaccharides found in brown seaweeds and are composed of linear polymers of β -(1 \rightarrow 4)-D-mannuronic (M) and α -L-guluronic (G) acids that differ in terms of their proportions and linear arrangements (**Fig.4.1**). The percentages of mannuronic acid (M) and guluronic acid vary with the algal species. These residues contribute to immobilize or encapsulate different cells [Kaplan et al, 2013]. Alginate matrix is of interest to most researchers, as it is a natural, biocompatible, biodegradable, non toxic orally and hydrophilic polymer. They produce thermally irreversible gels by association with most divalent cations. This gellation with the divalent cations is attributed mainly to G residue (especially to the pure polyguluronic (GG) chains), while the M residue contributes mainly to the cation exchange capacity of this naturally occurring polymer. This polymer is doped with huge number of hydroxyl groups that also aids in cation exchange.

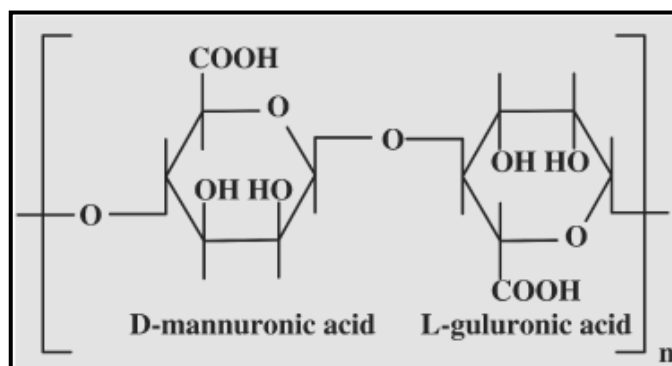


Figure 4.1: Structure of sodium alginate

Owing to all these reported potential advantages and utility of sodium alginate, it was chosen for immobilization of *Halomonas BVR 1* and consequent removal of lead, cadmium and zinc. Various parameters involved in an efficient biosorption process have been standardized for a batch study.

Most of the earlier investigations on M(II) biosorption were restricted only to batch equilibrium studies. The biosorption capacity of the biosorbent obtained from batch equilibrium experiments is useful in providing fundamental information about the effectiveness of metal sorbent system. However, this data may not be applicable to most metal remediation processes (such as column operations in practical application) where contact time is not sufficient for the attainment of the equilibrium [Kedziorek et al, 1998]. Therefore, a packed bed column is an effective process for continuous metal remediation, as it makes the best use of the difference in metal concentration that is known to be a driving force for heavy metal biosorption. Furthermore, it allows more efficient utilization of biosorbent and results in better quality treatment of the effluent. The dynamic behavior of a fixed bed column and its efficiency is described in terms of breakthrough curve [Xu et al, 2013]. A plot of effluent solute concentration versus time is referred as breakthrough curve which is an S-shaped curve. Breakthrough metal ion concentration is the point on the S-shaped curve at which the effluent solute concentration reaches its maximum allowable value. The point where the effluent solute concentration reaches 95% of the influent concentration is usually called the point of column exhaustion [Ansari et al, 2011]. The shape of the breakthrough curve depends on the nature of effluent being treated. If there is only one metal ion being remediated, the adsorption will be short and the breakthrough curve will be steep. If there is a mixture of ions having different adsorption capabilities, the sorption zone will be deep and the breakthrough will be flat.

This chapter, thus discusses the using *Halomonas BVR 1* immobilized in sodium alginate for removal of lead, cadmium and zinc. Modeling of column studies through generation of breakthrough curves using MATLAB software for the remediation of lead ions.

Materials and Methods

Preparation of the biosorbent

For immobilization in sodium alginate, the strain was inoculated into 100 mL LB medium containing 0.5 mol L⁻¹ NaCl and incubated at 37°C for 48 h till they reached the exponential phase [Manasi et al, 2014]. The cell suspension was harvested by centrifuging a 100 mL culture at 7200 rpm for 10 min. The pellet was washed twice with Milli Q water and then resuspended in 5 mL of autoclaved MilliQ water. Equal volumes of this cell suspension were mixed with 0.5% (w/v) sodium alginate (Himedia-MB-114 (Molecular Biology grade) and stirred for an hour [Park et al, 2004]. The cell suspension containing sodium alginate was added dropwise into 1% calcium chloride solution and maintained for 2 h at room temperature. These beads were dried in an hot air oven at 90° C and 0.4 g was used for batch sorption studies.

Physicochemical Characterizations of the biosorbent

Results and discussion

FTIR spectral characterization

The presence of various functional groups on the immobilized biomass necessary for metal binding can be identified by FT-IR spectroscopic analysis. In the FT-IR spectral analysis of this biomass (**Fig.4.2 A-D**) we observed characteristic bands corresponding to C-C stretching vibrations at 2359 cm⁻¹. [Talawar et al, 2004]. A strong peak at 1707 cm⁻¹ indicates the stretching vibration

corresponding to C=O group [Dumitriu et al, 2009]. The polyguluronate fraction consisting of the various carboxylate bands are represented by the peak at 946 cm^{-1} . This peak could be assigned to C-O, C-C-H, and C-O-H vibrations [Sakugawa et al, 2004]. The peaks at 3754 cm^{-1} , 3545 cm^{-1} , 3336 cm^{-1} corresponds to the O-H stretching mode. [Alam et al, 2013; Frost et al, 2007]. After adsorption of lead on the alginate bead surface, significant changes in the FTIR spectral pattern were observed. The peak at 1707 cm^{-1} shifted to 1700 cm^{-1} indicating the binding of the cationic lead to carboxyl groups. In case of cadmium and zinc the involvement of carbonyl group in metal binding was indicated by the spectral shift to 1710 cm^{-1} and 1713 cm^{-1} respectively. The peaks corresponding to the polyguluronates also yields a shift to 953 cm^{-1} after adsorption of lead. In case of cadmium adsorption the same peak shifted to 950 cm^{-1} , indicative of the polyguluronate fraction consisting of the various carboxylate in metal binding. The peak shifts from 3754 cm^{-1} to 3759 cm^{-1} , and 3336 cm^{-1} to 3342 cm^{-1} also suggests the involvement of the hydroxyl groups in metal binding. Appearance of peak at 1413 cm^{-1} in case of zinc adsorption suggest the formation of metal carboxylates. Hence, it is reasonable to hypothesize the complex formation and ionic interactions between the metal cation and functional groups present on the surface of immobilized bacteria [Frost et al, 2007].

SEM and EDAX analysis

The sodium alginate beads before and after adsorption of the metal were subjected to SEM – EDAX analysis. The SEM micrographs of the the alginate bead surface before adsorption exhibits smooth and clean surface while the surface showed a rougher appearance due to precipitation [Li et al, 2008] after adsorption indicating the deposition of metal ions on the beads (**Fig 4.3 A-D**). The EDAX pattern (**Fig 4.4 A-D**) after lead adsorption implies the ion exchange between the calcium and Pb^{+2} [Sone et al, 2009] similar to our earlier reported systems 1 and 2. On the contrary, the EDAX of the immobilized adsorbent after the adsorption of cadmium and zinc did not suggest this kind of

mechanism. However, distinct peaks corresponding to cadmium and zinc were observed indicative of effective adsorption of the metal ions on the surface of the adsorbent (**Fig. 4.4A-D**).

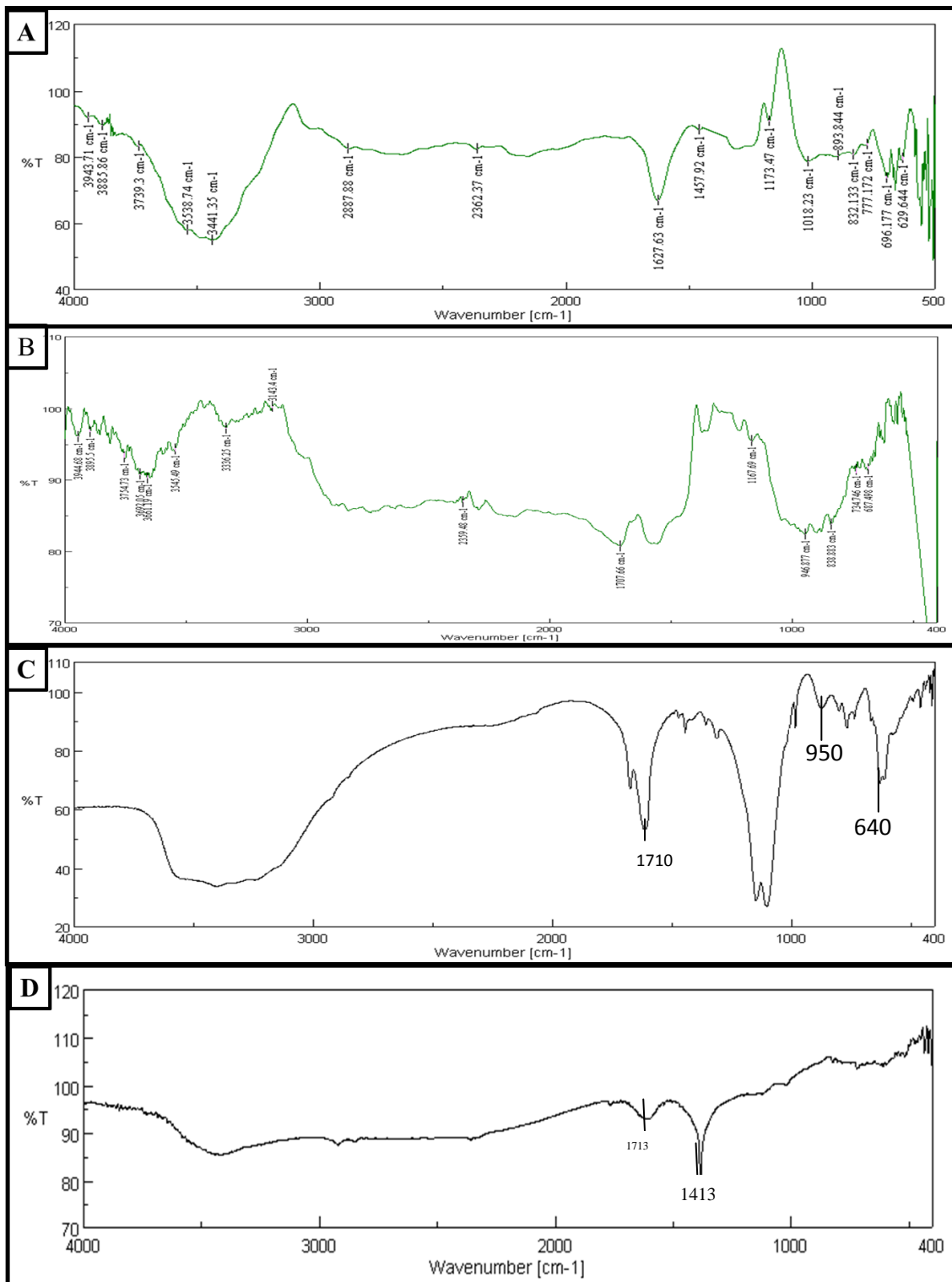


Figure 4.2: FTIR analysis of the adsorbent A) before metal adsorption B) after lead adsorption, C) after cadmium adsorption and D) after zinc adsorption

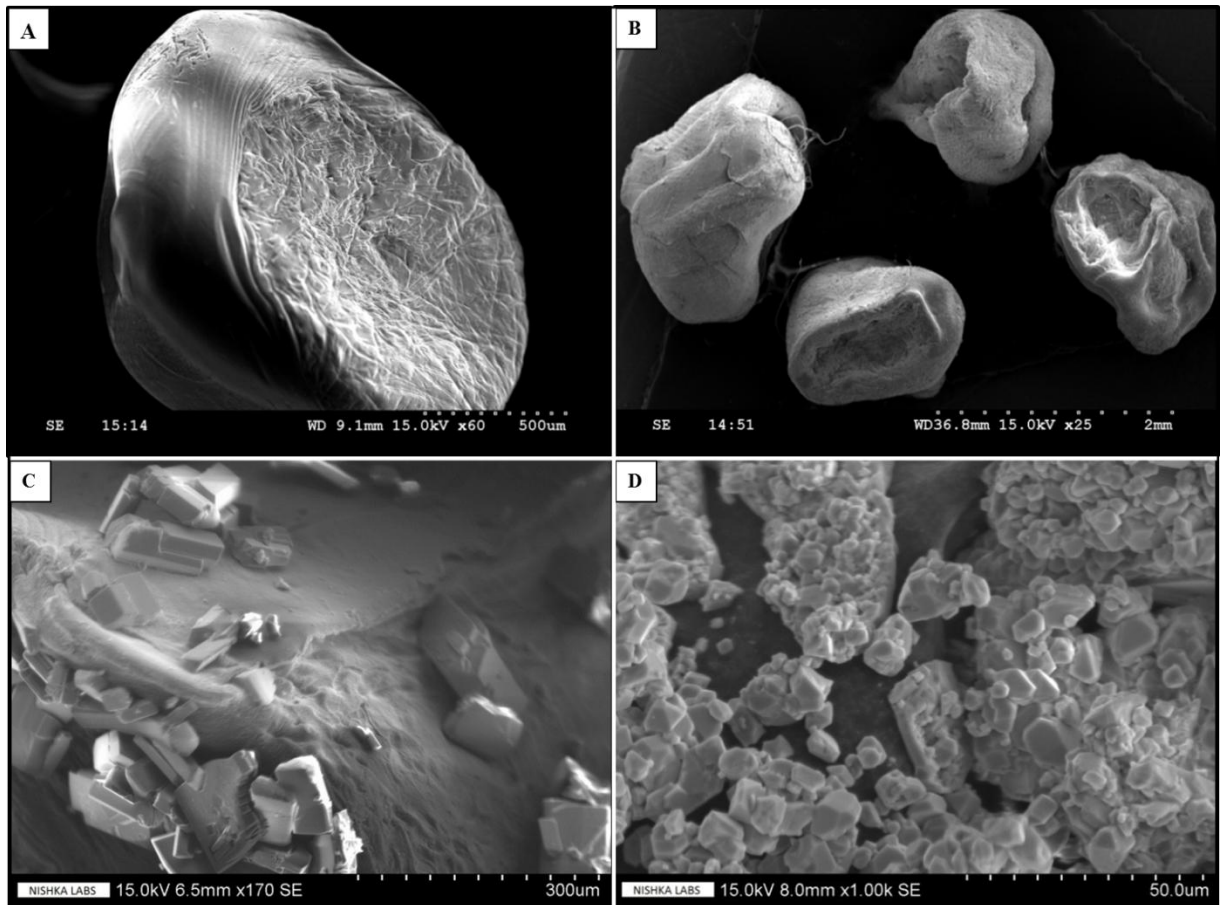


Figure 4.3 A) SEM image of the immobilized adsorbent before the metal adsorption. B) SEM analysis of the immobilized bacteria after the adsorption of lead C) Immobilized adsorbent after the adsorption of Zinc D) Immobilized adsorbent after the adsorption of Cadmium.

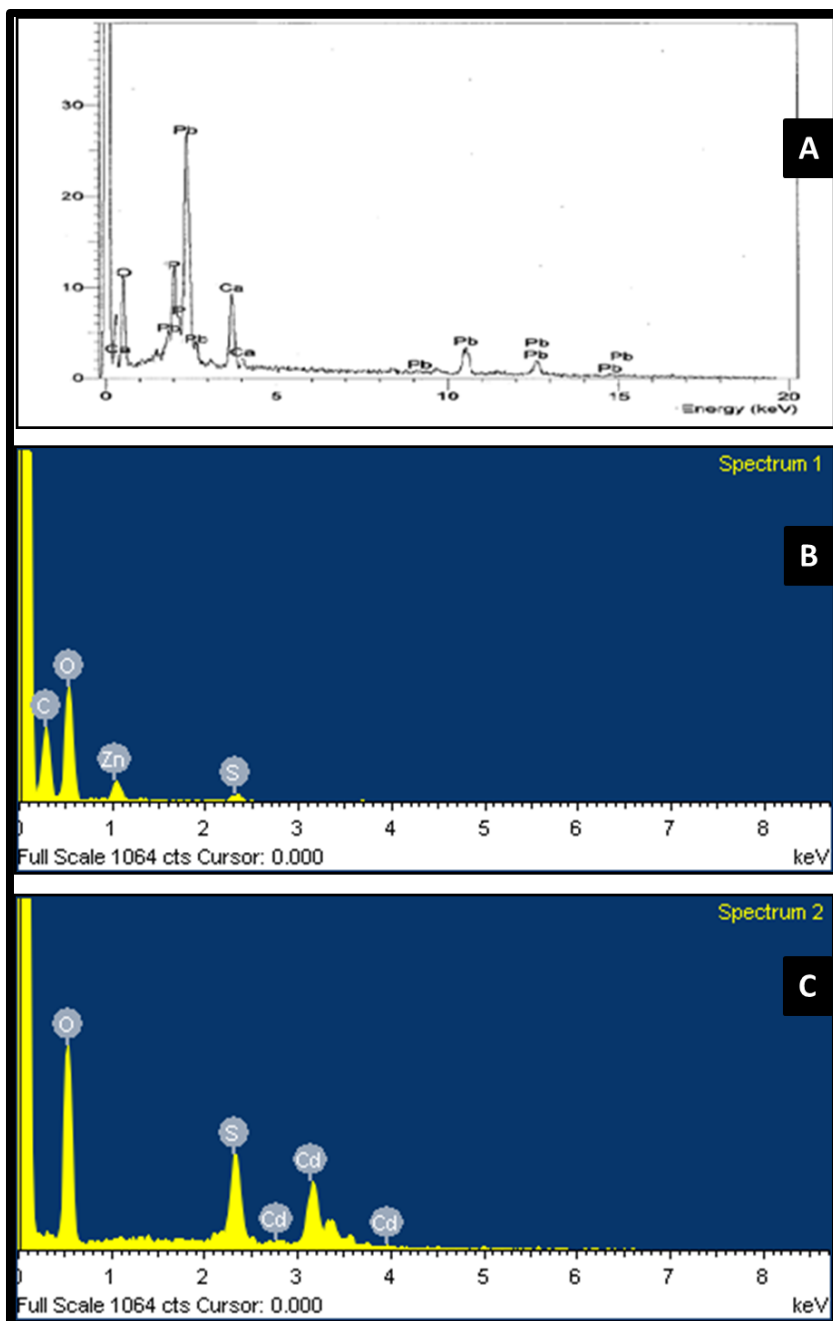


Figure 4.4 A) EDAX of the adsorbent after lead adsorption B) adsorbent after zinc adsorption C) adsorbent after cadmium adsorption.

Effect of pH on adsorption.

The adsorption of metal ions was found to be maximum in the alkaline pH range of 8.5 -10 (Fig 4.5). It is known that at higher pH, adsorption processes involve ion exchange mechanism while physical adsorption occurs at lower pH values [Cozmuta et al, 2012]. In acidic pH, there could be an

increase in the number of hydronium ions thus rendering the alginate adsorbent surface positively charged. An alkaline pH would foster a negatively charged adsorbent surface thus attracting the positively charged metal ion. [Onundi et al, 2010]. The effect of pH had a similar trend in case of cadmium and lead adsorption, where both the metal ions adsorbed effectively at pH 8.5. Adsorption of zinc was effective at neutral pH. As the pH increased, the percentage adsorption of zinc decreased gradually probably due to the interference from the H^+ ions.

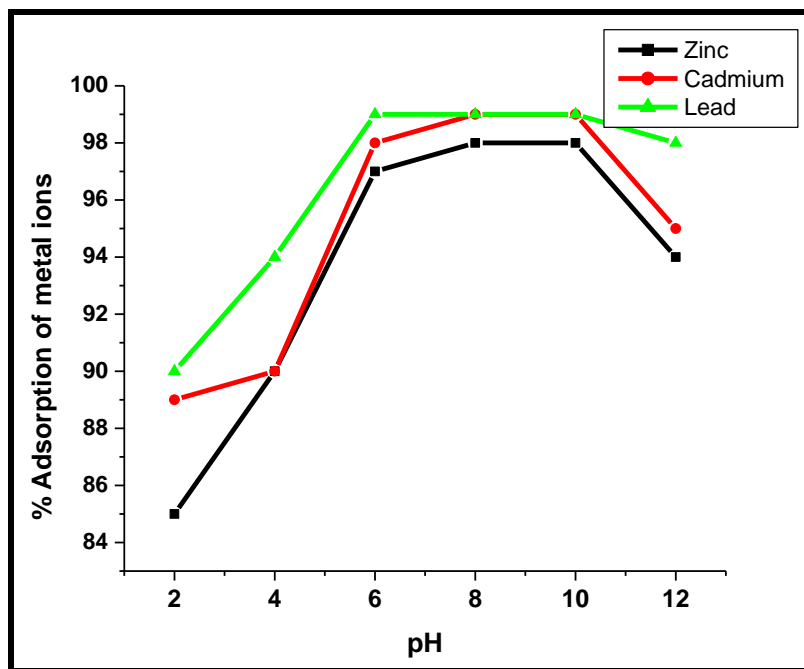


Figure 4.5 : Effect of pH on removal of metal ions

Isotherm studies

The detailed theory and detailed methodology of adsorption isotherms, kinetics and thermodynamics is given in Appendix I.

Langmuir isotherm

Langmuir [Langmuir et al, 1918] and Freundlich [Freundlich et al, 1906] isotherm models were used to study the adsorption behavior of metal ions on *Halomonas BVR 1* immobilized alginate beads.

The values of q_0 and b in the Langmuir equation were found to be 9.68 mg g^{-1} and 0.2969 L mg^{-1} for lead, 25.12 mg g^{-1} , 0.0155 L mg^{-1} for cadmium and 14.28 mg g^{-1} and 0.015 L mg^{-1} for zinc respectively. These were obtained from the slope and intercept of the plot of C_e/q_e against equilibrium metal concentration, C_e (**Fig. 4.6A**). Thus comparing the q_0 values it was deduced that this adsorbent was best suited for the removal of cadmium. R_L values in the range 0 to 1 signifies that adsorption process is effective [Mohan et al, 2012]. The other parameters are tabulated (**Table 4. 1**)

Freundlich isotherm

The Freundlich isotherm is represented as

$$\log q_e = \log K_F + \frac{1}{n} \log C_e$$

where q_e is the amount of M^{+2} adsorbed (mg g^{-1}), C_e is the equilibrium concentration of the adsorbate (mg L^{-1}), and K_f and n are the Freundlich constants which indicate the adsorption capacity and the adsorption intensity respectively (**Fig 4.6B**). The higher value of n in case of all the three metals indicates high affinity of this adsorbent towards the metal cations. Among the three metals, zinc adsorption obeyed the Freundlich adsorption isotherm owing to its higher regression coefficient. This isotherm does not predict any saturation of the adsorbent by the metal ions. Thus, it is predicted mathematically that infinite surface coverage is available for metal binding leading to a multilayer adsorption on the adsorbent surface. All the other calculated analytical parameters for the adsorption of all the metals have been tabulated in table 4.1

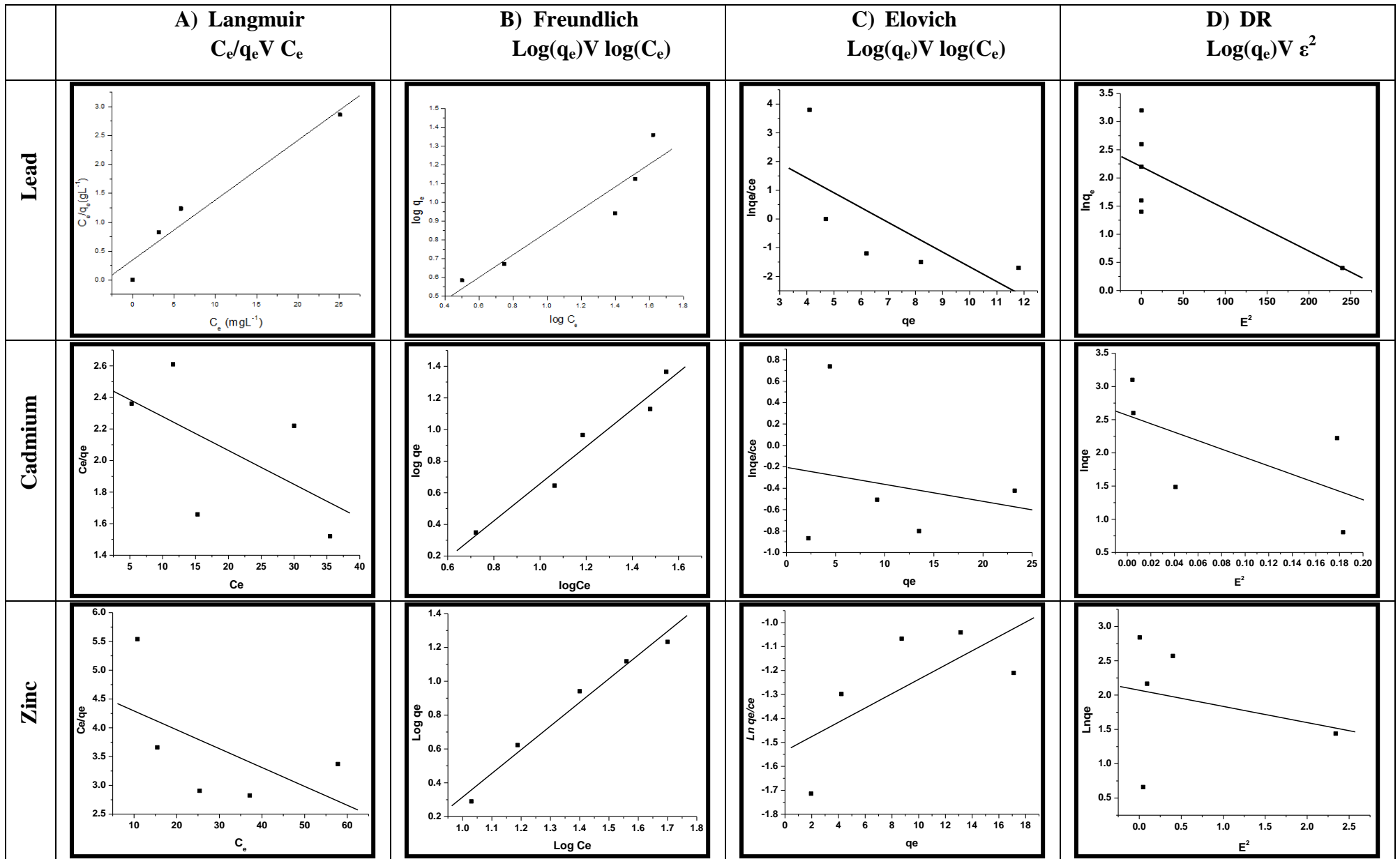


Figure 4.6: Adsorption isotherms A) Langmuir isotherm, B) Freundlich isotherm, C) Elovich isotherm and D) DR isotherm for Heavy Metals Lead, Cadmium and Zinc.

Table 4.1 Isotherm parameters obtained through various models

S.no.	Isotherm models	Parameters	Microorganism immobilized Sodium Alginate		
			Lead	Cadmium	Zinc
1.	Langmuir	q_0 (mg g ⁻¹) b (L mg ⁻¹) R_L r^2	9.68 0.2969 0.077 0.946	25.12 0.0155 0.55 0.958	14.28 0.015 0.019 0.652
2.	Freundlich	K_F (mg l ^{-1/n} g ⁻¹) L n r^2	1.733 1.66 0.89	3.28 0.852 0.978	12.105 0.719 0.987
3.	Dubinin-Radushkevich	q_m (mg g ⁻¹) β E (KJ Mol ⁻¹) r^2	8.652 0.0062 8.98 0.448	6.958 0.985 0.268 0.635	5.621 1.568 0.291 0.364
4.	Elovich	q_m K_E r^2	1.886 19.125 0.5126	6.25 8.94 0.715	4.352 0.724 0.678

Kinetics of adsorption

The uptake of the metal by *Halomonas BVR 1* immobilized sodium alginate depends on the contact time and hence the study of the kinetics of adsorption is a vital factor. The pseudo first order and second order kinetic models [Lagergren et al, 1898; Ho et al, 2006] relate the amount of metal ions adsorbed on the cell surface at equilibrium at various time intervals to the respective kinetic rate constants (k_1 and k_2). The first order and second order equations can be expressed as,

$$\log(q_e - q_t) = \log(q_e) - \frac{k_1 t}{2.303}$$

$$\frac{t}{q_t} = \frac{1}{k_2 q_e^2} + \frac{t}{q_e}$$

The respective kinetic plots (**Fig. 4.7A and 4.7B**) and the parameters (**Table 4.2**) gave a higher regression coefficient for the second order kinetic model indicating that lead and zinc adsorption data could fit well with pseudo second order kinetics. Further, the experimental and calculated equilibrium adsorption capacity [q_e] values were found to be 3.9 mg g^{-1} and 5.9 mg g^{-1} as per the second order kinetics for lead. A typical phenomenon observed in case of the cadmium adsorption was that the adsorption kinetics was favored by the pseudo first order model.

The details of all the other parameters are given in the **Table 4.2**

The intra- particle diffusion constant was calculated using the Weber and Morris intraparticle diffusion model [Weber et al, 1963]

$$q_t = k_{\text{int}} \sqrt{t} + C$$

where k_{int} is the intra-particle diffusion constant and q_t is the amount of metal adsorbed at time t .

Table 4.2 Kinetics and Intraparticle rate constant data for the adsorption of metal ions.

System	Second order rate constant k_2 ($\text{g mg}^{-1}\text{min}^{-1}$)	Regression Coefficient	First order rate constant k_1 (min^{-1})	Regression coefficient	Intraparticle rate constant k_{int} [$\text{mg/g/ min}^{-0.5}$]
Cadmium	0.015	0.0596	0.0016	0.995	0.963
Lead	0.0020	0.929	0.048	0.954	0.345
Zinc	0.048	0.999	0.025	0.981	0.980

Diffusion processes such as film, pore and surface diffusion could also influence the transport of the lead ion from the bulk to the alginate bead surface. Intraparticle diffusion of the metal ions from the bulk into the pores of the beads can also account for the kinetics of sorption. The Weber–Morris plot (**Fig. 4.7C**) yields a finite intercept and this is attributed to the fact that boundary layer effect also could influence the uptake of the metal ions from the bulk to the bacterium cell surface.

Thermodynamics of adsorption

The effect of temperature on the adsorption of divalent cations onto microbe alginate bead surface was studied. The free energy of adsorption [ΔG^0], standard enthalpy (ΔH^0) and standard entropy (ΔS^0) determined the adsorption studies at various temperatures.

The above parameters are given by the Van't Hoff equations [Pardo et al, 2003]. The equilibrium constant K was obtained from the ratio of the concentration of lead in the solid and liquid phase respectively. The $\ln K$ against $1/T$ plot gives ΔH^0 and ΔS^0 respectively (**Fig. 4.7D**).

The negative free energy change and the exothermic adsorption nature of the adsorption process (**Table 4.3**) indicates that metal ion adsorption on the microbe- alginate bead surface is feasible and spontaneous. The enthalpy of adsorption was low (less than 80KJ Mol⁻¹) indicative of a physisorption. Among the metals too, there was a wide degree of variation observed in terms of the calculated enthalpy due to the variation in their atomic radii. The immobilized *Halomonas BVR 1* in sodium alginate thereby acts as an effective secondary host for the adsorption of cations.

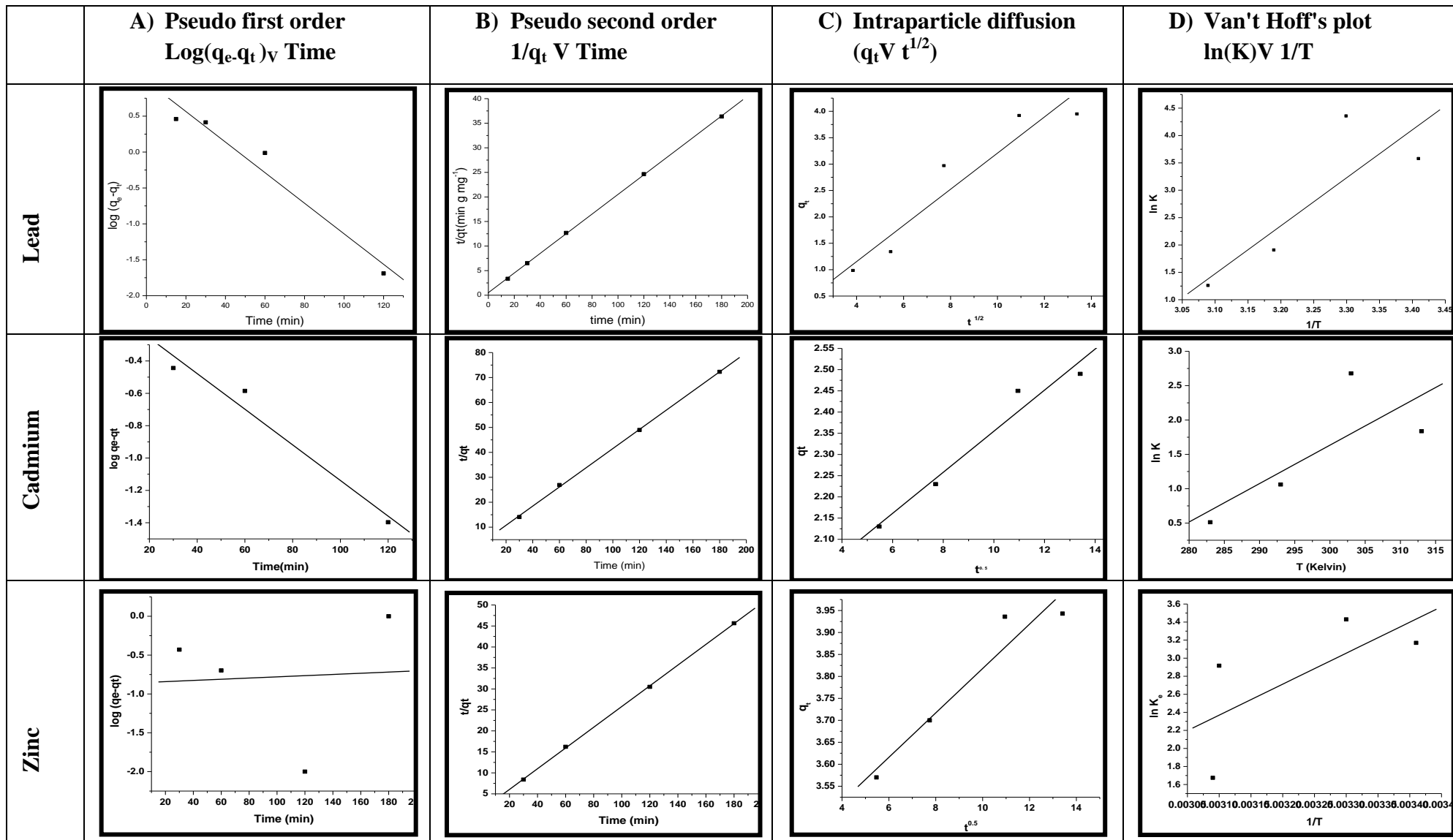


Figure 4.7: A) Pseudo first order B) Pseudo second order C) Intraparticle diffusion and D) Van't Hoff plots for heavy metals Lead, Cadmium and Zinc.

Table 4.3 Thermodynamic data for the adsorption of the metal ions.

System	Temperature (Kelvin)	ΔG° (kJ mol ⁻¹)	ΔS° (J mol ⁻¹ K ⁻¹)	ΔH° (kJ mol ⁻¹)
Immobilized bacteria in sodium alginate (Cadmium)	293	-7.741	-123.756	-28.534
	303	-8.650		
	313	-7.594		
	323	-4.478		
Immobilized bacteria in sodium alginate (lead)	293	-8.69	-213.713	-72.893
	303	-10.955		
	313	-4.94		
	323	-3.359		
Immobilized bacteria in sodium alginate (Zinc)	283	-1.205	-125.90	-4.257
	293	-2.585		
	303	-6.749		
	313	-4.780		

Interfering ion studies

The effects of foreign ions that are commonly present in the real effluents were investigated by preparing a synthetic mixture containing varying concentration of the metal ions. The aqueous volume was maintained at 10 mL. Anions such as nitrate, sulfate and chloride while cations such as Fe (II) and Cd (II) interfered with the adsorption of zinc significantly at higher concentrations. Adsorption of cadmium was significantly affected by the presence of cations such as zinc, iron and magnesium at 100 mg L⁻¹, 100 mg L⁻¹ and 50 mg L⁻¹ respectively. Effect of anions was negligible on cadmium adsorption. Lead adsorption reduced by 6% in the presence of iron and zinc at 100 mg L⁻¹ of each concentration. Presence of phosphate ions at 80 mg L⁻¹ reduced the adsorption of lead by 10% (**Table 4.4**)

Table 4.4: Effect of interfering ions metal adsorption

Concentration of Anions mgL ⁻¹	% adsorption of cadmium	% adsorption of lead	% adsorption of zinc	Concentration of Cations mg L ⁻¹	% adsorption of cadmium	% adsorption of lead	% adsorption of zinc
SO ₄ ²⁻ (70)	NI*	NI*	88±0.1	Zn ²⁺ (100)	95±0.5	96±0.8	NI*
PO ₄ ³⁻ (80)	99 ± 0.2	90±0.5	NI*	Ni ²⁺ (100)	NI*	NI*	NI*
Cl ⁻ (70)	NI*	NI*	85±0.4	Co ²⁺ (100)	NI*	NI*	NI*
NO ₃ ⁻ (80)	NI*	NI*	85±0.3	Mn ²⁺ (50)	NI*	NI*	NI*
				Fe ²⁺ (100)	93±0.9	96±0.4	86±0.5
				Mg ²⁺ (50)	92±0.7	NI*	NI*
				Cd ²⁺ (50)	NI*	NI*	89±0.9

NI*: No Interference

Regeneration of the alginate beads

The regeneration of the beads were tried using various reagents and percentage of metal eluted is shown in **Table 4.5**. The efficiency of these reagents are well known [Lin et al, 2005] and the recovery of lead was found to be maximum (90 %) with 5 mL of 0.1 mol L⁻¹ of HCl as the eluent. A 0.1 mol L⁻¹ HCl solution was found to be quite effective since in acidic medium the H⁺ ions are known to replace the metal ions from the adsorbent. With two 5 mL portions of the

eluent (0.1 mol L⁻¹ HCl) the adsorbent could be fully regenerated. However, poor recovery (50%) was observed with NaOH, owing to the deprotonation of the coordinating ligands. Thus the use of dilute HCl as an eluent makes the process greener and cost effective [Gotoh et al, 2004]. Diluted 0.1 mol L⁻¹ HCL was used for the regeneration of adsorbent after cadmium and zinc adsorption. About 90 % recovery of the metal ions was obtained after the regeneration procedure of both the heavy metals.

Table 4.5 Recovery of lead with various eluents

Eluent	Volume	Lead ions eluted (%)	cadmium ions eluted (%)	zinc ions eluted (%)	Volume
0.1 mol L⁻¹ HCl	5 mL	90	85	93	2 x 5 mL
0.1mol L⁻¹ NaOH	5 mL	50	65	70	2 x 5 mL

Comparison with other strains

The developed method for metal removal by immobilized cells was compared in terms of the adsorption capacity against other adsorbents [Lin et al, 2006; Mattuschka et al, 1993; Kapoor et al, 1995; Yan et al, 2000]. The comparison **Table 4.6** shows that the immobilized *Halomonas BVR 1* has good adsorption capacity for metal ions in comparison to other biosorbents.

Table 4.6: Comparison of the adsorption capacities with other similar adsorbents.

Sl.No.	Strain	Adsorption capacity (mg g ⁻¹)	Metal ions	Reference
1	<i>Pseudomonas aeruginosa</i> PU21	0.7	Lead	Gotoh et al, 2004
2	<i>Streptomyces noursei</i>	1.6	Lead	Lin et al, 2006
3	<i>Penicillium sp.</i>	5.0	Lead	Mattuschika et al, 1993
4	<i>Aspergillus niger (live)</i>	2.25	Lead	Kapoor et al, 1995
5	<i>Mucorrouxii (Na₂CO₃ pretreated)</i>	3.26	Lead	Yan et al, 2000
6 →	<i>Halomonas BVR 1+ Sodium alginate</i>	9.68	Lead	Present study
7	<i>Calcium alginate carbonate composite beads</i>	10.2	Cadmium	Mahmood et al, 2015
8	<i>Calcium alginate beads</i>	27.4	Cadmium	Akpomie et al, 2015
9	Chitosan	8.54	Cadmium	Krika et al, 2011
10	Granular activated carbon F400	8.00	Cadmium	Krika et al, 2011
11 →	<i>Halomonas BVR 1+ Sodium alginate</i>	25.12	Cadmium	Present study
12	<i>Alginate fly ash</i>	1.85	Zinc	Nadeem et al, 2014
13	<i>Hazelnut shells</i>	1.78	Zinc	Cimino et al, 2000
14	<i>Immobilized dead algal cells Chlorella vulgaris</i>	9.38	Zinc	Sheikha et al, 2008
15 →	<i>Halomonas BVR 1+ Sodium alginate</i>	14.28	Zinc	Present study

Column Studies: Experiments and Modeling

Column packing and parameters assessed

The earlier part of the chapter dealt with the removal of cations using *Halomonas BVR 1* immobilized in sodium alginate polymeric matrix. This adsorbent (**Fig. 4.8**) gave the least maximum adsorption capacity in case of lead adsorption when compared to zinc and cadmium batch adsorption. With this aspect in mind, column studies for treating larger volumes at higher concentration of lead using this adsorbent was deliberated upon.

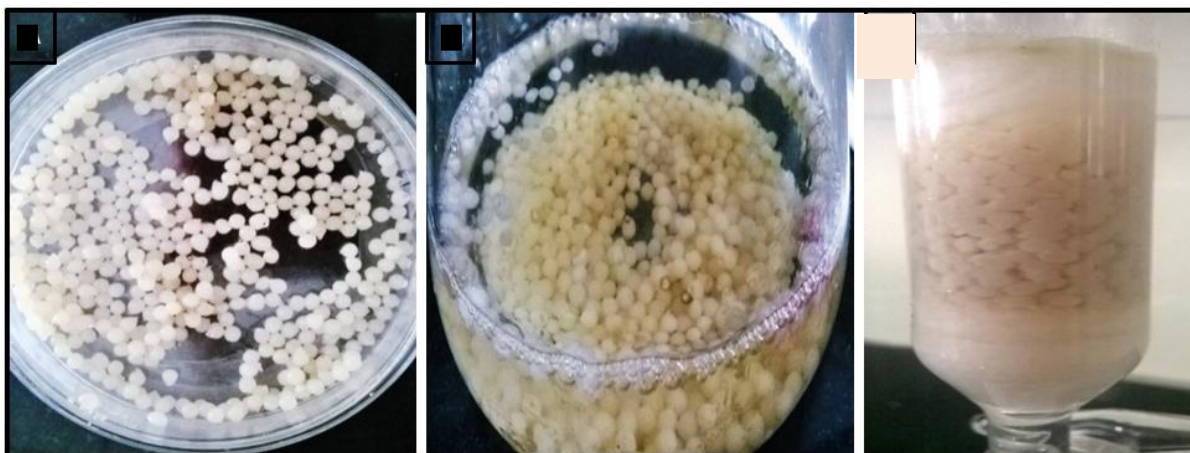


Figure 4.8: Depiction of the adsorbent used for column packing

Accordingly, a detailed column study for the removal of lead was carried out and a theoretical model for the upscale removal of the same was performed. The basic schematic representation of the experiments carried out is as follows (**Fig.4.9**):

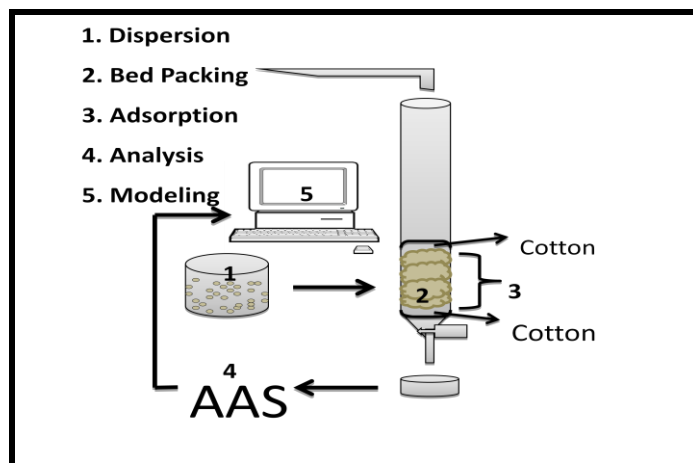


Figure 4.9: Schematic representation of the experiments carried out for modeling studies.

The biosorbent was packed homogenously in a 2x1.5 cm glass column by maintaining certain parameters constant such as a bead diameter of 3 mm, number of beads i.e. 250 beads/column which weighed 5.3g on an average, column height of 1.5cm and column diameter of 2 cm. Other parameters like concentrations of lead were varied from 20 to 60 mg L⁻¹. Volume of influent lead nitrate solution was taken as 100 mL and 250 mL and passed through the column at two different flow rates of 2.3 and 15 mL min⁻¹.

Materials and Methods

Varied concentrations lead nitrate solution, 20, 30, 40 and 50 mgL⁻¹ at a volume of 100 mL was run at two extreme flow rates 2.3 mL min⁻¹ and 15mL min⁻¹. The entire column experiment was performed manually. The output runs were collected at different time intervals of 5 min and 0.6 min for flow rates of 2.3 and 15 mL min⁻¹. respectively. Repetitive runs were performed on the same columns to analyze the efficiency and reusability of the column. The concentration of lead in the output metal solutions was analyzed by the Atomic Absorption Spectroscopy (AA-7000 Shimadzo)

Discussion: Breakthrough Curves

Plots showing C_t/C_o Vs time (t) was analyzed to determine the breakthrough concentration of lead with a respective volume at each flow rate considered for a certain height and mass of the column. Ideally, the concentration at particular time t where $C_t/C_o = 0.05$, determines the breakthrough concentration (C_b) of the column. The concentration of lead at $C_t/C_o = 0.95$ determines exhaustion concentration (C_e) indicating the saturation of the column. Such curves for concentrations of 20, 30, 40, 50 and 60 mg L⁻¹ lead solution for two different volumes of 100mL and 250mL at two different flow rates of 2.3 mL min⁻¹ and 15 mL min⁻¹ was generated (**Fig: 4.10-4.13**).

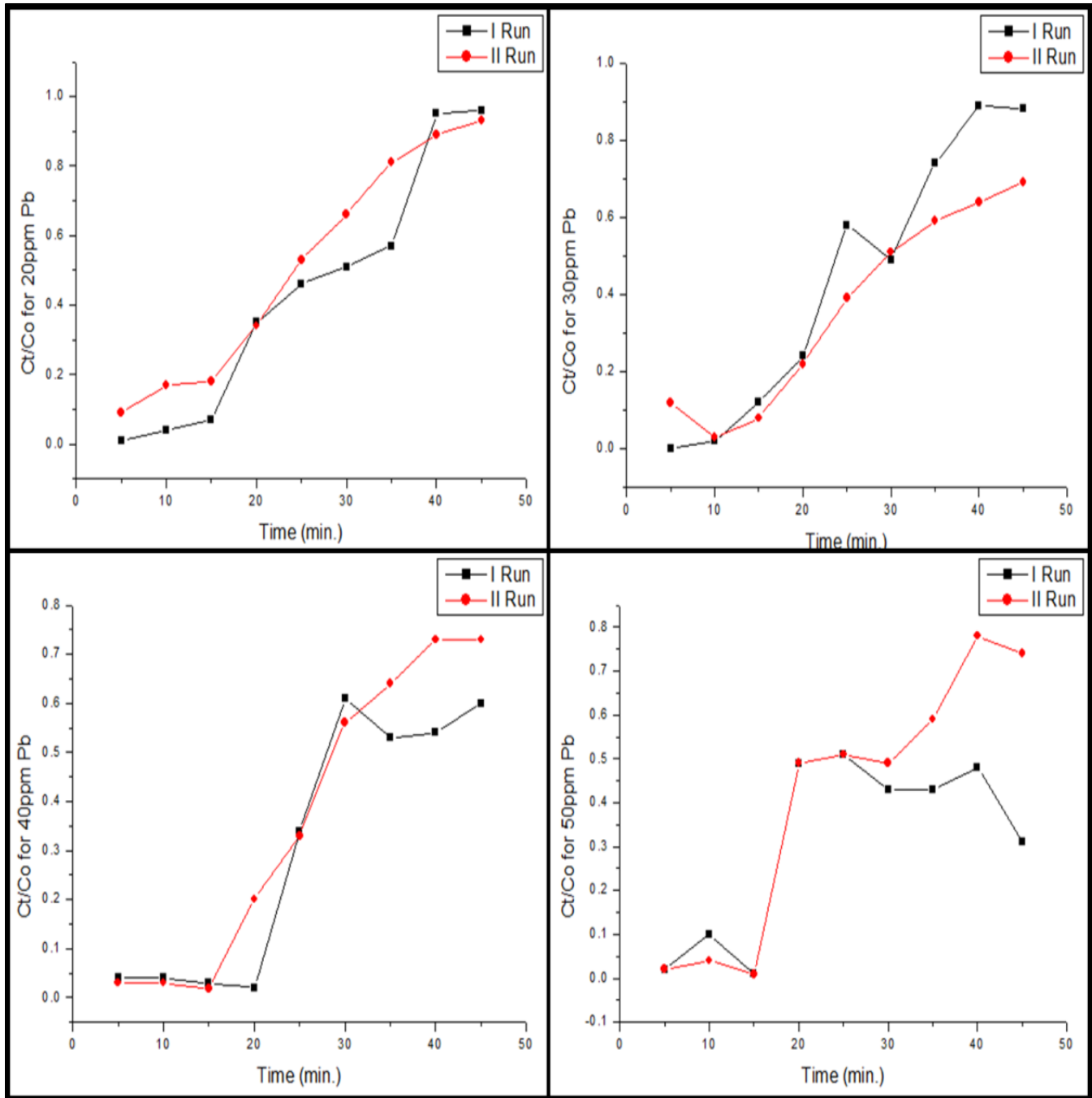


Figure 4.10. Breakthrough curves for 20, 30, 40 and 50 mg L⁻¹ of lead at 2.3mL min⁻¹.

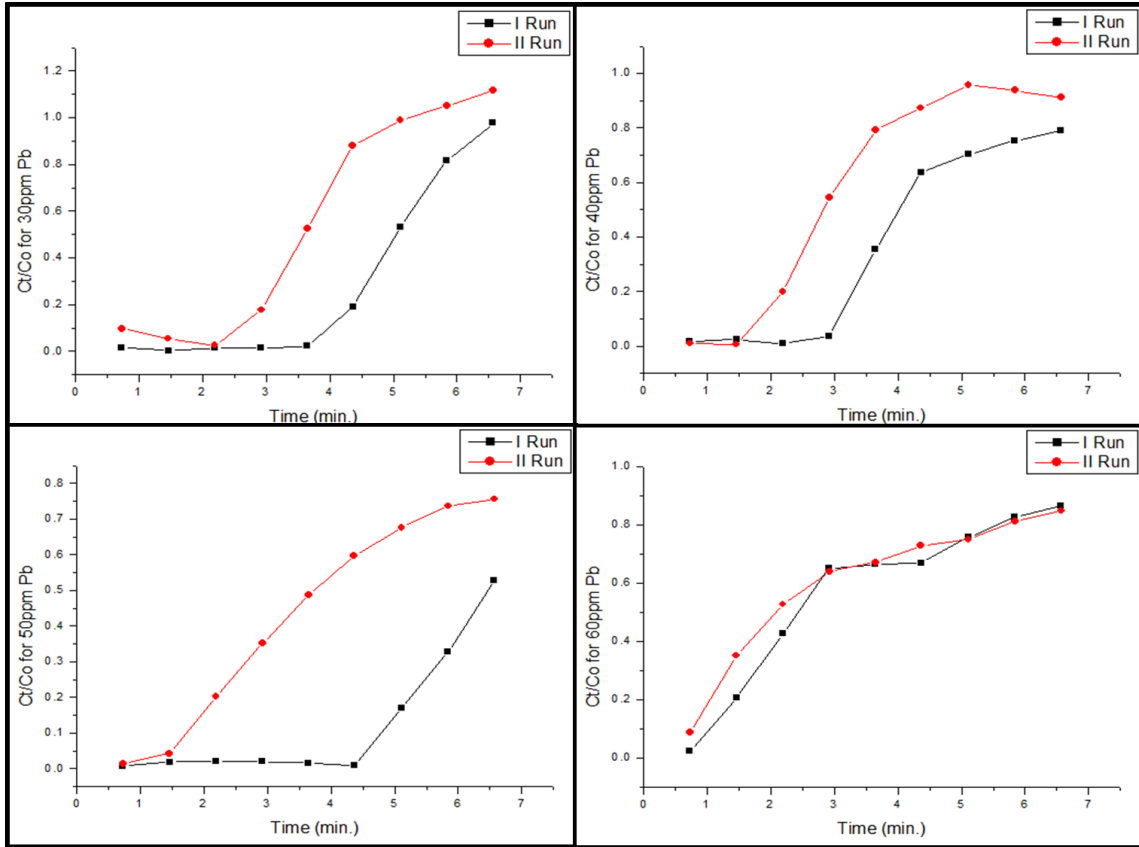


Figure 4.11. Breakthrough curves for 20, 30, 40 and 50 mg L⁻¹ of lead at 15 mL min⁻¹

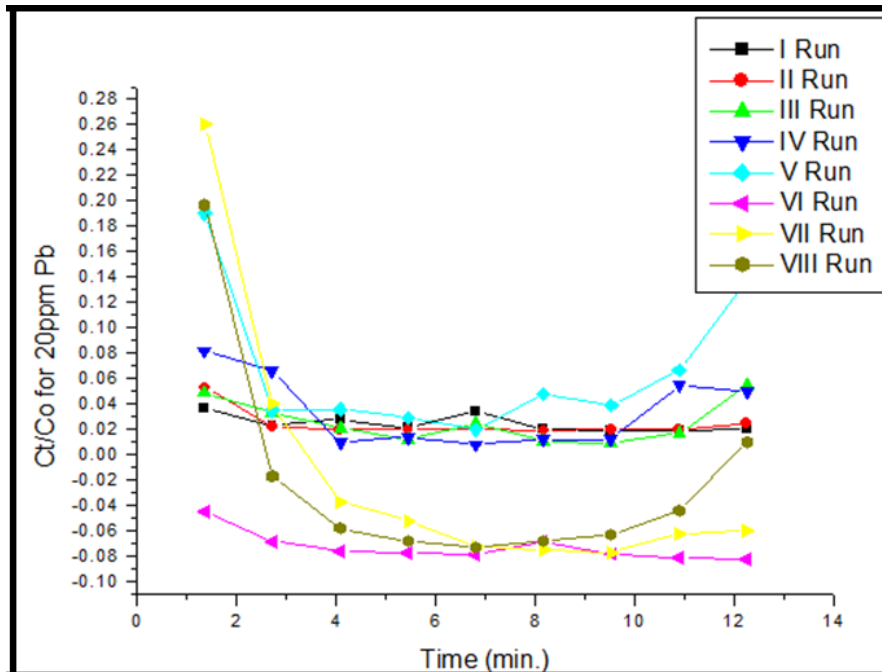


Figure 4.12 Breakthrough curves for 20 mg L⁻¹ concentration of Pb(NO₃)₂ in 100 mL MilliQ water at the maximum flow rate 15 mL min⁻¹. Eight runs performed with a total of 800 mL treated for 1 hr 45 mins.

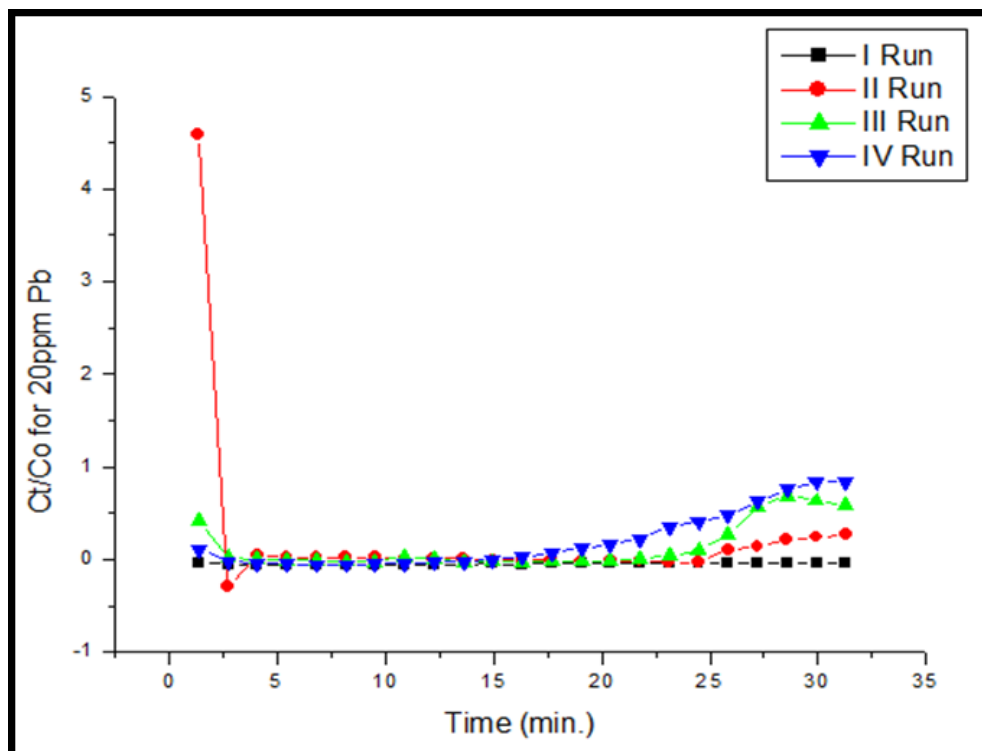


Figure 4.13. Breakthrough curves for 20mg L^{-1} concentration of $\text{Pb}(\text{NO}_3)_2$ in 250mL MilliQ water at the maximum flow rate 15mL min^{-1} . Four runs performed with a total of 800mL treated for $1\text{hr } 45\text{mins}$.

Dithizone Test

Dithizone is a reagent, which at pH 3 binds to lead ions to form red colored complex that indicates the presence and binding phenomenon of the lead ions [Diaper et al, 1957]. The Fig. 4.14 depicts the adsorbent before and after the metal adsorption occurs. The adsorbent clearly indicates effective metal adsorption which is indicated by the change in the color of the adsorbent .



Figure 4.14: Dithizone test for the *Halomonas BVR.1* immobilized sodium alginate beads before and after adsorption.

Column regeneration

Column regeneration is an important step that defines the efficiency, capacity and reusability of the column. Various concentrations (0.1-1 mol L⁻¹ range of CaCl₂ at pH 3 with varying volumes of 10-50 mL) of the eluent was used to desorb the metal adsorbed. Among these, 10 mL of 1.0 mol L⁻¹ CaCl₂ at pH 3 showed the highest efficiency in regenerating the column.

Transport Modeling of Adsorption Column Experiment: *Methodology*

The transport of metal species can be best described by the combination of three mechanisms: molecular diffusion, hydrodynamic dispersion, and heterogeneous advection. All these mechanisms differ fundamentally in their behavior and are considered separately while considering the change in solute concentration along the length of the column. The advection-dispersion equation [Logan, 2001] was used to monitor the change in concentration with respect to time. This equation was parameterized with terms that quantify both hydrodynamic advection

and dispersion. At the pore scale, diffusion turns out to be the most important mechanism of metal movement. At batch scale dispersion is significant and at larger scales advection governs the spreading. The dynamic behavior transport of metal ions in a simple column without packing can be thus written as

$$\frac{\partial C}{\partial t} = -u \frac{\partial C}{\partial x} + D \frac{\partial^2 C}{\partial x^2} \quad (1)$$

Eq. (1) represents advection convection equation that does not account for porous media. For transport in the case of porous media, the active flow region within the superficial volume V is $V\phi$, and accordingly the equation for the dynamic change of metal ions in aqueous phase is found to be:

$$V\phi \frac{\partial c}{\partial t} = -u(V\phi) \frac{\partial c}{\partial x} + D_L(V\phi) \frac{\partial^2 c}{\partial x^2} \quad (2)$$

For analysing the total mass of the solid phase $(1 - \phi)\rho V$, by assuming the rate of the sorption reaction k_d , the mass of the adsorption per unit mass of solid phase was given by the adsorption isotherms. Data from the laboratory studies (Refer Section kinetics and adsorption of this chapter) kinetics of adsorption and isotherms were estimated using Linear, Langmuir and Freundlich theories. For different empirical adsorption isotherm models, different Advection-Dispersion equations were developed using Eq. (2).

Advection-Dispersion model with Linear Adsorption

For Linear adsorption isotherm, where m (g g^{-1}) is concentration of solute adsorbed on the solid phase, C (g mL^{-1}) is equilibrium concentration of the solute in solution and K_d (mL g^{-1}) is the linear distribution coefficient, the isothermal is given by

$$m = K_d C \quad (3)$$

The molar rate of change due to adsorption is given as

$$V(1 - \varphi)\rho \frac{\partial m}{\partial t} = V(1 - \varphi)\rho \frac{\partial(K_d C)}{\partial t} = V(1 - \varphi)\rho K_d \frac{\partial C}{\partial t} \quad (4)$$

Equation (3) further can be improved by the combining Eq. (4) with rate of molar change due to advection-convection, and the transient change can be written as

$$[V\phi + V(1 - \phi)\rho K_d] \frac{\partial C}{\partial t} = -u(V\phi) \frac{\partial C}{\partial x} + D_L(V\phi) \frac{\partial^2 C}{\partial x^2} \quad (5)$$

By dividing each term by in equation (5) by $V\phi$ and introducing retardation factor ε , final developed model for sorption is:

$$\frac{\partial C}{\partial t} = -\frac{u}{\varepsilon} \frac{\partial C}{\partial x} + \frac{D_L}{\varepsilon} \frac{\partial^2 C}{\partial x^2} \quad (6)$$

Where $\varepsilon = [1 + \frac{(1-\varphi)}{\varphi} \rho K_d]$

Advection-Dispersion model with Freundlich Adsorption

Similar analysis was carried for Freundlich adsorption model by using a nonlinear empirical model which depicts the relation between the amount of an adsorbate adsorbed per unit weight (m , mg g^{-1}) of adsorbent and the adsorbate equilibrium concentration (C , moles L^{-1}) in the fluid. The relation used is given below:

$$m = K_d C^n \quad (7)$$

Where m is the amount of an adsorbate adsorbed per unit weight of adsorbent, x is the weight of adsorbate adsorbed on m unit weight of adsorbent, C is the adsorbate equilibrium concentration in the fluid and K and n are Freundlich coefficients. Carrying transient state

analysis of the phenomena, equation (7) was developed by using similar procedure as in case of linear model where elimination of K_d was done to arrive at a final model (14).

$$\frac{\partial m}{\partial t} = nK_d C_i^{n-1} \frac{\partial(C_i)}{\partial t} \quad (8)$$

$$V(1 - \varphi)\rho \frac{\partial(m)}{\partial t} = V(1 - \varphi)\rho nK_d C_i^{n-1} \frac{\partial(C)}{\partial t} \quad (9)$$

$$V\varphi \frac{\partial C}{\partial t} + V(1 - \varphi)\rho nK_d C_i^{n-1} \frac{\partial(C)}{\partial t} = -u(V\varphi) \frac{\partial C}{\partial x} + D_L(V\varphi) \frac{\partial^2 C}{\partial x^2} \quad (10)$$

$$\frac{\partial C}{\partial t} = -\frac{u}{\varepsilon} \frac{\partial C}{\partial x} + \frac{D_L}{\varepsilon} \frac{\partial^2 C}{\partial x^2} \quad (11)$$

Where the retardation factor $\varepsilon = \left[1 + \frac{(1-\varphi)}{\varphi} \rho nK_d C_i^{n-1}\right]$

Advection-Dispersion model with Langmuir Adsorption

Further analysis was carried out using the Langmuir adsorption isotherm where the adsorbent surface was considered to have a number of active interaction sites at which the phenomena of adsorption and desorption take place simultaneously.

$$m = \frac{X_m K_L C_i}{1 + K_L C_i} \quad (12)$$

Where, m is the concentration of solute adsorbed at equilibrium concentration (g g^{-1}), C is the concentration of the solute in solution (g mL^{-1}), X_m is the maximum amount of adsorbate for the formation of monolayer ($\text{g solute g adsorbent}^{-1}$) and K_L is the constant representing the strength with which the solute is bound to the substrate ($\text{Lm}_{\text{eq}}^{-1}$). Carrying transient state analysis of the phenomena, equation (15) was developed by using similar procedure as in case of linear model where elimination of K_d was done to arrive at a final model (18).

$$\frac{\partial m}{\partial t} = \frac{X_m K_L}{(1+K_L C)^2} \frac{\partial C}{\partial t} \quad (13)$$

$$V(1-\varphi)\rho \frac{\partial \left(\frac{X_m K_L C_i}{1+K_L C_i} \right)}{\partial t} = V(1-\varphi)\rho \frac{X_m K_L}{(1+K_L C)^2} \frac{\partial C}{\partial t} \quad (14)$$

$$V\varphi \frac{\partial C}{\partial t} + V(1-\varphi)\rho \frac{X_m K_L}{(1+K_L C)^2} \frac{\partial C}{\partial t} = -u(V\varphi) \frac{\partial C}{\partial x} + D_L(V\varphi) \frac{\partial^2 C}{\partial x^2} \quad (15)$$

$$\frac{\partial C}{\partial t} = -\frac{u}{\varepsilon} \frac{\partial C}{\partial x} + \frac{D_L}{\varepsilon} \frac{\partial^2 C}{\partial x^2} \quad (16)$$

$$\text{Where retardation factor } \varepsilon = \left[1 + \frac{(1-\varphi)}{\varphi} \rho \frac{X_m K_L}{(1+K_L C)^2} \right]$$

Numerical Implementation

For the different advection-dispersion models developed (i.e. equations (8), (14) and (18)) the basic assumptions that was considered are:

1. Flow doesn't exhibit velocity gradient along the cross section perpendicular to the flow direction i.e. frictional losses were not considered. Other assumptions made are:
2. Initial concentration in the column, $C(t=0,x)=0$
3. Boundary condition at Left Boundary, $C(t,x=0)=C_{in}$
4. Boundary condition at Right boundary, $\left. \frac{\partial C}{\partial x} \right|_{x=L} = 0$

Therefore, obtained AD equations for different empirical isothermal models were solved by dividing the column into n_x elements, each element of length Δx , and subsequently using the backward difference approximation and centred difference approximation for the terms $\frac{\partial C}{\partial x}$ (first derivative) and $\frac{\partial^2 C}{\partial x^2}$ (second derivative) respectively i.e.:

$$\frac{\partial C_i}{\partial x} = \frac{C_i - C_{i-1}}{\Delta x} \quad (19)$$

$$\frac{\partial^2 C}{\partial x^2} = \frac{C_{i+1} - 2C_i + C_{i-1}}{(\Delta x)^2} \quad (18)$$

Where $i=1, 2, 3, \dots, nx$

For linear model, by using equations (9), (20), and (21) the final model developed is:

$$\frac{\partial C_i}{\partial t} = -\frac{u}{\varepsilon} \left(\frac{C_i - C_{i-1}}{\Delta x} \right) + \frac{D_L}{\varepsilon} \left(\frac{C_{i+1} - 2C_i + C_{i-1}}{(\Delta x)^2} \right) \quad (20)$$

For $i=1$

$$\frac{\partial C_i}{\partial t} = -\frac{u}{\varepsilon} \left(\frac{C_1 - C_{in}}{\Delta x} \right) + \frac{D_L}{\varepsilon} \left(\frac{C_2 - 2C_1 + C_{in}}{(\Delta x)^2} \right) \quad (21)$$

$$\frac{\partial C_i}{\partial t} = -C_1 \left(\frac{u}{\varepsilon \Delta x} + \frac{2D_L}{\varepsilon (\Delta x)^2} \right) + C_{in} \left(\frac{u}{\varepsilon \Delta x} + \frac{D_L}{\varepsilon (\Delta x)^2} \right) + C_2 \left(\frac{D_L}{\varepsilon (\Delta x)^2} \right) \quad (22)$$

For $i=nx$

$$\frac{\partial C_i}{\partial t} = -\frac{u}{\varepsilon} \left(\frac{C_{nx} - C_{nx-1}}{\Delta x} \right) + \frac{D_L}{\varepsilon} \left(\frac{-C_{nx} + C_{nx-1}}{(\Delta x)^2} \right) \quad (23)$$

$$\frac{\partial C_i}{\partial t} = -C_{nx} \left(\frac{u}{\varepsilon \Delta x} + \frac{D_L}{\varepsilon (\Delta x)^2} \right) + C_{nx-1} \left(\frac{u}{\varepsilon \Delta x} + \frac{D_L}{\varepsilon (\Delta x)^2} \right) \quad (24)$$

For $1 < i < nx$

$$\frac{\partial C_i}{\partial t} = -C_i \left(\frac{u}{\varepsilon \Delta x} + \frac{2D_L}{\varepsilon (\Delta x)^2} \right) + C_{i-1} \left(\frac{u}{\varepsilon \Delta x} + \frac{D_L}{\varepsilon (\Delta x)^2} \right) + C_{i+1} \left(\frac{D_L}{\varepsilon (\Delta x)^2} \right) \quad (25)$$

Using above derived formulas (25), (26) and (27) the Advection-Dispersion equations for Freundlich, Langmuir and linear adsorption models were developed and their corresponding breakthrough curves were generated (**Fig 4.15-4.17**).

Comparison of Simulations with Column Experiments

The efficiency of column was explained by means of Breakthrough Curve. These were generated by plotting C versus time t, while keeping the flow rate constant. The breakthrough curves hence generated by using the data obtained through the column method operation exhibit a characteristic ‘S’ shape but each curve has a varying degree of steepness.

Adsorption of lead in accordance with various empirical adsorption isotherm models like Linear, Langmuir and Freundlich was taken into consideration. All of the required numerical modeling was done using MATLAB for different adsorption-dispersion models based on the experimental results obtained. To obtain the breakthrough curves using numerical modeling, the following parameters were considered that was obtained from the respective batch studies (**Table 4.7**).

Table 4.7: List of parameters considered to obtain the numerical model

Model	Dispersion Constant D_L	K_d	X_m	K_L	n
Linear	0.05	1.75	-	-	-
Langmuir	$2e^{-5}$	1.75	9.68	0.2969	-
Freundlich	$2e^{-5}$	1.733	-	-	1.766

Results and discussion

The following breakthrough curves have been generated using the mathematical models developed using empirical adsorption isotherms and comparisons have been made with the available experimental data. For all the models an acceptable extent of agreement between the

experimental data and computed results for inlet solution concentrations of 20, 30 and 40 mg L⁻¹ was observed. However, considerable deviation was observed between the two data sets for concentrations 50 and 60 mg L⁻¹ (Fig 4.15-4.17), which might be due to certain unaccounted change in the experimental conditions while carrying out the analysis. Also, on the basis of the simulation results, it can be concluded that the Linear model is the best model for simulating the adsorption behavior at low concentrations. This adsorption slowly shifts its behavior to the Freundlich isotherm that follows a multilayer kind of adsorption phenomenon.

The modeling studies could conclusively report that the column was effective in treating lead solutions up to a concentration of 40 mg L⁻¹. These columns treated volumes upto 800mL and 1L respectively in a period of 2hr 32min and 2hr 8min respectively. The regeneration showed best results with 10mL of 1mol L⁻¹ CaCl₂ at pH 3.

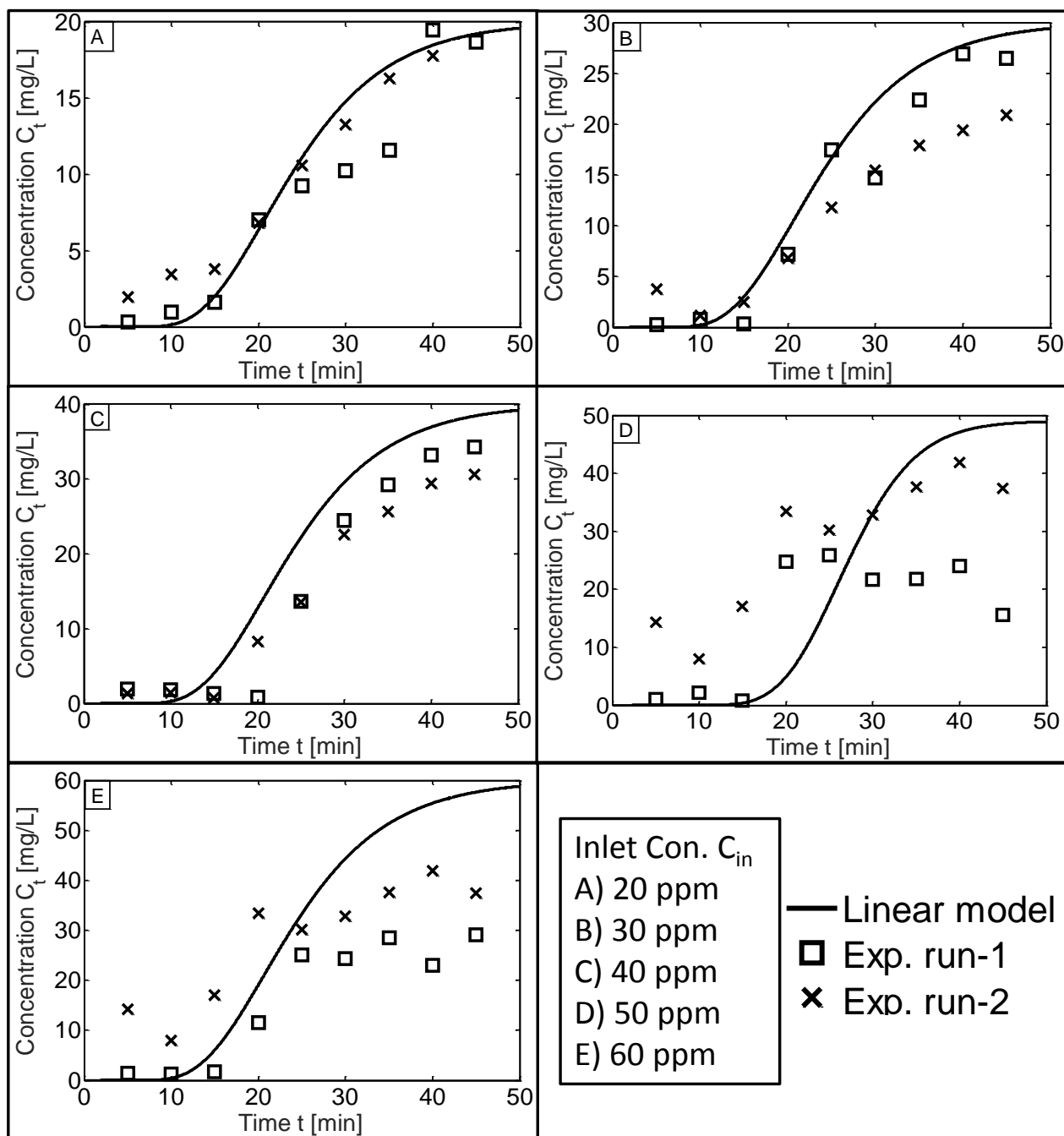


Figure 4.15: Comparison of Experimental data and Generated Breakthrough curves using Linear Model for 20, 30, 40 and 50mg L⁻¹ of Pb(NO₃)₂ in 100mL in MilliQ water at the least flow rate of 2.3mL min⁻¹.

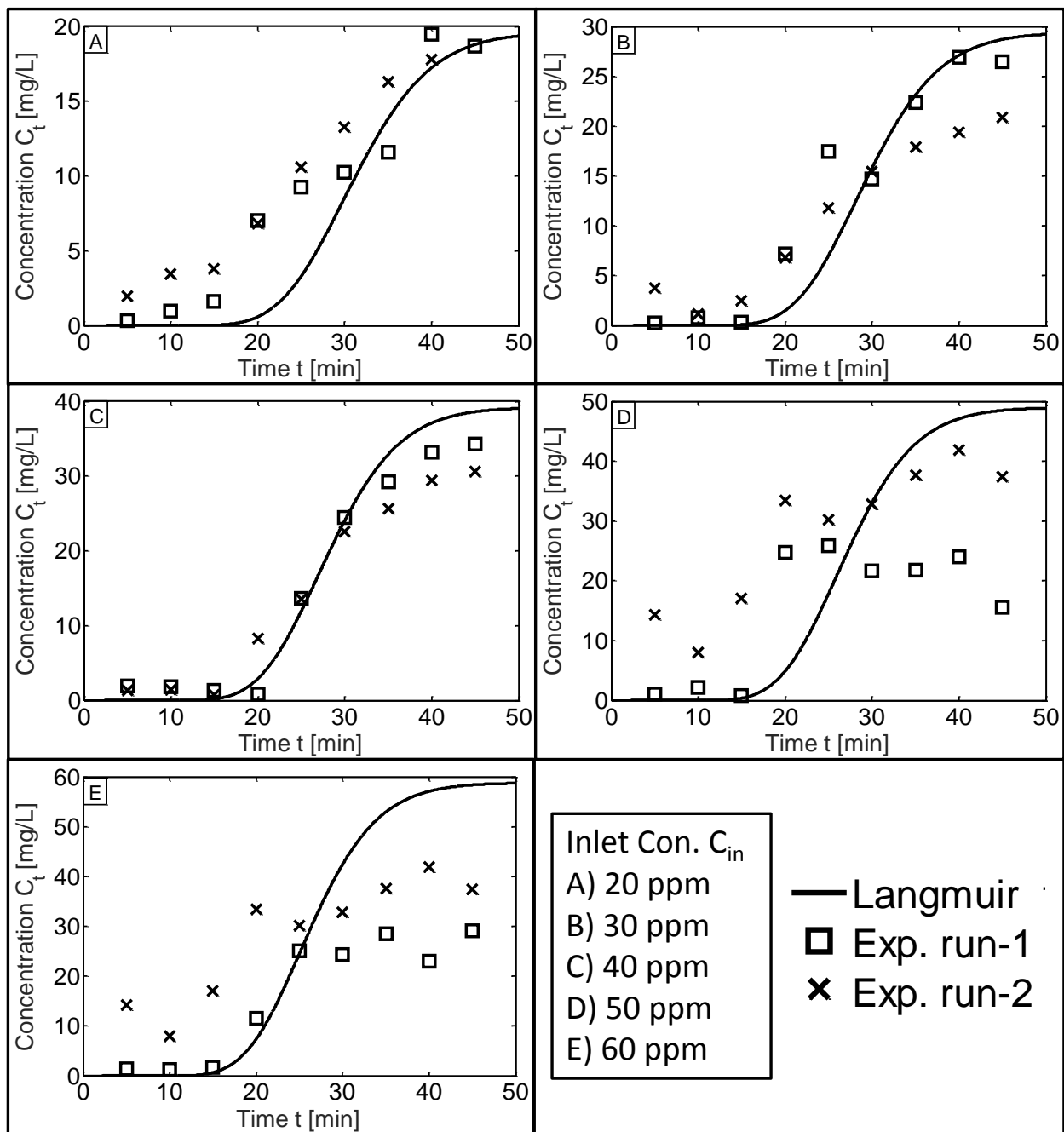


Figure 4.16: Comparison of Experimental data and Generated Breakthrough curves using Langmuir Model for 20, 30, 40 and 50mg L⁻¹ of Pb(NO₃)₂ in 100mL in MilliQ water at the least flow rate of 2.3mL min⁻¹.

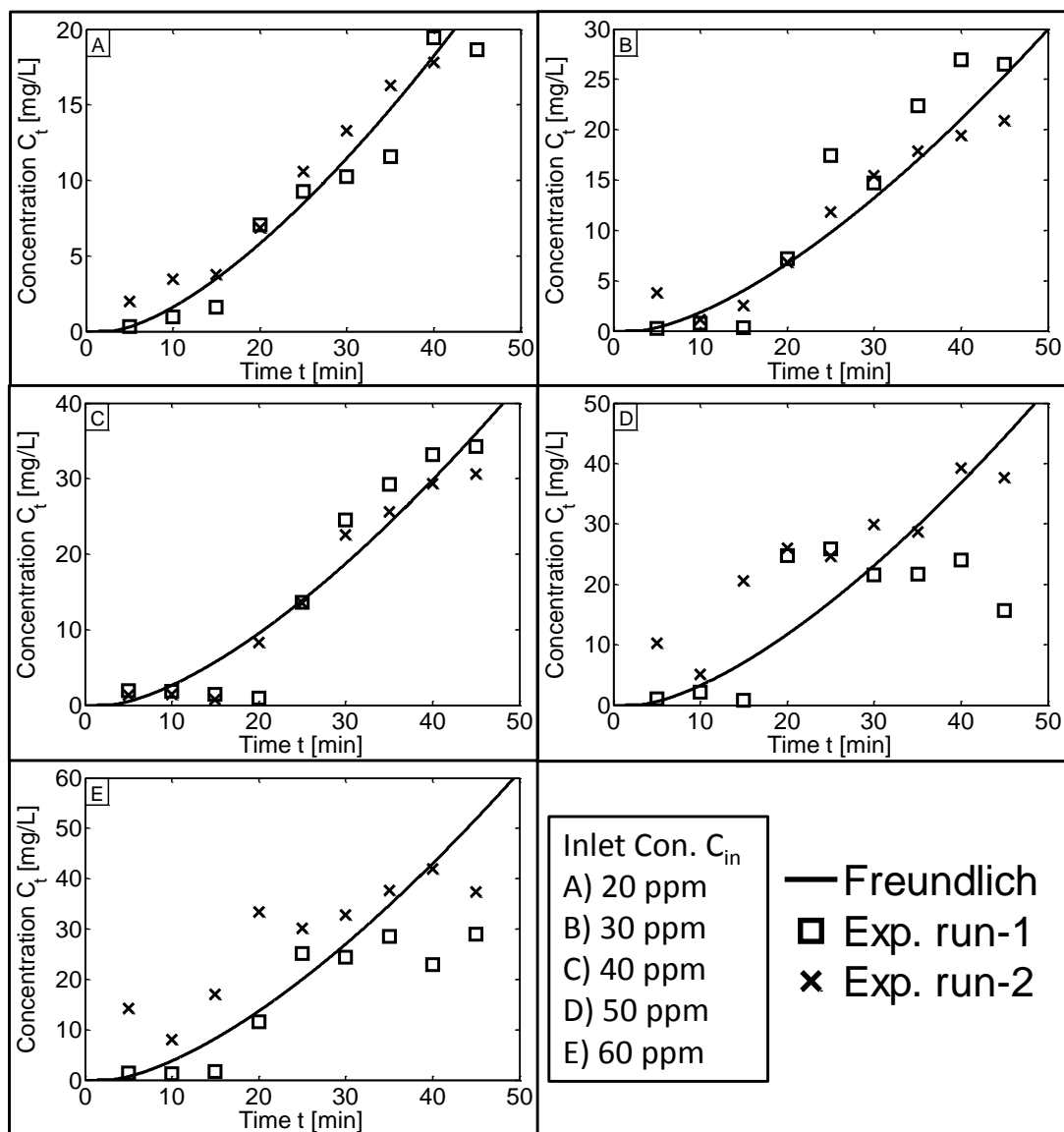


Figure 4.17: Comparison of Experimental data and Generated Breakthrough curves using Freundlich Model for 20, 30, 40 and 50 mg L^{-1} of $Pb(NO_3)_2$ in 100mL in MilliQ water at the least flow rate of 2.3 mL min^{-1} .

Additionally, the adsorbent was effective when used subsequent to soaking the *Halomonas BVR1* immobilized sodium alginate beads in 1.0 mol L^{-1} $CaCl_2$ solution at neutral pH for a week. These beads were then packed and soaked again in double distilled water for 3 days. One of the reasons for a better adsorption capacity after a prolonged soaking might be attributed

to the increase in the bead porosity due to swelling. Due to this surface area increases that leads to increase in number of sites being revealed for a better adsorption.

Conclusions

This work proved to be successful in developing a *Halomonas BVR 1* based biosorbent for the removal of cadmium, lead and zinc. The immobilized bacterium-alginate system functions as an effective host for the adsorption of metal ions due to the presence of functional groups on the surface of the bacterium and the carboxylate groups contributed by alginate. Langmuir isotherm gave a good fit to the experimental data with a maximum adsorption capacity of 9.68 mg g^{-1} and 25.12 mg g^{-1} for lead and cadmium respectively. The adsorption was found to be significantly dependent on the pH and temperature. The pseudo second order kinetic model was best suited for the adsorption of lead and zinc while that of cadmium obeyed the pseudo first order kinetics. Thermodynamics depicted the process to be spontaneous as well as exothermic. The adsorption process in all the cases was exothermic and spontaneous. Furthermore, the preparation of immobilized sodium alginate beads is simple and the process is robust and practically feasible. Hence, this system can remove lead up to a concentration of 75 mg L^{-1} thus making the process economical and green for diverse applications. This adsorbent was also able to remediate cadmium and zinc upto a concentration of 80 mg L^{-1} . Extrapolating the batch data obtained for the adsorption of lead, to column studies revealed certain important findings. The column could treat up to 800mL and 1L respectively in a period of 2hr 32min and 2hr 8min respectively with 5.3 gm of the adsorbent. The column showed high efficiency both in terms of capacity and reusability when the concentration of lead was within 40 mg L^{-1} . The regeneration showed best results with 10mL of $1 \text{ mol L}^{-1} \text{ CaCl}_2$ at pH 3.

CHAPTER V

UNDERSTANDING THE EFFECT OF POLYAMINE EXPRESSION UNDER LEAD STRESS ON *Halomonas BVR 1* AND DELINEATING THE GENETIC BASIS OF ITS HEAVY METAL RESISTANCE

Understanding the effect of heavy metal stress on *Halomonas BVR 1* and delineating the genetic basis of its heavy metal resistance

Deciphering the physiology of *Halomonas BVR 1* under heavy metal stress

Our isolate *Halomonas BVR 1* has proved to be an excellent biosorbent for the remediation of heavy metals like lead, cadmium and zinc. One of the main reason for this strain being able to remediate is its tolerance to high concentration of heavy metals. It was therefore important and interesting to identify the genetic basis of its metal resistance and also understand the fate of the bacterial cells under heavy metal stress.

The ability of bacterial strains to cope with sudden changes in the environment ensures their ecological dominance under stress conditions. Heavy metal pollution is one such stress condition that has turned into a major issue. This kind of stress triggers the production of myriad metabolites which act as potential mechanisms for combating stress in living systems. Stress in bacteria leads to increased metabolite production due to changes in physiological processes contributing to their protective mechanisms [Ramakrishna et al, 2011] Some of the stress related adaptive and protective responses include, alteration of gene expression patterns, changes in the control of transcription, translation, stability of transcripts and proteins etc [Ron et al, 2013] This is one of the major reasons why microbes are used to remediate metals ie; their biochemical versatility which is a result of their genetic plasticity and ability to modify physiology so as to make them best the competitor in a constantly changing environment (Murugesan and Maheswari, 2007)

The fluctuations in nitrogen metabolism is central to the heavy metal response in terms of physiology of a bacteria [Chen et al, 2011, Ramakrishna et al, 2011]. Among these, the major

players are polyamines (PA), which are ubiquitous polycationic aliphatic amines present in all living organisms. The three major PA's include putrescine, spermidine and spermine. Putrescine, the diamine precursor to spermidine and spermine is synthesized from amino acid arginine and ornithine via the enzymes arginine decarboxylase (ADC) and ornithine decarboxylase (ODC) respectively. The PA metabolic pathway is intricately connected to the metabolism of several amino acids and other important metabolites like ethylene and γ -aminobutyric acid (GABA), thus forming a crucial, complicated network of nitrogen sequestration. The polycationic chemistry of these molecules provides direct structural evidence for their roles in metal sequestration through lone-pair-bond-pair reactions. Therefore, in our study we have attempted to concentrate on this aspect of polyamine expression in *Halomonas BVR 1* under heavy metal stress.

Furthermore, metal ion homeostasis in a bacterial cell is governed by extensive regulatory and metal coding machinery that aids bacteria to regulate metal uptake and maintain an optimal bioavailable concentration. With this available literature, a study was also carried out to analyze the protein profile of *Halomonas BVR 1* under metal stress.

Overall, the adaption of a bacterial cell to adverse habitat can be natural or acquired through plasmids. The genetic determinants of heavy metal resistance in bacteria might be present on the plasmid DNA, transposons or chromosomal DNA [Cervantes et al, 1991, Carattoli et al, 2003]. Recently, these innate resistance mechanisms in bacteria have also contributed to enhanced metal adsorption capacity by microorganisms and hence has been exploited to carry out bioremediation. With these aspects in mind, we have analyzed the three centered interaction between polyamines, heavy metal and the physiology of *Halomonas BVR 1* in the presence of lead. The protein profile and the genetic basis of heavy metal resistance of *Halomonas BVR 1* under metal stress has also been decoded.

A) Evidence for Polyamines Mediated Mitigation of Lead Induced Stress in *Halomonas BVR 1*

Introduction

The potential role of PA in modulating plant stress due to heavy metals is well documented, but there are no reports on PA mediated modulation of metals in bacteria. Literature survey shows some of the following mechanisms that have been proposed to justify the increase in PA levels and their precise role in scavenging metals:

1. Heavy metal stress leads to the production of OH^\cdot and O_2^- due to oxidative stress, leading to disintegration of biomembranes by lipid peroxidation. Polyamines are known to scavenge free radicals *in-vitro* [Schrader et al, 1763].
2. Polyamines block one major vacuolar channel, and their accumulation decreases inward ion conductance at the vacuolar membrane to facilitate metal ion compartmentation [Girdhar et al, 2014].
3. Polyamines being positively charged tend to bind to metals and nucleic acids for their stability and can also help in sequestration of metals [Casale et al, 2009].

There is no clear information till date on the role of polyamines as a possible player in combating heavy metal stress in bacteria. This study adds to the existing literature of polyamines in bacteria and throws light on their heavy metal stress mitigation phenomenon. The results demonstrated in this paper, depicts a simple and easy measurement of polyamines using mass detection and fluorescence spectrophotometer in bacterial cells in the presence of heavy metal lead.

Materials and Methods

Bacterial growth and Metal stress

Heavy metal resistant bacterial strain, *Halomonas sp. strain BVR 1* (KC178681) was isolated from an electronic industry effluent and has been identified after a detailed biochemical and molecular characterization involving 16S r- DNA sequencing [Manasi et al, 2014]. This isolate was found to be resistant to a range of heavy metals and antibiotics. The Minimum Inhibitory Concentration (MIC) of the strain towards cadmium and lead was found to be 200 mg L⁻¹ and 400 mg L⁻¹ respectively, while it could tolerate zinc up to 250 mg L⁻¹ and chromium up to 150 mg L⁻¹. For the analysis of modulations in PA levels in the presence of metal, the strain (being a halophile), was cultured overnight under aerobic conditions at 37°C and constant shaking at 120 rpm in Luria Bertani broth (LB) supplemented with 3% NaCl and lead with pH of the medium set to 7.2 for better growth [Manasi et al, 2014]. Growth medium supplemented with 300 mg L⁻¹ of Pb²⁺ was inoculated with 100 µl of overnight *Halomonas sp. strain BVR 1* (O.D. 600 value of 0.2; approx. 1x10⁴ cells) to study the impact of heavy metal toxicity. This concentration of the metal solution was chosen to induce metal stress, as this was slightly lower than the calculated Minimum Inhibitory Concentration (MIC) [Manasi et al, 2014]. Metal concentration in the medium was tested using a HI98185 ion meter equipped with lead ion selective electrode (Hanna Instruments, USA). There was no reduction in the metal concentration indicating no complexation with the constituents in the medium. Bacterial cells grown without lead supplementation were used as controls. Control and treated cells were grown and harvested at varied time intervals of 6h, 12h, 18h and 24h for further analysis.

Analysis of Lead uptake by Bacteria

Analysis of lead uptake by bacteria was done by measuring Pb^{2+} concentration in spent Vs. fresh medium. About 25 mL of LB medium supplemented with $300\text{ mg L}^{-1} Pb^{2+}$ (treated cells) was inoculated with 100 μl of the overnight bacterial culture (O.D₆₀₀ of 0.8; approx. 2×10^6 cells) and incubated at 37°C. Both the treated and control tubes were taken out at various time intervals of 6h to 24h. The samples were centrifuged at 5670 xg for 10 min. Subsequently, the supernatant was used for measurement of extracellular heavy metal concentration using Atomic Absorption Spectrophotometer (AAS).

Extraction and dansylation of free, endogenous PAs.

Polyamines were extracted by the standard freeze-thaw method as proposed by Minocha et al [Minocha et al, 1990]. Bacterial cultures were pelleted down, supernatant was discarded and about 450 + 20 mg of cells was mixed with four volumes of 5% perchloric acid and frozen at -20°C. Following three rounds of freezing and thawing, these samples were vortexed and centrifuged for 10-15 minutes. About 100 μl of the supernatant was collected and used for dansylation. To the supernatants, 100 μl of saturated Na_2CO_3 solution and 100 μl of dansyl chloride (in acetone) was added. After 1 h of incubation at 60°C, 50 μl of 20 mg mL^{-1} asparagine made in distilled water was added to the above mixture. After an additional incubation of half an hour, about 400 μl of toluene was added. Samples were vortexed and allowed to stand for 5 min. These were then centrifuged at 18000 xg for 1 min to facilitate separation of aqueous and organic phases. Organic phase containing the polyamines was transferred to a new eppendorf tube and vacuum evaporated using a rotary evaporator. Samples were reconstituted using 1mL of methanol. Dansylation was also performed on PA standards in a similar fashion. The standards used were putrescine, spermidine and spermine (Sigma-Aldrich). Concentration of the standards

ranged from 0.1 mMol L⁻¹ to 1 mMol L⁻¹, which falls in the same range as the physiological polyamine levels in an active bacterial cell [Shah et al, 2008]. An internal standard 1,7 diaminoheptane was used to account for error due to spillage, evaporation etc.

Analysis of total PAs using Fluorescence Spectrophotometry

Total dansyl-PAs were analyzed using fluorescence spectrophotometry (Spectramax M4). The cell free extracts containing dansyl-PAs were analyzed at an excitation wavelength of 365 nm and an emission wavelength of 510 nm respectively against a blank sample as a reference [Smith et al, 1985].

Analysis of individual PAs using Liquid Chromatography Mass Spectrometry (LC-MS).

Liquid Chromatography Mass Spectrometry (LC-MS) was performed using a Shimadzu HP series to quantify the individual polyamines [Ducros et al, 2009]. A C18 Column (Phenomenox) was used for the separation of PAs. The mobile phase used for the separation of compounds was a gradient established between acetonitrile (A) and water (B) both acidified with 0.1 % formic acid. The gradient program was set up as follows: the gradient used was 0 to 2 min, 60% A/40% B. This was followed by a linear increase of B, reaching 100% at 8 min; from 8 to 10 min, 100% B; at 11 min, 40% A and 60% B; and from 11 to 15 min, 60% A and 40% B. The injected amount was 50 µl and the flow rate was maintained at 200 µl/min. The mass analysis was performed on a Shimadzu HP Series Single Quadrupole. The source was operated in both positive and negative mode at an ion spray voltage of 1000 V. The oven temperature was set to 25°C at a flow rate of 1mL min⁻¹. All these experiments were carried out in triplicates.

Fourier Transform Infrared Spectroscopy (FT-IR) analysis

FTIR spectra was generated for polyamines extracted from the 6h control and metal treated samples using a Jasco 4200 FT-IR spectrometer in the range 400–4000 cm⁻¹. The

samples were dried overnight, followed by encapsulation into dry KBr powder. The prepared pellet was then scanned and the spectra of polyamines from control and metal treated bacterial cells were recorded.

Cytotoxicity assay

Cytotoxicity assays of the bacterial cells were carried out at 6 and 12h post metal treatment using two methods - Trypan Blue method and MTT assay. The Trypan Blue assay is based on the principle that a larger quantity of the blue dye enters cells which have damaged/compromised cell membranes as opposed to cells with healthy/ intact membranes. Hence, injured cells tend to stain a deeper blue than healthier cells. For Trypan Blue assay about 100 mg wet weight of the bacterial cells at 6 h and 12h time period were incubated in 1mL of 0.05 % Trypan blue dye for 15 minutes. This mixture was centrifuged at about 22000 xg for 15 min. The supernatant was discarded and the pellet was washed till the supernatant appeared colourless. The pellet was now resuspended in 1 mL of 1% SDS and was spun at 22,000 xg. Absorbance of the supernatant was measured spectrophotometrically (Beckman Coulter DU 730) at 600 nm.

The chemical 3-(4,5-dimethylthiazol-2-yl)-2,5-diphenyl tetrazolium bromide, abbreviated as MTT is used to test for cell viability by measuring respiratory activity. Colorless MTT interacts with the electron transport chain and is reduced to a blue colored product called formazan [Mosmann et al, 1983]. Thus, actively respiring cells tend to exhibit greater intensity of the blue color. The assay was carried out according to a standard protocol [Ikewage et al, 1998]. According to this protocol, 100 mg wet weight of the bacterial cell pellet harvested after 6h and 12h of growth was taken and suspended in 250 µg of MTT reagent, followed by gentle mixing at room temperature for an hour. The mixture was centrifuged at 22000 xg for 10 minutes. The supernatant was discarded and the pellet was resuspended in 1mL of 0.04 Mol L⁻¹ acid propanol.

This suspension was again centrifuged to obtain the supernatant for further analysis. This supernatant was measured spectrophotometrically at 590 nm.

Analysis of Growth curve

For growth curve measurement, about 20 mL culture volume of the LB medium, supplemented with 100 mg L⁻¹ Pb²⁺ (permissible lead concentration for growth) was inoculated with 100 µl of the overnight bacterial culture (Optical Density at 600 nm (O.D₆₀₀ of 0.8; approx. 2x10⁶)) and incubated at 37 °C. Bacterial growth was measured at 600 nm at regular time intervals of 6, 12, 18, 24, 30 and 36h. Growth curve comparison of *Halomonas* sp. strain *BVR 1* in the presence and absence of metal was analyzed.

Statistical analysis

Statistical analysis was carried out using student's t-test (Microsoft- Excel) or two factor ANOVA (Graph pad prism 7.0) as required.

Results and Discussion

Bacterial growth in the presence of Heavy Metal

The trend of bacterial growth was similar between metal treated and untreated bacterial cells, as is evident from **Fig. 5.1**, though the metal treated cells exhibited significantly higher O.D values at all time periods. This observation is as per the expected outcome, as *Halomonas* sp. strain *BVR 1* [Manasi et al, 2014] has been isolated from a heavy metal rich effluent and is thus likely to be better adapted to heavy metals, thereby leading to enhanced induction of bacterial growth in the presence of metal [Manasi et al, 2014]. For the first 6h after sub culturing, the growth trend was identical in both control and metal treated bacteria. A sharp surge in growth was observed in the metal treated cells against the untreated ones. This indicates a shorter lag phase in the metal treated bacteria and could be a response due to the presence of heavy metal in the

media. A less steep surge was seen in the control cells after 12h of growth. Overall, similar growth rates were observed in both metal treated and untreated bacteria respectively.

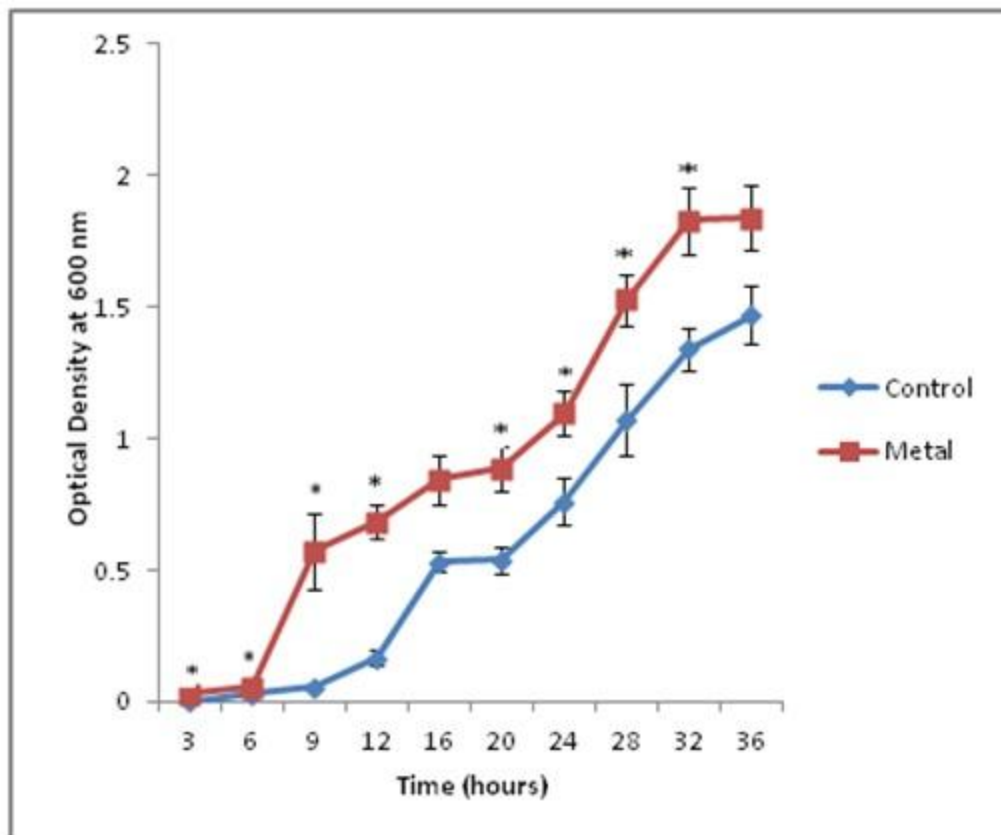


Figure 5.1: Growth curve of *Halomonas sp.* strain *BVR 1* in the presence and absence of metal. The * represents significant difference ($p \leq 0.05$) between control and metal treated sample within the same time period. Blue indicates control cells; Red indicates treated cells.

Analysis of Lead uptake by Bacteria

To establish that the Pb^{2+} supplemented in the medium is indeed being endogenously taken up by the bacteria, we analyzed the disappearance of Pb^{2+} in the spent medium using Atomic Absorption Spectrophotometry (AAS) (Fig. 5.2). In the treated, there was a gradual decline in the extracellular concentration of metal from a period of 6h to 24h (Fig. 5.2), indicating a relative uptake of metal ions by the cells. Overall, this decrease of extracellular metal concentration in the medium during the period of 6h to 24h in metal treated cells is an

indirect measure of metal contributing to polyamine increase in these cells. The other mechanisms adopted by the bacteria to tolerate metal contamination include cell wall absorption, chelation, extracellular sequestration, etc [Rajendran et al, 2003].

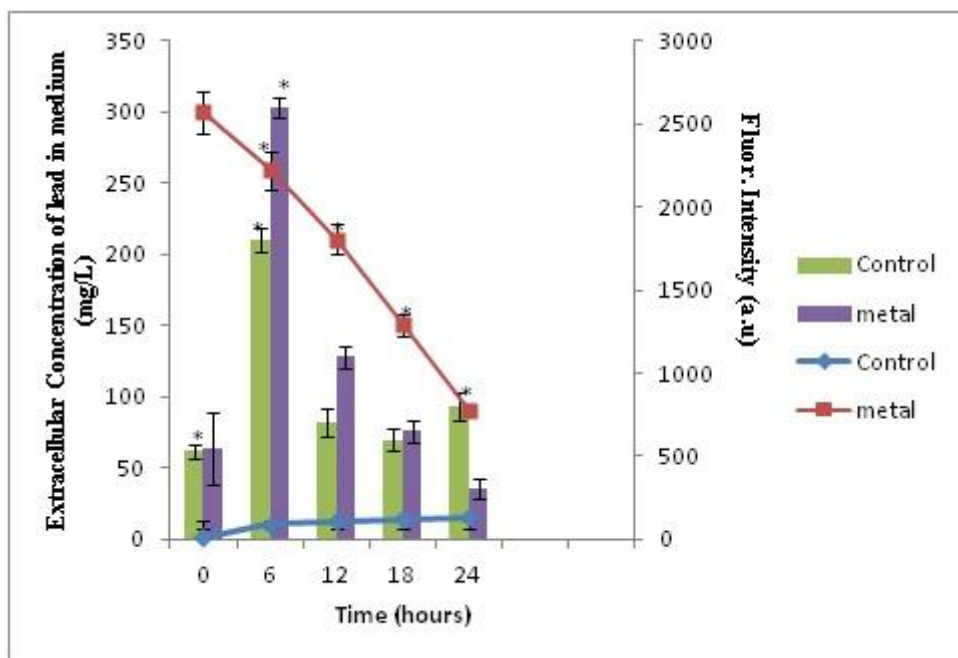


Figure 5.2: Comparing extracellular concentration of metal in growth medium and total polyamine content across various time points. Data are mean (\pm) standard error of 6 replicates from 2 experiments. The * represents significant difference ($p \leq 0.05$) between control and metal treated sample within the same time period. Bars represent the polyamine data while line represents the extracellular concentration of lead in medium.

Analysis of total Polyamines using Fluorescence Spectrophotometry

Polyamines are considered to be part of the General Adaptation Syndrome (GAS) generated in response to various environmental stresses, including heavy metal stress [Leshman et al, 1996; Hossain et al, 2012]. Heavy metals are directly involved in the redox reactions in cells and results in the formation of O_2^- . This reactive oxygen species leads to the generation of H_2O_2 and $\cdot OH$ and brings about the membrane disruption [Anjum et al, 2014]. Polyamines are known to scavenge these Reactive Oxygen Species (ROS) and other free radicals thereby acting as antioxidants and helping in combating heavy metal stress [Ha et al, 1998]. *In-vivo* and *in-vitro*

studies have suggested that in this way, they can effectively protect and stabilize the membrane systems against hazardous effects of redox active metal ions in bacteria [Pegg et al, 2011].

Under normal conditions, endogenous levels of polyamines in cells are regulated by both, polyamine synthesis and catabolism. Simultaneous regulated expression of polyamine biosynthetic and degradation genes (like amine oxidases causing oxidative deamination of polyamines) is required to maintain the intracellular levels of polyamines [Rouchad et al, 2015]. As dansylated polyamines exhibit fluorescence [Minoha et al, 1990], the total polyamine concentration in the metal treated and control samples were calculated by the amount of fluorescence generated by these molecules when excited at 365 nm (emission was at 510 nm) (**Fig 5.3**). Both control and metal treated samples exhibited an overall decrease in total PA concentration between 6 and 24h post sub-culturing and metal addition.

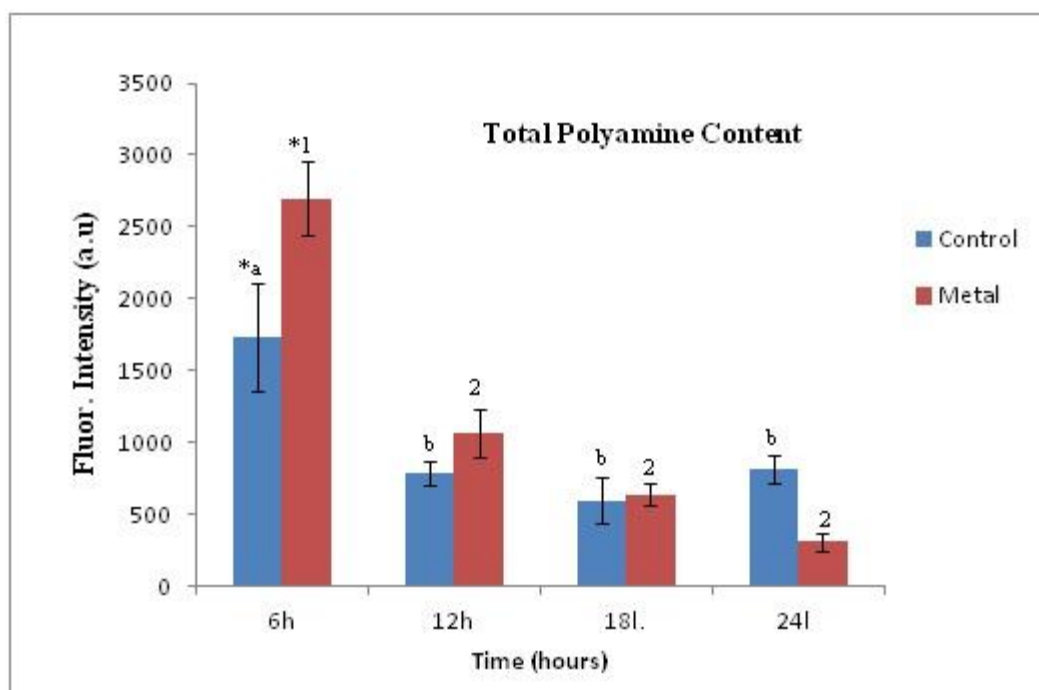


Figure 5.3: Total polyamine concentration in the control and metal treated cells as determined through fluorescence. Data are mean (\pm) standard error of 6 replicates from 2 experiments. * represents significant difference ($p \leq 0.05$) between control and metal treated samples within the same time period, a,b represents significant difference ($p \leq 0.05$) between control samples across

time periods and 1,2 significant difference ($p \leq 0.05$) between treated samples across time periods. Blue indicates control cells; Red indicates treated cells.

Two way ANOVA test for both treated and control cells, depicted that the polyamine content at 6h was significantly different from the results obtained across the other time periods. Individual trend analysis of control samples showed that, there was a significant decrease (about 2-folds) in fluorescence from 6 to 12h, followed by insignificant fluctuations upto 24h (decrease at 18h followed by marginal increase at 24h). In case of metal treated cells, a similar pattern with even more sharp and significant decrease (about 2.5-folds) was observed between 6 and 12h post metal addition. This decrease continued subsequently all the way up to 24h but turned out to be statistically insignificant. (as determined by 2-way ANOVA).

Comparison at individual time points indicated that the total PA concentration in metal treated cells was significantly higher at 6h post metal treatment as compared to controls. The leveling out of the total PA concentration in the control samples post 12h and a decreasing trend in the metal treated cells resulted in overall low PA presence in the metal treated cells as compared to controls in the 24h time point.

The exact mechanistic role of polyamines in bacteria under metal stress is not well established. But based on literature available in plants, PAs are hypothesized to chelate the heavy metal ions [Norris et al, 2014] reducing their availability for causing metal toxicity.

Analysis of individual PAs using Mass Spectrometry

After understanding the trends in total PA concentration within the bacterial cell, it was important to assess and understand the trends with respect to the three individual PAs – putrescine, spermidine, spermine. Since these are highly charged cationic molecules with a very small size, we used a well- established derivatization technique to tag the individual polyamines

(details in materials and methods) and used LC-MS for their detection and quantification. Derivatization leads to a significant increase in the molecular masses of these polyamines depending on the number of the dansyl groups being attached. Hence, the resultant mass of the PAs does not impede with the masses of any other biological molecules. Spectral analysis was done in the positive mode, owing to a stronger signal in this mode as compared to the negative one. The electrospray mass spectra selected from the first quadruple gave a single charged protonated molecule at m/z 555 corresponding to putrescine. Spermine and spermidine are tetra and tridansylated polyamines respectively and gave their ion product spectra at m/z 1135 and m/z 845 respectively [Ducros et al, 2009].

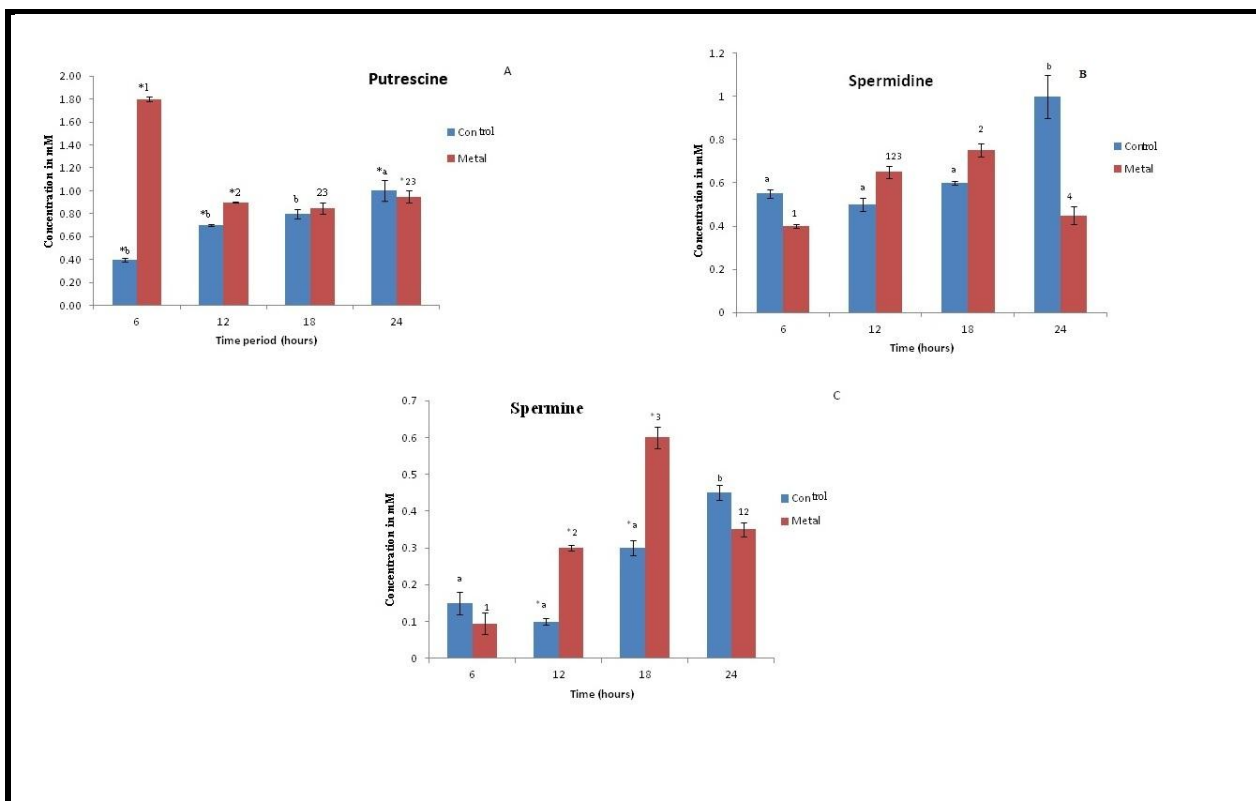
The putrescine concentration gradually increased from 6 to 24h in the control cells (the putrescine levels at 24h was significantly higher from all the other time periods, as determined by 2 way ANOVA), an overall significant decrease in the same was observed in the metal treated cells (**Fig. 5.4A**).

Considering changes at individual time periods, at 6h, the putrescine concentration in metal treated cells was significantly higher (about 5 folds) than the control cells. Significant differences in putrescine levels continued to exist in the metal treated vs. untreated cells at 12h & 24h period also, albeit to a lower extent. Overall, the cellular putrescine concentration increased significantly in the first 6h of inducing heavy metal stress, correlating positively with bacterial growth at 6h (**Fig. 5.1**). Earlier reports with plants have indicated similar enhancement in putrescine production as an early protective response against heavy metals, since putrescine is the precursor molecule for the production of other polyamines [Pang et al, 2007]. Putrescine levels increased significantly in apple callus under salt stress [Liu et al, 2006]. Metal stress

(Cu⁺²) increased the putrescine levels in 7 day old raddish seedlings, aiding in oxidative stress management [Choudhary et al, 2012].

The cellular concentration of spermidine in the treated cells shows a gradual increase from 6h to 18h following which the spermidine concentration decreases significantly at 24h (**Fig. 5.4B**). On the other hand, there was a different pattern seen in untreated cells. The levels in the untreated cells did not show any change from 6 to 12h followed by a significant increase at 24h (as confirmed by the 2 way-ANOVA). Surprisingly (and negatively correlating with putrescine data), comparison at different time points indicated low spermidine in the metal treated cells as opposed to control cells at 6h and 24h. However, at 12 and 18h the spermidine concentration was higher in treated cells as compared to control. None of these differences at individual time periods between metal and control cells were statistically significant though. Spermine cellular levels followed a similar trend like spermidine in both metal treated and untreated cells till 18h (**Fig. 5.4C**). Spermine levels gradually increased in concentration over a time period from 6h-18h in case of metal treated cells. There was however a significant fall observed in the concentration beyond 18h. In case of untreated cells, there was a dip in 12h similar to spermidine and then a subsequent gradual rise in the levels beyond 12h. The spermine levels at 24h was significantly higher in comparison to all the other time periods, as showed by 2 way-ANOVA.

To summarize, in metal treated cells, over a period of time from 6h to 24h, putrescine concentration gradually decreased (**Fig 5.4A**) with a concomitant increase in spermidine and spermine levels up to 18h. Hence, it can be speculated that the synthesized putrescine is now being utilized for the synthesis of other polyamines (along with simultaneous, possible catabolism of putrescine) (**Fig. 5.4A,B,C**).



5.4. A) Variation in putrescine levels (Obtained from mass spectrometry data) over a period of time. * represents significant difference ($p \leq 0.05$) between control and metal treated samples within the same time period, a,b represents significant difference ($p \leq 0.05$) between control samples across time periods and 1,2,3 represents significant difference ($p \leq 0.05$) between treated samples across time periods.

B) Mass data of the variation in spermidine levels over a period of time. a,b represents significant difference ($p \leq 0.05$) between control samples across time periods and 1,2,3,4 represents significant difference ($p \leq 0.05$) between treated samples across time periods.

C) Mass data of the variation in spermine levels over a period of time. * represents significant difference ($p \leq 0.05$) between control and metal treated samples within the same time period, a,b represents significant difference ($p \leq 0.05$) between control samples across time periods and 1,2,3 represents significant difference ($p \leq 0.05$) between treated samples across time periods.

Data are mean (\pm) standard error of 6 replicates from 2 experiments. Blue indicates control cells; Red indicates treated cells.

It is likely that, after an initial spurt of putrescine at 6h, the other polyamines, spermine and spermidine start contributing towards defending the cell from the heavy metal. In our study,

spermine increase was more predominant as compared to spermidine between the 6h to 24h period. This could be ascribed to the fact that the antioxidant activities of these polyamines are associated with the number of amine groups and spermine, being a tetra-polyamine is likely to be more efficient in scavenging ROS [Drolet et al,1986; Lovaas et al, 1997]. The levels increased significantly according to the bacterial cell density during the logarithmic and stationary phases. Production of all the polyamines shows a decline between 18 to 24h indicating enhanced polyamine catabolism.

FT-IR assay

FT-IR of the polyamines of the control and the cells exposed to the metal was carried out to determine whether the metals are involved in binding to the polyamines. Few characteristic changes have been observed in the FTIR spectrum of both control and metal treated samples. A shift in the peak was observed from 1565 cm^{-1} in the control samples to 1570 cm^{-1} in metal treated samples [Quameur et al, 2004]. This wave number corresponds to the N-H vibrations. This shift in the peak was accompanied by a reduction in the percentage transmittance from 38.1943 to 18.2595 (**Fig. 5.5**). The C-N peak in the control sample may correspond to single C–N bonds that is present at 1116 cm^{-1} [Meija et al, 2014]. This peak also shifted slightly to 1120 cm^{-1} in the metal treated samples. The results obtained from the FTIR analysis do suggest a role of these polyamines in direct metal chelation in these bacteria under high Pb conditions (**Fig. 5.5**).

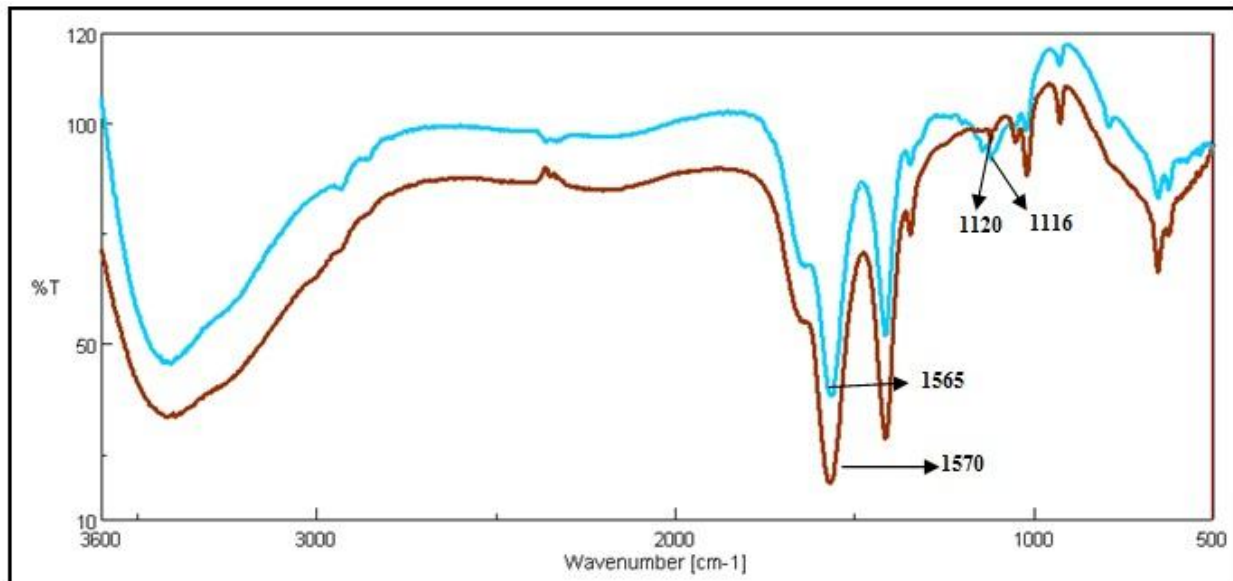


Figure 5.5: FTIR analysis of the polyamines from control and metal treated bacterial cells. (Red :Polyamines from metal treated samples, Blue : Polyamines from control samples)

Cytotoxicity assay

Cell viability assays were done at 6h and 12h post metal addition. At a 6h time period, when the cells are in lag phase, adjusting to the growth environment, there is no significant change in growth statistics in the control and metal treated samples as is evident from the Trypan blue and MTT assay. Results from Trypan blue assay can be very well supported with the growth curve data, where there is a surge in the growth at 6h time period, indicating that there is not much membrane damage at this time interval and the cells are actively growing. At 12h, where cells are in an actively dividing phase, the quantity of cells exhibiting membrane damage in metal treated cells was higher as compared to the untreated cells (**Fig. 5.6**).

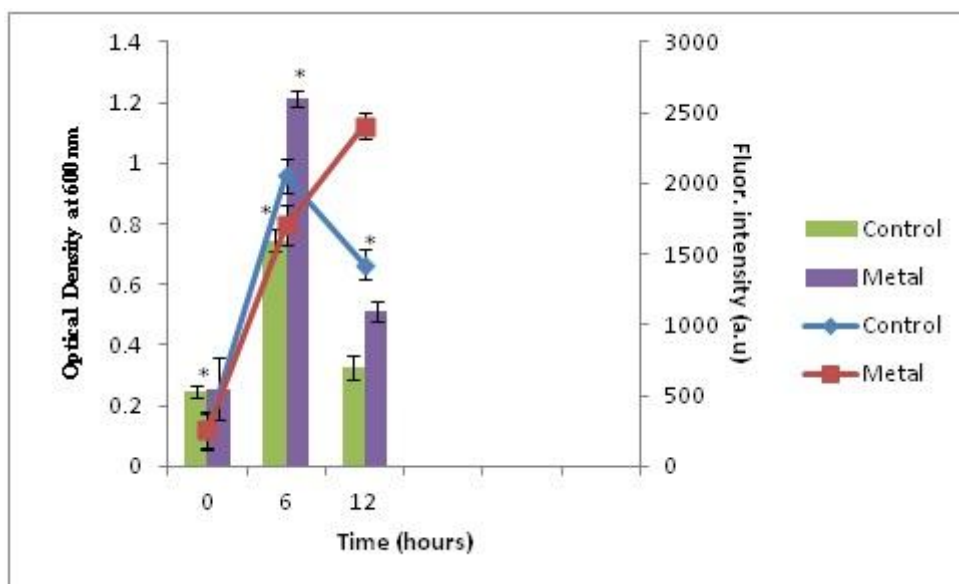


Figure 5.6. Comparing membrane damage assay of the cells in the presence of metal and total polyamine content at various time points. Data are mean (\pm) standard error of 6 replicates from 2 experiments. The * represents significant difference ($p \leq 0.05$) between control and metal treated sample within the same time period. Blue indicates control cells; Red indicates treated cells. Bars represent polyamine content while line represents Optical Density at 600nm.

No significant difference is seen in the MTT data between the control and metal treated cells, although it can be seen that membrane compromised metal treated cells show slightly low respiratory activity at 12h as against the bacterial cells at 6h post metal treatment (**Fig. 5.7**). In order to corroborate our data with the physiological status of *Halomonas sp.* strain *BVR 1* under Pb treated conditions, growth and viability assays were conducted to assess the physiological response of these bacteria to Pb^{2+} treatment. These results point towards a complex regulation of physiological processes in these bacteria due to Pb^{2+} addition. For example, at 6h post metal treatment, the growth curve (**Fig. 5.1**) indicates a surge in bacterial growth, while the MTT assay (**Fig. 5.6**) does not exhibit a corresponding increase in respiratory activity of these bacteria. However, after a prolonged period (12h) of post metal addition, the Trypan blue assay

(Fig. 5.7) did exhibit an increase in membrane damage. In this context, further experimentation will be required to elucidate the reasons for some of these observations.

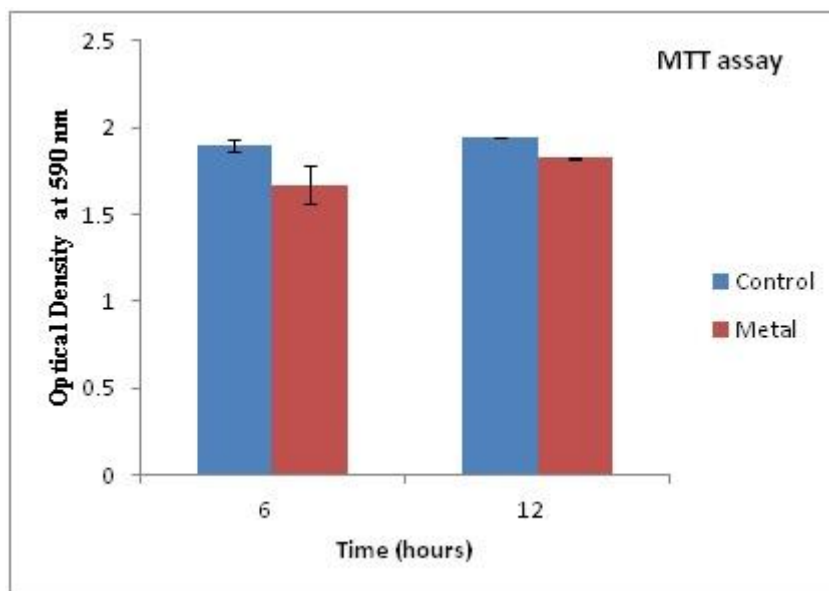


Figure 5.7: Respiratory activity of the cells in the presence of the metal. Blue indicates control cells; Red indicates treated cells.

Proteomic expression assays in *Halomonas BVR 1*

The proteomes from the *Halomonas BVR 1* were extracted by sonication process. The control set of samples (bacterial cells without the exposure of lead) and the treated set (bacterial cells with the exposure of lead) from mid-log phases of cellular growth (Optical Density 0.3–0.4) were taken and centrifuged separately at 7300 rpm for 10 min. Subsequently, the cells were suspended in 100 mM Tris HCl (pH 8.0) buffer for lysis. The sonication process was then carried out for 8 min at 40 s pulse with a 30 s break time and the pattern of proteomic expression was analyzed by 12% SDS– PAGE using Laemmli’s method

Twelve percent SDS – PAGE analysis showed the expression of proteins from *Halomonas BVR 1* after its exposure to 100 mg L⁻¹. The cell samples were taken from the logarithmic phase in which the cells adapt to the metal toxicity. Control samples (without lead) were also run on the

PAGE gel along with the treated samples (**Fig. 5.8**). The treated samples showed considerable increase in the proteomic expression indicating that, various proteins are upregulated during stress response in presence of lead. The difference in protein expression profile, in the presence and absence of the heavy metal, suggests the role of some metal sequestering proteins towards lead resistance. Notable observation was an up regulation of a distinct polypeptide (14.3 kDa) corresponding to a cysteine rich metallothionein - metal binding protein which is consistent with earlier report [Murthy et al., 2011].

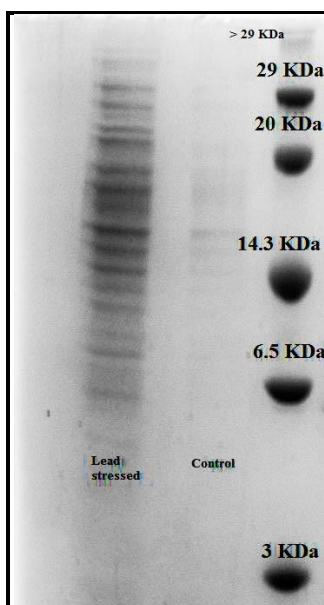


Figure 5.8: SDS gel analysis of the varying proteome expression profiles of the control bacteria and under stress.

B) Genetic determinants contributing to heavy metal resistance in *Halomonas BVR 1*

Introduction

Several plasmids have been identified in halophilic bacteria specifically *Halomonas* genera which confer resistance to various heavy metals. These plasmids may subsequently be used for the genetic transformation of the lower resistant strain to boost up its metal resistance. Such inherited resistance can thus be used as a tool for remediating heavy metals.

Here, we report the isolation of a plasmid from *Halomonas BVR 1*, that is grown under high concentrations of lead and evaluation of the genetic basis for plasmid mediated heavy metal resistance. The genetic transformation of this plasmid into organism with low tolerance to metals increased its resistance to double the initial concentration. Also transforming the same to a cured strain of *Halomonas* strain brought back their resistance to normal.

Materials and Methods

All the experiments were carried out after approval from the Institutional Biosafety Committee (IBSC).

Sampling site, characterization and selection of the organism.

The electronic industry effluent was characterized to identify the microbial population. The detailed procedure and the outcome of this characterization has already been reported in our earlier publication [Manasi et al, 2014]. Out of the ten strains isolated, three strains belonged to the genera *Halomonas*. The organisms belonging to this genera has not been exploited as a potential biosorbent for metal remediation. Among the three strains belonging to *Halomonas*

genera, *Halomonas BVR 1* was selected for further studies owing to its high tolerance level to metals and antibiotics [Manasi et al, 2014].

Determination of the Minimum Inhibitory Concentrations (MIC).

The Minimum inhibitory concentration (MIC) of this selected microbe was tested against various heavy metals like cadmium, lead and Zinc. A fixed inoculum volume of 10 μl (1.3×10^7 cells) was inoculated into Luria Bertani medium with varied concentrations of heavy metals. Analytical grade heavy metal salts ($\text{CdCl}_2 \cdot 8\text{H}_2\text{O}$, $\text{ZnSO}_4 \cdot 7\text{H}_2\text{O}$, $\text{Pb}(\text{NO}_3)_2$) were used to prepare 1000 mg L^{-1} stock solutions. Each of these solutions were autoclaved separately and added to LB medium at a concentration of 50-400 mg L^{-1} . The growth of *Halomonas BVR 1* in this medium was analyzed by measuring the Optical Density (OD) at 600nm [Aleem et al, 2003]. This species was found to be highly resistant to cadmium with a minimal inhibitory concentration of 200 mg L^{-1} . The detailed MIC of *Halomonas BVR 1* against cadmium has already been reported earlier [Manasi et al, 2014].

Plasmid DNA isolation and digestion.

Plasmid DNA was isolated using the standard alkaline lysis method proposed by Sambrook [Sambrook, 2001]. The isolated product was detected by an agarose gel (0.8%) run. The product was visualized and compared with a standard 1 kb ladder. Single digestion of the plasmid was carried out using BamH1 with the conditions recommended by the manufacturer (New England Biolabs). The digested products were separated using 0.8% agarose gel electrophoresis. A 10kb standard DNA ladder was run along with the digested product to assess the size of the isolated plasmid.

Plasmid curing experiments

To determine if the heavy metal resistance genes are encoded by the plasmid, plasmid curing experiments were carried out with ethidium bromide as the curing agent. The colonies from the highest concentration of ethidium bromide ($100 \mu\text{g mL}^{-1}$) were selected for testing its plasmid curing efficiency. Appropriate dilutions of the inoculum was plated onto LB agar plates. Colonies from this master plate were picked up by the process of replica plating. Accordingly, a sterilized whatman filter paper was placed upon the master plate and subsequently transferred to a selective medium of LB with optimal concentration (200 mg L^{-1}) of heavy metal lead (secondary plate). The master plate and secondary plate were compared to assess the plasmid curing efficiency. Isolation of plasmid from the cured strain of *Halomonas BVR 1* from the master plate and non cured strains from the secondary plate was carried out to confirm the success of the curing experiments [Shahid et al, 2003].

Genetic transformations of the isolated plasmid.

Plasmid DNA obtained from a 10 mL culture in an exponential phase was eluted in a 30 μl TE buffer (10 mM-Tris/HCl/1 mM-EDTA, pH 8). Approximately, 50ng of this isolated plasmid was used to transform 100 μl of *E.coli DH5 α* competent cells [Coral et al, 2005]. Similar procedure was followed for cloning the plasmid into the cured strains of *Halomonas BVR 1* strain. This was done to know if the resistance was gained from the plasmid in the control and cured strains by this cloning experiment. These transformed strains were tested for their uptake of plasmid after transformation and increased threshold of heavy metal tolerance.

Assessment of the heavy metal tolerance

The transformed and non cured strains of *Halomonas BVR 1* were grown in LB medium with different lead concentrations ranging from 100 mg L⁻¹ to 400 mg L⁻¹. Bacterial growth was measured by taking their Optical density (O.D) at 600nm. One non metal resistant *E.coli DH5α*, was taken as a control strain to compare the metal tolerance level of *Halomonas BVR 1*.

Decontamination of the genetically transformed strains.

All the strains that were genetically modified have been discarded with utmost care. Proper decontamination of these cultures were carried out. The genetically modified organisms were developed only for the experimental purpose.

Results and discussion

Our isolated *Halomonas BVR 1*, was observed to have more resistance towards lead in comparison to cadmium and Zinc. It could tolerate lead till 400 mg L⁻¹ levels while the concentration of cadmium and zinc that inhibited the growth of the organism was 200 mg L⁻¹ and 150 mg L⁻¹ of cadmium as shown in the graph (**Fig. 5.12**). Beyond these concentrations there was total cessation of bacterial growth. Considering these tolerance levels to various metals, this strain was selected as a test model for evaluating the genetic basis for the lead resistance in this strain.

Are genetic determinants present on plasmid ?

The presence of plasmid mediated metal resistance in *Halomonas BVR 1* was substantiated by knocking out the plasmids using a plasmid curing agent. Replica plating of the cured strains on to a selective medium (LB medium supplemented with lead) reduced the growth by 50 %. This is

also reflected in the plasmid curing efficiency that was calculated to be around 50 %. This experiment thus delineates the proof of plasmid mediated heavy metal in *Halomonas BVR 1*.

Plasmid isolation from non cured/ wild type strains, cured strains and transformed strains confirmed the success of the plasmid curing experiments (**Fig 5.9**). The agarose gel image depicted the presence of plasmid in the wild type strain while the cured strains were devoid of any plasmid. The gel image manifested that the plasmid had multiple bands indicative of different conformations of the plasmid involving multimer, nicked circular, linear and super coiled forms.

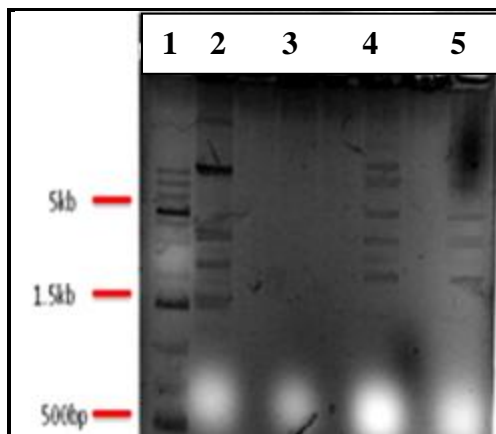


Fig 5.9. Plasmids isolated from various strains. (Lane 1: Marker, Lane 2: Plasmid isolated from *Halomonas BVR 1*, Lane 3: Plasmid cured from *Halomonas BVR 1*, Lane 4: Plasmid isolated from a transformed strain of *E. coli* with the plasmid of *Halomonas BVR 1*, Lane 5: Non-cured strain of *Halomonas BVR 1*).

The single cut restriction digestion of this plasmid with *Bam HI* yielded a linear plasmid of size > 10kbp (**Fig 5.10**). The sequencing and other characterization of the plasmid are in progress in our lab.

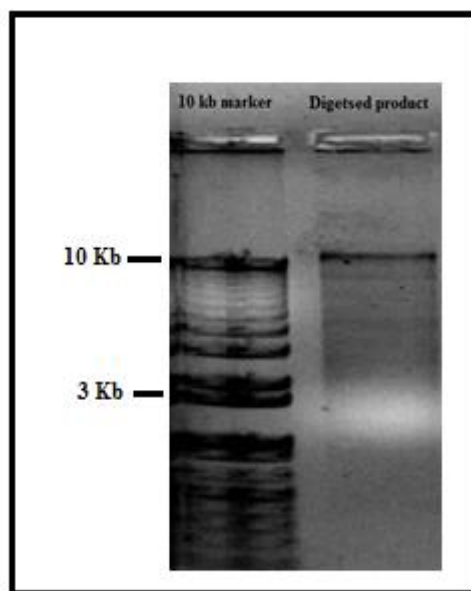


Fig 5.10. Restriction digestion of the isolated plasmid from *Halomonas BVR 1*.

Subsequent to genetic transformation, several individual colonies appeared on the transformed plate consisting of LB medium supplemented with lead, while there was no growth in case of competent cells. Additionally, there was one more observation made in terms of the color change in bacteria in presence of the heavy metal (**Fig 5.11**). There was an increase in brown pigmentation observed at 400 ppm metal concentration. Bacterial pigments are known to protect the cell against any photo oxidative damage caused due to the toxic metal ions. It is already reported that at low metal concentrations, bacterial pigmentation is inhibited [Agostinho et al, 2012]. Isolation of plasmids from the transformed strains also showed a similar kind of plasmid pattern as the wild type *Halomonas BVR 1*. This proves that the genetic transformation of heavy metal resistant plasmid in the test strain E.coli was successful.



Fig 5.11: Transformed bacterial growth in the presence of heavy metal

The transformants, *Ecoli DH5 α* strain and the wild type *Halomonas BVR 1* were tested for their metal resistance. It was clearly observed that *Ecoli DH5α* was the least resistant to lead and could tolerate heavy metal concentration only up to 300 ppm. The wild type strain *Halomonas BVR 1* had the highest metal tolerance level and could resist the metal concentration upto 400 ppm. A positive clone of *Ecoli DH5α* obtained after successful transformation also was tested for its metal tolerance. The experimental results showed that transformation of heavy metal resistant plasmid in the cured strains of *Halomonas BVR 1*, restored the metal tolerance level to 400 ppm after (**Fig 5.12**). This increase in metal resistance might be attributed to the uptake of the heavy metal resistance plasmid. Overall, the plasmid curing experiments, genetic transformations and evaluation of the metal tolerance level in different strains suggested the localization of the genetic determinant bearing the property of heavy metal resistance to be present on the plasmid.

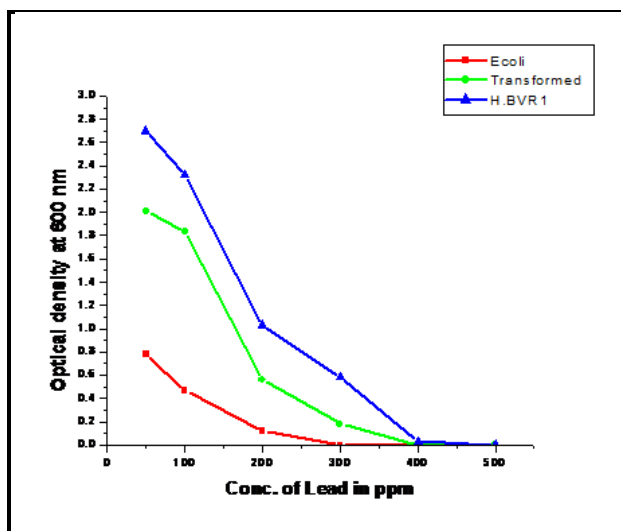


Fig 5.12. Metal evaluation of *E. coli* (test strain), *E. coli* strain transformed with the plasmid from *Halomonas BVR 1* (transformed strain) and *Halomonas BVR 1* (wild strain).

Thus, results from this study, will aid in generating microorganism with higher metal adsorption capacity along with greater efficiency and specificity. Such strains can be exploited commercially as novel biosorbents for the bioremediation of metals.

Conclusions

The results demonstrated in this chapter, depicts a simple and easy measurement of polyamines using mass detection and fluorescence spectrophotometer in bacterial cells. A detailed analysis of the production of polyamines in bacterial cell under the exposure of heavy metal at varied time intervals has been studied. There was a significant increase in the levels of polyamines under metal stress particularly, putrescine, the precursor to the other polyamines (Spermidine and Spermine) in the initial 6h. This was the major polyamine produced in the presence of heavy metal. However a time dependent increase in the levels of spermine and spermidine was also observed in the bacterial cells till a period of 18h, followed by a gradual dip in the production beyond this period

of time was seen owing to its utilization in the stability of the cell and as a part of the cell's protective response. The cytotoxicity assays shows that with increased exposure to heavy metal, there is a gradual increase in the membrane damage, as was observed at the 12h time period.

Our study unravelled the genetic basis of heavy metal resistance in *Halomonas BVR 1*. Experiments like plasmid curing, genetic transformations and evaluation of heavy metal resistance paved way for this confirmation. Results from this study, will aid in generating microorganism with higher metal adsorption capacity along with greater efficiency and specificity.

CHAPTER VI
CONCLUSIONS AND SUGGESTIONS FOR FUTURE
WORK

SUMMARY AND CONCLUSIONS

Summary and Conclusions

The first chapter gives a comprehensive overview of electronic waste and their effluents as a major source of heavy metals and its hazardous effects. It also summarizes the existing remediation technologies available for removal of heavy metals. The toxic nature of heavy metals vividly describes the need to remove these heavy metals from industrial effluents, which constitutes the major source of heavy metal pollution. Hence, efforts were directed towards the development of effective methods and biosorbents for the detoxification of metals.

The second chapter explains the detailed chemical, microbiological and molecular characterization of the electronic effluents that was collected from an industry located in the outskirts of Hyderabad, to assess the microbiota in the effluent. Various physical parameters like colour, pH, etc. were tested on site while the chemical parameters like COD, BOD, DO and alkalinity were carried out in our lab. Biochemical characterizations involving IMVIC tests, citrate test, motility, starch hydrolysis, carbohydrate fermentation were carried out for strain identification. A total of ten bacterial strains and two fungal strains were isolated from this effluent. These strains belonged to four different genera of *Bacillus*, *Halomonas*, *Pseudomonas* and *Kocuria*. Confirmation of identity of these strains was done by the 16S rDNA sequencing and FAME analysis. Among the ten strains isolated, three organisms belonged to the genera *Halomonas*. Organisms from this genera have not been researched upon as a potential use as a biosorbent. Hence one organism belonging to *Halomonas* genera was selected as a test organism for further studies. The biomass as such was used for the remediation of lead, cadmium and zinc. Optimization of parameters like pH, temperature, contact time, metal concentration were studied in detail for attaining maximum adsorption capacity and efficient removal of heavy metals. This microbe functions as an effective adsorbent for the remediation of heavy metals due to the presence of functional groups such as carboxyl, amine, hydroxyl and phosphate that facilitate metal binding and removal from aqueous solutions. The surface characterization of the adsorbent also

showed binding of the heavy metals ion on to the surface of the adsorbent. Langmuir isotherm gave good fit to the experimental data with a maximum adsorption capacity of 12.023 mg g⁻¹, 11.11 mg g⁻¹ and 9.152 mg g⁻¹ for cadmium, zinc and lead respectively. This microbial adsorbent seemed to have more specificity to cadmium owing to its higher adsorption capacity in comparison to the other heavy metals. The adsorption was found to be significantly dependent on the pH, contact time and temperature. The adsorption favored Langmuir adsorption in case of cadmium and lead while it obeyed Freundlich isotherm for zinc adsorption. The pseudo second order kinetic model was best suited for the adsorption of all the metals and thermodynamics depicted the process to be spontaneous and exothermic. The highlight of the method is that although the effluent contains higher concentrations of salts (chlorides, nitrates and phosphates), their effect on the adsorption of metal ions was not significant. Overall the novel bacterium is able to remove cadmium upto a concentration of 100 mg l⁻¹. This biomass was able to remove Lead and zinc upto a concentration of 80 mg l⁻¹ and 50 mg l⁻¹ respectively thus making the process economical and green in environmental remediation.

The third chapter of the thesis deals with the enhancement in the biosorption capacity of the metal ions by immobilizing *Halomonas BVR 1* strain in various biopolymer matrices like chitosan and Graphene Oxide. The surface characterization of the adsorbent before and after adsorption showed characteristic changes in the indicating effective binding of the heavy metals ion on to the surface of the adsorbent. The enhancement in the metal adsorption capacity increased around two folds than the native adsorbent that consisted only *Halomonas BVR 1* cells. Among all the various adsorbents used for the removal of lead, cadmium and zinc, adsorbent that was best suitable for the removal of lead and zinc was *Halomonas BVR 1* immobilized in Graphene Oxide. The maximum adsorption capacity for lead and zinc was found to be 73.58 mg g⁻¹ and 42.53 mg g⁻¹ respectively. *Halomonas BVR 1* immobilized in sodium alginate was successful in maximum removal of cadmium. The adsorption capacity was found to be 25.12 mg g⁻¹. The other parameters like the kinetics, thermodynamics, influence of other interfering ions (cations and anions) were also optimized to achieve the maximum adsorption capacity. Majorly all the processes were exothermic and were favored at relatively lower temperatures. Maximum adsorption was observed by maintaining the average contact time to 2-3 hrs between the adsorbent and the metal ions.

The fourth chapter deals with the immobilizing the microbe in another bioadsorbent ie sodium alginate and modeling studies to specifically simulate the upscale removal of lead ions The experimental data from the Column studies was used to develop a mathematical model generate breakthrough curves and thus simulate the upscale removal of metal ions.

The fifth chapter deals with understanding the physiology of the cell under metal stress and also the genetic basis of the heavy metal resistance in *Halomonas BVR 1*. The genetic basis of heavy metal resistance in our isolated strain was assessed by experiments like plasmid curing ad genetic transformations it was concluded that the basis of metal resistance resided in the plasmid The role of polyamines as a possible player in combating heavy metal stress in bacteria has not been studied till date. A detailed analysis of the production of polyamines in bacterial cell under the exposure of heavy metal at varied time intervals was studied. There was a significant increase in the levels of polyamines under metal stress particularly, putrescine, the precursor to the other polyamines (Spermidine and Spermine) in the initial 6 h. This was the major polyamine produced in the presence of heavy metal. This indicates that putrescine is the first response even in bacterial cells owing to exposure to metal stress. This fact is also corroborated with the data available from plants, in which putrescine is proved to be the first response against heavy metal stress in plants.

Application to real samples and Validation of the method

The validation and application of the adsorption method was performed with real electronic industry effluents using the developed adsorbent that gave the highest adsorption capacity. The compositions of the effluents are shown in **Table 2.2**. The effluent samples were digested with HNO₃-H₂SO₄ mixture to remove the organic matter. Among the prepared adsorbents, microbe immobilized in GO was selected as a test adsorbent to remediate the effluent, owing to its highest adsorption capacity. This adsorbent was significantly able to remediate the heavy metals (98%) in the effluents.

Summary of the developed biosorbents for the removal of metal cations is as follows.

S. No	Adsorbent	Metal	Langmuir adsorption capacity (mg/g)
1.	<i>Halomonas BVR 1</i>	Lead	9.152
2.	<i>Halomonas BVR 1</i>	Cadmium	12.023
3.	<i>Halomonas BVR 1</i>	Zinc	11.11
4.	<i>Halomonas</i> +Sodium Alginate crosslinked CaCl ₂	Lead	9.68
5.	<i>Halomonas</i> +Sodium Alginate crosslinked CaCl ₂	Cadmium	25.12
6.	<i>Halomonas</i> +Sodium Alginate crosslinked CaCl ₂	Zinc	14.28
7.	<i>Halomonas</i> + Chitosan crosslinked glutarladehyde	Lead	24.15
8.	<i>Halomonas</i> + Chitosan crosslinked glutarladehyde	Cadmium	23.88
9.	<i>Halomonas</i> + Chitosan crosslinked glutarladehyde	Zinc	12.535
10.	<i>Halomonas</i> + GO	Lead	73.58
11.	<i>Halomonas</i> + GO	Cadmium	20.30
12.	<i>Halomonas</i> + GO	Zinc	42.53

Scope for future work

The results obtained in this study offered many new and interesting possibilities for future research. Some of them are listed below:-

1. Use combination of microbes to generate a consortium and study its efficacy.
2. Decoding the plasmid sequence responsible for the heavy metal resistance
3. Analyzing the expression of various other proteins (Metallothioneins, glutathione's etc.) responsible for the bacterial resistance to various heavy metals.
4. Assessing the trends in other organisms in the presence of metals other than lead is of paramount importance to delineate the resistance mechanism in bacteria.
5. The molecular mechanism's involving polyamines and heavy metal scavenging needs to be addressed.

REFERENCES

REFERENCES

Ababio, O. (2012). Electronic Waste Management in Ghana – Issues and Practices, Chapter 7, **INTECH, Open Minds**. 149-160.

Abbas, S. Z., Rafatullah, M., Ismail, N., Lalung, J. (2014). Isolation, Identification, and Characterization of Cadmium Resistant *Pseudomonas sp. M3* from Industrial Wastewater. **Journal of Waste Management**. Article ID 160398. 1-6.

Agostinho, A., De Lima, E. S., Marcia, A. et al. (2012). Heavy metal tolerance (Cr, Ag and Hg) in bacteria isolated from sewage. **Brazilian Journal of Microbiology**. 43, 1620-1631.

Ahluwalia, S. S., Goyal, D. (2007). Microbial and plant derived biomass for removal of heavy metals from waste water. **Bioresource Technology**. 98, 2243-2257.

Akpomie, K.G., Dawodu, F. A., Adebowale, K.O. (2015). Mechanism on the sorption of heavy metals from binary-solution by a low cost montmorillonite and its desorption potential. **Alexandria Engineering Journal**. 54, 757-767.

Alam, M.A., Sherif, E.S.M., Zahrani, S.M.A. (2013). Fabrication of various epoxy coatings for offshore application and evaluating their mechanical properties and corrosion behaviour. **International Journal of Electrochemical Science**. 8, 8388–8400.

Alcazar, R., Altabella, T., Marco, F., Bortolotti, C., Reymond, M., Koncz, C., Carrasco, P., Tiburcio, A.F. (2010). Polyamines: molecules with regulatory functions in plant abiotic stress tolerance. **Planta**. 231, 1237–1249.

Aleem, A., Isar, J., Malik, A. (2003). Impact of long-term application of industrial wastewater on the emergence of resistance traits in *Azotobacter Chroococcum* isolated from rhizospheric soil. **Bioresource Technology**. 86, 7-13.

Alkorta, I., Hernández-Allica, J., Becerril, J., Amezaga, I., Albizu, I., Garbisu, C. (2004) Recent findings on the phytoremediation of soils contaminated with environmentally toxic heavy metals and metalloids such as zinc, cadmium, lead, and arsenic. **Reviews in Environmental Science and Biotechnology**. 3, 71–90.

Amiri, A., Shanbedi, M., Ahmadi, G., Eshghi, H., Kazi, S.N., Chew, B.T., Savari, M., Zubir, M. N. M. (2016). Mass production of highly-porous graphene for high-performance supercapacitors. **Scientific Reports**. DOI: 10.1038/srep32686.

Ammar, A., Enizi, A. M. A., Almaadeed, M. A., Karim, A. (2016). Influence of graphene oxide on mechanical, morphological barrier, and electrical properties of polymer membranes. **Arabian Journal of Chemistry**. 9, 274-286.

Amoozegar, M. A., Hamed, J., Dadashpour, M., Shariatpanahi, S. (2005). Effect of salinity on the tolerance to toxic metals and oxyanions in native moderately halophilic spore forming bacilli. **World Journal of Microbiology and Biotechnology**. 21, 1237-1243.

Amoozegar, M.A., Ghazanfari, N., Didari, M. (2012). Lead and cadmium bioremoval by Halomonas sp. an exopolysaccharide-producing Halophilic Bacterium. **Progress in Biological Sciences**. 2, 1-11.

Ang, X.W., Sethu, V.S., Andersen, J.M., Sivakumar, M. (2013). Copper(II) ion removal from aqueous solutions using biosorption technology: thermodynamic and SEM–EDX studies. **Clean Technologies and Environmental Policy**. 15, 401-407.

Anjum, N. A., Aref, I. M., Duarte, A.C., Pereira, E., Ahmad, I., Iqbal, M. (2014). Glutathione and proline can coordinately make plants withstand the joint attack of metal(loid) and salinity stresses. **Frontiers in Plant Science**. 5, 1-4.

Ansari, R., Mosayebzadeh, Z., Khan, A.M. (2011). Application of a Cost Effective Biosorbent for Basic Dye Removal from Textile Industries. **Journal of Advanced Scientific Research**. 2, 25-31.

Atlas, R. M., Unterman, R., Bioremediation. In: Atlas, R.M . and Unterman. R eds. Industrial microbiology and biotechnology. Washington, D.C., American Society for Microbiology (ASM) Press, 2nded., 1999, p. 666-681.

Aygan, A., Arikan, Burhan. (2007). An Overview on Bacterial Motility Detection. **International Journal of Agriculture and Biology**. 1, 193-196.

Babel, S., Kurniawan, T. A. (2003). Low-cost adsorbents for heavy metals uptake from contaminated water: a review. **Journal of Hazardous Materials**. 97, 219-243.

Bae, W., Chen, W., Mulchandani, A., Mehra, R.K. (2000). Enhanced bioaccumulation of heavy metals by bacterial cells displaying synthetic phytochelatin. **Biotechnology and Bioengineering**. 70, 518-524.

Bansode, R. R., Losso, J. N., Marshall, W.E., Rao, R. M., Portier, R. J. (2004). Pecan shell-based granular activated carbon for treatment of chemical oxygen demand (COD) in municipal wastewater. **Bioresource technology**. 94, 129-135.

Barakat, M.A. (2011). New trends in removing heavy metals from industrial waste water. **Arabian Journal of chemistry**. 4, 361-377.

Barathi, M., Kumar, A.S.K., Kumar, C. U., Rajesh, N. (2014). Graphene oxide–aluminium oxyhydroxide interaction and its application for the effective adsorption of fluoride. **RSC Advances**. 4, 53711-53721.

Bartholomew, J. W., Mittwer, T. (1952). The Gram Stain. **Bacteriology Reviews**. 16, 1-29.

Bergey, D. H., Buchanan, R. E., Gibbons, N. E., & American Society for Microbiology. (1974). *Bergey's manual of determinative bacteriology*. Baltimore: Williams & Wilkins.

Boddu, V. M., Smith, E. D. (2004). Composite biosorbent for treatment of waste aqueous system(s) containing heavy metals. US Patent No: 6786336.

Bohli, T., Villaescusa, I., Ouederni, A. (2013). Comparative Study of Bivalent Cationic Metals Adsorption Pb(II), Cd(II), Ni(II) and Cu(II) on Olive Stones Chemically Activated Carbon. **Journal of Chemical Engineering and Process Technology**. 4, 1-7.

Borneman, J., Hartin, R. J. (2000). PCR Primers that amplify fungal r RNA genes from environmental samples. **Applied and Environmental Microbiology**. 66, 4356–4360.

Brandl, H., Bosshard, R., Wegmann, M. (2001). Computer-munching microbes: Metal leaching from electronic scrap by bacteria and fungi. **Hydrometallurgy**. 59, 319–326.

Carattoli, A. (2003). Plasmid-mediated antimicrobial resistance in *Salmonella enterica*. **Current Issues in Molecular Biology**. 5, 113-122.

Casale, A., C, De Stefano., Manfredi, G., Milea, D., Sammartano, S. (2009). Sequestration of alkyltin (IV) compounds in aqueous solution: Formation, stability, and empirical relationships for the binding of dimethyltin (IV) cation by N- and O-donor ligands. **Bioinorganic chemistry and applications**. 2009, 1-17.

Cervantes, C., Chavez, K., Vaca, S. (1991). Mechanisms of bacterial resistance to heavy metals. **Revista latinoamericana de microbiología**. 33, 61-70.

Chakraborty, S., Mukherjee, A, Bukhsh, K., Das, T.K. (2014). Cadmium induced oxidative stress tolerance in cadmium resistant *Aspergillus Foetidus*: its Possible role in cadmium bioremediation. **Ecotoxicology and Environmental Safety**. 106, 46-53.

Chakravarty, R., Banerjee, P.C. (2012). Mechanism of cadmium binding on the cell wall of an acidophilic bacterium. **Bioresource Technology**. 108, 176–183.

Chakravorty, S., Helb, D., Burday, M., Connell, N., Alland, D. (2007). A detailed analysis of 16s ribosomal RNA gene segments for the diagnosis of pathogenic bacteria. **Journal of Microbiological Methods**. 69, 330-339.

Chen, A.H., Yang, C.Y., Chen, C.Y., Chen, C.Y., Chen, C.W. (2013). The chemically crosslinked metal-complexed chitosans for comparative adsorptions of Cu(II), Zn(II), Ni(II) and Pb(II) ions in aqueous medium. **Journal of Hazardous Material**. 163, 1068–1075.

Chen, G.I., Mi, J., Wu, X., Luo, C., Li, J., Tang, Y., Li, J. (2011). Electrospun chitosan-graft-poly (ϵ -caprolactone)/poly (ϵ -caprolactone) cationic nanofibrous mats as potential scaffolds for skin tissue engineering. **International Journal of Biological Macromolecules**. 49, 543–547.

Chen, J.Y., Hao, Y.M., Liu, Y., Gou, J.J. (2013). Magnetic graphene oxides as highly effective adsorbents for rapid removal of a cationic dye rhodamine B from aqueous solutions. **RSC Advances**. 3, 7254–7258.

Chen, L., Han, Y., Jiang, H., Korpelainen, H., Li, C. (2011) Nitrogen nutrient status induces sexual differences in responses to cadmium in *Populus yunnanensis*. **Journal of Experimental Botany**. 62, 5037-5050.

Chen, X. C., Wang, Y. P., Lin, Q., Shi, J. Y., Wu, W.X., Chen, Y. X. (2005). Biosorption of copper(II) and zinc(II) from aqueous solution by *Pseudomonas putida* CZ1. **Colloids Surf B Biointerfaces**. 46, 101-107.

Chen, Y. L., Lee, C. C., Lin, Y. L., Yin, K. M., Ho, C. L., Liu, T. (2015). Obtaining long 16S rDNA sequences using multiple primers and its application on dioxin-containing samples, **BMC Bioinformatics**. 16, 2-11.

Choudhary, S.P.C., Kanwar, M., Bhardwaj, R., Yu, J.Q., Tran, L.S.P. (2012). Chromium stress mitigation by polyamine -brassinosteroid application involves phytohormonal and physiological strategies in *Raphanus sativus* L. **Plos One**. doi: 10.1371/journal.pone.0033210.

Cicatelli, A., Lingua, G., Todeschini, V., Biondi, S., Torrigiani, P., Castiglione, S. (2010). Arbuscular mycorrhizal fungi restore normal growth in a white poplar clone grown on heavy metal-contaminated soil, and this is associated with upregulation of foliar metallothionein and polyamine biosynthetic gene expression. **Annals of botany**. 106, 1-12.

Cimino, G., A. Passerin., G. Toscano (2000). Removal of toxic cations and Cr (VI) from aqueous solution by hazelnut shell. **Water Research**. 34, 2955-2962.

Clarridge, J.E. (2004). Impact of 16S rRNA Gene Sequence Analysis for Identification of Bacteria on Clinical Microbiology and Infectious Diseases. **Clinical Microbiology Reviews**. 17, 840-862.

Cong, M., Wu, H., Liu, X., Zhao, J., Wang, X., Lv, J., Hou, L. (2012). Effects of heavy metals on the expression of a zinc-inducible metallothionein-III gene and antioxidant enzyme activities in *Crassostrea gigas*. **Ecotoxicology**. 12, 1928-1936.

Coral, M. N. U., Korkmaz, H., Arikan, B., Coral, G. (2005). Plasmid mediated heavy metal resistance in *Enterobacter* spp. isolated from Sofulu landfill, in Adana, Turkey. **Annals of Microbiology**. 55, 175-179.

Cozatl, D. M., Loza-Tavera, H., Hernandez-Navarro, A., Moreno-Sanchez, R. (2005). Sulfur assimilation and glutathione metabolism under cadmium stress in yeast, protists and plants. **FEMS Microbiology Reviews**. 29, 653-671.

Cozmuta, L.M., Cozmuta, A.M., Peter, A., Nicula, C., Nsimba, E.B., Tutu, H. (2012). The influence of pH on the adsorption of lead by Naclinoptilolite: kinetic and equilibrium studies, **Water S.A.** 38, 269–272.

Crist, R.H., Oberholser, K., Shank, N., Nguyen, M. (1981). Nature of bonding between metallic ions and algal cell walls. **Environmental Science and Technology**. 15 1212–1217.

Das, N., Vimala, R., Karthika, P. (2008). Biosorption of heavy metals An overview. **Indian Journal of Biotechnology**. 7, 159-169.

Diaper, D. G. M., Kuksis, A. (1957). Determination of lead by dithizone in a single phase water acetone system. **Canadian Journal of Chemistry**. 35, 1278-1284.

Dinis, M. D. L., Fiuza, A. (2011). Exposure assessment to heavy metals in the environment: measures to eliminate or reduce the exposure to critical receptors. **Environmental Heavy Metal Pollution and Effects on Child Mental Development**.1, 27-50.

Dong, Y., Kumar, C. G., Chia, N., Kim, P. J., Miller, P. A., Price, N. D., Cann, I. K. O., Flynn, T. M., et al. (2014). *Halomonas sulfidaeris*-dominated microbial community inhabits a 1.8 km-deep subsurface cambrian sandstone reservoir. **Environmental Microbiology**. 16,1695-1708.

Donia, A.M. Atia, H. A., Boraey, El.,Mabrouk, D. (2006). Uptake studies of copper (II) on glycidyl methacrylate chelating resin containing Fe₂O₃ particles. **Separation and Purification Technology**. 49, 64-70.

Drolet, G., Dumbroff, E. B., Legge, R. L., Thompson, J. E. (1986). Radical scavenging properties of polyamines. **Phytochemistry**. 25, 367-371.

Du, H., Chen, W., Cai, P., Rong, X., Dai, Ke., Pecocock, C. L., Huang, Q. (2016). Cd(II) Sorption on Montmorillonite-Humic acid-Bacteria Composites. **Scientific Reports**. 6, Article number: 19499.

Ducros, V., Ruffieux, D., Belva-Besnet, H., Florence de Fraipont, Berger, F., Favier, A. (2009). Determination of dansylated polyamines in red blood cells by liquid chromatography-tandem mass spectrometry. **Analytical Biochemistry**. 390, 46–51.

Dumitriu, R.P., Oprea, A.M., Vasile, C (2009). A drug delivery system based on stimuli responsive Alginate/n-isopropylacryl amide hydrogel. **Chemical Cell Technology**. 43, 251–262.

Duruibe, J. O., Ogwuegbu, M. O. C., Egwurugwu, J. N. (2007). Heavy metal pollution and human biotoxic effects. **International Journal of Physical Sciences**. 2, 112-118.

Elzinga, E.J., Sparks, D.L. (2007). Phosphate adsorption onto hematite: An in situ ATRFTIR investigation of the effects of pH and loading level on the mode of phosphate surface complexation. **Journal of Colloid and Interface Science**. 308, 53–70.

EPA guidelines, Office of air and radiation, 2010. Available and Emerging Technologies for Reducing Greenhouse Gas Emissions from Municipal Solid Landfills.

E-Waste In India Reserach Unit (Larrdis) Rajya Sabha Secretariat New Delhi June, 2011.

Fan, L., Luo, C., Sun, M., Li, X., Qiu, H. (2013). Highly selective adsorption of lead ions by water-dispersible magnetic chitosan/graphene oxide composites. **Colloids and Surfaces B:Biointerfaces**. 103, 523-529.

Farkas, V., Felinger, A., Hegedusova, A., Dekany, I., Pernyeszi, T. (2013). Comparative study of the kinetics and equilibrium of phenol biosorption on immobilized white-rot fungus *Phanerochaete chrysosporium* from aqueous solution, **Colloids and Surfaces B**. 103, 381–390.

Fein, J.B. (2006). Thermodynamic modelling of metal adsorption onto bacterial cell walls: current challenges. **Advances in Agronomy**. 90, 179 -202.

Fischer, E. R., Hansen, B. T., Nair, V., Hoyt, F. H., Dorward, D.W. (2012). Scanning Electron Microscopy. **Current Protocols in Microbiology**. Chapter: Unit 2B.2. doi:10.1002/9780471729259.mc02b02s25.

Freundlich, H.M.F. (1906). Over the adsorption in solution. **Zeitschrift für Physikalische Chemie**. 57, 385–470.

Frost, R.L., Reddy, B.J., Wain, D.L., Martens, W.N. (2007). Identification of the rosasite group minerals an application of near infrared spectroscopy. **Spectrochimica Acta A**. 66, 1075–1081.

Futalan, C.M., Tsai, W. C., Lin, S. S., Hsien, K.L., Dalida, M. L., Wan, M. W. (2012). Copper, nickel and lead adsorption from aqueous solution using chitosan-immobilized on bentonite in a ternary system. **Sustainable Environmental Research**. 22, 345-355.

G.M. Gadd, Accumulation and transformation of metals by microorganisms, in *Biotechnology: A MultiVolume Comprehensive Treatise*, Vol. 10 **Special Processes**, H.J. Rehm, G. Reed, A. Puhler, and P. Stadler, eds., Wiley-VCH Verlag, Weinheim, 2001, pp. 225–264.

Gadd, G.M. (1990). Heavy metal accumulation by bacteria and other microorganisms. **Experientia**. 46, 834-840.

Gadd, G.M., Fry, J.C., Herbert, G.M., Jones, R. A., Craik, C.W. (1992). *Microbial Control of Heavy Metal Pollution*, Cambridge University Press, Cambridge (United Kingdom). 59-87.

Gairola, C. G., Wagner, G. J. (1991). Cadmium accumulation in the lung, liver and kidney of mice and rats chronically exposed to cigarette smoke. **Journal of Applied Toxicology**. 11, 355–358.

Gedam, A. H., Dongre, R. S., Bansiwala, A. K. (2014). Synthesis and characterization of graphite doped chitosan composite for batch adsorption of lead (II) ions from aqueous solution. **Advanced Materials Letters**. 10.5185/amlett.2014.7592.

George, Z.K., Eleni, A.D. (2013). Mercury(II) Removal with Modified Magnetic Chitosan Adsorbents. **Molecules**. 18, 6193–6214.

Gill, S. S., Tuteja, N. (2010). Polyamines and abiotic stress tolerance in plants. **Plant Signalling and Behavior**. 5, 26–33.

Girdhar, M., Sharma, N. R., Rehman, H., Kumar, A., Mohan, A. (2014). Comparative assessment for hyperaccumulatory and phytoremediation capability of three wild weeds. **3 Biotech**. 4, 579–589.

Groppa, M. D., Tomaro, M. L., Benavides, M. P. (2007b). Polyamines and heavy metal stress: The antioxidant behavior of spermine in cadmium- and copper-treated wheat leaves. **Biomaterials**. 20,185-195.

Guibal, E.(2004). Interactions of metal ions with chitosan-based sorbents: a review. **Separation and Purification Technology**. 38, 43–74.

Guide manual waste water analysis by Central Pollution Control board, MINARS/27/2007-08.

Guidelines for Environmentally Sound Management of E-waste (As approved vide MoEF letter No. 23-23/2007-HSMD dt. March 12, 2008 (Guidelines for environmentally sound management of e-waste) .

Guo, J., Zheng, X.D., Chen, Q. B., Zhang, L., Xu, X.P. (2012). Biosorption of Cd(II) from aqueous solution by *Pseudomonas plecoglossicida*: kinetics and mechanism. **Current Microbiology**. 65, 350–355.

Gupta, V.K., Suhas., Tyagi, I., Agrawal, S., Singh, R., Chaudhary, M., Harit, A., Kushwaha, S. (2016). operation studies for the removal of dyes and phenols using a low cost adsorbent. **Journal of Environmental Science and Management**. 2, 1-10.

Ha, H. C., Sirisoma, N. S., Kuppusamy, P., Zweier, J. L., Woster, P. M., Casero, R. A. (1998). The natural polyamine spermine functions directly as a free radical scavenger. **Proceedings of National Academy of Science** 1998, USA 95, 11140-11145.

Haferburg, G., Kothe, E. (2007). Microbes and metals: interactions in the environment. **Journal of Basic Microbiology**. 47, 453-467.

Hamdaoui, O., Naffrechoux, (2007). E. Modeling of adsorption isotherms of phenol and chlorophenols onto granular activated carbon Part I. Two-parameter models and equations allowing determination of thermodynamic parameters. **Journal of Hazardous Material**. 147, 381–394.

Handbook of chlor alkali technology Volume I: Fundamentals, Volume III: Facility Design and product Handling, Vol IV: Operations, Volume V: Corrosion, Environmental Issues, and Future Developments, Springer.

Hazarika, J., Pakshirajan, K., Sinharoy, A., Syiem, M. B. (2015). Bioremoval of copper, zinc, lead, and cadmium by *Nostoc muscorum* isolated from a coal mining site. **Journal of Applied Phycology**. 27, 1525-1534.

Ho, Y.S. (2006). Review of second-order models for adsorption systems. **Journal of Hazardous Materials**. B136, 681-689.

Hossain, M. A., Piyatida, P, Jaime, A., Teixeira da Silva, Fujita, M. (2012). Molecular mechanism of heavy metal toxicity and tolerance in plants: Central role of glutathione in detoxification of reactive oxygen species and methyl glyoxal and in heavy metal chelation. **Journal of Botany**. Article ID 872875. 1-37.

<https://www.epa.gov/eg/effluent-guidelines-plan-2016> (EPA guidelines, 2016).

Hu, L., Li, Y., Zhang, X., Wang, Y., Cui, L., Wei, L., Ma, H., Yan, L., Du, B. (2016). Fabrication of magnetic water-soluble hyperbranched polyol functionalized graphene oxide for high-efficiency water remediation. **Scientific Reports**, 6, 1-13.

Huff, J., Lunn, R.M., Waalkes, M.P., Tomatis, L., Infante, P. F. (2007). Cadmium-induced cancers in animals and in humans. **International Journal of Occupational Environmental Health**. 13, 202-212.

Hur, J., Shin, J., Yoo, J., Seo, Y. S. (2015). Competitive Adsorption of Metals onto Magnetic Graphene Oxide: Comparison with Other Carbonaceous Adsorbents. **Scientific World Journal**. Article ID 836287. 1-11.

Igwe, J. C., Abia, A.A. (2007). Adsorption isotherm studies of Cd (II), Pb (II) and Zn (II) ions bioremediation from aqueous solution using unmodified and EDTA modified maize cob. **Ecl. Quím. São Paulo**. 32, 33–42.

Ikewaga, H., Yamamoto, Y., Matsumoto, H. (1998). Cell death caused by a combination of aluminum and iron in cultured tobacco cells. **Plant Physiology**. 104, 474-478.

Jain, P. K., Bajpai, V. (2011). Biotechnology of bioremediation- a review. **International Journal of Environmental Sciences**. 3, 535-549.

Jarup, L. (2003). Hazards of heavy metal contamination. **British Medical Bulletin**. 68, 167-182.

Johnson, A. M., Thurlow, L. R., Swenger, S. R., Gillock, E. T. (2007). Partial characterization of two moderately halophilic bacteria from a Kansas salt marsh. **Prairie**. 39, 29-39.

Johnson, K. J., Ams, A. A., Wedel, A.N., Szymanowski, J.E.S., Weber, D.L., Schneegurt, M.A., Joo, J. H., Hussein, K. A., Hassan, S. H. A. (2011). Bacteria and Fungi as Alternatives for Remediation of Water Resources Polluting Heavy Metals. **Korean Journal of Soil Science and Fertility**. 44, 600-614.

Joutey, N.T., Sayel, H., Bahafid, W., Ghachtouli, N. E. (2013). Mechanisms of hexavalent chromium resistance and removal by microorganisms Springer; D.M. Whitacre (ed.), **Reviews of environmental contamination and toxicology**. 45-69.

Kaplan, D.L. (2013). Biopolymers from renewable resources. Methods of isolation, purification and characterization. **Springer Berlin Heidelberg**. ISBN 9783540635673.

Kapoor, A., Viraraghavan, T. (1995). Fungal biosorption-an alternative treatment option for heavy metal bearing wastewaters: a review. **Bioresource Technology**. 53, 195–206.

Kaniyoor, A., Baby, T. T., Ramaprabhu, S. (2010). Graphene synthesis via hydrogen induced low temperature exfoliation of graphite oxide. **Journal of Materials Chemistry**. 20, 8467-8469.

Kedziorek, M. A.M., Dupuy, A., Bourg, A., Compere, F. (1998). Leaching of Cd and Pb from a polluted soil during the percolation of EDTA: Laboratory column experiments modeled with a non-equilibrium solubilization step. **Environmental Science and Technology**. 32, 1609-1614.

Kirkelund, G.M., Damoe, A.J., Ottosen, L.M. (2012). Electrodialytic removal of Cd from biomass combustion fly ash suspensions. **Journal of Hazardous Material**. 250-251, 212-219.

Klaus, H., Dabo, G., Anamika, B. (2005). Proceedings: Sustainable Consumption: The Contribution of Research, Workshop, 10-12 February 2005. Ind Ecol Report Series 2005/1, Norwegian University of Science and Technology, **Industrial Ecology Program**. ISBN 82-7948-046-3.

Klimmek, S., Holz, Stan, H. J., Wilke, A., Bunke, G., Buchholz, R. (2001). Comparative analysis of the biosorption of cadmium, lead, nickel, and zinc by algae. **Environmental Science and Technology**. 35, 4283-4288.

Kocak, N., Sahin, M., Arslan, G., Ucan, H.I. (2012) Synthesis of crosslinked chitosan possessing Schiff base and its use in metal removal. **Journal of Inorganic and Organometallic Polymers and Materials**. 22, 166–177.

Kostal, J., Prabhukumar, G., Lao, U.L., Chen, A., Matsumoto, M., Mulchandani, A., Chen, W. (2005). Customizable biopolymers for heavy metal remediation. **Journal of nanoparticle research**. 7, 517-523.

Kouakou, U., Ello, A. S., Yapo, J. A., Trokourey, A. (2013). Adsorption of iron and zinc on commercial activated carbon. **Journal of Environmental Chemistry and Ecotoxicology**. 5, 168-171.

Krika, F., Azzouz, N., Ncibi, M. C. (2016). Adsorptive removal of cadmium from aqueous solution by cork biomass: Equilibrium, dynamic and thermodynamic studies. **Arabian Journal of Chemistry**. 9, S1077-S1083.

Krishnani, K. A., Anirudhan, T. S. (2008a). Kinetic and equilibrium modeling of cobalt (II) adsorption onto bagasse pith based sulphurized activated carbon. **Chemical Engineering Journal**. 137, 257-264.

Krishnaswamy, R., Wilson, D. B. (2000) Construction and characterization of an Escherichia coli strain genetically engineered for Ni(II) bioaccumulation. **Applied and Environmental Microbiology**. 66, 5383–5386.

Lagergren, S. (1898). Zur theorie der sogenannten adsorption gelöster Stoffe, **K.S. Vetenskapsakad. Handl.** 24, 1–39.

Langmuir, I. (1918). The adsorption of gases on plane surface of glass, mica and platinum. **Journal of American Chemical Society**. 40, 1361–1403.

Leshem, Y., Kuiper, P. J. C. (1996). Is there a GAS (general adaptation syndrome) response to various types of environmental stress? **Biology Plantarum**. 38, 1-18.

Li, H., Li, Z., Liu, T., Xiao, X., Peng, Z., Deng, L. (2008). A novel technology for biosorption and recovery hexavalent chromium in waste water by biofunctional magnetic beads. **Bioresource Technology**. 99, 6271–6279.

Lin, C.C., Lai, Y.T. (2006). Adsorption and recovery of lead (II) from aqueous solutions by immobilized *Pseudomonas aeruginosa* PU21 beads. **Journal of Hazardous Material**. 137, 99–105.

Lin, C.C., Lin, H.L. (2005). Remediation of soil contaminated with the heavy metal (Cd^{2+}). **Journal of Hazardous Material**. 122, 7–15.

Liu, J. H., Nada, K., Honda, C., Kitashiba, H., Wen, X. P., Pang, X. M., Moriguchi, T. (2006). Polyamine biosynthesis of apple callus under salt stress: importance of the arginine decarboxylase pathway in stress response. **Journal of Experimental Botany**. 57, 2589-2599.

Liu, Y., Zhou, J., Zhu, E., Tang, J., Liu, X., Tang, W. (2015). Covalently intercalated graphene oxide for oil-water separation. **Carbon**. 82, 264-272.

Logan, J.D. (2001). Transport modelling in Hydrogeochemical systems. Chapter 2, Reaction-Advection dispersion equation. Springer Eds.

Lord, S. E. (1984). TRAC: Trends in Analytical Chemistry. Vol 3, 126.

Lovaas, E. (1997). Antioxidative and metal-chelating effects of polyamines. **Advanced pharmacology**. 38, 119-149.

Lu, C., Chiu, H. (2006). Adsorption of zinc(II) from water with purified carbon nanotubes. **Chemical Engineering Science**. 61, 1138-1145.

M.C. Stern, Ph.D Thesis, 2013. Massachusetts Institute of Technology, Department of Chemical Engineering.

Mahamadi, C., Mawere, E. (2014). High adsorption of dyes by water hyacinth fixed on alginate. **Environmental Chemistry Letters**. 12, 313-320.

Mahmood, Z., Amin, A., Zafar, U., Raza, M. A., Hafeez, I., Akram, A. (2015). Adsorption studies of cadmium ions on alginate–calcium carbonate composite beads. **Applied Water Science**. 1-7.

- Maitani, T., Kubota, H., Sato, K., Yamada, T. (1996). The Composition of metals bound to Class 111 Metallothionein (Phytochelatin and Its Desglycyl Peptide) induced by various metals in root cultures of *Rubia tinctorum*. **Plant Physiology**. 110, 1145-1150.
- Malik, A. (2004). Metal bioremediation through growing cells. **Environment International**. 30, 261-278.
- Mameri, N., Boudries, N., Addour, L., Pauss, A. (1999). Batch Zinc Biosorption by a Bacterial Nonliving *Streptomyces rimosus* Biomass. **Water Research**. 33, 1347-1354.
- Manasi, Rajesh, V., Kumar, A. S. K., Rajesh, N. (2014). Adsorption isotherms, kinetics and thermodynamic studies towards understanding the interaction between a microbe immobilized polysaccharide matrix and lead. **Chemical Engineering Journal**. 248, 342-35.
- Manasi, Rajesh, V., Kumar, A. S. K., Rajesh, N. (2014). Biosorption of cadmium using a novel bacterium isolated from an electronic industry effluent. **Chemical Engineering Journal**. 235,176-185.
- Marcano, D. C., Kosynkin, D. V., Berlin, J. M., Sinitskii, A., Sun, Z., Slesarev, A., Alemany, L. B., Lu W., Tour, J. M. (2010). Improved Synthesis of Graphene Oxide **ACS Nano**. 4, 4806-4814.
- Mattuschka, B., Straube, G. (1993). Biosorption of metals by a waste biomass. **Journal of Chemical Technology and Biotechnology**. 58, 57–63.
- Mejare, M., Bulow, L. (2001). Metal-binding proteins and peptides in bioremediation and phytoremediation of heavy metals. **Trends in Biotechnology**. 19, 67-73.
- Mejia, V. C., Solis, E. B., Jimenez, J. C., Garcia, R. M., Gatica, J. C., Martinez, G. M., Ortega, Y. R. (2014). Branched polyamines functionalized with proposed reaction pathways based on ¹H-NMR, Atomic Absorption and IR Spectroscopies. **American Journal of Analytical Chemistry**. 5,1090-1101.
- Merle, S.S., Cuine, S., Carrier, P., Pradines, C.L., Luu, D.T., Peltier, G. (2003). Enhanced toxic metalaccumulation in engineered bacterial cells expressing *Arabidopsis thaliana* phytochelatin synthase. **Applied and Environmental Microbiology**. 69, 490-494.
- Michalak, I., Chojnacka, K., Krowiak, A. W. (2013). State of the Art for the Biosorption Process—a Review. **Applied Biochemistry and Biotechnology**. 170, 1389-1416.
- Minocha, S. C., Minocha, R., Robie, C. A. (1990). High-performance liquid chromatographic method for the determination of dansyl- polyamines. **Journal of Chromatography**. 511, 177-183.

Miretzky P, Cirelli A. F. (2009) Hg(II) removal from water by chitosan and chitosan derivatives: a review. **Journal of Hazardous Materials**. 167, 10-23.

Mishra, S. K., Tripathi, S. N., Choudhary, V., Gupta, B. D. (2014). SPR based fibre optic ammonia gas sensor utilizing nanocomposite film of PMMA/reduced graphene oxide prepared by in situ polymerization. **Sensors and Actuators**. 199, 190-200.

Mmolawa, A., Likuku, S., Gaboutloeloe, G. K. (2011). Assessment of heavy metal pollution in soils along major roadside areas in Botswana K. B. **African Journal of Environmental Science and Technology**. 5, 186-196.

Moat, A.G., Foster, J.W., Spector, M.P. (2000). Microbial stress responses, in microbial physiology, Fourth Edition, Chapter 18, John Wiley & Sons, Inc. Hoboken, NJ, USA.

Mohajer, R., Hassan, M.S., Mohammadi, J., Emami, M.H., Azarm, T. (2013). The status of lead and cadmium in soils of high prevalence gastrointestinal cancer region of Isfahan. **International Journal of Research in Medical Science**. 18, 210-214.

Mohan, D., Sharma, R., Singh, V.K., Steele, P., Pittman, C.U. (2012). Fluoride removal from water using bio-char, a green waste, low cost adsorbent: equilibrium uptake and sorption dynamics modelling. **Industrial & Engineering Chemical Research**. 51, 905–914.

Mohapatra, S., Minocha, R., Long, S., Minocha, S. C. (2010). Transgenic manipulation of a single polyamine in poplar cells affects the accumulation of all amino acids. **Amino Acids**. 38, 1117-1129.

Mohapatra, M., Mohapatra, L., Singh, P., Anand, S., Mishra, B.K. (2010). A comparative study on Pb(II), Cd(II), Cu(II), Co(II) adsorption from single and binary aqueous solutions on additive assisted nano-structured goethite. **International Journal of Engineering, Science and Technology**. 2, 89-103.

Moller, E. M., Bahnweg, G., Sandermann, Geiger, H. H. (1992). A simple and efficient protocol for isolation of high molecular weight DNA from filamentous fungi, fruit bodies and infected plant tissues. **Nucleic Acids Research**. 20, 6115-6116.

Molyneux, P. (1984). Langmuir isotherm in relation to mobility and molecular size of the adsorbate. **Nature**. 202, 368–370.

Morrow, H., Kirkothmer (2010). Encyclopedia of Chemical Technology, **Wiley publications**, 1–36

Mosmann, T. (1983). Rapid colorimetric assay for cellular growth and survival: application to proliferation and cytotoxicity assays. **Journal of Immunological Methods**. 65, 55-63.

- Muhammad, I., Puschenreiter, M., Wenzel, W. W. (2012). Cadmium and Zn availability as affected by pH manipulation and its assessment by soil extraction, DGT and indicator plants. **Total Environment**. 416, 490–500
- Murthy, S., Bali, G., Sarangi, S. K. (2011). Effect of lead on metallothionein concentration in lead resistant bacteria *Bacillus cereus* isolated from industrial effluent. **African Journal of Biotechnology**. 10, 15966-15972.
- Muthoosamy, K., Bai, R. G., Abubakar, I. B., Sudheer, S. M., Lim, H. N., Loh, H. S., Huang, N.M., Chia, C. H., Manickam, S. (2015). Exceedingly biocompatible and thin-layered reduced graphene oxide nanosheets using an eco-friendly mushroom extract strategy. **International Journal of Nanomedicine**. 10, 1505-1519.
- Nadeem, U., Datta, M. (2014). Adsorption studies of Zinc ions on biopolymer composite beads of alginate fly ash. **European Chemistry Bulletin**. 3, 682-691.
- Najafi, F. (2015). Removal of Zinc ion by Graphene Oxide (GO) and functionalized graphene oxide-glycine (GO-G) as adsorbents from aqueous solution :Kinetic studies. **International Nano Letters**. 5, 171-178..
- Norris, V., Reush, R. N., Igarashi, K. (2014). Root-Bernstein R. Molecular complementarity between simple, universal molecules and ions limited phenotype space in the precursors of cells. **Biology Direct**. 9, 1-20.
- Nourbakhsh, M.N., Kilicarslan, S., Ilhan, S., Ozdag, H. (2002). Biosorption of Cr^{6+} , Pb^{2+} and Cu^{2+} ions in industrial waste water on *Bacillus* sp. **Chemical Engineering Journal**. 85, 351-355.
- Nriagu, J.O. (1979). Global inventory of natural and anthropogenic emissions of trace metals to the atmosphere. **Nature**. 279, 409-411.
- Onundi, Y.B., Mamun, A.A., Al Khatib, M.F., Ahmed, Y.M. (2010). Adsorption of copper nickel and lead ions from synthetic semiconductor industrial wastewater by palm shell activated carbon. **International Journal of Environmental Science and Technology**. 7, 751–758.
- Oancea, S., Nfoca, A., Airinei, A., Jarup, L. (2003). Effects of lead on plant growth and photosynthetic activity. **Hazards of heavy metal contamination**. 68, 167-182.
- Ornek, A., Ozacar, M., Sengil, I.A. (2007). Adsorption of lead onto formaldehyde or sulphuric acid treated a corn waste: equilibrium and kinetic studies. **Biochemical Engineering Journal**. 37, 192–200.

Ouameur, A.A., Tajmir-Riahi, H. A. (2004). Structural analysis of DNA interactions with biogenic polyamines and cobalt(III)- hexamine studied by Fourier transform infrared and capillary electrophoresis. **Biological Chemistry**. 279, 42041-42054.

Oteng-Ababio, M. (2012). Electronic Waste Management in Ghana – Issues and Practices **INTECH Open minds**. Chapter 7. 149-166.

Pang, X. M., Zhang, Z.Y., Wen, X.P., Ban, Y., Moriguchi, T. (2007). Polyamines, all purpose players in response to environmental stresses in plants. **Plant Stress**.1, 173-188.

PangPardo, R., Herguedas, M., Barrado, E., Vega, M. (2003). Biosorption of cadmium, copper, lead and zinc by inactive biomass of *Pseudomonas putida*. **Analytical and Bioanalytical Chemistry**. 376, 26–32.

Park, H.G., Chae, M.Y (2004). Novel type of alginate gel-based adsorbents for heavy metal removal. **Journal of Chemical Technology and Biotechnology**. 79, 1080–1083.

Paschalidis, K. A., Roubelakis-Angelakis, KA. (2005). Spatial and temporal distribution of polyamine levels and polyamine anabolism in different organs/tissues of the tobacco plant. correlations with age, cell division/expansion, and differentiation. **Plant Physiology**. 138, 142–152.

Paschalidis, K.A., Roubelakis-Angelakis, K.A. (2005). Spatial and temporal distribution of polyamine levels and polyamine anabolism in different organs/tissues of the tobacco plant. correlations with age, cell division/expansion, and differentiation. **Plant Physiology**. 138,142–152.

Pegg, E., Jr. Robert, A C. (2011). Current status of the polyamine research field. **Methods of Molecular Biology**. 720, 3-35.

Perpetuo, E. A., Souza, C. B., Nascimento, C.A.O. (2011). Engineering Bacteria for Bioremediation, Progress in Molecular and Environmental Bioengineering - From Analysis and Modeling to Technology Applications, Prof. Angelo Carpi (Ed.), ISBN: 978-953-307-268-5, InTech.

Petrone, L., Easingwood, R., Barker, M. F., McQuillan, A.J. (2011). In situ ATR-IR spectroscopic and electron microscopic analyses of settlement secretions of *Undaria pinnatifida* kelp spores. **Journal of the Royal Society Interface**. 8, 410–422.

Phoenix, V. R., Martinex, R.E. (2002). Characterization and Implications of the Cell Surface Reactivity of *Calothrix sp.* Strain. **AEM**. 68, 4827-4834.

Pieschel, F., Lange, E., Camacho, J., Körber, H. (2004). Starch phosphates method for the production thereof and their use, United States patent.

Piner, R. D., Nguyen, S.T., Ruoff, R. S. (2006). Synthesis and exfoliation of isocyanate-treated graphene oxide nanoplatelets. **Carbon**. 44, 3342-3347.

Pinto, V.N. (2008). E-waste hazard: The impending Challenge. **International Journal of Occupational and Environmental medicine**. 12, 65-70.

Quintelas., Cristina., Pereira, R., Kaplan, E., Tavares, T. (2013). Removal of Ni(II) from aqueous solutions by an *Arthrobacter viscosus* biofilm supported on zeolite: From laboratory to pilot scale. **Bioresource Technology**. 142, 368–374.

Rajendran, P., Muthukrishnan, J., Gunasekaran, P. (2003). Microbes in heavy metal remediation. **Indian Journal of Experimental Biology**. 41, 935-944.

Ramakrishna, A., Ravishankar, G.A. (2011). Influence of abiotic stress signals on secondary metabolites in plants. **Plant Signalling and Behaviour**. 6, 1720-1732.

Rani, A., Goel, R. (2009). Microbial strategy for crop improvement. Springer-Verlag Berlin Heidelberg. 2009, 85-104.

Reddad, Z., Gerente, Z.C., Andres, Y., Le Cloirec, P. (2002). Adsorption of several metal ions onto a low-cost biosorbent: kinetic and equilibrium studies. **Environmental Science and Technology**. 36, 2067–2073.

Rhee, H. J., Kim, E. J., Lee, J.K. (2007). Physiological polyamines: simple primordial stress molecules. **Journal of Cellular and Molecular Medicine**. 11, 685- 703.

Riccardi, C., Papacchini, M., Mansi, A., Ciervo, A., Petrucca, A., La, R. G., Marianelli, C., Muscillo, M., Marcelloni, A. M., Spicaglia, S. (2005). Characterization of bacterial population coming from a soil contaminated by polycyclic aromatic hydrocarbons [PAHs] able to degrade pyrene in slurry phase. **Annals of Microbiology**. 55, 85-90.

Robertson, Veonica., Haltli, B., McCauley, E.P., Overy, D.P., Kerr, R. G. (2016). Highly Variable Bacterial Communities Associated with the Octocoral *Antilloorgia elisabethae*. **Microorganisms**. 4, 1- 23.

Ron, E. Z. (2013). The prokaryotes-prokaryotic physiology and biochemistry, Bacterial stress responses. **Springer**, 589-598.

Rouached, H., Pal, S., Rachmilevitch, S., Libault, M., Lam-Son P. H. (2015). Plants Coping Abiotic and Biotic Stresses: A Tale of Diligent Management. **Biomed Research International**. Article ID 754754, 1-2.

Ruiz, J. D.C., Quackenboss, J. J., Tulve, N. S. (2016). Contributions of a Child's Built, Natural, and Social Environments to Their General Cognitive Ability: A Systematic Scoping Review. **Plos One**. 11, doi: 10.1371/journal.pone.0147741

Sowmyaa, S., Sudheesh Kumara., P.T., Chennazhia., K.P., Naira., S.V., Tamurab., H., Jayakumara. R. (2011). Biocompatible β -chitin Hydrogel/Nanobioactive Glass Ceramic Nanocomposite Scaffolds for Periodontal Bone Regeneration. **Trends in Biomaterials and Artificial Organs**. 25, 1-11.

Sabate, J., Vinas, M., Solanas, A.M. (2004). Laboratory-scale bioremediation experiments on hydrocarbon-contaminated soils. **International Biodeterioration & Biodegradation**. 54, 19-25.

Sakugawa, K., Ikeda, A., Takemura, A., Ono, H. (2004). Simplified method for estimation of composition of alginates by FTIR. **Journal of Applied Polymer Science**. 93, 1372–1377.

Sambrook, J. (2001) Cloning and sequencing. In: Sambrook J Russel, D.W. (Eds.), Molecular cloning- A laboratory manual. Cold Spring Harbor Laboratory Press, Cold Spring Harbor.

Sanchez, V.C., Jachak, A., Hurt, R.H., Kane, A.B. (2012). Biological Interactions of Graphene-Family Nanomaterials – An Interdisciplinary Review. **Chemical Research Toxicology**. 25, 15-34.

Santhosh, C., Kollu, P., Komarala, E. V. P. K., Doshi, S. N. et al. (2015). Solvothermal synthesis of MnFe₂O₄-Graphene composite - Investigation of its adsorption and antimicrobial properties. **Applied Surface Science**. 327, 27-36.

Sarkar, B.K., Patel, R., Bhadoriya, U. (2011). Antimicrobial activity of some novel pyrazoline derivatives. **Journal of Advanced Pharmaceutical Technology and Research**. 1, 243–250.

Sengil, I.A., Ozacar, M., Turkmenler, H. (2009). Kinetic and isotherm studies of Cu (II) biosorption onto valonia tabninin resin. **Journal Hazardous Material**. 162, 1046–1052.

Serbus, C., Hora, K., Rezae, J., Pribil, S., Marvan, P., Krejdirik, L., et al. (1973). Sorbent and method of manufacturing same. U.S. Patent No: 3725291.

Seymour, J., Ahmed, T., Marcos., Stocker, R. A. (2008). microfluidic chemotaxis assay to study microbial behavior in diffusing nutrient patches. **Limnology Oceanography Methods**. 6,477–488.

Shah, P., Swiatlo, E. A. (2008). multifaceted role for polyamines in bacterial pathogens. **Molecular Microbiology**. 68, 4-16.

Shahid, M., Malik, A., Sheeba. (2003). Multidrug-resistant *Pseudomonas aeruginosa* strains harbouring R-plasmids and Amp C L-lactamases isolated from hospitalised burn patients in a tertiary care hospital of North India. **FEMS Microbiology Letters**. 228 , 181-186.

Sharma, R. K., Agrawal, M. (2005). Biological effects of heavy metals: An overview. **Journal of Environmental Biology**. 26, 301-313.

Sharma, S. B., Suman, J., Praveen, K., Sunisha, K. (2013). The effects of airpollution on the environment and human health. *Indian Journal of Research in Pharmacy and Biotechnology*. 1, 391- 396.

Sharma,S.S., Dietz,K.J. (2006). The significance of amino acid and amino acid- derived molecules in plant responses. **Journal of Experimental Botany**. 57, 711-726.

Sheikha, D., Ashour, I., Rub, F.A.A.A. (2008). Biosorption of Zinc on Immobilized Green Algae: Equilibrium and Dynamics Studies. **The Journal of Engineering Research**. 5, 20-29.

Silhavy, T.J., Kahne, D., Walker, S. (2010). The bacterial Cell envelope. **Cold Spring Harbor Perspectives in Biology**. 5, 1-16.

Silva, L. A. A., De, Carvalho, MA., De, Souza, S. A., Dias, P. M., et al. (2012). Heavy metal tolerance (Cr, Ag and Hg) in bacteria isolated from sewage. **Brazilian Journal of Microbiology**. 43, 1620-1631.

Simões Campos Tavares, T. M. J., & Pontes Correia Neves, I. M. (2008). Biosorption system produced from biofilms supported in faujasite (FAU) zeolite, process obtaining it and its usage for removal of hexavalent chromium (Cr(VI)). US Patent No: 20080169238.

Singh,R., Gautam, N., Mishra, A., Gupta, R. (2011). Heavy metals and living systems: An overview. **Indian Journal of Pharmacology**. 43, 246-253.

Smith, M. A., Davies, P. J. (1985). Separation and quantitation of polyamines in plant tissue by high performance liquid chromatography of their dansyl derivatives. **Plant Physiology**. 78, 89-91.

Smrithi, A., Usha, K. (2012). Isolation and characterization of chromium removing bacteria from tannery effluent disposal site. **IJABR**. 3, 644-652.

Sone, H., Fugetsu, B., Tanaka, S. (2009). Selective elimination of lead (II) ions by alginate/polyurethane composite foams. **Journal of Hazardous Material**. 162, 423–429.

Souza, L. D., Devi, P., Shridhar, D., Naik, C.G. (2008) .Use of fourier transform Infrared (FTIR) spectroscopy to study cadmium-induced changes in *Padina Tetrastromatica* (Hauck). **Analytical Chemistry Insights**. 3, 135–143.

Spiegelman, D., Whissell, G., Greer, C.W. (2005). A survey of the methods for the characterization of microbial consortia and communities. **Canadian Journal of Microbiology**. 51, 355-386.

Srivastava, P.K., Yadav, p., Ghosh, S. (2012). Non-Oxidative, Controlled Exfoliation of Graphite in Aqueous Medium. **Nanoscale**. 00, 1-3.

Studham, E., Macintosh, G. C. (2013). Multiple phytohormone signals control the transcriptional response to soybean aphid infestation in susceptible and resistant soybean plants. **Molecular Plant Microbial Interaction**. 26, 116-129.

Sun, P., Wang, Y., Liu, H., Wang, K., Wu, D., Xu, Z., Zhu, H. (2014). Structure Evolution of Graphene Oxide during Thermally Driven Phase Transformation: Is the Oxygen Content Really Preserved? **Plos one**. <http://dx.doi.org/10.1371/journal.pone.0111908>.

Sun, X., Peng, B., Ji, Y., Chen, J., Li, D. (2009). Chitosan(chitin)/cellulose composite biosorbents prepared using ionic liquid for heavy metal ions adsorption. **AIChE Journal**. 55, 2062-2069.

Sun, X.F., Wang, S.G., Liu, X.W., Gong, W.X., Bao, N., Ma, Y. (2008). The effects of pH and ionic strength on fulvic acid uptake by chitosan hydrogel beads. **Colloids and surfaces: Physicochemical and engineering Aspects**. 324, 28–34.

Talawar, M.B., Agrawal, A.P., Chhabra, J.S., Asthana, S.N (2004). Studies on lead-free initiators: synthesis, characterization and performance evaluation of transition metal complexes of carbonylhydrazide. **Journal of Hazardous Material**. A113, 57–65.

Tan, W. G., Fu, B., Li, S. F. (2015). Metallomics and NMR-based metabolomics of *Chlorella* sp. reveal the synergistic role of copper and cadmium in multi-metal toxicity and oxidative stress. **Metallomics**. 7, 426-438.

Tchounwou, P. B., Yedjou, C.G., Patlolla. A. K., Sutton, D. J. (2012). Heavy Metals Toxicity and the Environment. **Molecular, Clinical and Environmental Toxicology**. 101, 133-164.

Tchounwou, P.B., Yedjou, C. G., Patlolla, A.K., Sutton, D. J. (2012). Heavy metals toxicity and the environment. **EXS**. 101, 133-164.

Tehrani, M. S., Azar, P. A., Namin, P. E., Dehaghi, S.M. (2014). Removal of Lead Ions from Aqueous Solution Using Multi-Walled Carbon Nanotubes: The Effect of Functionalization. **Journal of Applied Environmental and Biological Sciences**. 4, 316- 326.

Tehrani, M. S., Azar, P. A., Namin, P.E., Dehaghi, S.M. (2014). Removal of Lead Ions from Aqueous Solution Using Multi-Walled Carbon Nanotubes: The Effect of Functionalization. **Applied Environmental and Biological Sciences**. 4, 316-326.

Tong, S., Yasmin, E., Schirnding, V., Prapamontol, T. (2000). Environmental lead exposure: a public health problem of global dimensions. **Bulletin of the World Health Organization**, 78 1068-1077.

Umrانيا, V.V. (2006). Bioremediation of toxic heavy metals using acidothermophilic autotrophies. **Bioresource Technology**. 97, 1237-1242.

Varadarajan, H., Shikha, S. (2014). Biodiversity characterization of bacterial and fungal isolates from gold electroplating industry. **JAEM**. 2, 212-219.

Varma, A.J., Deshpande, S.V., Kennedy, J.F. (2004). Metal complexation by chitosan and its derivatives: a review. **Carbohydrate Polymers**. 55, 77-93.

Veeraiah, K., Venkatrao, G., Vivek, CH., Hymaranjani, G. (2013). Heavy metal, cadmium chloride induced biochemical changes in the Indian major carp *Cirrhinus mrigala* (Hamilton). **International journal of bioassays**. 2, 1028-1033.

Veglio, F., Beochini, F. (1997). Removal of metals by biosorption A review. **Hydrometallurgy**. 44, 301-316.

Venckatsh, R., Amudha, T., Sivaraj, R., Chandramohan, M., Jamulingam, M. (2010). Kinetics and equilibrium studies of adsorption of direct Red-28 onto *Punica Granatum* carbon. **International Journal of Engineering Science and Technology**. 2, 2040-2050.

Ventosa, A., Nieto, J. J., Oren, A. (1998). Biology of Moderately Halophilic Aerobic Bacteria. **Microbiology and Molecular Biology Reviews**. 1998, 504–544.

Vijayaraghavan, K., Palanivelu, K., Velan, M. (2006). Biosorption of copper and cobalt from aqueous solutions by crab shell particles. **Bioresource Technology**. 97, 1411-1419.

Viswanathan, N., Meenakshi, S. (2010). Enriched fluoride sorption using alumina/ chitosan composite. **Journal of Hazardous Material**. 178 , 226–232.

Valls, M., Lorenzo, V. D. (2002). Exploiting the genetic and biochemical capacities of bacteria for the remediation of heavy metal pollution. **FEMS Microbiology Reviews**. 26, 327-338.

Vold, I.M.N., Varum, K.M., Guibal, E., Smidsrod, O. (2003). Binding of ions to chitosan. Selectivity studies. **Carbohydrate Polymers**. 54, 471–477.

Wan, M.W., Kan, C. C., Rogel, B.D., Dalida, M.L.P. (2010). Adsorption of copper (II) and lead (II) ions from aqueous solution on chitosan-coated sand. **Carbohydrate Polymers**. 80, 891-899.

Wang, G., Qian, F., Saltikov, C. W., Jiao, Y. (2011). Microbial reduction of graphene oxide by *Shewanella*. **Nano Research**. 4, 563-570.

Wang, J., Chen, C. (2009). Biosorbents for heavy metals removal and their future. **Biotechnology Advances**. 27, 195-226.

Wang, Y., Liang, S., Chen, B., Guo, F., Yu, S., Tang, Y. (2013). Synergistic Removal of Pb(II), Cd(II) and Humic Acid by Fe₃O₄@Mesoporous Silica-Graphene Oxide Composites. **Plos One**. <http://dx.doi.org/10.1371/journal.pone.0065634>.

Weber, F.A., Hofacker, A.F., Kretzschmar, R. (2010). Temperature dependence and coupling of iron and arsenic reduction and release during flooding of a contaminated soil. **Environmental Science and Technology**. 44, 116–122.

Weber, W.J., Morris, J.C. (1963). Kinetics of adsorption on carbon from solution. **Journal of the Sanitary Engineering Division (American Society of Civil Engineering)** 89, 3–60.

Weiss, B. (1984). Chapter 1, Behavior as a Measure of Adverse Responses to Environmental, Contaminants Drugs, Neurotransmitters, and Behavior.

Widmer, F., Seidler, R. J., Gillevet, P. M., Watrud, L.S., Giovanni, D.D. (1998). A Highly Selective PCR Protocol for Detecting 16S rRNA Genes of the Genus *Pseudomonas* (*Sensu Stricto*) in Environmental Samples. **Applied and Environmental Microbiology**. 64, 2545-2553.

Xu, Z., Cai, J. G., Pan, B. C. (2013). Mathematically modeling fixed bed adsorption in aqueous systems. **Applied Physics and Engineering**. 14, 155- 176.

Yan, G., Viraraghavan, T. (2000). Effect of pretreatment on the bioadsorption of heavy metals on *Mucor rouxii*. **Water S.A.** 26, 119–123.

Yang, C.H., Wang, M.X., Haider, H., Yang, J.H., Sun, J.Y., Chen, Y.M., Zhou, J., Suo, Z. (2013). Strengthening alginate/polyacrylamide hydrogels using various multivalent cations, **ACS Applied Material and Interfaces**. 5, 10418–10422.

Yoshida, N., Ikeda, R., Okuno, T. (2006). Identification and characterization of heavy metal-resistant unicellular alga isolated from soil and its potential for phytoremediation. **Bioresource Technology**. 97, 1843-1849.

Yoshizawa, K., Rimm, E.B., Morris, J.S., Spate, V.L., Hsieh, C.C., Spiegelman, D., Stampfer, M.J., Willett, W.C.(2002). Mercury and the risk of coronary heart disease in men. **The New England Journal of Medicine**. 347,1755-1760.

Youssef, N.H., Savage, A. K. N., Mc Cully, A.L., Luedtke, B., Shaw,E.I., Hoff, W. D., Elshahed, M.S. (2014). Trehalose 2- sulfotrehalose biosynthesis and glycine-betaine uptake are widely spread mechanisms for osmoadaptation in the Halobacteriales. **ISME J**. 8, 636-649.

Zhang, G., Qu, R., Sun, C., Ji, C., Chen, H., Wang, C., Niu, Y. (2008). Adsorption for metal ions of chitosan coated cotton fiber. **Journal of Polymer Science**. 110, 2321-2327.

Zhang, J., Xu, Y., Liu, Z., Yang, W., Liu, J. (2013). Highly conductive porous graphene electrode prepared via in-situ reduction of graphene oxide using Cu nanoparticles for the fabrication of high performance supercapacitors. **RSC Advances**. 5, 54275-54282

Zhang, X., Wang, X. (2015). Adsorption and Desorption of Nickel(II) Ions from Aqueous Solution by a Lignocellulose/ Montmorillonite Nanocomposite. **PlosOne**.10, e0117077.

Zhao, G., Wu, X., Tan,X., Wang,X. (2011). Sorption of Heavy Metal Ions from Aqueous Solutions: A Review. **The Open Colloid Science Journal**. 4, 19-31.

Zhou, Y.F., Haynes, R. (2010). Sorption of Heavy Metals by Inorganic and Organic Components of Solid Wastes: Significance to Use of Wastes as Low-Cost Adsorbents and Immobilizing Agents. **Critical Reviews in Environmental Science and Technology**. 40, 909-977.

Zone size interpretative chart in accordance to performance standards for antimicrobial disk susceptibility tests, CLSI [formerly NCCLS].

Zu, Y., Zhang, Y., Zhao,X., Shan,C., Zu, S., Wang, K., Li, Y., Ge, Y. (2012). Preparation and characterization of chitosan-polyvinyl alcohol blend hydrogels for the controlled release of nano-insulin. **International Journal of Biological Macromolecules**. 50, 82-87.

APPENDIX I

APPENDIX I

Isolation of genomic DNA.

To isolate DNA from microbial cells the following materials and methods were used:

Materials and reagents

- 1) GET buffer.(Glucose- 20%, Tris- 50mM and EDTA- 50mM)
- 2) Lysozyme working concentration of 100ug/mL
- 3) 10% SDS
- 4) Tris-saturated phenol (pH-8)
- 5) Chloroform- Isoamyl Alcohol mix (24:1)
- 6) Ethanol-100%
- 7) Ethanol-70%
- 8) TE (Tris-EDTA buffer) for dissolution of DNA
- 9) Micropipettes
- 10) Eppendorfs

Genomic DNA was isolated by the standard DNA extraction procedure [Sambrook et al., 2001]. Isolated microorganisms were grown in 5 mL LB medium at 37 °C for overnight by constant agitation. The culture was spun down and DNA pellet was lysed using GET buffer.(Glucose- 20%, Tris- 50mM and EDTA- 50mM). This was followed by lysozyme treatment at 37 °C for 30-40 min. Subsequently extraction was carried out using 10 % SDS at 37 °C for 1-2 h. Extraction, by adding equal volumes of PCI (Phenol: Chloroform: Isoamyl alcohol) was done by transferring the supernatant into fresh eppendorf tubes and adding PCI . The lysate was collected subsequent to centrifugation at 10,000 rpm for 10min. DNA precipitation was done by adding 1.5 volumes of 100% ethanol to supernatant transferred from earlier step into fresh tubes. The

precipitated DNA was finally washed with 70% ethanol and air dried by inverting tubes on filter paper till last traces of ethanol evaporates. DNA pellets were dissolved in 30 μ l of Tris-EDTA buffer (pH-8) and 2 μ l of it was loaded on to agarose gel electrophoresis to check for DNA bands. The primer used has a T_m of 55⁰C. In accordance to this Polymerase Chain Reaction (PCR) was set up with reaction mixture containing 100 ng/ μ l of the extracted genomic DNA, 200ng each of forward and reverse primer (27F and 1492 R) , 200 μ M each dNTP, 1 unit of *Taq polymerase*, 2.5 μ l of 10X PCR buffer, and 1.5mM of MgCl₂. Some of the genomic DNA obtained were of very low concentration, even on repeated optimization of the isolation procedures. Such samples were subjected to colony PCR. In this procedure pure single colonies were developed on Luria Bertani agar plates. Single colony representing a pure culture was taken using sterilized toothpick and rubbed on the bottom of the surface of an eppendorf tube. All the required components needed for the PCR amplification of the DNA were added into this tube.

Adsorption isotherm models

The adsorption isotherm curves was used to assess the mechanism involving the interaction between the adsorbent and adsorbate molecules. Adsorption isotherm equations interprets the experimental adsorption parameters mathematically. The nature of the adsorption process can be postulated from the experimental observations. The isotherm studies also allows calculation of metal uptake (q_e) at equilibrium, which has a major impact on the adsorption process.

The relationship between the amount of metal adsorbed and the equilibrium concentration is well expressed using well known Langmiur and Freundlich isotherm models. The relative performance of the adsorbents is ascertained from the maximum adsorption capacity obtained from these models.

Langmuir adsorption isotherm

The Langmuir adsorption isotherm is based on the following assumptions:

1. Adsorption is homogeneous containing the adsorbing sites on a flat surface without any corrugations .
2. Adsorption occurs as a monolayer coverage.
3. All the sites are equivalent that can hold only one adsorbate molecule at a time.
4. The ability of a molecule to adsorb at a given site is independent of the occupation of neighbouring sites.
5. One sorbate molecule reacts with only one active site and does not interact with the molecules on the adjacent sites.

According to this isotherm a given adsorbent has certain number of fixed adsorption sites and each adsorbate can stick either by means of a physisorption or chemisorption [Langmuir et al., 1918; Atkins et al, 2006]. This is applicable to the physical or chemical adsorption on solid surface with one type of adsorption active center. The Langmuir equation can be used for describing equilibrium conditions for the adsorption behavior in different adsorbate-adsorbent systems. The Langmuir isotherm assumes monolayer adsorption on a uniform surface with a finite number of adsorption sites. Once a site is filled with the adsorbate molecule, no further sorption can take place at that site. The surface eventually will reach a saturation point where the maximum adsorption of the surface will be achieved. The Langmuir isotherm can be expressed as

$$\frac{C_e}{q_e} = \frac{1}{q_m b} + \frac{C_e}{q_m}$$

Where q_e is the amount of metal ions adsorbed at equilibrium (mg g^{-1}), q_0 is the maximum adsorption capacity (mg g^{-1}), C_e is the equilibrium concentration of the adsorbate (mg L^{-1}), and b (L mg^{-1}) is the Langmuir constant. This monolayer adsorption model gives the maximum adsorption capacity in the linearized Langmuir expression.

$$q_e = \frac{bC_e}{1+C_e b}$$

Where ‘ C_e ’ is the equilibrium concentration and ‘ q_e ’ is the amount of adsorbate adsorbed per gram of adsorbent at equilibrium (mg g^{-1}); ‘ q_0 ’ and ‘ b ’ are Langmuir constants related to the sorption capacity and intensity respectively. A plot of $\frac{C_e}{q_e}$ vs C_e gives the q_0 and b . The feasibility of the adsorption process is also determined by R_L [Crini et al., 2007]. R_L a dimensionless parameter relates the effectiveness of adsorption of the metal and is given by the expression.

$$R_L = \frac{1}{1 + bC_0}$$

where C_0 (mg L^{-1}) is the initial metal concentration and b is Langmuir constant.

3.2.3. Freundlich isotherm

This isotherm [Freundlich et al., 1906] is applicable to both monolayer (chemisorption) and multilayer adsorption (physisorption). This empirical relation is based on the assumptions that the adsorbate molecules adsorb on a heterogenous surface unlike langmuir isotherm. The Freundlich adsorption equation [Ozacar et al., 2003] can be written as,

$$q_e = K_F C_e^{1/n}$$

The linear form of the Freundlich isotherm model is described as:

$$\log q_e = \log K_F + \frac{1}{n} \log C_e$$

where q_e is amount of metal adsorbed at equilibrium (mg g^{-1}), C_e is the equilibrium concentration of the adsorbate in solution, K_F , and n are constants related to the adsorption process such as adsorption capacity and intensity respectively. This parameters suggests the feasibility of the reaction favouring Freundlich isotherm.

Other models that were considered apart from these two were DR isotherm and Elovich isotherm. These isotherms are considered to be extensions of the langmuir isotherm [Dabrowski et al., 2001]. The parameters obtained from these isotherms like the adsorption energy, polanyi potential etc also suggests the nature of the adsorption.

Adsorption kinetics

Since, the adsorption capacity of an adsorbent depends upon the contact time, the study of the kinetics of adsorption is a vital parameter that needs to be studied. The kinetics of adsorption process depends on the time and the concentration distribution of the solute in both bulk solution and adsorbent. The two major kinetic models studied are the pseudo first /Lagergren and second order kinetic models. The experimental data obtained were applied to these equations to obtained and investigate the adsorption mechanism of metal ions on a specific adsorbent.

The study of adsorption kinetics in wastewater is important as it provides valuable insights into the reaction mechanism. Furthermore, it is important to predict the time at which the adsorbate is effectively removed from aqueous solution to aid in the design of an appropriate treatment plant for the upscale studies. Generally, the kinetics of adsorption is governed by three probable models [Wu et al., 2001]

- (i) external mass transfer or the film diffusion that involves the transfer of metal ions from the aqueous solution onto the external surface of the adsorbent.

- (ii) particle diffusion that helps in diffusion of the metal ions through the pores of the adsorbent.
- (iii) physical / chemical adsorption of the adsorbate molecules on the interior of the adsorbent.

The rate of adsorption of metal ions can also be expressed in terms of the sticking probability (S) and the molecular flux (F) The probability of adherence of metal ions onto the adsorbent surface is a characteristic feature of a particular adsorbent–adsorbate system. Essentially, this would mean that S is also a function of the surface coverage. It is given by the following equation:

$$R_{ads} = S \cdot F$$

Lagergren / Pseudo first order kinetics

The first-order rate expression of Lagergren can be expressed mathematically as [Lagergren et al., 1898; Ozacar et al, 2005]

$$\log (q_e - q_t) = \log q_e - \frac{k_1 t}{2.303}$$

where q_e and q_t (mg g^{-1}) are the amounts of metal adsorbed per unit mass of adsorbent at equilibrium and time, t (min), respectively, and k_{ad} is the rate constant. The value of adsorption rate constants (k_{ad}) for the different adsorbents at different initial metal concentrations were obtained from slopes of the plots of $\log (q_e - q_t)$ vs time. Depending on the regression coefficient being closer to 1, favourability of the adsorption process towards these kinetic models is ascertained.

Pseudo-second order kinetics

A pseudo second order reaction model [Gerente et al, 2007; Ho et al, 2006] utilized to study the process of adsorption can be expressed mathematically as:

$$\frac{t}{q_t} = \frac{1}{k_2 q_e^2} + \frac{t}{q_e}$$

Where k_2 ($\text{g mg}^{-1} \text{min}^{-1}$) is the equilibrium rate constant of pseudo second order adsorption. The slope and intercept of the plot of $\frac{t}{q_t}$ vs t gives the parameters q_e and k_2 respectively.

Intraparticle diffusion

Weber Morris model of intraparticle diffusion is used to interpret the adsorption mechanism particularly the overall steps that govern the adsorption kinetics and its mechanism. This model involves the uptake of metal ions by the adsorbent [Weber et al., 1963].

- (i) Transport of metal from bulk solution to the external surface of the adsorbent.
- (ii) Transport of metal ions into the pores of the adsorbent.
- (iii) Adsorption of metal ions on the surface of the sorbent.

The Weber Morris equation is given as follows

$$q_t = k_{\text{int}} \cdot t^{0.5} + C$$

where K_{int} is the intra-particle diffusion constant and q_t is the amount of the heavy metals adsorbed at time t .

In the first step, a thin film is formed around the adsorbent due to the transport of the adsorbate to the boundary thereby creating a concentration gradient around the adsorbent. The second step rightly called as pore diffusion involves the probable diffusion of the adsorbate molecules into

the pores of the adsorbent matrix. The Weber Morris plot relating the initial concentration of the adsorbate and the rate of adsorption is linear in case this stage limits the adsorption process. A linear plot of q_t vs \sqrt{t} with non-zero intercept manifests that the intraparticle diffusion is not the only rate limiting step.

Adsorption thermodynamics

The study of thermodynamics involving parameters like the free energy (ΔG_0), entropy (ΔS_0) and enthalpy (ΔH_0) changes is an important factor in the study of metal adsorption to ascertain the feasibility and nature of the adsorption process. These parameters are determined at various temperature ranges and were obtained from the following equations [Sun et al., 2007; Ho et al., 2000; Ozcan et al., 2004]

$$\Delta G^0 = -RT \ln K$$

$$\Delta G^0 = \Delta H^0 - T \Delta S^0$$

$$\ln K = \frac{-\Delta H^0}{RT} + \frac{\Delta S^0}{R}$$

Where R is gas constant ($J K^{-1} mol^{-1}$), T is the temperature (Kelvin) and K_{ad} is the equilibrium constant that is obtained from the ratio of the concentration of metal ions adsorbed on the solid adsorbent to that in the liquid phase. Calculation of the free energy changes depicts the adsorption mechanism being either exothermic or endothermic. The Van't Hoff plot of $\ln K$ vs $\frac{1}{T}$ gives the parameters ΔH^0 and ΔS^0 respectively.

PUBLICATIONS

LIST OF PUBLICATIONS

Publications from the thesis work

1. **Manasi**, Vidya Rajesh, N. Rajesh, "An indigenous *Halomonas BVR1* strain immobilized in crosslinked chitosan for adsorption of lead and cadmium" *International Journal of Biological Macromolecules*, 79, (2015), 300 – 308.
2. **Manasi**, Vidya Rajesh, N. Rajesh, "Adsorption Isotherms, Kinetics and Thermodynamic studies towards understanding the interaction between a microbe immobilized polysaccharide matrix and lead." *Chemical Engineering Journal*, 248, (2014), 342 - 351.
3. **Manasi**, Vidya Rajesh, A. Santhana Krishna Kumar, N. Rajesh, " Biosorption of cadmium using a novel bacterium isolated from an electronic industry effluent", *Chemical Engineering Journal*, 235, (2014), 176 - 185.
4. **Manasi**, N Rajesh, Vidya Rajesh Evaluation of genetic determinants contributing to heavy metal resistance in an isolate from electronic industry effluent, *Journal of Genetic Engineering and biotechnology*,14, (2016), 177–180.
5. **Manasi**, Sridev Mohapatra, N Rajesh, Vidya Rajesh, Evidence for Polyamines Mediated Mitigation of Lead Induced Stress in *Halomonas BVR 1*, *Scientific Reports*, 2017, 7: 13447 DOI:10.1038/s41598-017-13893-0.
6. **Manasi**, Aditya Tibrewal, N.Rajesh, Vidya Rajesh, Identification and Characterization of the microbial communities found in electronic industrial effluent and their potential for bioremediation, *Chemosphere* (Under Review).
7. **Manasi**, Vidya Rajesh, N Rajesh, Chemistry and biotechnology converge in the synergistic influence of reduced graphene oxide and a halophilic bacteria for the sequestration of heavy metal ions, (Under Communication)

Publications from biosorption studies.

1. T. Sathvika, **Manasi**, Vidya Rajesh, N. Rajesh, "Microwave assisted immobilization of yeast in cellulose biopolymer as a green adsorbent for the sequestration of chromium." *Chemical Engineering Journal* , 279, (2015), 38 – 46.
2. T. Sathvika, **Manasi**, Vidya Rajesh, N. Rajesh, " Prospective application of *Aspergillus* sps. immobilized in sodium montmorillonite to remove toxic hexavalent chromium from waste water", *RSC Advances*, 5, (2015), 107031 - 107044.
3. T. Sathvika, **Manasi**, Vidya Rajesh, N. Rajesh, Adsorption of chromium supported with various column modeling studies through the synergistic influence of *Aspergillus* and cellulose, *Journal of Environmental Chemical Engineering*, 4 (2016), 3193-3204.
4. A. Santhana Krishna Kumara, Timsi Gupta, Shruti Singh Kakan, S. Kalidhasan, **Manasi**, Vidya Rajesh, N. Rajesh, "Effective adsorption of hexavalent chromium through a three center (3c) co-operative interaction with an ionic liquid and biopolymer". *J. Hazardous Material*, 239-240, (2012), 213 - 224.

Papers presented in conferences / workshops

1. **Manasi**, Vidya Rajesh, N. Rajesh, " A graphene oxide microbe combination as an effective adsorbent for the remediation of zinc", International conference on Frontiers in Biological Sciences, NIT, Rourkela, 22nd - 24th January, 2015.
2. **Manasi**, Vidya Rajesh, Satvika T., N. Rajesh, " Removal of zinc using a novel microbe-polysaccharide adsorbent', 16th CRSI National Symposium in Chemistry, IIT, Bombay, 7th - 9th February, 2014.

3. **Manasi**, A. Santhana Krishna Kumar, Vidya Rajesh, N. Rajesh, "Adsorption of Cadmium and Lead using a novel bacterial strain isolated from E-waste", Indian Analytical Science Congress, Goa, 15th - 17th August, 2013.

4.T. Sathvika, S. Akhil, **Manasi**, Vidya Rajesh, N. Rajesh, " Nitrogen fixing bacteria (Rhizobium) immobilized in clay as a sustainable option for the removal of hexavalent chromium from waste water", ICMG, IISc, Bangalore, 17th Feb - 20th Feb, 2016.

5.T. Sathvika, **Manasi**, Vidya Rajesh, N. Rajesh, "Rhizobium sps. immobilized in multi walled carbon nanotubes (MWCNT) for the effective adsorption of chromium", NFCFA, BITS, Pilani - Goa campus, 18th - 19th December, 2015.

6. T. Sathvika, S. Akhil, **Manasi**, Vidya Rajesh, N. Rajesh, " A symbiotic nitrogen fixer immobilized in sodium montmorillonite for the effective sequestration of chromium from waste water", Nascent Development in Chemical Sciences - NDCS 2015, BITS, Pilani, Pilani Campus, Rajasthan, 16th - 18th October, 2015.

BIOGRAPHY OF PROF. VIDYA RAJESH

Prof. Vidya Rajesh is Associate Professor in the Department of Biological Sciences. She is also Associate Dean of Academic Research Division of BITS, Pilani – Hyderabad Campus. Prof. Vidya Rajesh completed her M. Sc. in Microbiology from Nagpur University in the year 1995. She completed her M. E. in Biotechnology (2000) and Ph. D from BITS, Pilani – Pilani campus in the year 2007. The topic of her doctoral thesis was “*Studies on Sequence Diversity and Characterization of the Apical Membrane Antigen of Plasmodium in Indian Isolates*”. Prof. Vidya Rajesh is an extremely dedicated and hard core team player with commitment to teaching and research. She has been actively involved and has gained 17 yrs of teaching, research and administrative experience during her tenure in various capacities at BITS. Her primary research interest is in the area of molecular genetics of human diseases. As collaborative research with Prof. N. Rajesh of Department of Chemistry, her interest has expanded to microbe based heavy metal remediation. She has nearly 30 research publications and equal number of conference presentations. She has completed three research projects as principal investigator and has an

ongoing DST project as an investigator and co-investigator. She has extended her work by focusing on projects like Thyroid receptor mutations in Autism and analysis of urinary biomarkers in autistic patients. Prof. Vidya Rajesh is also part of other institutional projects like DST – FIST and DST – TBI at BITS, Pilani – Hyderabad campus.

BIOGRAPHY OF PROF. N. RAJESH

Prof. N. Rajesh, Department of Chemistry, Birla Institute of Technology and Science, Pilani, Hyderabad Campus, India obtained his Master's degree and Ph.D from Indian Institute of Technology (IIT), Madras, India. He is involved in teaching and research over the past 20 years. He is a fellow member of the Royal Society of Chemistry (FRSC) London. His research interests include development of greener sorbents for the effective detoxification of heavy metals and dyes from industrial effluents. He has several research publications in peer reviewed journals and is also an expert reviewer for various international journals. He has been recognized by Elsevier as an outstanding reviewer for 2015 for his reviewing contributions to the Journal of Environmental Chemical Engineering. Currently, his group is engaged in the development of novel biopolymer, graphene and clay based sorbents for heavy metal remediation. He has research collaborations with Prof. Ranjit Koodali, Department of Chemistry, University of South Dakota, USA. He is a member of American Chemical Society (ACS) and a life member of Chemical Research Society of India (CRSI), Association of Separation Scientists and Technologists (ASSET), India, Indian Council of Chemists and Indian Science Congress (ISC). He has successfully completed projects sponsored by UGC and DST, India.

BIOGRAPHY OF MRS. MANASI

Mrs. Manasi obtained her Master's degree (M. Sc) in Biotechnology from Sri Padmavati Mahila Visvavidyalaya (SPMVV) , India in 2008 and started her research as an institute fellow in the Department of Biological Sciences at BITS Pilani, Hyderabad campus, India. She has been awarded the Dr. KV Rao award for the young scientist award in the year 2014. She is well versed in microbiology, molecular biology based procedures and various analytical procedures involving HPLC, LC-MS, AAS and FTIR. She has good number of publications to her credit and has presented her work in several national and international conferences. Currently, her research

interests focus on the microbial characterization of the industry effluents and its subsequent utilization in the bioremediation of heavy metals.

*Genetic, Metabolic and Physiological Studies of Indigenous Halomonas BVR 1
Isolated from Electronic Industry Effluent for Remediation of Heavy Metals*

THESIS

Submitted in partial fulfillment of
the requirements for the degree of

DOCTOR OF PHILOSOPHY

by

MANASI

ID. No: 2010PHXF432H

Under the Supervision of

Prof. VIDYA RAJESH

Department of Biological Sciences

&

Prof. N. RAJESH

Department of Chemistry



BIRLA INSTITUTE OF TECHNOLOGY AND SCIENCE, PILANI

Hyderabad Campus, Hyderabad, INDIA

2017

CHAPTER VI
CONCLUSIONS AND SUGGESTIONS FOR FUTURE
WORK

SUMMARY AND CONCLUSIONS

Summary and Conclusions

The first chapter gives a comprehensive overview of electronic waste and their effluents as a major source of heavy metals and its hazardous effects. It also summarizes the existing remediation technologies available for removal of heavy metals. The toxic nature of heavy metals vividly describes the need to remove these heavy metals from industrial effluents, which constitutes the major source of heavy metal pollution. Hence, efforts were directed towards the development of effective methods and biosorbents for the detoxification of metals.

The second chapter explains the detailed chemical, microbiological and molecular characterization of the electronic effluents that was collected from an industry located in the outskirts of Hyderabad, to assess the microbiota in the effluent. Various physical parameters like the colour, pH, etc. were tested on site while the chemical parameters like the COD, BOD, DO and alkalinity were carried out in our lab. Biochemical characterizations involving IMVIC tests, citrate test, motility, starch hydrolysis, carbohydrate fermentation were carried out for strain identification. A total of ten bacterial strains and two fungal strains were isolated from this effluent. These strains belonged to four different genera of *Bacillus*, *Halomonas*, *Pseudomonas* and *Kocuria*. Confirmation of identity of these strains was done by the 16S rDNA sequencing and FAME analysis. Among the ten strains isolated, three organisms belonged to the genera *Halomonas*. Organisms from this genera have not been researched upon as a potential use as a biosorbent. Hence one organism belonging to *Halomonas* genera was selected as a test organism for further studies. The biomass as such was used for the remediation of lead, cadmium and zinc. Optimization of parameters like pH, temperature, contact time, metal concentration were studied in detail for attaining maximum adsorption capacity and efficient removal of heavy metals. This microbe functions as an effective adsorbent for the remediation of heavy metals due to the presence of functional groups such as carboxyl, amine, hydroxyl and phosphate that facilitate metal binding and removal from aqueous solutions. The surface characterization of the adsorbent also

showed binding of the heavy metals ion on to the surface of the adsorbent. Langmuir isotherm gave good fit to the experimental data with a maximum adsorption capacity of 12.023 mg g⁻¹, 11.11 mg g⁻¹ and 9.152 mg g⁻¹ for cadmium, zinc and lead respectively. This microbial adsorbent seemed to have more specificity to cadmium owing to its higher adsorption capacity in comparison to the other heavy metals. The adsorption was found to be significantly dependent on the pH, contact time and temperature. The adsorption favored Langmuir adsorption in case of cadmium and lead while it obeyed Freundlich isotherm for zinc adsorption. The pseudo second order kinetic model was best suited for the adsorption of all the metals and thermodynamics depicted the process to be spontaneous and exothermic. The highlight of the method is that although the effluent contains higher concentrations of salts (chlorides, nitrates and phosphates), their effect on the adsorption of metal ions was not significant. Overall the novel bacterium is able to remove cadmium upto a concentration of 100 mg l⁻¹. This biomass was able to remove Lead and zinc upto a concentration of 80 mg l⁻¹ and 50 mg l⁻¹ respectively thus making the process economical and green in environmental remediation.

The third chapter of the thesis deals with the enhancement in the biosorption capacity of the metal ions by immobilizing *Halomonas BVR 1* strain in various biopolymer matrices like chitosan and Graphene Oxide. The surface characterization of the adsorbent before and after adsorption showed characteristic changes in the indicating effective binding of the heavy metals ion on to the surface of the adsorbent. The enhancement in the metal adsorption capacity increased around two folds than the native adsorbent that consisted only *Halomonas BVR 1* cells. Among all the various adsorbents used for the removal of lead, cadmium and zinc, adsorbent that was best suitable for the removal of lead and zinc was *Halomonas BVR 1* immobilized in Graphene Oxide. The maximum adsorption capacity for lead and zinc was found to be 73.58 mg g⁻¹ and 42.53 mg g⁻¹ respectively. *Halomonas BVR 1* immobilized in sodium alginate was successful in maximum removal of cadmium. The adsorption capacity was found to be 25.12 mg g⁻¹. The other parameters like the kinetics, thermodynamics, influence of other interfering ions (cations and anions) were also optimized to achieve the maximum adsorption capacity. Majorly all the processes were exothermic and were favored at relatively lower temperatures. Maximum adsorption was observed by maintaining the average contact time to 2-3 hrs between the adsorbent and the metal ions.

The fourth chapter deals with the immobilizing the microbe in another bioadsorbent ie sodium alginate and modeling studies to specifically simulate the upscale removal of lead ions The experimental data from the Column studies was used to develop a mathematical model generate breakthrough curves and thus simulate the upscale removal of metal ions.

The fifth chapter deals with understanding the physiology of the cell under metal stress and also the genetic basis of the heavy metal resistance in *Halomonas BVR 1*. The genetic basis of heavy metal resistance in our isolated strain was assessed by experiments like plasmid curing ad genetic transformations it was concluded that the basis of metal resistance resided in the plasmid The role of polyamines as a possible player in combating heavy metal stress in bacteria has not been studied till date. A detailed analysis of the production of polyamines in bacterial cell under the exposure of heavy metal at varied time intervals was studied. There was a significant increase in the levels of polyamines under metal stress particularly, putrescine, the precursor to the other polyamines (Spermidine and Spermine) in the initial 6 h. This was the major polyamine produced in the presence of heavy metal. This indicates that putrescine is the first response even in bacterial cells owing to exposure to metal stress. This fact is also corroborated with the data available from plants, in which putrescine is proved to be the first response against heavy metal stress in plants.

Application to real samples and Validation of the method

The validation and application of the adsorption method was performed with real electronic industry effluents using the developed adsorbent that gave the highest adsorption capacity. The compositions of the effluents are shown in **Table 2.2**. The effluent samples were digested with HNO₃-H₂SO₄ mixture to remove the organic matter. Among the prepared adsorbents, microbe immobilized in GO was selected as a test adsorbent to remediate the effluent, owing to its highest adsorption capacity. This adsorbent was significantly able to remediate the heavy metals (98%) in the effluents.

Summary of the developed biosorbents for the removal of metal cations is as follows.

S. No	Adsorbent	Metal	Langmuir adsorption capacity (mg/g)
1.	<i>Halomonas BVR 1</i>	Lead	9.152
2.	<i>Halomonas BVR 1</i>	Cadmium	12.023
3.	<i>Halomonas BVR 1</i>	Zinc	11.11
4.	<i>Halomonas</i> +Sodium Alginate crosslinked CaCl ₂	Lead	9.68
5.	<i>Halomonas</i> +Sodium Alginate crosslinked CaCl ₂	Cadmium	25.12
6.	<i>Halomonas</i> +Sodium Alginate crosslinked CaCl ₂	Zinc	14.28
7.	<i>Halomonas</i> + Chitosan crosslinked glutarladehyde	Lead	24.15
8.	<i>Halomonas</i> + Chitosan crosslinked glutarladehyde	Cadmium	23.88
9.	<i>Halomonas</i> + Chitosan crosslinked glutarladehyde	Zinc	12.535
10.	<i>Halomonas</i> + GO	Lead	73.58
11.	<i>Halomonas</i> + GO	Cadmium	20.30
12.	<i>Halomonas</i> + GO	Zinc	42.53

Scope for future work

The results obtained in this study offered many new and interesting possibilities for future research. Some of them are listed below:-

1. Use combination of microbes to generate a consortium and study its efficacy.
2. Decoding the plasmid sequence responsible for the heavy metal resistance
3. Analyzing the expression of various other proteins (Metallothioneins, glutathione's etc.) responsible for the bacterial resistance to various heavy metals.
4. Assessing the trends in other organisms in the presence of metals other than lead is of paramount importance to delineate the resistance mechanism in bacteria.
5. The molecular mechanism's involving polyamines and heavy metal scavenging needs to be addressed.